UNIVERSIDAD AUTÓNOMA DE MADRID

Departamento de Biología

Facultad de Ciencias

THE KISS ME DEATHLY FAMILY OF E3 UBIQUITIN LIGASES ARE INVOLVED IN NUTRITIONAL CROSSTALKS, REGULATING PHENYLPROPANOIDS BIOSYNTHESIS IN *ARABIDOPSIS THALIANA* (L.)

TESIS DOCTORAL

Mónica Rojas Triana

Madrid, 2015

Departamento de Biología

Facultad de Ciencias

UNIVERSIDAD AUTÓNOMA DE MADRID

THE KISS ME DEATHLY FAMILY OF E3 UBIQUITIN LIGASES ARE INVOLVED IN NUTRITIONAL CROSSTALKS, REGULATING PHENYLPROPANOIDS BIOSYNTHESIS IN *ARABIDOPSIS THALIANA* (L.)

Mónica Rojas Triana

Licenciada en Biología

Directores de Tesis

Dr. Vicente Rubio Munoz **Dr. Fco. Javier Paz-Ares Rodríguez**

Centro Nacional de Biotecnología CNB, CSIC, Madrid, España

Memoria presentada, para optar al grado de

Doctor en Ciencias, por

Mónica Rojas Triana

Universidad Autónoma de Madrid

Noviembre de 2015

Vº Bº de los directores de Tesis

Dr. Vicente Rubio Muñoz **Dr. Fco. Javier Paz-Ares Rodríguez**

Tutor

Dr. Rafael Rivilla

El Doctorando

Mónica Rojas Triana

ACKNOWLEDGMENTS

Quiero expresar mis más sinceros agradecimientos a todas las personas que han colaborado en la realización de este trabajo.

En primer lugar, agradezco a mis co-directores de Tesis, Dr. Vicente Rubio Muñoz y Prof. Javier Paz-Ares Rodríguez, por la excelente labor de dirección realizada, por la oportunidad que se me ha brindado y por la invaluable mentoría que han representado en el desarrollo de mi carrera profesional.

Deseo agradecer a mi tutor de Tesis, Prof. Rafael Rivilla y a la Dra. Francisca Fernández del Campo de la Universidad Autónoma de Madrid, su amabilidad, colaboración y diligencia durante el desarrollo de esta tesis doctoral.

A Jennifer Esteban (Q. E. P. D.) por su inestimable labor técnica desarrollada día a día.

Al Dr. Juan Carlos del Pozo del Instituto Nacional de Investigación y tecnología Agraria y Alimentaria INIA, Madrid, España, por la aportación de construcciones para la técnica de doble híbrido en levaduras.

A la Pr. Salomé Prat por la aportación de las semillas *pub27/28/29*.

Al Dr. Antonio Leyva Tejada por albergarme en su laboratorio por una larga temporada.

A los miembros de los laboratorio 311, 312 y 20-B del Centro Nacional de Biotecnología CNB-CSIC cuya colaboración ha permitido la obtención de los resultados aquí descritos.

Al Departamento de Genética Molecular de Plantas del Centro Nacional de Biotecnología CNB-CSIC, especialmente al servicio de cultivo *in vitro*, coordinado por la Dra. Raquel Piqueras, y al servicio de invernadero, por facilitar el proceso de experimentación. Igualmente, a la unidad de Imagen y Fotografía por la realización de la mayor parte de las fotografías que aparecen en este documento.

I would like to thank to Dr. Wolf-Rudiger Scheible, for giving me the opportunity to complete my research process in the Max Planck Institute of Molecular Plant Physiology, Golm, Germany, and in The Samuel Roberts Noble Foundation, Ardmore, Oklahaoma, USA, and for his support and valuable scientific feedback.

To Professors Mark Estelle and Pascal Genschik for the *cul1–6* and *cul3*^{hyp} mutants seeds, respectively.

Finally, to Prof. Joachim Kopka from the Max Planck Institute of Molecular Plant Physiology, Golm, Germany, for his collaboration in the metabolite profiling presented in this research.

Este trabajo ha sido realizado en el Departamento de Genética Molecular de Plantas del Centro Nacional de Biotecnología-CSIC y ha sido financiado por el Consejo Superior de Investigaciones Científicas CSIC dentro de su programa de becas Junta para la Ampliación de Estudios JAE-preDoc.

ABBREVIATIONS

3-AT: 3-amino-1,2,4-triazole

3-D: three dimensional

A. thaliana: *Arabidopsis thaliana* L.

A. tumefaciens: *Agrobacterium tumefaciens*

aa: amino acid

ABA: abscisic acid

AD: activation domain

AGI: Arabidopsis Genome Initiative

AM: arbuscular mycorrhizae

AMF: arbuscular mycorrhizal fungi

APC: Anaphase Promoting Complex

APC/C: APC/cyclosome

ATP: adenosine triphosphate

BINs: hierarchical functional pathways according to MAPMAN

CKs: cytokinins

CLR3: CUL3 type E3 Ub ligases

CO_2: carbon dioxide

Co-IP: co-immunoprecipitation

Col-0: Columbia-0

CRL1: CUL1 type E3 Ub ligases

CRL3: CUL3–RING E3s

CUL3-RBX1-BTB/POZ: CUL3, RBX1, Broad complex, Tramtrack, Bric-a-brac/Pox virus and Zinc finger

CRL4: CUL4-–RING E3 ligase

CRLs: culling-Ring ligases

CUL: Cullin

Cys: cysteine

DCAF: DDB1 CUL4 Associated Factors

DNA: deoxyribonucleic acid

DWD: DDB1 Binding WD40

E. coli: *Escherichia coli*

E1: Ub-activating enzyme

E2: Ub-conjugating enzyme

E3: Ub-ligase enzyme

EMS: ethyl methanesulfonate

ER: endoplasmic reticulum

FBX: F-box

FN: full nutrition

FW: fresh weight

GA: gibberellins

Gly: glycine

GFP: green fluorescent protein

HECT: Homology to E6AP C Terminus

His: histidine

IP: immunoprecipitation

KFB: Kelch F-box

KMD: Kiss Me Deathdly

Log: logarithmic

L-Phe: phenylalanine

LR: lateral root

LRR: leucine-rich repeat

Lys: Lysine

miRs: microRNAs

MS: Murashige and Skoog

N. benthamiana: *Nicotiana benthamiana*

-N: nitrogen starvation

N: nitrogen

OA: organic acids

P1BS: PHR1-binding sequence

P: phosphorus

PAL: Phenylalanine ammonia-lyase

PCR: polymerase chain reaction

Pi: inorganic phosphate

-Pi: Pi starvation

PHR1: Phosphate Starvation Response1

PHL1: PHR1-like1

PM: plasma membrane

PR: primary root

PSI: Pi-starvation inducible

PSR: Pi-starvation response

PSR genes: Pi-starvation responsive genes

qRT-PCR: quantitative reverse transcription-polymerase chain reaction

QTL: quantitative trait locus

RBX1: RING-Box1

RH: root hair

RING: Real Interesting New Gene

RNA: ribonucleic acid

rpm: revolutions per mimute

RSA: root system architecture

S. cerevisae: *Saccharomyces cerevisae*

SCF: SKP1-like, CDC53, F-box

SLs: strigolactones

-Suc: sucrose starvation

Suc: sucrose

t-CA: trans-cinnamic acid

T-DNA: transfer DNA

TFs: transcriptional factors

TRs: transcriptional regulators

Ub: Ubiquitin

UPL: Ubiquitin-Protein Ligase

UPS: ubiquitin-26S proteasome system

v/v: volume/volume

WT: wild-type

w/v: weight/volume

Y2H: yeast-two hybrid

A mi madre,

a mi familia.

TABLE OF CONTENTS

SUMMARY

1. SUMMARY

Phosphorus (P) is an essential element for life as it is a structural component of nucleic acids, membrane lipids, energy metabolites or activated intermediates in the photosynthetic carbon cycle and throughout primary metabolism. Inorganic phosphate (Pi) also plays a crucial role in signal transduction cascades. Pi is a macronutrient for plants and its availability limits plant growth and development in many soils throughout different climatic zones. To cope with growth under a low Pi supply, plants count on a battery of morphological, physiological, metabolic, biochemical and molecular changes collectively called the Pi-starvation response (PSR), that are regulated at the transcriptional level, mainly by the key transcriptional factors (TFs) PHOSPHATE STARVATION RESPONSE1 (PHR1) and PHR1-like1(PHL1), and at the post-transcriptional level by a pool of mechanisms that, together with ubiquitination, affect Pi uptake and long-distance Pi signaling, thus modulating Pi-starvation responses.

In this work, we have identified and characterized a family of E3 ubiquitin (Ub) ligases (E3), called KISS ME DEATHDLY (KMDs) that are responsive to Pi-starvation at the transcriptional level and are negatively controlled by PHR1/PHL1. KMD proteins are substrate adaptors into an S-PHASE KINASE-ASSOCIATED PROTEIN1 (SKP1)/Cullin (CUL)/F-box protein (SCF) E3 complex and directly interact with phenylalanine ammonia-lyase 2 (PAL2), mediating PAL2 proteolytic turnover via the ubiquitin-26S proteasome system (UPS). PAL catalyzes the first rate-limiting step in the phenylpropanoids biosynthesis pathway. In *Arabidopsis KMD* mutants and overexpressors, the biosynthesis of phenylpropanoids is reciprocally impaired at the level of the (i) precursor phenylalanine (L-Phe), (ii) intermediates like ferulic and sinapic acid, and (iii) products like anthocyanin pigments.

Moreover, Arabidopsis *KMD*s mutants and overexpressors displayed hypersensitivity and insensitivity to cytokinin (CK) treatments, respectively, and such an effect is altered according to Pi and sucrose (Suc) availability. Based on our findings, KMDs act as an integrator node of the previously reported (i) bidirectional antagonistic interactions between cytokinin and both sugar and Pi-starvation signaling, as well and more importantly in the focus of this research, of the (ii) positive bidirectional interaction between sugar and Pi-starvation signaling, by means of the post-transcriptional regulation of PAL stability, among others. *KMD* genes respond to developmental and environmental cues, however the major transcriptional effect over *KMD*s transcription is produced by the availability of metabolizable sugars in the medium. Thus, we propose that KMDs contribute in sugar and Pi-starvation signaling interaction acting as integrators of the two pathways, by controlling the stability of the common effector PAL, which alters the carbon flux directed to the phenylpropanoids biosynthesis and, in consequence, the fine-tuned balance between Pi and sugar status in the cell.

RESUMEN

2. RESUMEN

El fósforo (P) es un macronutriente esencial para todos los organismos vivos. Las plantas absorben el P como ortofosfato (Pi) y su disponibilidad limita el desarrollo y crecimiento de las plantas en muchos suelos en diferentes zonas climáticas del mundo. Las plantas han desarrollado una serie de respuestas adaptativas, que incluyen cambios metabólicos y en el desarrollo que les permiten sobrellevar situaciones de estrés por carencia de Pi en el suelo. Dichos cambios adaptativos son el producto de variaciones en la expresión génica, reguladas principalmente por los factores de transcripción (TFs; del inglés Transcription Factors) PHOSPHATE STARVATION RESPONSE1 (PHR1) y PHR1-like1 (PHL1), y de modificaciones post-traduccionales, mediadas por un conjunto de mecanismos que junto con la ubiquitinación, afectan la captación y señalización a larga distancia de Pi, modulando así las respuestas adaptativas al ayuno de Pi en plantas. En este trabajo, hemos identificado y caracterizado una familia de E3 ubiquitina (Ub) ligasas (E3), llamada KISS ME DEATHDLY (KMDs) que a nivel transcripcional responden a la carencia de Pi y que son controladas negativamente por PHR1/PHL1. Las proteínas KMD son adaptadores de sustrato en complejos E3 del tipo S-PHASE KINASE-ASSOCIATED PROTEIN1 (SKP1)/Cullin (CUL)/F-box protein (SCF) e interactúan físicamente con la fenilalanina amonia liasa 2 (PAL2; del inglés Phenylalanine Ammonia-Lyase 2), mediando su degradación proteolítica a través del sistema ubiquitina-proteosoma 26S (UPS; del inglés Ubiquitin-26S Proteasome System). PAL cataliza la primera etapa limitante en la biosíntesis de los fenilpropanoides. En los mutantes y sobre-expresores de *KMD*s de Arabidopsis, la biosíntesis de los fenilpropanoides está recíprocamente alterada a nivel (i) del precursor fenilalanina (L-Phe), (ii) de intermediarios como ácido ferúlico y ácido sinápico, y (iii) de productos tales como las antocianinas. Adicionalmente, los mutantes y sobre-expresores de *KMD*s muestran hipersensibilidad e insensibilidad a tratamientos con citoquininas (CKs), respectivamente, y este efecto es dependiente de la disponibilidad de Pi y sacarosa (Suc; del inglés Sucrose). Según nuestros hallazgos, las proteínas KMD actúan como un nodo integrador de (i) la interacción antagónica bidireccional entre las CKs y las rutas de señalización de azúcares y Pi y, aún más relevante dentro del foco de esta investigación, de (ii) la interacción positiva bidireccional entre las rutas de señalización de azucares y del ayuno de Pi, por medio de la regulación post-traduccional de la estabilidad de PAL, entre otros. Los genes *KMD* responden a diferentes estímulos ambientales, sin embargo, la disponibilidad de azúcares metabolizables en el medio surge el mayor efecto transcripcional sobre éstos. Por lo tanto, basados en los resultados obtenidos en esta investigación, proponemos que las proteínas KMD contribuyen en la interacción conocida entre las rutas de señalización del ayuno de Pi y de azucares, actuando como integradores de las dos rutas, mediante el control de la estabilidad del efector común, PAL. Así, KMDs contribuyen en la regulación del flujo de carbón destinado a la biosíntesis de los fenilpropanoides y, en consecuencia, en el mantenimiento del balance entre el Pi y los azucares en la célula.

INTRODUCTION

3. INTRODUCTION

3.1. THE UBIQUITIN-26S PROTEASOME PATHWAY

Ub is a small peptide that acts as a post-translational modifier to virtually regulate all aspects of cell biology in eukaryotes, including cell division, growth, communication, movement and death (Hershko & Ciechanover, 1998). In plants, Ub has been related to the control of many physiological, developmental and stress responses, such as phytohormone signaling, flowering, circadian clock function, plant defense, heat shock and cold stresses, DNA damage repair, nutrient deprivation and drought tolerance (reviewed in Smalle & Vierstra, 2004). Also, Ub helps the cell to get rid of proteins with biosynthetic/folding errors (Raasi *et al*., 2007). In many cases, this control is exercised by the degradation of target proteins through the 26S proteasome, which is a 2MDa ATP-dependent proteolytic complex (reviewed in Voges *et al*., 1999; Hartmann-Petersen *et al*, 2003) with multiple isoform assembles in plants (Fu, *et al*. 1999; Shibahara *et al*. 2002; Yang *et al*. 2004). Given the relevance on this process (known as the ubiquitin-26S pathway), it discovery and description, during the 70's and 80's, earned the 2004 Noble Prize in Chemistry to the Drs. Aaron Ciechanover, Avram Hershko and Irwin Rose (Hershko *et al*., 1980; Hershko & Ciechanover, 1982).

Ub is present in all examined eukaryotic organisms and it is the most structurally conserved protein yet identified; its 76 amino acid (aa) sequence is invariant in the plant kingdom and only differs in two residues from the yeast Ub, and in three residues from animal Ub (Callis *et al*., 1995). At the three dimensional (3-D) level, it has a globular shape with five beta strand structures forming a cavity into which an alpha helix fits (Vierstra, 1996). Protruding from the globular shape is the C-terminal glycine (Gly) 76 that covalently interacts, via the carboxyl group, with ubiquitination enzymes and participates in the attachment to its targets (Figure 1-A).

3.1.1. The ubiquitination cascade

Ub is covalently linked to target proteins by an isopeptidic bond between the Ub C-terminal Glycine (Gly)76 and lysine (Lys) residues of the intracellular target protein. The attachment is the result of an adenosine triphosphate (ATP)-dependent specific enzymatic cascade (ubiquitination) (Figure 1-B). These cascades begins with the binding of the Ub (Gly76) with a cysteine (Cys) in an E1 Ub-activating enzyme (E1), via a thiol-ester linkage, and the transference of the activated Ub to a Cys in an E2 Ub-conjugating enzyme (E2 or UBC), via transesterification. E3 Ub-ligases (E3) represent the last step in the cascade, working as a recognition element that brings together

the Ub-E2 intermediate and the protein target, that is then ubiquitinated. Therefore, E3s play a key role in ubiquitination by providing substrate specificity (reviewed in Smalle & Vierstra, 2004).

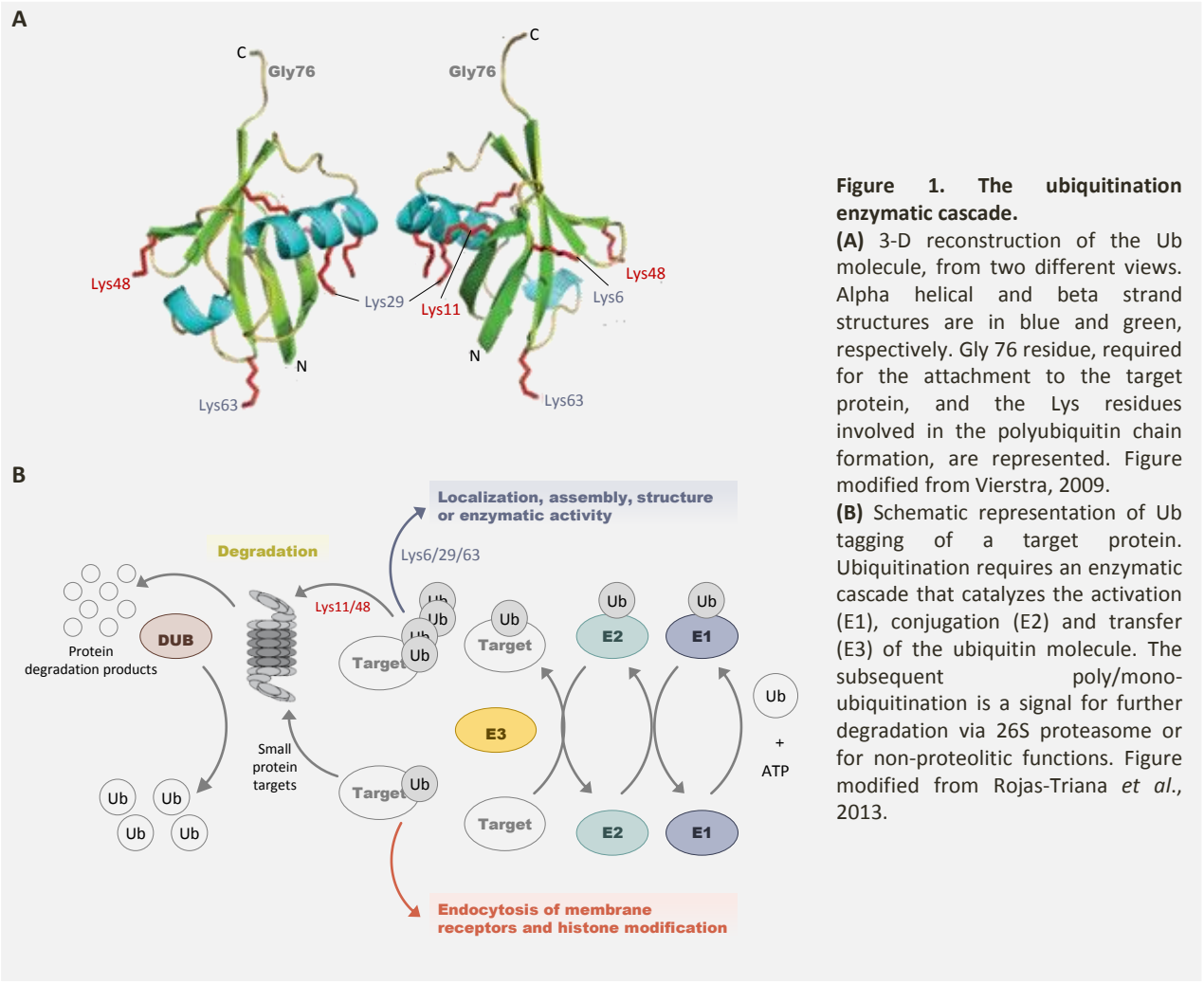

Figure 1. The ubiquitination enzymatic cascade.
(A) 3-D reconstruction of the Ub molecule, from two different views. Alpha helical and beta strand structures are in blue and green, respectively. Gly 76 residue, required for the attachment to the target protein, and the Lys residues involved in the polyubiquitin chain formation, are represented. Figure modified from Vierstra, 2009.
(B) Schematic representation of Ub tagging of a target protein. Ubiquitination requires an enzymatic cascade that catalyzes the activation (E1), conjugation (E2) and transfer (E3) of the ubiquitin molecule. The subsequent poly/mono-ubiquitination is a signal for further degradation via 26S proteasome or for non-proteolitic functions. Figure modified from Rojas-Triana *et al.*, 2013.

Consecutive cycles of ubiquitination may result in polyubiquitination and subsequent recognition by the 26S proteasome for degradation (Hershko & Ciechanover, 1998). Despite the well-established function of ubiquitination in regulated proteolysis via the proteasome, recent evidence has shown that this mechanism can modulate protein function through additional means. In this context, it has been found that different poly-Ub chain conformations determine different fates for the targeted protein. Thus, substrates for proteosomal degradation are labeled with chains in which Ubs are linked via their Lys11 or 48, whereas Ub chains linked via Lys6, 29 or 63 modulate other aspects of protein functionality, such as localization, assembly, structure or enzymatic activity (Deshaies & Joazeiro, 2009). A similar effect is found in the case of protein monoubiquitination, which is involved, for example, in endocytosis of membrane receptors and histone modification (Sigismund *et al.*, 2004). However, it has recently been shown that monoUb can trigger proteasomal degradation of small protein targets (≤150aas;

Shabek *et al*., 2012). Target ubiquitination can be reversed by Ub hydrolases (i.e., deubiquitinases or Ub deconjugases), adding an additional level of complexity to the regulatory mechanisms involved in this posttranslational modification (Kim *et al*., 2003). *Arabidopsis* genome expresses two E1 isoforms of ~1100aa (Hatfield *et al*., 1997), with high catalytic efficiency that ensure the activated Ub pool needed in the ubiquitination cascade (Pickart, 2001). E2s are identified by a Cys active-site surrounded by a catalytic core (150aa) (Hamilton *et al*., 2001), that is well conserved between the at least 37 E2s, reported in the *Arabidopsis* genome (Vierstra, 1996; Bachmair *et al*., 2001). Is well know that some E2s have N and/or C-terminal motifs that may contribute in appropriate E3s association, localization and target recognition (Smaller & Vierstra, 2004).

The organization of the UPS is hierarchical with most of the complexity residing in the E3 protein families that decide which proteins should be ubiquitinated. Indeed, whereas *Arabidopsis* genome contains 2 E1 genes and 37 E2 genes, it contains ~1300 genes encoding E3 components (Vierstra, 2003). In the next section, we will focus in the review of the E3s mechanism of action and functions in plants.

3.1.2. E3 ligases

As the enzymes responsible for identifying Ub-target proteins, E3s confer the specificity to the ubiquitination process and, therefore, they are the most abundant and diverse factors of the cascade. It is reported that there are more than 1300 genes that encode putative E3s in the Arabidopsis genome (Gagne *et al*., 2002; Vierstra, 2003). Originally, E3s were described in mammals (Hershko *et al*., 1982) and they can act as monomers or as multimeric complexes (Choi *et al*., 2014) (Figures 2 and 3). In plants, there are three major E3 types, grouped based on subunit composition and mechanism of action. The main types are: (i) Homology to E6AP C Terminus (HECT), (ii) monomeric Real Interesting New Gene (RING)/U-Box, and (iii) cullin (CUL)-based E3 ligases. Four major E3 ligase families are known in plants that contain either a CUL (CUL1, 3, or 4) or a CUL-like protein ANAPHASE-PROMOTING COMPLEX2 (APC2). They are known as: (i) CUL1-based E3s (CRL1) or SCF, (ii) CUL3–RING E3s (CRL3) or CUL3-RBX1-BTB/POZ (for CUL3, RBX1, Broad complex, Tramtrack, Bric-a-brac/Pox virus and Zinc finger) , (iii) CUL4-based E3s (CRL4; CUL4–RING E3 ligase), and (iv) APC/cyclosome (APC/C) (Figure 3).

3.1.2.1. Monomeric E3 ligases

Unlike the other types of E3s, HECT and RING/U-box E3s acts as monomers, without the help of additional substrate adaptor proteins. HECT E3s belongs to a small gene family in *Arabidopsis* (7 members; Downes *et al*., 2003), that have been named UBIQUITIN-PROTEIN LIGASE (UPL) 1 to UPL7.

Although HECT represents a small family of E3s, nowadays there is only functional descriptions for a few of them, including UPL1, UPL3 and UPL5 (Table 1). UPLs are characterized by a ~350aa domain, relatively conserved

among the family, and variable regions that add up to molecular weights greater than 100kDa (Huibregtse *et al*., 1995; Schwarz *et al*., 1998). The most striking feature about HECT E3s is the unique ubiquitynation mechanism, characterized by the formation of an Ub-HECT intermediate (thiol-ester linkage), previous to the Ub transfer to the target protein (Scheffner *et al*., 1995) (Figure 2).

Table 1. Examples of monomeric E3 ligases from plants (modified from Chen & Hellmann, 2013).

TYPE	NAME	AGI CODE	PROPOSED FUNCTION	REFERENCES
HECT	UPL1	At1g55860	Unknown	Bates & Vierstra, 1999; Downes *et al*., 2003
HECT	UPL3	At4g38600	Endoreduplication cycles in trichomes; GA signaling	Perazza *et al*., 1999; Downes *et al*., 2003
HECT	UPL5	At4g12570	Leaf senescence	Miao & Zentgraf, 2010
RING	Rma1H1	At4g03510	Tolerances for water/drought/salt	Lee *et al*., 2009; Seo *et al*., 2012b
RING	XBAT32	At5g57740	Ethylene signaling	Lyzenga *et al*., 2012
RING	RGLG1	AT3G01650	Water	Cheng *et al*., 2012
RING	DIS1 (*Oryza sativa*)		Drought	Ning *et al*., 2011
RING	SIE3 (*Lotus japonicas*)		Nodule organogenesis	Yuan *et al*., 2012
RING	WAV3	At2g22680	Root gravitropism, root growth and blue-light phototropic responses	Sakai *et al*., 2012
RING	LOG2	AT3G09770	Metabolic processes	Pratelli *et al*., 2012
U-box	CHIP	At3g07370	Low- or high-temperature stress	Yan *et al*., 2003; Shen *et al*., 2007a; Shen *et al*., 2007b
U-box	PUB9	At3g07360	ABA signaling and drought responses	Samuel *et al*., 2008
U-box	PUB18/19	At1g10560 At1g60190	Seed germination	Seo *et al*., 2012a
U-box	PUB44/SAUL1	At1g20780	Senescence process	Rabb *et al*., 2009
U-box	PUB13	At3g46510	SA-dependent defense signaling and floweringtime regulation	Li *et al*., 2012

In contrast, monomeric RING-finger E3s simultaneously bind an E2 and a target protein, facilitating Ub transfer from the Ub-E2 intermediate to a substrate (Figure 2). E2-binding capacity displayed by RING-finger E3s is conferred by the ~40-60aa RING motif, similar to zinc-finger domains (Cys and histidine (His) residues coordinating

binding of two zinc ions). In *Arabidopsis*, more than 469 proteins are being assigned as RING type (Stone *et al.*, 2005), and even if most are likely E3s, few display roles as part of multimeric E3 complexes (e.g. RBX1; see 3.1.2.2. CUL-based E3 ligases; Stone *et al.*, 2005).

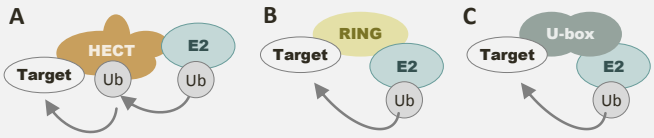

Figure 2. Monomeric E3 Ub ligases. Schematic representation of the organization of **(A)** HECT, **(B)** Ring, and **(C)** U-box E3s, in association with a Ub-E2 intermediate and a protein target.

The last class of monomeric E3s are the U-box or PUB E3s (Figure 2). They harbor a ~70aa U-box motif, that differs from the RING in the absence of the zinc-chelating Cys and His residues (Ohi *et al.*, 2003). Approximately 64 Arabidopsis proteins are being annotated as members of the U-box family, and they appear to be widely involved in stress-related responses (Table 1).

3.1.2.2. CUL-based E3 ligases

In plants, the highest diversity among E3s is found in the CUL-based E3 ligases. The CUL protein act as scaffolding and central subunit recruiting a RING-finger protein at its C-terminal region, and a substrate adapter protein at its N-terminal part.

CUL3-based E3s, better known as CUL3-RBX1-BTB/POZ, are a large class of CRLs, characterized by an ensemble between CUL3 (CUL3a or CUL3b; Weber *et al.*, 2005), RBX1 and a substrate adaptor BTB/POZ protein (80 annotated members in *Arabidopsis*; Gingerich *et al.*, 2005). The BTB/POZ fold is required to interact with CUL3 and, by means of the direct interaction, bring target proteins to the CUL3-RBX1 core (Figueroa *et al.*, 2005; Gingerich *et al.*, 2005; Weber *et al.*, 2005; Yoshida *et al.*, 2005; Dieterle *et al.*, 2005; Zhuang *et al.*, 2009) (Figure 3). Noteworthy are the CUL3-RBX1-BTB/POZ E3s implications in the phytohormone regulation and pathogen responses, that are being described by dissecting BTB/POZ substrate adaptors individual roles (Wang *et al.*, 2004a; Fu *et al.*, 2012; Shi *et al.*, 2012; Pajerowska-Mukhtar *et al.*, 2013; Spoel *et al.*, 2009) (Table 2).

Recently, the CRL4 complexes were described as conserved E3s among diverse organisms (Biedermann & Hellmann, 2011), in which RBX1 and DNA DAMAGED BINDING PROTEIN 1 (DDB1) binds to CUL4 C-terminal and N-terminal regions, respectively. DDB1 (125kDa) helps binding substrate adaptors to the E3 core (Angers *et al.*, 2006; Bernhardt *et al.*, 2006; Lee *et al.*, 2008), sometimes by means of interactions with the so called DDB1 CUL4 ASSOCIATED FACTORS (DCAF) (Biedermann and Hellmann, 2011). Some DCAF proteins are characterized by multiple WD40 repeats and a conserved 16-17aa sequence called DDB1 BINDING WD40 (DWD)-box (Lee *et al.*, 2008) (Figure 3). However, DCAF are called all substrate adaptor proteins able to interact with DDB1, with CUL4

exception. Since its description in plants, CRL4 E3s are being reported as key factors in abiotic stress responses, DNA repair, flowering, phytohormone signaling and photomorphogenesis, among others (Table 2).

Table 2. Examples of CUL-based E3 ligases from plants (modified from Choi *et al*., 2014).

TYPE	NAME	AGI CODE	PROPOSED FUNCTION	REFERENCES
CRL3	ARIA	At5g19330	ABA signaling	Kim *et al.*, 2004; Lee *et al*., 2009b
	BPM1-6	At1g19000/ At3g06190/ At2g39760/ Etc.	ABA signaling, ABA-stomatal response, Drought response, wounding response, senescence, ethylene signaling, cytokinin signaling, fatty acid biosynthesis, seed development	Lechner *et al*., 2011; Weber *et al*., 2005; Weber & Hellmann, 2005; Chen *et al*., 2013
	EOL1/ EOL2	At4g02680/ At5g58550	Ethylene biosynthesis	Wang *et al*., 2004a; Christians *et al*., 2009
	ETO1	At3g51770	Ethylene biosynthesis	
	NPH3	At5g64330	Blue light-dependent bending, blue light regulation	Pedmale & Liscum, 2007; Roberts *et al*., 2011
	NPR1/ NPR3/ NPR4	At1g64280/ At5g45110/ At4g19660	Basal and SA-dependent pathogen response; cellular redox potential; effector triggered immunity	Spoel *et al*., 2009; Fu *et al*., 2012; Zhang *et al*., 2006
	SR1IP1	At5g67385	Calcium signaling, pathogen response	Zhang *et al*., 2014
CRL4	ABD1	AT4G38480	ABA signaling, salt tolerance	Seo *et al*., 2014
	COP1/ COP10	AT2G32950/ AT3G13550	Photomorphogenesis, flowering time, UV-induced morphogenesis	Chen *et al*., 2010; Huang *et al*., 2013b; Jang *et al*., 2008; Lau & Deng, 2009;
	DDB2	AT5G58760	NER, UV- sensitivity	Biedermann & Hellmann 2010; Molinier *et al*., 2008
	DET1	AT4G10180	Photomorphogenesis, circadian rhythm, DNA repair	Schroeder *et al.,* 2002; Bernhard *et al.,* 2006
	DWA1-3	AT2G19430/ AT1G76260/ AT1G61210	ABA signaling, salt tolerance	Lee *et al.,* 2010; Lee *et al.,* 2011
	PRL1	AT4G15900	ABA signaling, cytokinin signaling, sugar sensitivity	Lee *et al.,* 2008; Fragoso *et al.,* 2009
	SPA1-4	At2g46340/ At4g11110/ Etc.	Photomorphogenesis, flowering time, UV-induced morphogenesis	Chen *et al.,* 2010; Huang *et al.,* 2013b; Zhu *et al.,* 2008
	TRIP1/eIF3i	AT2G46280	Brassinosteroid signaling	Jiang & Clouse, 2001; Lee *et al.,* 2008
APC/C	APC2/ APC6/ APC10	At4g36920/ At1g78770/ At2g18290/	Megagametogenesis Leaf epidermal development, vascular vein development, shoot development, ploidy	Marrocco *et al.,* 2009; Perez-Perez *et al.,* 2008
	CCS52A1 CCS52A2	At4g22910/ At4g11920	Ploidy, root meristem, pathogen response	Vanstraelen *et al.,* 2009; Lammens *et al.,* 2008
	CDC20.1	At4g33270	Cell cycle regulation	Kevei *et al.,* 2011
	CDC27a	At3g16320	Gametogenesis, embryogenesis	Blilou *et al.,* 2002; Perez-Perez *et al.,* 2008
	HBT	At2g20000	Gametogenesis, embryogenesis, auxin insensitivity, ploidy	Blilou *et al.,* 2002; Perez-Perez *et al.,* 2008
	OsMOC1	Q84MM9	Tillering control	Xu *et al.,* 2012
	OsRAA1	AAT94064	Spindle apparatus	Xu *et al.,* 2010b

Table 2. (Continued)

TYPE	NAME	AGI CODE	PROPOSED FUNCTION	REFERENCES
SCF	COI1	At2g39940	JA signaling, pathogen response, wounding, pollen fertility	Xie *et al.*, 1998; Feys *et al.*, 1994; Thines *et al.*, 2007
	DOR	At2g31470	Drought tolerance, ABA-stomatal response	Zhang *et al.*, 2008b
	EBF1/ EBF2	At2g25490/ At5g25350	Ethylene signaling, Guo & Ecker 2003; Potuschak et al 2003;	Binder *et al.*, 2007
	EDL3	At3g63030	ABA signaling, seed germination, flowering time, root development, osmotic stress	Koops *et al.*, 2011
	EID1	At4g02440	Photomorphogenesis, skotomorphogenesis; far-red response	Dieterle *et al.*, 2001; Marroco *et al.*, 2006
	ETP1/ ETP2	At3g18980/ At3g18910	Ethylene signaling	Alonso *et al.*, 1999; Qiao *et al.*, 2009
	FBL17	At3g54650	Cell cycle regulation, gametogenesis	Gusti *et al.*, 2009; Kim *et al.*,. 2008
	FKF1/ LKP2	At1g68050/ At2g18915	Blue light response, flowering time, photomorphogenesis,	Sawa *et al.*, 2007; Ito *et al.*,. 2012
	MAX2	At2g42620	ABA signaling, ABA-stomatal response, drought tolerance, osmotic stress, strigolactone signaling, lateral shoot branching	Bu *et al.*, 2014; Stirnberg *et al.*, 2007
	SGT1a / SGT1b	At4g23570 / At4g11260	Auxin signaling, pathogen response	Austin *et al.*, 2002; Azevedo *et al.*, 2002; Gray *et al.*, 2003
	SKP2a/ SKP2b	At1g21410/ At1g77000	Cell cycle regulation, auxin	del Pozo *et al.*, 2002a; Jurado *et al.*, 2010; Ren *et al.*, 2008
	SLY1/ SLY2	At4g24210 / At5g48170	GA signaling	Strader *et al.*, 2004; Ariizumi *et al.*, 2011
	TIR1	At3g62980	Auxin signaling, root development, shoot growth, embryogenesis, drought tolerance, nitric oxide production	Gray *et al.*, 1999; Dharmasirii *et al.*, 2005b; Gray *et al.*, 2001; Greenham *et al.*, 2011
	AFB1-5	At4g03190/ At3g26810/ Etc.		
	UFO	At1g30950	Flower organogenesis, floral meristem development	Levin & Meyerowitz, 1995; Chae *et al.*, 2008
	ZTL	At5g57360	Blue light response, flowering time, photomorphogenesis, circadian rhythm	Kiba *et al.*, 2007; Ito *et al.*, 2012

Arabidopsis APC2 shares homology to CUL proteins and act as scaffold in the APC/C E3 complexes, the bigger E3s in size so far described in the plant kingdom. APC/C comprise at least 11 core subunits (Capron *et al*., 2003a), from which APC2 and APC11 (similar to RBX1; Gieffers *et al*., 2001; Zhang *et al*., 2013) acts as catalytic subunits in Ub-E2 intermediate binding, target protein recognition and Ub transfer to the substrate (Zhang *et al*. 2013) (Figure 3). Studies on plant APC/C E3s indicated that subunits 1, 4, 5, 6, and 8 help as scaffolding moieties, while APC3 and APC7 contribute in binding of APC10, that together with APC2, are involved in target binding (Van Leene *et al*., 2010; Zhang *et al*., 2013). It is worth noting that, for the full action of the E3 complex, extra co-activator subunits are required to facilitate target protein binding. So far, WD40-repeat-containing protein families,

CELL DIVISION CYCLE20/FIZZY (CDC20/FZ) and CDC20 HOMOLOG1/FIZZY-RELATED (CDH1/FZR), are being described as co-activators (Capron *et al*., 2003b; Vodermaier *et al*., 2003; Fulop *et al*., 2005; da Fonseca *et al*., 2011). Processes related with the biological relevance of APC/C complexes are the control of the auxin sensing, cell cycle and ploidy (Table 2).

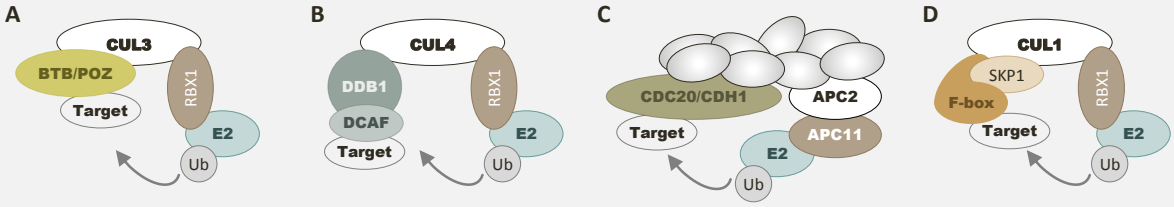

Figure 3. CUL-based E3 ligases. Schematic representation of the organization of **(A)** BTB/POZ-CUL3-RBX, **(B)** CRL4, **(C)** APC/C, and **(D)** SCF E3 complexes, in association with a Ub-E2 intermediate and a target.

Finally, the best-described and diverse CRL E3s are the CUL1-based E3s, better known as SCF complexes, characterized by an assemble of at least four polypeptides, as follow: CUL1 with RBX1 (or ROC1 and HRT1; RING H2–type domain protein), that employs SKP1-like and F-box proteins as substrate adaptors (Craig & Tyers, 1999; Gagne *et al*., 2002; Gray *et al*., 2002) (Figure 3). Alike in the above mentioned CRL E3 complexes, CUL1 displays a scaffolding performance, binding the substrate adaptor complex, and the RBX1/Ub-E2 complex, at its N- and C-terminal regions, respectively. By this means, CUL1 brings the F-box and the Ub-E2 intermediate into close physical proximity to enable Ub transfer to a target protein (Zheng *et al*., 2002b). In a broad view, CUL1-RBX1-ARABIDOPSIS SKIP (ASK) subcomplex provides Ub-transferase activity and the F-Box proteins confer target specificity (Deshaies *et al*., 1999).

In contrast with the only two CUL1-like (CUL1 and CUL1b) and two RBX1 codified by the *Arabidopsis* genome, 21 ASK-like proteins and 692 F-box proteins are being predicted (Gagne *et al*., 2002; Xu *et al*., 2009). In other plant species like *Oryza sativa*, *Populus trichocarpa* and *Vitis vinifera*, 779, 337 (Xu *et al*., 2009), and 156 (Yang *et al*., 2008) F-box genes were identified, respectively.

Typically, ASKs interacts with CUL1 via an N-terminal domain (125aa), similar to the BTB/POZ (Schulman *et al*., 2000), while the F-box proteins interact with both the ASKs and CUL1 via it characteristic F-box motif (at the N-terminal region) (Schulman *et al*., 2000). Located a t the C-termini of the F-box proteins, several protein-protein interaction motifs can be found, that presumably identifies specific target proteins (Gagne *et al*., 2002). Worth notice that, extra post-translational modifications (e.g. phosphorylation) over the substrate may be required for the proper E3 target recognition (Deshaies *et al*., 1999).

According to reiterative BLAST searches of the *Arabidopsis* genome, using as queries a group of F-box proteins from diverse and distant organisms (yeast, animals and plants), Gagne and collaborators (2002) established a collection of putative *Arabidopsis* FBX loci (from F-Box). The predicted F-box proteins are characterized by a long region C-terminal to the F-box motif, with a wide array of protein-protein interaction domains, presumably involved in target protein recognition. The most ample F-box types (or subfamilies) are those harboring leucine-rich (LRR) or Kelch repeats, however, WD-40, Armadillo (Arm) and tetratricopeptide (TPR) repeats, and Tub, actin, DEAD-like helicase, and jumonji (Jmj)-C domains, can be found. Approximately, 202 F-box proteins contain the 20-29aa LRR motifs, with positionally conserved leucines or other aliphatic residues. For example, the biologically relevant and very well known TRANSPORT INHIBITOR RESPONSE 1 (TIR1) and CORONATINE INSENSITIVE 1 (COI1) F-box proteins (see Table 2), matched a LRR consensus sequences when using the SMART (Simple Modular Architecture research Tool) tool (Gagne *et al*., 2002), however, most the *Arabidopsis* predicted F-box proteins were found to contain a plant-specific derivative of the cysteine-containing LRR (Gagne *et al*., 2002).

In plants, a very interesting F-box subfamily is constituted by the F-box Kelch proteins (FBKs), that contains from one to five kelch repeats, C-terminal to the N-terminal F-box motif. FBKs represent a distinctive class of F-box proteins in plants, since only one FBK has been functionally described in humans (Sun *et al*., 2009), and its occurrence as an uncommon event in non-plant organisms. In contrast, kelch repeat containing proteins (without a F-box motif) are wide spread and have been described in *Arabidopsis* (Leung *et al*., 2004; Mora-García *et al*., 2004) as well as in distant non-plant organisms like *Drosophila melanogaster*, *Caenorhabditis elegans*, *Schizosaccharomyces pombe* and *Homo sapiens sapiens* (Prag & Adams, 2003).

The potential protein-protein interaction domain, formed by the kelch repeats in the FBKs, more likely displays a tertiary β-propeller structure, as predicted by Andrade and collaborators (2001), based on molecular modelling according with the kealch-repeats-containing galactose oxidase crystal structure (Andrade *et al*., 2001). Supporting this prediction, the crystal structure of the human kelch protein KEAP1 (Kelch-like ECH-associated protein 1 regulator), form a β-propeller structure (Li *et al*., 2004).

Arabidopsis genome codes for approximately 100 FBKs (Gagne *et al*., 2002), most of which are not been functionally characterized. Some examples are being related with flowering and circadian rhythms in *Arabidopsis*, like the putative flavin-containing photoreceptors FLAVIN-BINDING KELCH-REPEAT F-BOX1 (FKF1), LOV KELCH PROTEIN2 (LKP2) and ZEITLUPE (ZTL), and with the positive regulation of the phytochrome A-mediated light signaling by ATTENUATED FAR-RED RESPONSE (AFR) (Harmon & Kay, 2003).

3.1.2.3. Regulation of CUL-based E3 ligases

The regulation of the CRL E3s (except for APC/C) is represented by loosely associations with some accessory factors, which are affecting the assembly and/or activity of the CRL core subunits. CUL subunit activation/deactivation is a key step in the dynamic regulation of CRLs, and is driven by a single RUB (Related to Ubiquitin)/NEDD8 conjugation/de-conjugation process (del Pozo *et al*., 2002b; Gray *et al*., 2002; Dharmasiri *et al*., 2003, 2007). Boh and collaborators (2011), has indicated that a rapprochement occurs between CUL and a bound substrate (requirement for ubiquitination), as a result of RUB attachment to a CUL C-terminal region Lys residue (del Pozo & Estelle, 1999) (Boh *et al*., 2011). RUB modification is de-conjugated by the COP9 signalosome (CSN), a protein complex that comprises eight subunits and resembles the 19S lid of the 26S proteasome (Dohmann *et al*., 2005; Stuttmann *et al*., 2009). Another regulatory factor is CULLIN ASSOCIATED AND NEDDYLATION DISSOCIATED 1 (CAND1) that interacts with unmodified CUL (Zhang *et al*., 2008a; Helmstaedt *et al*., 2011), preventing CUL binding with substrate adaptors as well as a RUB modification (Duda *et al*., 2011). Therefore, RUB conjugation enables assembly of target-loaded substrate adaptor modules to the CUL-RBX1 core for target ubiquitination. Afterwards, RUB deconjugation by CSN complexes allows binding of CAND1 to CUL proteins, triggering dissamsembly of CRL complex and release of substrate adaptor modules that can, subsequently, interact with new targets.

3.2. PHOSPHATE STARVATION IN PLANTS

P is an essential element for life as it is a structural component of nucleic acids, membrane lipids, energy metabolites or activated intermediates in the photosynthetic carbon cycle and throughout primary metabolism. Pi also plays a crucial role in signal transduction cascades (Poirier & Bucher, 2002). Pi is a macronutrient for plants and its availability limits plant growth and development in many soils throughout different climatic zones (Marschner, 1995; Raghothama, 1999; Lynch, 2011). Low bioavailability of Pi is mainly due to its propensity to form sparingly soluble salts with oxides/hydroxides of aluminum and iron in acidic soils and with calcium and magnesium in alkaline soils (Marschner, 1995; Raghothama, 1999; Poirier & Bucher, 2002). Pi-fertilizers are supplied in large amounts to increase or maintain crop yields, but minable global P-resources are non-renewable and finite. Broader awareness of this alarming situation was generated when in 2008-2009 Pi-fertilizer prices spiked and some reports (Cordell *et al*., 2009; Vaccari, 2009) forecasted that the production of Pi-fertilizers will peak as early as 2030, and insufficient P-availability might thus lead to increased famine among a rising global human population. Although other reports (Fixen & Johnston, 2012; Van Kauwenbergh *et al*., 2013) assume that global P-reserves last for another couple hundred years, it is a matter of fact that P-fertilizers are a considerable cost factor for

farmers/producers world-wide. Hence it is important, if not crucial, to (i) understand how plants sense, signal, respond to and cope with Pi-limitation, (ii) determine what genes and molecular mechanisms are involved, and (iii) apply generated knowledge to improve Pi-efficiency in agricultural production systems, and thus maintain food security as well as reduce environmental damage caused by Pi-fertilizer application (Scheible & Rojas-Triana, 2015).

3.2.1. The plant phosphate starvation response

To cope with growth under a low Pi supply, plants count on a battery of morphological, physiological, metabolic, biochemical and molecular changes collectively called the PSR and aiming at improved Pi-acquisition, sensible Pi-reallocation and remobilization, and thus increased Pi-efficiency (Figure 4). Plants usually increase their root/shoot ratio when P becomes limiting, by reducing shoot growth more than root growth. Sometimes root growth is maintained or even stimulated, and especially the number and length of lateral roots and root hairs increase, while primary root growth becomes inhibited, although not necessarily in all plant species or cultivars (Chevalier *et al*., 2003). During Pi-limitation plants also produce special roots, such as proteoid (cluster) roots (Lambers *et al*., 2011), establish connections to fungal hyphae networks (arbuscular mycorrhizae, AM) (Bucher, 2007; Smith *et al*., 2011), or produce more shallow roots to improve Pi-acquisition from Pi-rich top-soil (Lynch & Brown, 2001; Zhu *et al*., 2005). Such developmental strategies increase the root surface, root-soil contact and thus help to more efficiently explore/mine the soil for Pi (Bates & Lynch, 2001; Williamson *et al*., 2001; Lambers et al., 2011; Lynch, 2011).

At the physiological and biochemical levels plants increase their capacity for Pi uptake, transport and translocation by induction of high-affinity Pi transporters and stimulation of production and secretion of organic anions, such as malate and citrate, into the soil and the apoplastic space (Raghothama, 1999) to solubilize otherwise insoluble phosphates. Similarly, the production and secretion of acid phosphatases, phosphodiesterases, nucleases and ribonucleases (Taylor *et al*., 1993; Bariola *et al*., 1994) help to liberate, scavenge and recycle Pi from organic matter in the soil and inside the plant (Li *et al*., 2002; Hurley *et al*., 2010). Nucleic acids (especially ribosomal RNA), membrane phospholipids and major phosphorylated metabolites (e.g. glucose 6-phosphate or fructose 6-phosphate) represent the bulk of organically bound P in plant cells (Chapin & Bieleski, 1982; Lambers *et al*., 2011; Plaxton & Tran, 2011). Plants control these P pools tightly and increase recycling/remobilization of Pi from these pools during Pi-limitation. Membrane phospholipids are degraded during Pi-limitation and replaced by sulfolipids and galactolipids in Arabidopsis and other plant species (Nakamura, 2013). During Pi-limitation plants also contain considerably less ribosomal RNA (Hewitt *et al*., 2005; Sulpice *et al*., 2014).

Other biochemical and metabolic responses of plants to Pi-limitation comprise the use of alternative, Pi- and adenylate-saving metabolic pathways such as for cytosolic glycolysis and mitochondrial electron transport (Plaxton & Tran, 2011), the accumulation of sugars, starch or many amino acids (Morcuende *et al*., 2007; Hammond & White, 2008; Pant *et al*., 2014). Similar to green algae, plants like *Arabidopsis* also accumulate triacylglycerides, i.e. storage lipids, during P-limitation (Pant, Burgos & Scheible, personal communication). Furthermore, reduction of photosynthesis (Fredeen *et al*., 1989; Wissuwa *et al*., 2005) and protein synthesis (Israel *et al*., 1990; Morcuende *et al*., 2007) and reduced levels of many phosphorylated metabolites were reported in Pi-limited plants, while secondary metabolites, including glucosinolates and phenylpropanoids (anthocyanin) may increase (Pant *et al*., 2014). In general, the effect of P-limitation on the plant metabolome is quite pronounced.

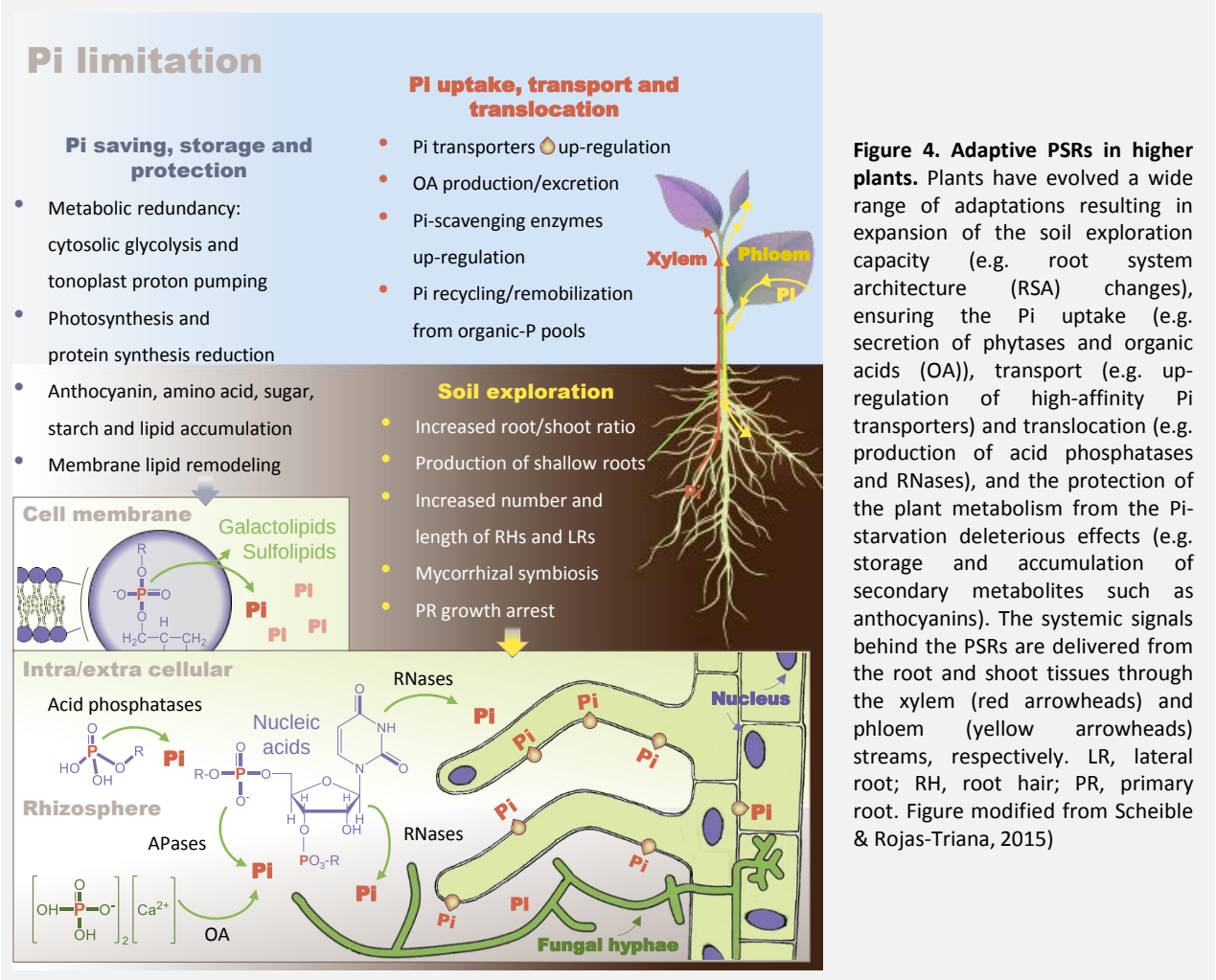

Figure 4. Adaptive PSRs in higher plants. Plants have evolved a wide range of adaptations resulting in expansion of the soil exploration capacity (e.g. root system architecture (RSA) changes), ensuring the Pi uptake (e.g. secretion of phytases and organic acids (OA)), transport (e.g. up-regulation of high-affinity Pi transporters) and translocation (e.g. production of acid phosphatases and RNases), and the protection of the plant metabolism from the Pi-starvation deleterious effects (e.g. storage and accumulation of secondary metabolites such as anthocyanins). The systemic signals behind the PSRs are delivered from the root and shoot tissues through the xylem (red arrowheads) and phloem (yellow arrowheads) streams, respectively. LR, lateral root; RH, root hair; PR, primary root. Figure modified from Scheible & Rojas-Triana, 2015)

At the gene level plants respond to Pi-limitation by major changes in gene expression. Hundreds to thousands gene transcripts are induced or repressed in response to Pi-limitation in a spatial and temporal manner

(see 3.2.2.1. Transcriptional control of Pi-starvation responses; Misson *et al*., 2005; Morcuende *et al*., 2007; Secco *et al*., 2013)

3.2.1.1. The phenylpropanoid pathway

A severe drop in intracellular Pi levels provokes harmful effects, such as a reduction in photosynthetic capacity (e.g. photoinhibition), that can be alleviated by increased biosynthesis of anthocyanins and other photoprotective pigments (Takahashi *et al*., 1991; Trull *et al*., 1997; Nilsson *et al*., 2007) (Figure 5).

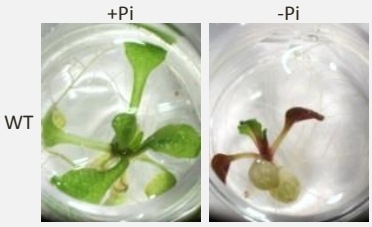

Figure 5. Anthocyanin accumulation in response to Pi starvation. *Arabidopsis* seedlings accumulate anthocyanins in the shoot, in response to Pi starvation, which protect the plant from the deleterious effects caused by –Pi-derived photoinhibition.

Anthocyanins are water-soluble vacuolar flavonoids, synthesized via the phenylpropanoid pathway, in which the essential aa L-phenylalanine (L-Phe) is converted into various aromatic compounds, together called (poly) phenolics (often known as phenylpropanoids). In plants, they are being categorized into benenoids, coumarins, flavonoids, stilbenes, hydroxycinnamates, lignans, and the macromolecule lignin, that all together sum up to more than 800 aromatic metabolites (Vogt, 2010; Fraser & Chapple, 2011).

The general phenylpropanoid pathway is originally connected to the aromatic amino acids production from the central carbon metabolism, which takes place in the so called shikimate pathway (Figure 6-A). The L-Phe from the primary metabolic pool, is used to synthetized trans-cinnamic acid (*t*-CA), by the entry-point enzyme of the phenylpropanoid pathway, Phenylalanine ammonia-lyase (PAL). PAL catalyzes the non-oxidative elimination of ammonia from L-Phe to yield *t*-CA (Cochrane *et al*., 2004) (Figure 6-B). The *t*-CA produced by PAL, is further transformed into several phenylpropanoids (Bate *et al*., 1994; Cochrane *et al*., 2004) (Figure 6-A). In plants, PAL acts as a 275-330kDa enzyme, with multiple tetrameric forms that indicates PAL ability to form heterotetramers (Havir & Hanson, 1973; Zimmermann & Hahlbrock, 1975; Appert *et al*., 1994; Bolwell *et al*., 1985). The three dimensional reconstructions of PAL, shows PAL as a helix-containing protein with a mobile N-terminal extension and a specific shielding domain sited over the active center (Calabrese *et a*l., 2004; Ritter & Schulz, 2004). PAL proteins are encoded by a multi-gene family, fluctuating from four members described in *Arabidopsis* (*PAL1-PAL4*), to more than a dozen in potato and tomato (Chang *et al*., 2008). *PAL* have long been known to be regulated in response to environmental stresses and to developmental cues (Dixon and Paiva, 1995; Anterola *et al*., 2002; Pawlak-Sprada *et al*., 2011). PAL differentially respond to environmental stresses and *PAL* genes have functional specialization in environmentally caused phenolic synthesis. For example, nitrogen (N) limitation particularly

induces *PAL1-2* expression, and together with the presumable induction of the downstream phenylpropanoid–flavonoid biosynthetic genes, it increases the accumulation of anthocyanins, flavonoids (kaempferol and quercetin), and sinapic acid (Olsen *et al*., 2008).

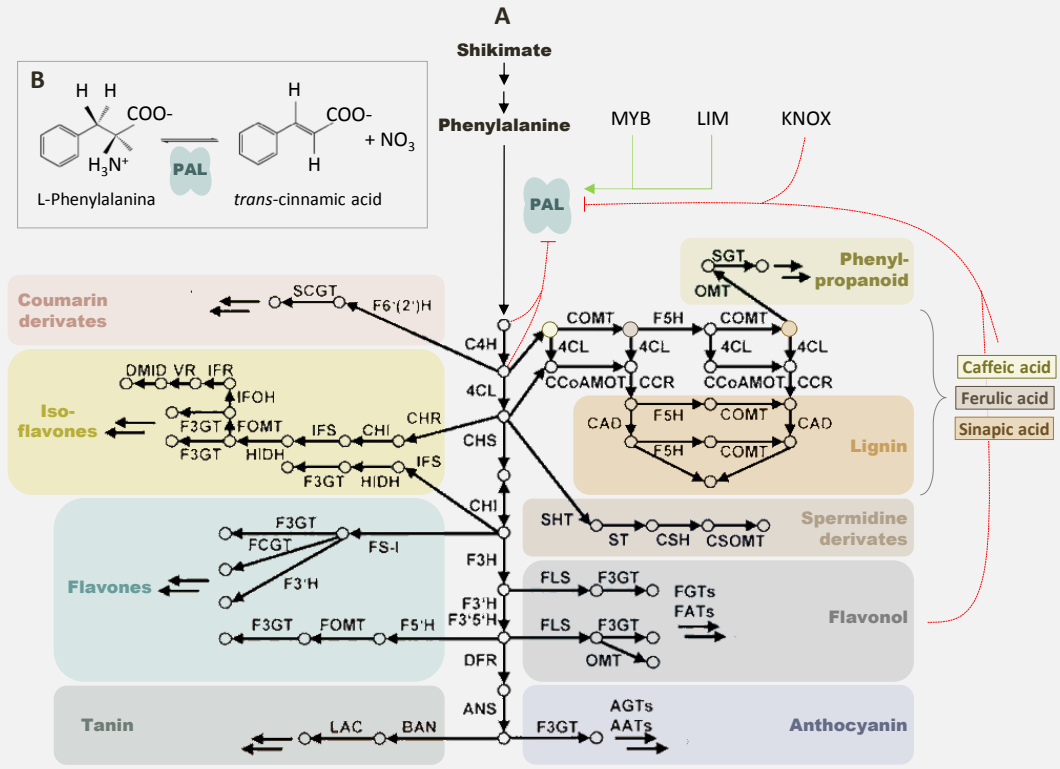

Figure 6. The phenylalanine derived secondary metabolite biosynthesis in plants. (A) Deamination of L-phenylalanine (L-Phe) by L-phenylalanine ammonia-lyase (PAL). **(B)** L-Phe derived major phenolic secondary mebolite biosynthesis in plants. Arrow indicates enzymatic reaction, circle indicates metabolite. Ferulic acid and sinapic acid are highlighted, as well as the precursor caffeic acid. Figure modified from Tohge *et al*., 2013 and Zhang *et al*., 2015. Abbreviations:

C4H, cinnamate-4-hydroxylase;
4CL, 4-coumarate CoA ligase;
CAD, cinnamoyl-alcohol dehydrogenase;
F5H, ferulate 5-hydroxylase;
C3H, coumarate 3-hydroxylase;
ALDH, aldehyde dehydrogenase;
CCR, cinnamoyl-CoA reductase;
HCT, hydroxycinnamoyl-Coenzyme A shikimate/quinate hydroxycinnamoyltransferase;
CCoAOMT, caffeoyl/CoA-3-O-metheltransferase;
COMT, caffeic acid 3-O-methyltransferase;
CHS, chalcone synthese;
CHI, chalcone isomerase;
F3H, flavanone 3-hydroxylase;
F30H, flavonoid-30-hydroxylase;
F3GT, flavonoid-3-O-glycosyltransferase;
FS, flavone synthase;
FOMT, flavonoid O-methyltransferase;
FCGT, flavone-C-glycosyltransferase;
FLS, flavonol synthese;
F3GT, flavonoid-3-O-glycosyltransferase;
DFR, dihydroflavonol reductase;
ANS, Anthocyanidin synthese;
AGT, Flavonoid-O-glycosyltransferase;
AAT, anthocyanin acyltransferase;
BAN, oxidoreductase|dihydroflavonol reductase like;
LAC, laccase

PAL promoter regions typically contain multiple cis-regulatory elements, in particular MYB TFs binding sites like the AC-rich motifs (AC-I, ACCTACC; AC-II, ACCAACC; and AC-III, ACCTAAC) (Yang *et al*., 2001; Rohde *et al*.,

2004). MYB R2R3 TFs like AmMYB305 (from *Antirrhinum majus*) and NtMYBAS1/2 (from *Nicotiana tabacum*) are known to control PAL expression in a tissue specific manner (Martin & Paz-Ares, 1997; Sablowski *et al*., 1994; Yang *et al*., 2001). Moreover, in *Arabidopsis* is been documented that MYB58, MYB63 and MYB85 are specifically involved in regulating lignin biosynthesis (Zhou *et al*., 2009), however wether these TFs can directly target *PAL* expression is still unknown.

In addition to the MYB TFs, KNOX family of TFs, which function in maintaining cells in an indeterminate state (Tsiantis, 2001), also affect PAL expression. Mutations in the KNOX gene BREVIPEDICELLUS (BP) upregulate the expression of *Arabidopsis* PAL1 and other enzymes from the phenylpropanoid pathway, and cause premature lignification of the vasculature (Mele *et al*., 2003), suggesting a negative regultation of PAL expression driven by KNOX. Furthermore, LIM domain-containing proteins bind the AC-rich motif and positively regulate PAL gene expression (Kawaoka *et al*., 2000; Kawaoka & Ebinuma, 2001).

Separately from transcriptional regulation, PAL and phenylpropanoid biosynthetic activity seem to be regulated by particular biosynthetic intermediates (Figure 6-A), indicating a metabolite feedback regulation (for review see Zhang *et al*., 2015). The feedback regulation is not only triggered by the immediate product of PAL, *t*-CA (Lamb, 1979; Bolwell *et al*., 1986; see Figure 6-B), but also by intermediates from branch pathways. Some known molecular regulators are: trans-cinnamate (Blount *et al*., 2000), caffeic acid (in *Glycine max*) (Bubna *et al*., 2011), flavonols (Yin *et al*., 2012), etc. (Figure 6-A).

In summary, the regulation of the phenylpropanoid pathway, and in particular of PAL, seem to be driven by multifaceted regulatory mechanisms, namely, transcriptional regulation, product inhibition, metabolite feedback regulation, among others (Zhang *et al*., 2015). This noticeable complexity, responds to the wide range of physiological functions dependent on the aromatic compounds, which are essential for development, growth and response to biotic and abiotic stimuli. For instance, soluble phenolics act as anti-pathogenic phytoalexins, antioxidants, or UV absorbing compounds (Dixon and Paiva, 1995). Moreover, lignin is a structural constituent placed in the vasculature, and gives mechanical support and produces a hydrophobic environment that is important for transporting water and nutrients in plants (Whetten & Sederoff, 1995; Vanholme *et al*., 2010).

3.2.2. Regulation of the phosphate starvation response in plants

To coordinate all of the PSRs, plants require a Pi-monitoring system that involves the perception and integration of information on local and whole-plant Pi (reviewed in Franco-Zorrilla *et al*., 2004; Ticconi & Abel 2004: Doerner, 2008; Rouached *et al*., 2010; Vance, 2010; Yang & Finnegan, 2010; Chiou & Lin, 2011). Although the

nature of Pi sensor(s) is unknown, many components of the Pi-starvation signaling pathway have been identified during the last decade. These regulatory components act at the transcriptional or posttranscriptional level to maintain plant Pi homeostasis and adequate responses to low Pi stress conditions (Figure 7).

3.2.2.1. Transcriptional control of Pi-starvation responses

Transcriptional control of the so-called Pi-starvation responsive genes (PSR genes) greatly underlies the adaptive response program of plants to Pi-deficiency. According to this idea, early studies showed that expression of many genes involved in the control of the Pi starvation rescue system increases under Pi-deficient conditions (reviewed in Franco-Zorrilla *et al*., 2004). Among these are genes involved in Pi transport, breakdown of Pi-containing molecules (e.g. nucleases, ribonucleases, phosphoesterases, phosphatases), photosynthesis, respiration, aa and lipid metabolism, as well as regulatory genes involved in signaling events, including genes encoding transcriptional regulators (TRs), microRNAs (miRs), components of the UPS for targeted protein degradation, genes involved in growth and development and genes of yet unknown function.

Subsequent expression profiling studies have further supported the complexity of the transcriptional control network underlying PSRs, which may be composed of at least two or more transcriptional programs, that responds to the gradual development of Pi-starvation upon Pi withdrawal (i.e. early and late PSRs; Hammond *et al*., 2003; Wu *et al*., 2003). Early responsive genes include many related to signal transduction events (e.g. TRs, miRs, MAP kinases, protein kinases), general stress-related genes (e.g. cytochrome P450s, glutathione S-transferase), genes encoding Pi transporters, SPX-domain proteins, acid phosphatases and ribonucleases, and even cell wall-related genes. Late responsive genes are rather related to primary carbon metabolism, secondary metabolism, photosynthesis, protein synthesis or hormone synthesis/signaling. These studies have also shown that the over-all change in gene expression is conserved between distant higher plants, such as rice and *Arabidopsis* (Wasaki *et al*., 2003). In this regard, genome-wide transcriptional analyses have been used for monitoring the short-, medium- and long-term transcriptional responses of plants (mainly *Arabidopsis*) to Pi starvation, and the Pi-specificity of the corresponding transcriptional changes, using different Pi re-supply experimental designs (Misson *et al*., 2005; Morcuende *et al*., 2007; Muller *et al*., 2007 ; Lan *et al*., 2012). Additionally, distinction among groups of genes that are controlled by Pi deprivation either locally or systemically (i.e. long-distance responsive genes) was observed by means of “split root” techniques and transcriptomic assays (Thibaud *et al*., 2010). Recently, Bustos *et al*. (2010) contributed to the overall panorama by performing an organ (roots and shoots)- specific transcriptomic analysis under long-term Pi-deficiency conditions in *Arabidopsis* wild-type (WT) and in *phr1* and *phr1/phl1* mutants. These analyses elucidated the central role of the PHR1 TF and its (partially)

functionally redundant homolog PHL1 in the control of transcriptional activation and repression of the PSRs in *Arabidopsis*.

The MYB-type TFs PHR1 and PHL1, together with their homolog proteins in rice (OsPHR2) and wild bean (*Phaseolus*; Fabaceae; PvPHR1) belong to the MYB-Coiled Coil (MYBCC) family of TFs (Wykoff *et al*., 1999; Rubio *et al*., 2001; Valdes-López *et al*., 2008; Zhou *et al*., 2008; Bustos *et al*., 2010), and are arguably the most influential TR of PSRs described in plants so far (Rubio *et al*., 2001) (Figure 7). PHR1 expression is constitutive, i.e. unaffected by Pi-status, but post-translational regulation through the SUMO E3 ligase SIZ1 probably modulates its activity in response to Pi-limitation (Miura *et al*., 2005; see 3.2.2.2.1. Sumoylation).

PHR1 was identified in a screen for mutants displaying altered PSRs. Thus, *phr1* mutants grown in low Pi conditions showed reduced expression of PSR genes, decreased accumulation of anthocyanins, and a reduced root/shoot ratio relative to WT plants. In addition, *phr1* mutants displayed lower levels of Pi content in shoots under all Pi regimens (Rubio *et al*., 2001). Bustos *et al*. (2010) showed that these defects are enhanced in *phr1/phl1* double mutants, where up to 80% and 60% of the Pi starvation-inducible genes in shoots and roots, respectively, display lower levels of expression compared to WT plants under –Pi conditions. Such major control in gene expression activation is in part exerted directly, as indicated by the fact that promoters of Pi starvation-induced genes are enriched in PHR1-binding sequences (P1BS), and by induction of PSR genes upon activation of a PHR1:GR fusion protein upon treatment with dexamethasone, even when protein translation is inhibited with cycloheximide (Bustos *et al*., 2010). Interestingly, PHR1/PHL1 direct targets include the majority of the genes that are systemically controlled by low Pi, as was shown by Thibaud *et al*., (2010). Moreover, PHR1 overexpression was reported to enhance phosphate uptake in *Arabidopsi*s (Nilsson *et al*., 2007) probably due to increased expression of *miR399* and reduced PHOSPHATE2 (PHO2) activity (see 3.2.2.2.3. miRNA-mediated long-distance Pi signaling and target mimicry and 3.2.2.2.4.4. Ubiquitination pathway components controlling Pi homeostasis), and similar results were also obtained in rice (Zhou *et al*., 2008). Overexpression of PHR1 in wheat also resulted in the up-regulation of a subset of PSI genes, improved Pi uptake and promoted wheat growth and grain yield (Wang *et al*., 2013a). Targeting *PHR1* thus appears as a useful approach for molecular breeding of plants with more efficient Pi uptake/assimilation and increased yield. More recent results also established that *AtPHR*1 exerts major control over the P-starvation metabolome (Pant *et al*., 2014) and lipid remodeling, i.e. degradation of phospholipids and synthesis of glyco-/sulfolipids, during P-limitation (Pant, Burgos and Scheible, personal communication).

Additional proteins belonging to different TF families also act as regulators of PSR gene expression, although to a lesser extent than PHR1/PHL1 family members (Figure 7) (recently reviewed in Scheible & Rojas-Triana, 2015). Further TRs known to affect PSR are: AtWRKY75 (Devaiah *et al*., 2007a; Rishmawi *et al*., 2014),

AtWRKY6 and AtWRKY42 (Chen *et al*., 2009), AtWRKY45 (Wang *et al*., 2014b), BHLH32 (Chen *et al*., 2007), ZAT6 (Devaiah *et al*., 2007b), AtMYB62 (Devaiah *et al*., 2009), AtMYB2 (Baek *et al*., 2013), AtHRS1 (Liu *et al*., 2009), OsARF16 (Shen *et al*., 2013), OsARF12 (Wang *et al*., 2014), OsPTF1 (Yi *et al*., 2005), OsMYB2P-1 (Dai *et al*., 2012).

Chromatin remodeling is another scenario that appears to be important during Pi-starvation signaling, via transcriptional regulation (reviewed in Scheible & Rojas-Triana, 2015). Some examples are: ARP6 (Smith *et al*., 2009), NAP1;2 (Iglesias *et al*., 2013) and AL6 (Chandrika *et al*., 2013).

Several proteomic studies performed in different plant species indicate that there is a high correlation between transcriptional changes that occur in response to Pi deprivation, and variations in the abundance of the corresponding proteins (Li *et al*., 2007; Tran & Plaxton, 2008; Chevalier & Rossignol, 2011; Lan *et al*., 2012; Iglesias *et al*., 2013). Such correlation is more evident in the case of genes that are highly upregulated in response to low Pi. However, in a significant number of cases, protein levels did not match gene expression variation, especially in the case of proteins whose abundance is reduced under Pi deprivation (Lan *et al*., 2012). These discordances between mRNA and protein levels highlight the relevance of post-transcriptional regulation during Pi starvation stress adaptation.

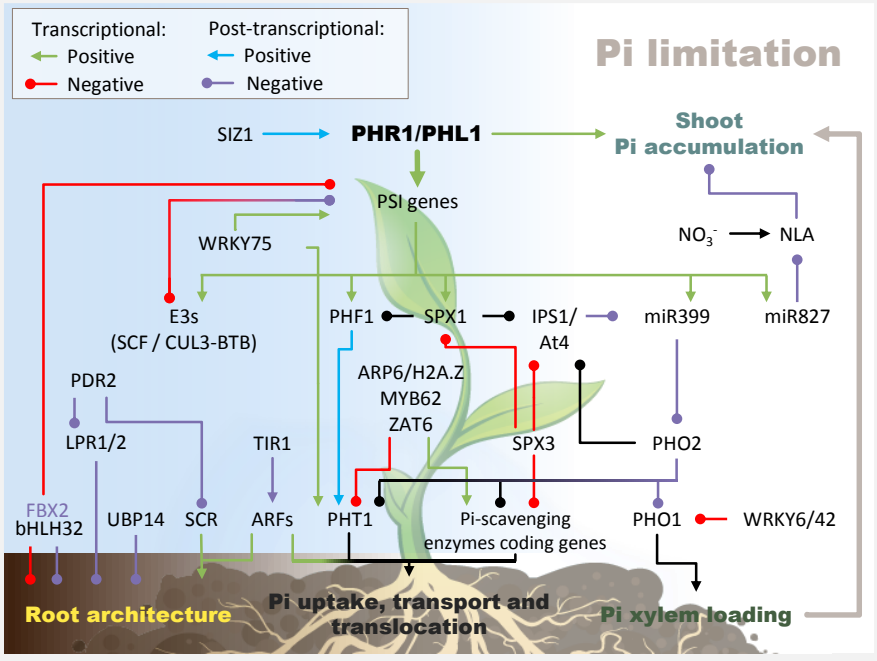

Figure 7. Regulatory elements relevant to PSR. Typical PSRs are controlled transcriptionally and post-transcriptionally by an increasingly complex network of local/systemic signals and effectors. The MYB-type TFs PHR1/PHL1 are master regulators controlling most of the PSI-gene transcripts. Post-transcriptional mechanisms like microRNA silencing (e.g. miRNA399), target mimicry (e.g. IPS/At4), ubiquitination (e.g. PHO2), sumoylation (e.g. SIZ1), and trafficking of Pi transporters (e.g. PHF1) complement the molecular mechanisms controlling the Pi homeostasis during Pi-starvation. The color code of the lines and the lines endings (arrowheads or dots) indicates the level of regulation (transcriptional or post-transcriptional) and the effect (positive or negative). Black lines represent unknown levels of regulation. Figure modified from Scheible & Rojas-Triana, 2015.

3.2.2.2. Post-transcriptional control of phosphate starvation responses

Different posttranscriptional mechanisms, together with ubiquitination (the main focus of this section; see 3.2.2.2.4. Ubiquitin-mediated modulation of Pi-starvation responses), affect Pi uptake and long-distance Pi signaling, and modulate Pi starvation responses (Figure 7). Further details on the molecular basis of these mechanisms are provided by several excellent reviews (Doerner, 2008; Rouached *et al*., 2010; Yang & Finnegan, 2010; Chiou & Lin, 2011; Peret *et al*., 2011).

3.2.2.2.1. Sumoylation

Similarly to ubiquitin, small ubiquitin-like modifier (SUMO) peptide is attached to protein targets by a specific enzymatic cascade. Modification of proteins with SUMO rarely triggers their degradation through the 26S proteasome, but alters protein activity, localization or interaction abilities (Ulrich, 2005). In plants, sumoylation has been involved in the control of developmental processes, such as flowering control, and responses to different stresses, including cold, drought, pathogen attack and Pi starvation. Most of these regulatory effects of sumoylation have been obtained from the characterization of mutants in E3 SUMO-ligase SIZ1 (review by Miura & Hasegawa, 2010). Among other pleitropic phenotypes, *Arabidopsis siz1* mutants displayed enhanced local and systemic Pi starvation responses, such as reduced growth of the primary root, increased lateral root proliferation, and higher accumulation of anthocyanins. *siz1* mutants also displayed upregulation of a subset of PSR genes under Pi-sufficient conditions (Miura *et al*., 2005). Interestingly, SIZ1 was able to sumoylate PHR1 *in vitro*. Substantiating this result, PHR1 was isolated together with SUMO-protein conjugates purified from *Arabidopsis* (Miller *et al*., 2010). SIZ1-mediated sumoylation of PHR1 may account for many Pi-related phenotypes found in *siz1* mutants. However, it has recently been shown that SIZ1 negatively regulates root architecture responses to Pi limitation by controlling auxin regulated gene expression and auxin patterning (Miura *et al*., 2011). These results indicate that SIZ1 may target additional yet-unknown proteins within the auxin-signaling pathway to control specific Pi starvation responses.

3.2.2.2.2. Pi transporter phosphorylation and trafficking

Certain Pi starvation responses are shared between organisms that rely on Pi availability in the external media (e.g., bacteria, fungi and plants), including increased expression and accumulation of high-affinity Pi transporters, aimed at facilitating Pi uptake into cells (Raghothama, 1999). In plants, accumulation of high-affinity Pi transporters (PHT1 family members) at the plasma membrane (PM) is subject to tight regulation. Thus, upon Pi deprivation, expression of PHT1 genes is upregulated, and newly-synthesized PHT1 proteins are sorted from the endoplasmic reticulum (ER) to the PM into COPII coated secretory vesicles (Bayle *et al*. 2011). Proper ER-to PM trafficking of PHT1 proteins requires the function of PHOSPHATE TRAFFIC FACILITATOR 1 (PHF1), an ER-localized

protein structurally related to SEC12 proteins, and is modulated by phosphorylation of specific residues at the C-terminal end of PHT1 proteins. PHF1 is apparently not necessarily used for COPII vesicle recruitment, but instead it may act as a packaging chaperone of incorrectly-folded PHT1 proteins (Gonzalez *et al*. 2005; Bayle *et al*. 2011). Once at the PM, adequate PHT1 protein levels are maintained according to the Pi requirement of cells. Thus, under Pi-sufficient conditions, excess PHT1 proteins that are no longer necessary are removed from the PM by internalization into endosomes, and subsequent sorting and degradation into the vacuole. Under Pi-limiting conditions, PHT1 proteins are also subjected to endocytosis, although they are mainly redirected to the PM by endosome recycling processes, therefore allowing sustained Pi uptake rates.

3.2.2.2.3. miRNA-mediated long-distance Pi signaling and target mimicry

Pi homeostasis requires long-distance signaling mechanisms that allow integration of Pi status at different plant organ levels (reviewed in Doerner, 2008; Chiou and Lin, 2011). The nature of the signaling molecule(s) has been the focus of intense debate in the field. Recent studies have proposed that specific miRNAs (i.e., miR399 family members) can have this function based on key features of these molecules. Thus, *miR399* genes are highly responsive to Pi starvation, their products can move from the shoot to the root through the phloem, and, moreover, they recognize as targets the transcripts of *PHO2*, a gene encoding a putative E2/E3 ubiquitin ligase that acts as a negative regulator of shoot Pi accumulation (Fujii *et al*., 2005; Aung *et al*., 2006; Bari *et al*., 2006; Chiou *et al*., 2006; Lin *et al*., 2008; Pant *et al*., 2008). Therefore, the proposed model is that, upon Pi deprivation, intracellular Pi levels will drop in the aerial part, triggering *miR399* expression and transport to the root where they recognize specific target sites on the 5'UTR of *PHO2* mRNA to promote its degradation through the RNAinduced silencing complex. As a result of PHO2 degradation, there is an increase in both Pi transport into root cells and Pi loading into the xylem that aims to normalize Pi levels in the shoot. Additional studies added a new level of complexity to this regulatory mechanism by identifying non-coding RNAs that mimic miR399's targets (Franco-Zorrilla *et al*., 2007). In this regard, it was found that the products of the *At4/IPS1* gene family (conserved in different eudicots, such as rice, tomato, *Medicago* and *Arabidopsis*) show partial complementarity to miR399. Thus, *At4/IPS1* members share a 23-nt region that is complementary to the *miR399* sequence, with the exception of a 2- or 3-nt mismatch in the predicted miRNA cleavage site. In this way, *At4/IPS1* RNA molecules are able to compete with *PHO2* transcripts for binding *miR399*. Importantly, imperfect pairing between *At4/IPS1* and *miR399* molecules prevents cleavage of *At4/IPS1*, resulting in *miR399* sequestration and leading to stabilization of *PHO2* transcripts (Franco-Zorrilla *et al*., 2007). Interestingly, *At4/IPS1* and *miR399* gene expression is induced by PHR1 under low Pi conditions. It has been suggested that *At4/IPS* genes may act as a negative feedback regulatory loop that limits miR399 function under fluctuating Pi supply conditions. The regulatory mechanism mediated by *At4/IPS1* genes was termed "target mimicry", and since its identification in the context of Pi signaling in plants, it

has also been found in animals, where it provides a framework for a dialogue among RNAs sharing the same miRNA binding sites (Rubio-Somoza *et al*., 2011).

3.2.2.2.4. Ubiquitin-mediated modulation of Pi starvation responses

Several reports have demonstrated that specific enzymes mediating Ub conjugation or deconjugation are involved in the control of adaptive responses to Pi starvation in plants (Figure 7; reviewed in Rojas-Triana *et al*., 2013). Below, we describe the best-known examples.

3.2.2.2.4.1. E3 Ub ligases as negative regulators of Pi responses

FBX2, a protein that contains both WD40 and F-box domains, was identified as a negative regulator of molecular, developmental, physiological and metabolic responses to Pi starvation in Arabidopsis (Chen *et al*., 2008). Indeed, a T-DNA insertion mutant in the corresponding gene, *fbx2*, displayed constitutive low Pi responses, such as higher levels of Phosphoenolpyruvate Carboxylase Kinase 1 (PPCK1) transcripts, a higher number of root hairs, and increased contents of intracellular Pi and anthocyanins under Pi-sufficient conditions (Chen *et al,*. 2008). According to microarray data, *FBX2* gene expression is not responsive to differences in Pi supply, which indicates that FBX2 function is controlled post-transcriptionally by a yet-unknown mechanism (Bustos *et al*., 2010). The molecular mechanism by which FBX2 modulates PSR is not clear either, since the identity of its potential ubiquitination substrates is unknown. Although PHR1 might be an ideal target candidate due to its central role in the control of PSR, no evidence for direct interaction between FBX2 and PHR1 was found (Chen *et al*., 2008). Another TF, bHLH32, was found to strongly interact with FBX2 *in vitro*. However, it is unlikely that bHLH32 is targeted by FBX2 activity, since both proteins act as negative regulators of similar PSRs, as observed in the analysis of *fbx2* and *bhlh32* mutants (Schiefelbein, 2003; Zhang *et al*., 2003; Chen *et al*., 2007, 2008). It has been proposed that FBX2 acts as part of an SCF E3 complex that recruits target proteins for ubiquitination through its interaction with bHLH32 (Figure 7). The identification of the targets recognized by FBX2 will likely unveil novel regulatory elements within the Pi starvation-signaling pathway.

3.2.2.2.4.2. Crosstalk between auxin and Pi starvation signaling

Another F-box protein, Transport Inhibitor Response 1 (TIR1), also controls (to some extent) plant growth and developmental responses to Pi starvation. TIR1 acts as an auxin receptor that triggers ubiquitination of AUXIN/INDOLE-3-ACETIC ACID (AUX/IAA) proteins, and further degradation by the 26S proteosome (Gray *et al*., 2001; Dharmasiri *et al*., 2005; Kepinski & Leyser, 2005). Removal of AUX/IAA proteins releases Auxin Response Factor (ARF) TFs that regulate expression of auxin-responsive genes (Tiwari *et al*., 2001). Interestingly, Perez-Torres *et al*. (2008) reported that, contrary to WT seedlings, *tir1–1* mutants failed to enhance lateral root production in response to Pi starvation, indicating that SCF^{TIR1}-mediated auxin signaling is required for root architecture

modification in response to low Pi availability. Additional data showed that changes in Pi availability do not cause differences in free IAA concentration in either the roots or shoots of WT seedlings (Jain *et al*., 2007; Perez-Torres *et al*., 2008). Indeed, it was found that the increase in the formation and emergence of lateral roots under Pi starvation conditions is due to an enhancement in auxin sensitivity as a consequence of increased expression of TIR1 in Pi-deprived plants (Perez-Torres *et al*., 2008). Therefore, upon Pi deprivation, accumulation of TIR1 would enhance degradation of AUX/IAA proteins, liberating ARF transcription factors and modulating the expression of genes involved in lateral root formation.

3.2.2.2.4.3. Ub deconjugases

The previous examples demonstrate that enzymes mediating Ub conjugation to protein targets play important roles in the control of Pi starvation responses. Likewise, deconjugation of Ub from targets should affect plant adaptation to Pi deprivation. This is the case of Ubiquitin-specific Protease 14 (UBP14), a Ub deconjugase (or deubiquitinase) that is required for regulation of Pi homeostasis at the posttranslational level, and which affects the root hair developmental program in response to Pi availability (Li *et al*., 2010). UBP14 had been previously described as being essential for the optimal functioning of the UPS pathway during the early stages of plant development, through its roles in Ub recycling and in the maintenance of an adequate balance between free Ub molecules and poly-ubiquitin chains (Doelling *et al*., 2001). In fact, in the absence of UBP14, the embryos reach the globular stage, but are unable to produce viable seeds as a consequence of a limited number of cell divisions before the embryo arrest, resulting in an embryo-lethal phenotype (Doelling *et al*., 2001).

By means of a screen of an ethyl methanesulfonate (EMS)-mutagenized *Arabidopsis* population, Li *et al*. (2010) isolated *per1* (*PI DEFICIENT ROOT HAIR DEFECTIVE1*), a weak mutant allele of *UBP14*, which allowed further functional characterization of this gene. *per1* plants displayed Pi-specific defects in root hair elongation under Pi starvation conditions, and a battery of phenotypes that resembled Pi-deficient plants under Pi-rich conditions. These results suggest that an adequate balance between Ub monomers and Ub chains is necessary for sustaining proper root responses to Pi deprivation (Li *et al*. 2010).

3.2.2.2.4.4. Ubiquitination pathway components controlling Pi homeostasis

As mentioned before, PHO2 protein acts as a negative regulator of Pi starvation responses by controlling Pi transport from roots and Pi allocation in shoots (Fujii *et al*. 2005; Bari *et al*. 2006). Thus, *pho2* mutants accumulate excessive Pi in shoots (from 3- to 6-times the level in WT plants), which may cause toxic effects and leaf senescence (Delhaize & Randall 1995; Dong *et al*., 1998).

PHO2, also known as UBC24, belongs to an atypical E2 Ub conjugase family that includes four members in *Arabidopsis* (UBC23–26; Bachmair *et al*., 2001; Kraft *et al*., 2005). UBC family members display sequence similarity

to mammalian UBE2O (E2–230K) and BIRC6 (Apollon), two E2 enzymes that do not interact with E3 Ub ligases, but rather contain a chimeric E2/E3 domain that may allow them to directly target specific proteins for ubiquitination (Berleth & Pickart, 1996; Hauser *et al*., 1998; Bartke *et al*., 2004; Hao *et al*., 2004). Both BIRC6 and UBE2O may have similar cellular localization, since BIRC6 localizes in the Golgi and Trans-Golgi network and in small vesicles, and UBE2O interacts with proteins associated with the endomembrane system, such as copine (Hauser *et al*., 1998; Tomsig *et al*., 2003). Interestingly, it has recently been shown that PHO2 also colocalizes with endomembrane compartments, where it may trigger ubiquitination and degradation of specific substrates involved in Pi transport to the shoot (Liu *et al*., 2012).

Increased PSI gene transcripts in Pi-replete *pho2* mutants suggest that PHO2/UBC24 acts via an intermediate target. While a transcriptional regulator would be an obvious candidate given the up-regulation of a considerable number of PSI genes in *pho2* mutants, the first PHO2-target identified through a genetic suppressor screen and biochemical experiments was PHO1 (Liu *et al*., 2012), a transmembrane protein involved in the loading of Pi into the xylem (Hamburger *et al*., 2002) (Figure 7). Thus, it was found that mutations in *PHO1* are able to rescue *pho2* Pi levels to normal conditions (Poirier *et al*., 1991; Arpat *et al*., 2012; Liu *et al*., 2012). Interestingly, both *PHO2* and *PHO1* are expressed in vascular cells, where they colocalize at the endomembrane system (Hamburger *et al*., 2002; Arpat *et al*., 2012; Liu *et al*., 2012). Additional analyses demonstrated that PHO2 and PHO1 physically interact, and, moreover, that PHO2 is able to trigger degradation of PHO1 in transient expression assays in *N. benthamiana* leaves, although in a proteasome independent manner. Further experiments have indicated that PHO1 proteolysis may occur in the vacuole, and is mediated by trafficking into multivesicular bodies (Liu *et al*., 2012). Therefore, PHO2 acts in the root as a negative regulator of Pi transport to the aerial part by promoting degradation of PHO1 under high Pi conditions (when *PHO2* transcripts accumulate; Figure 7). However, whether or not PHO1 is directly ubiquitinated by PHO2 still needs to be demonstrated through further research. Further downstream components of PHO2 identified using proteomics include PHT1-family proteins and PHF1 (Huang *et al*., 2013). PHO2 apparently controls the degradation of several proteins directly or indirectly involved in Pi transport to maintain Pi homeostasis in plants.

Another UPS component, NITROGEN LIMITATION ADAPTATION (NLA), is involved in Pi homeostasis maintenance (Kant *et al*., 2011). NLA contains a RING domain, and has been proposed to act as an E3 Ub ligase. Additionally, it contains an SPX domain, which is present in many proteins involved in Pi sensing, and in transport in yeast and plants (e.g., PHO1 family members; Wang *et al*., 2004; Stefanovic *et al*., 2007). NLA ubiquitination targets have not been identified to date. However, it was found that Pi transporters accumulate in nla mutants, although whether this effect is direct or indirect remains unknown. Lack of *NLA* function causes an increase in Pi

accumulation in shoots, similar to *PHO2* mutation (Kant *et al*., 2011). Interestingly, high accumulation of Pi in these mutants depends on nitrate concentration. Thus, *nla* plants show enhanced Pi levels only under low-nitrate conditions, and *pho2* displays higher increased Pi accumulation under these conditions. On the other hand, it was found that Pi starvation induces high expression of *miR827*, which displays complementarity to *NLA* transcripts and promotes their destabilization, allowing accumulation of PHT1 transporters and increased Pi uptake and transport to the shoot (Kant *et al*., 2011). More recently, NLA was shown to recruit PHO2 and mediate degradation of plasma membrane Pi transporters (Lin *et al*., 2013; Park *et al*., 2014). Further characterization of the mechanisms that involve PHO2 and NLA function will surely shed light on the sophisticated regulatory crosstalk between Pi and nitrate signaling pathways.

3.2.3. The role of phytohormones in Pi homeostasis

Upon sensing of Pi limitation in the root or elsewhere in the plant, signaling pathways/cascades become activated resulting in the generation of local (cell-autonomous) and systemic (long-distance) signals. In multicellular organisms local signaling and long-distance signaling between organs and tissues are needed to adjust and coordinate plant physiology, growth and development of various organs. Besides typical secondary messenger molecules, such as Ca2+, inositol phosphates or reactive oxygen species (Chiou & Lin, 2011), phytohormones have long been discussed as messengers in the context of Pi stress signaling. Pi-deficiency can change the expression of hormone biosynthetic genes, hormone production, sensitivity, signaling and transport (Rubio *et al*., 2009; Chiou & Lin, 2011) to regulate root growth including the inhibition of primary root growth, the promotion of lateral root growth, root hair and cluster root formation (Bates & Lynch, 1996; Williamson *et al*., 2001; López-Bucio *et al*., 2002; Zhang *et al*., 2003; Jain *et al*., 2007). For several phytohormone classes there is convincing evidence for their involvement in the regulation of PSRs (Figure 8), either by acting as local or systemic signaling intermediates.

Ethylene also plays a role in regulating plant responses to Pi starvation. Transcriptome analyses showed that transcript levels of ethylene biosynthesis genes are increased in lupin and *Arabidopsis* under low Pi (Uhde-Stone *et al*., 2003; Morcuende *et al*., 2007; Thibaud *et al*., 2010), and Pi-starved roots of common bean produce twice as much ethylene than Pi-sufficient roots (Borch *et al*., 1999) (Figure 8). In maize, Pi-starvation increases the sensitivity of roots to ethylene (He *et al*., 1992). The role of ethylene in the Pi-starvation-mediated inhibition of primary root growth and the stimulation of root hair formation is well documented (López-Bucio *et al*., 2002; Ma *et al*., 2003; Zhang *et al*., 2003; Kim *et al*., 2008). The *hps2* mutant in Arabidopsis displays enhanced responses to Pi-starvation, such as PSR gene expression, induction of acid phosphatases and anthocyanin production, and harbors a T-DNA insertion in the protein kinase gene CTR1 (Lei *et al*., 2011a), which acts downstream of ethylene

receptors in ethylene signaling. The *hsp3* mutant is an allele of ETO1, a negative regulator of ethylene biosynthesis (Wang *et al*., 2012). *hps3* alleles have altered expression of PSR genes and enhanced production of acid phosphatase under Pi-sufficient and –deficient conditions, but accumulate less anthocyanin than wild type under Pi-starvation. The *hps4* mutant in Arabidopsis also exhibits enhanced responses to Pi starvation, such as inhibition of primary root growth, enhanced expression of PSR genes or overproduction of root-associated acid phosphatases (Yu *et al*., 2012).

Gibberellic acid (GA) has also been implicated in the regulation of PSRs in Arabidopsis (Jiang *et al*., 2007). Exogenous application of GA or mutations in DELLA proteins, which are core-components of GA-signaling, led to repression of several shoot and root PSRs including characteristic changes in root system architecture and anthocyanin accumulation. Pi starvation was also found to promote the accumulation of the DELLA protein RGA (repressor of *ga1-3*) and to cause a decrease of bioactive GA and transcripts encoding enzymes of GA metabolism (Jiang *et al*., 2007) (Figure 8). GA and GA signaling however were not found to be involved in the regulation of Pi uptake efficiency or the expression of PSR gene transcripts. The Pi-starvation induced transcription factor MYB62 in turn affects the expression of several GA biosynthetic genes (Devaiah *et al*., 2009).

Strigolactones (SLs) are a more recently recognized class of carotenoid-derived plant hormones and are now recognized as important local and systemic signals to regulate the acclimation of plants to Pi-starvation. SLs were known for some time to promote hyphal branching and root colonization of arbuscular mycorrhizal fungi (AMF) (Akiyama *et al*., 2005; Besserer *et al*., 2006), a developmental trait intimately connected with Pi-limitation. Using SL-deficient and –insensitive max mutants and the synthetic SL GR24, SLs were also found to suppress lateral shoot branching, regulate root hair elongation, lateral and adventitious root formation or root nodulation (Gomez-Roldan *et al*., 2008; Ruyter-Spira *et al*., 2011; Czarnecki *et al*., 2013). Pi deficiency induces SL biosynthesis in roots of many plant species (Yoneyama *et al*., 2007) and gene transcripts encoding enzymes for SL biosynthesis (Umehara *et al*., 2010). Pi deficiency also stimulates SL exudation from roots (Yoneyama *et al*., 2007; Umehara *et al*., 2010) which is important for beneficial plant-microbe interactions and thus for improving Pi acquisition from soil. Using max mutants and GR24, SLs were implicated in plant perception of or response to low Pi conditions (Ruyter-Spira *et al*., 2011; Mayzlish-Gati *et al*., 2012), including an effect on the expression of PSR genes and the auxin receptor gene TIR1 (Mayzlish-Gati *et al*., 2012) (Figure 8).

Abscisic acid (ABA) might also be involved in some aspects of the PSR. Induction of some PSR gene transcripts was reported to be inhibited by ABA and increased in *aba1-3* mutants (Ribot *et al*., 2008) (Figure 8). Also similarity of growth patterns of P-limited and ABA-treated plants, e.g. increased root-to-shoot ratio, led to the speculation that ABA might be involved in Pi-starvation signaling (Trull *et al*., 1997). However ABA concentration

was not found to be altered in Pi-deficient cotton plants (Radin, 1984), nor were the investigated biochemical and developmental responses to Pi-limitation altered in aba1 or abi2-1 mutants (Trull *et al.*, 1997). Hence in comparison to other phytohormones, ABA appears to play a minor only.

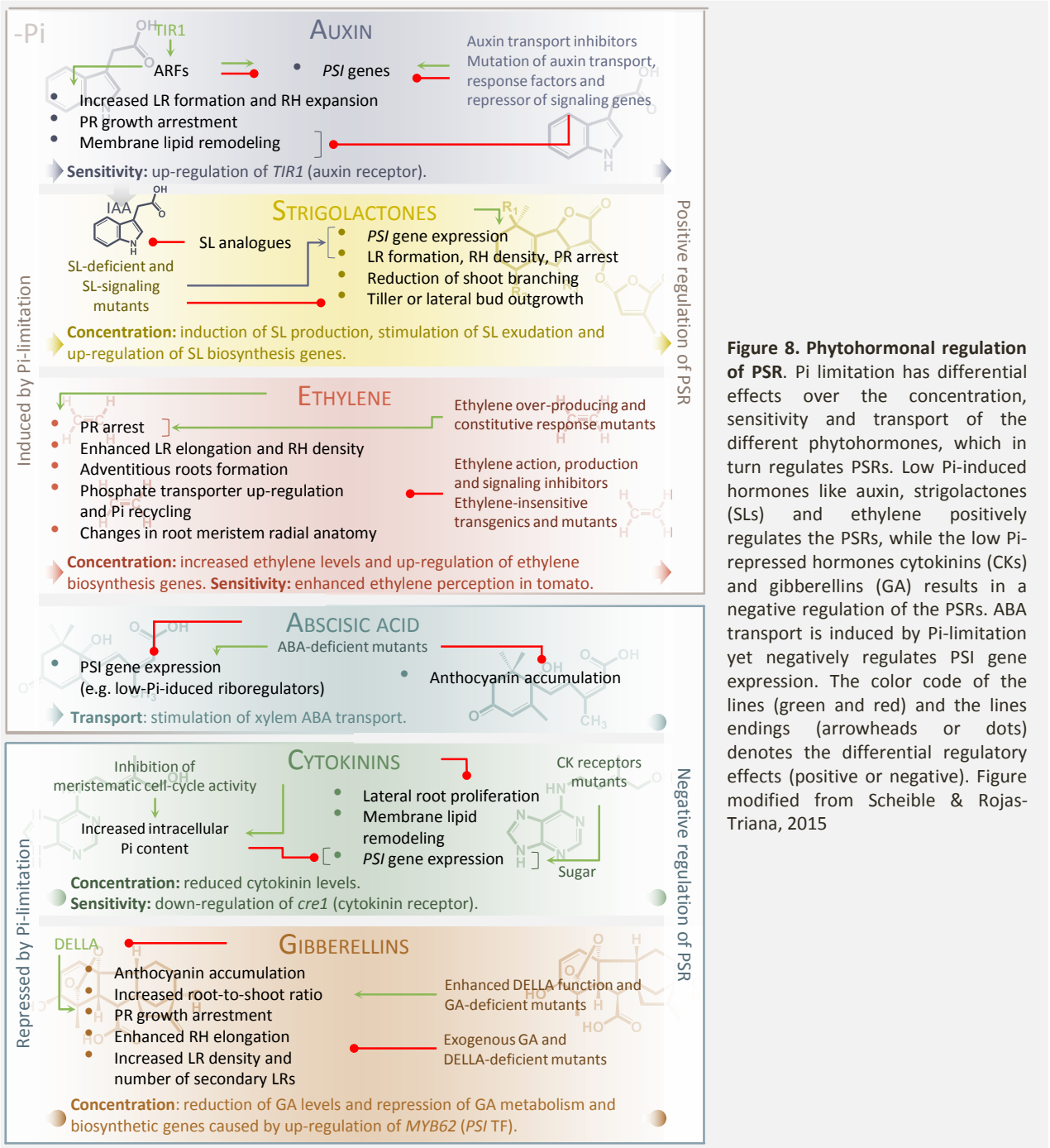

Figure 8. Phytohormonal regulation of PSR. Pi limitation has differential effects over the concentration, sensitivity and transport of the different phytohormones, which in turn regulates PSRs. Low Pi-induced hormones like auxin, strigolactones (SLs) and ethylene positively regulates the PSRs, while the low Pi-repressed hormones cytokinins (CKs) and gibberellins (GA) results in a negative regulation of the PSRs. ABA transport is induced by Pi-limitation yet negatively regulates PSI gene expression. The color code of the lines (green and red) and the lines endings (arrowheads or dots) denotes the differential regulatory effects (positive or negative). Figure modified from Scheible & Rojas-Triana, 2015

Cytokinins (CKs) are usually associated with a stimulation of shoot- but an inhibition of root growth. Decrease in CKs has been associated with P-starvation and N-limitation (Horgan & Wareing, 1980; Kuiper *et al.*,

1988) and lower CK concentrations in roots during P-limitation could alleviate the inhibition of root growth. CK is known to repress the induction of PSI genes in Arabidopsis, whereas the increase in root hair number and length during P-limitation is not dependent on CK (Martín *et al*., 2000; Franco-Zorrilla *et al*., 2005). CK repression of PSI gene expression is dependent on CK receptors CRE1/AHK4 and AHK3 (Franco-Zorrilla *et al*., 2005), and could be due, at least in part, to the release of Pi from internal sources and a concomitant increase in intracellular Pi content that occurs upon treatment with CK in Pi-deprived rice (Wang *et al*., 2006). The observations that CKs affect PSRs that are dependent upon whole-plant Pi status, and do not repress the increase in root hair number and length induced by Pi starvation, a response dependent on local Pi concentration, suggest that CKs act as systemic signals (Martín *et al*., 2000), similar to their function in the control of N assimilation and status in plants (Sakakibara, 2006). Split-root experiments however also demonstrated that the *cre1/ahk3* double mutant is not significantly affected in long-distance systemic repression of PSI gene expression (Franco-Zorrilla *et al*., 2005), suggesting that systemic signaling of P-status involves further signals.

In summary, there is nowadays overwhelming evidence for the involvement of several phytohormones in P-limitation signaling in plants (Figure 8). However, understanding the precise roles of each hormone and their cross-talk at the cellular, tissue or organ level, as well as the relative importance of and interaction with additional local and systemic signals requires more.

OBJECTIVES

4. OBJECTIVES

The characterization of the KMD family and the identification of their target proteins, potentially involved in the regulation of the Pi-starvation signaling, are the main objectives of this research, whose specific objectives are:

1. Identification of E3 ubiquitin ligases that respond transcriptionally to Pi starvation in Arabidopsis.

2. Functional characterization of the E3 ubiquitin ligases family KISS ME DEATHDLY (KMD) in the nutritional signaling in Arabidopsis.

3. Identification and characterization of target proteins of the E3 ubiquitin ligases KMDs.

4. Study of the metabolic implications of the post-traductional reglation of the enzyme PAL, mediated by KMD proteins.

MATERIALS AND METHODS

5. MATERIAL AND METHODS

5.1. BIOLOGICAL MATERIAL

5.1.1. Bacterial strains

- *Agrobacterium tumefaciens* (*A. tumefaciens*) C58C1: (Yanofsky & Nester, 1986).
- *Escherichia coli* (*E. coli*) DH5α: (Woodcock *et al*., 1989).

5.1.2. Yeast strains

- *Saccharomyces cerevisae* (*S. cerevisae*) AH109: (Clontech).
- *Saccharomyces cerevisae* Y187: (Clontech).

5.1.3. Plant material

- *Arabidopsis thaliana* L. (*A. thaliana*) (L. Heynh), ecotype Columbia (Col-0).
- *Nicotiana benthamiana* (*N. benthamiana*).
- *A. thaliana* mutant alleles in Col-0 background (Table 3).

Table 3. *A. thaliana* mutant alleles in Col-0 background.

STABLE LINE	REFERENCE	OBSERVATIONS
pub27/28/29	Rojas-Triana *et al*., 2013	Provided by Prof. Salomé Prat
phr1/phl1	Bustos *et al*., 2011	Provided by Prof. Javier Paz-Ares
cul1-6	Moon *et al*., 2007	Provided by Prof. Mark Estelle
cul3^{hyp}	Thomann *et al*., 2009	Provided by Prof. Pascal Genschik
kmd1	Alonso *et al*. 2003	Salk_129095 obtained from ABRC
kmd2	Alonso *et al*. 2003	Salk_01438 obtained from ABRC
kmd4	Alonso *et al*. 2003	Salk_080250 obtained from ABRC
kmd1/2	Rojas-Triana, unpublished data	Crossed
kmd1/4	Rojas-Triana, unpublished data	Crossed
kmd1/2/4	Rojas-Triana, unpublished data	Crossed

- *Arabidopsis* transgenic lines in Col-0 background (Table 4).

Table 4. *Arabidopsis* transgenic lines in Col-0 background.

STABLE LINE	REFERENCE	CONSTRUCTION
oeKMD1-GFP-45	Rojas-Triana, unpublished data	35S::KMD1-GFP
oeKMD1-GFP-82	Rojas-Triana, unpublished data	35S::KMD1-GFP
oeKMD4-GFP-12	Rojas-Triana, unpublished data	35S::KMD4-GFP
oeKMD4-GFP-15	Rojas-Triana, unpublished data	35S::KMD4-GFP
oeKMD1-MYC-8	Rojas-Triana, unpublished data	35S::KMD1-10xMYC
oeKMD1-MYC-10	Rojas-Triana, unpublished data	35S::KMD1-10xMYC
oePAL2-GFP-32	Rojas-Triana, unpublished data	35S::PAL2-GFP
oePAL2-GFP-42	Rojas-Triana, unpublished data	35S::PAL2-GFP
oePAL2-GFP-32/oeKMD1-MYC-8	Rojas-Triana, unpublished data	Crossed
oePAL2-GFP-32/oeKMD1-MYC-10	Rojas-Triana, unpublished data	Crossed
oePHR1-MYC	Dr. Vicente Rubio	35S::PHR1-10xMYC
oeSPX1-GFP	Dra. Maria Isabel Puga	35S::SPX1-GFP

5.2. CULTURE METHODS

5.2.1. Bacterial culture methods

Lysogeny broth (LB) medium was used for all the bacterial cultures (10 g/L Tryptone, 5g/L yeast extract and 10 g/L NaCl). pH was adjusted to 7.0 with NaOH. 15 g/L bactoagar were added for solid media (Sambrook *et al*., 1989). *E. coli* and *A. tumefaciens* were cultured at 37°C and 28°C respectively with agitation at 250 r.p.m (revolutions per minute). Media were supplemented with the corresponding antibiotics: ampicilin (100 µg/mL), gentamicin (50 µg/mL), hygromycin (40 µg/mL), kanamycin (50 µg/mL), rifampicin (50 µg/mL), spectinomycin (50 µg/mL) and streptomycin (10 µg/mL).

5.2.2. Yeast culture methods

AH109 and Y187 *S. cerevisae* cells were grown in YPAD and YPD media, respectively. Both media have almost the same composition (20 g/L peptone/tryptone, 10 g/L yeast extract, 40% glucose, 40 mg/L adenine only in YPAD medium, pH adjusted to 5.8 with HCl 37 % and 20 g/L bactoagar added only for solid media) (Clontech

Yeast Protocols Handbook). Transformation of pGADT7 and pGBKT7 led to normal growth of AH109/Y187 yeast cells on the selective media SD-WL. Selective medium, SD, contained 6.7 g per liter of yeast nitrogen base without amino acids with a pH of 5.8, adjusted with KOH, and for solid media 20 g/L of bactoagar was added. Drop out (DO) mix (1x) was used as follow:

- SD-WL: Yeast nitrogen base without amino acids supplemented with-Trp/-Leu DO supplement (Clontech, No. 630417).
- SD-WLH: Yeast Nitrogen Base without amino acids supplemented with-Leu/-Trp/-His/ DO supplement (Clontech, No. 630419).
- SD-WLA: Yeast Nitrogen Base without amino acids supplemented with-Ade/-His/-Leu/-Trp DO supplement (Clontech, No. 630428) and 0.002% histidine.
- SD-WLHA: Yeast Nitrogen Base without amino acids supplemented with -Ade/-His/-Leu/-Trp DO supplement (Clontech, No. 630428).

5.2.3. Plant cultivation

5.2.3.1. Cultivation of Arabidopsis in vitro

5.2.3.1.1. Arabidopsis seed surface sterilization

Seeds of Arabidopsis were surface sterilized for 15 minutes in 70% (v/v) bleach and 0.01% (v/v) Tween-20, and washed four times with bi-distilled water.

5.2.3.1.2. Solid media plant cultures

Seeds were sterilized as described above, stratified 3 days at 4°C in the dark, and planted on sterile solid medium in plates. Growing conditions were 100 µmol/(m2*s) light at 22°C, under long day conditions (16h light / 8h darkness). Unless stated otherwise, plants were grown in Johnson medium (Johnson *et al*., 1957; Bates & Lynch, 1996) with pH 5.7 (KOH). Bactoagar concentration was 0.6% (w/v; 6g/L) for horizontal growth and 1% (w/v; 10g/L) for vertical growth.

5.2.3.1.3. Liquid medium plant cultures

Sterile liquid cultures, as described by (Scheible *et al*., 2004), were grown in full nutrition (FN), low Pi,-Pi, low N,-N and-Suc conditions (Table 5). Arabidopsis sterilized and stratified seeds were cultivated in three different systems:

- In sterile 125mL Erlenmeyer flasks in 30 mL of sterile liquid medium. Approximately 120 surface sterilized and stratified Arabidopsis seeds, corresponding to 3mg of dried seeds, were added to each flask.
- In sterile 24-wells Falcon™ tissue culture plates, each well containing 3ml of liquid medium and one Arabidpsis seed.
- In a sterile hydroponic system (see Figure 23) in 150ml of liquid medium.

Unless stated otherwise, plants in liquid cultures were grown in continuous 100 µmol/(m^2*s) light at 22°C on shakers set to 45 revolutions per mimute (rpm).

Table 5. Liquid culture medium compositions.

COMPOUND	FN	Low Pi 200µM	-Pi	Low N 150µM	-Suc
KNO_3	2mM	2mM	2mM	0.1mM	2mM
NH_4NO_3	1mM	1mM	1mM	50µM	1mM
K_2HPO_4/KH_2PO_4 (pH 5.7-5.8)	3mM	0.2mM	-	1mM	1mM
KCl	-	2.5mM	2.5mM	1.5mM	-
$CaCl_2$	4mM	4mM	4mM	4mM	4mM
$MgSO_4$	1mM	1mM	1mM	1mM	1mM
K_2SO_4	2mM	2mM	2mM	2mM	2mM
2-(N-morpholino)ethanesulfonic acid (MES)	3mM	3mM	3mM	3mM	3mM
Microelements*	1x	1x	1x	1x	1x
Sucrose	0.5%	0.5%	0.5%	0.5%	-
Glutamine**	1mM	1mM	1mM	-	1mM
Sucrose	0.5%	0.5%	0.5%	0.5%	-

* Oligoelements consist of the following: 40µM $Na_2FeEDTA$, 60µM H_3BO_3, 14µM $MnSO_4$, 1µM $ZnSO_4$, 0.6µM $CuSO_4$, 0.4µM $NiCl_2$, 0.3µM $HMoO_4$, 20nM $CoCl_2$. ** Sterile filtered glutamine was added after medium sterilization.

5.2.3.2. Soil grown plant conditions

Seedlings were transplanted into a mix of soil and vermiculite (ratio 3:1). Growing was carried out in greenhouse conditions at 22°C with a photoperiod of 16 hours of light and 8 hours of darkness in long-day conditions, and 8 hours of light and 16 hours of darkness in short-day conditions.

5.3. CLONING METHODS

To generate expression vectors for plants and yeast, Gateway cloning techniques were used according to the manufacture's instructions (Gateway, Invitrogen). As template either cDNA from FN and Pi limited Arabidopsis plants, or commercially available full-length cDNAs clones (Table 6), were used.

Table 6. Full-length cDNA templates source.

NAME	AGI	SOURCE*
ASK3	At2g25700	Arabidopsis seedling cDNA
ASK4	At1g20140	Arabidopsis seedling cDNA
ASK5	At3g60020	Arabidopsis seedling cDNA
ASK9	At3g21850	Arabidopsis seedling cDNA
ASK11	At4g34210	Arabidopsis seedling cDNA
ASK16	At2g03190	Arabidopsis seedling cDNA
ASK19	At2g03160	Arabidopsis seedling cDNA
ASK20	At2g45950	pda02182; RIKEN stock
KMD1	At1g80440	U18578; ABRC stock
KMD2	At1g15670	pda02271; RIKEN stock
KMD4	At3g59940	U18085; ABRC stock
PAL2	At3g53260	pda01530; RIKEN stock

* RIKEN: Institute of Physical and Chemical Research of Japan / ABRC: Arabidopsis Biological Resource Center.

The full-length expressed fragment was amplified was amplified by polymerase chain reaction (PCR) with Pwo DNA polymerase (Roche), using adaptor specific primers.

Table 7. Primers used for Gateway pDONR207 cloning. Universal adaptor sequences are given in bold letters.

AGI	Name	Sequence 5'- 3
At2g25700	ASK3_BF2	**GGGGACAAGTTTGTACAAAAAAGCAGGCTAT**ATGGCAGAAACGAAGAAGATGATCATC
	ASK3_BR	**GGGGACCACTTTGTACAAGAAAGCTGGGTA**CTCGAACGCCCACCTGTTCTCAT
At1g20140	ASK4_BF2	**GGGGACAAGTTTGTACAAAAAAGCAGGCTAT**ATGGCAGAAACGAAGAAGATGATCAT
	ASK4_BR	**GGGGACCACTTTGTACAAGAAAGCTGGGTA**CTCGAACGCCCACTTGTTCTC
At3g60020	ASK5_BF2	**GGGGACAAGTTTGTACAAAAAAGCAGGCTAT**ATGTCGACGAAGATCATGTTGAAGA
	ASK5_BR	**GGGGACCACTTTGTACAAGAAAGCTGGGTA**TTGAAAAGCCCATTGATTCTCCT
At3g21850	ASK9_BF2	**GGGGACAAGTTTGTACAAAAAAGCAGGCTAT**ATGTCGACGAAGAAGATCATATTGAAG
	ASK9_BR	**GGGGACCACTTTGTACAAGAAAGCTGGGTA**TTCAAAAGCCCATTTATTCT
At4g34210	ASK11_BF2	**GGGGACAAGTTTGTACAAAAAAGCAGGCTAT**ATGTCTTCGAAGATGATCGTGTTGAT
	ASK11_BR	**GGGGACCACTTTGTACAAGAAAGCTGGGTA**TTCAAAAGCCCATTGATTCTCCT
At2g03190	ASK16_BF2	**GGGGACAAGTTTGTACAAAAAAGCAGGCTAT**ATGTCTTCGAACAAGATTGTGTTG
	ASK16_BR	**GGGGACCACTTTGTACAAGAAAGCTGGGTA**CTTTAGATCCTCAAAAGCCCAA
At2g03160	ASK19_BF2	**GGGGACAAGTTTGTACAAAAAAGCAGGCTAT**ATGTCTTCGAAAAAGATTGTGTTGAC
	ASK19_BR	**GGGGACCACTTTGTACAAGAAAGCTGGGTA**GGGTTTTGGAACTTGTTGTTTTCCA
At2g45950	ASK20_BF2	**GGGGACAAGTTTGTACAAAAAAGCAGGCTAT**ATGTCAGAAGGTGATTTGGCCGT
	ASK20_BR	**GGGGACCACTTTGTACAAGAAAGCTGGGTA**AAAAAGAGTAAACATACAT
At1g80440	KMD1_BF2	**GGGGACAAGTTTGTACAAAAAAGCAGGCTAT**ATGGAACTTATCCCCAATCTTCCCGA
	KMD1_BR	**GGGGACCACTTTGTACAAGAAAGCTGGGTA**GACCTCCAAGAAGCAGCCAGCT
At1g15670	KMD2_BF2	**GGGGACAAGTTTGTACAAAAAAGCAGGCTAT**ATGGAGCTTATTCCTGATCTTCCCGA
	KMD2_BR	**GGGGACCACTTTGTACAAGAAAGCTGGGTA**TATCTCCAAGAAGCAACCAGCTTGAACGT
At3g59940	KMD4_BF2	**GGGGACAAGTTTGTACAAAAAAGCAGGCTAT**ATGGGAGTGTCAAAGAAGAAATCA
	KMD4_BR	**GGGGACCACTTTGTACAAGAAAGCTGGGTA**AACGTAGATTGAAGAACACGA
At3g53260	PAL2_BF2	**GGGGACAAGTTTGTACAAAAAAGCAGGCTAT**ATGGATCAAATCGAAGCAATGT
	PAL2_BR	**GGGGACCACTTTGTACAAGAAAGCTGGGTA**GCAAATCGGAATCGGAGCTCCGTT

Gel purification of the *attB*-PCR products was performed using the Qiaquick Gel Extraction Kit (QIAGEN). Subsequently, fragments were cloned into the Gateway entry vector pDNOR207 in BP reactions.

The BP reactions were used for transformation of chemo-competent *E. coli* DH5α cells (see 5.4.1. Bacterial transformation). Plasmid DNA was isolated from liquid bacteria cultures using the QIAPrep Spin Miniprep kit (QIAGEN). Correct identity was confirmed by sequencing. Positive clones, containing mutation-free sequence of interest, were re-cloned by LR reactions into different Gateway-compatible destination vectors (Table 8). Some constructions for Y2H assays were kindly provided by collaborators (Table 8).

Table 8. Constructions used for expression *in planta* and for the yeast two hybrid system (Y2H).

PLASMID	CONSTRUCTION	SELECTION	OBSERVATIONS
pGADT7	AD-ASK1	Ampicillin	Dr. Juan Carlos del Pozo
pGADT7	AD-ASK2	Ampicillin	Dr. Juan Carlos del Pozo
pGADT7	AD-ASK3	Ampicillin	Rojas-Triana, unpublished data
pGADT7	AD-ASK4	Ampicillin	Rojas-Triana, unpublished data
pGADT7	AD-ASK5	Ampicillin	Rojas-Triana, unpublished data
pGADT7	AD-ASK6	Ampicillin	Dr. Juan Carlos del Pozo
pGADT7	AD-ASK8	Ampicillin	Rojas-Triana, unpublished data
pGADT7	AD-ASK9	Ampicillin	Rojas-Triana, unpublished data
pGADT7	AD-ASK10	Ampicillin	Dr. Juan Carlos del Pozo
pGADT7	AD-ASK11	Ampicillin	Rojas-Triana, unpublished data
pGADT7	AD-ASK14	Ampicillin	Dr. Juan Carlos del Pozo
pGADT7	AD-ASK16	Ampicillin	Rojas-Triana, unpublished data
pGADT7	AD-ASK18	Ampicillin	Dr. Juan Carlos del Pozo
pGADT7	AD-ASK19	Ampicillin	Rojas-Triana, unpublished data
pGADT7	AD-ASK20	Ampicillin	Rojas-Triana, unpublished data
pGADT7	AD-KMD1	Ampicillin	Rojas-Triana, unpublished data
pGADT7	AD-KMD2	Ampicillin	Rojas-Triana, unpublished data
pGADT7	AD-KMD4	Ampicillin	Rojas-Triana, unpublished data
pGADT7	AD-PAL2	Ampicillin	Rojas-Triana, unpublished data
pGADT7	AD-SPX1	Ampicillin	Dra. Maria Isabel Puga
pGBKT7	BD-ASK1	Kanamycin	Dr. Juan Carlos del Pozo
pGBKT7	BD-ASK2	Kanamycin	Dr. Juan Carlos del Pozo
pGBKT7	BD-ASK3	Kanamycin	Rojas-Triana, unpublished data
pGBKT7	BD-ASK8	Kanamycin	Dr. Juan Carlos del Pozo
pGBKT7	BD-ASK14	Kanamycin	Dr. Juan Carlos del Pozo
pGBKT7	BD-ASK18	Kanamycin	Dr. Juan Carlos del Pozo
pGBKT7	BD-ASK19	Kanamycin	Rojas-Triana, unpublished data
pGBKT7	BD-ASK20	Kanamycin	Rojas-Triana, unpublished data
pGBKT7	BD-KMD1	Kanamycin	Rojas-Triana, unpublished data
pGBKT7	BD-KMD2	Kanamycin	Rojas-Triana, unpublished data
pGBKT7	BD-KMD4	Kanamycin	Rojas-Triana, unpublished data
pGBKT7	BD-PAL2	Kanamycin	Rojas-Triana, unpublished data
pGBKT7	BD-PHR1	Kanamycin	Dra. Maria Isabel Puga
pGWB5	35S::KMD1-GFP	Kanamycine	Rojas-Triana, unpublished data
pGWB5	35S::KMD4-GFP	Kanamycin	Rojas-Triana, unpublished data
pGWB5	35S::PAL2-GFP	Kanamycin	Rojas-Triana, unpublished data
pGWB5	35S::SPX1-GFP	Kanamycin	Dra. Maria Isabel Puga
pGWB20	35S::KMD1-10xMYC	Kanamycin	Rojas-Triana, unpublished data
pGWB20	35S::PHR1-10xMYC	Kanamycin	Dr. Vicente Rubio

5.4. TRANSFORMATION METHODS

5.4.1. Bacterial transformation

Transformation of competent DH5α *E. coli* cells was carried out by heat-shock as described in (Sambrook, *et al*., 1989) or by electroporation as described in (Chassy & Flickinger, 1987). Competent cells were prepared through a calcium chloride treatment. Transformation of competent C58C1 *A. tumefaciens* cells was carried out as described in (Weigel & Glazebrook, 2002). Competent cells were generated through a freezing method using also calcium chloride. Transformed *E. coli* and *A. tumefaciens* cells were plated onto selective media (LB with corresponding antibiotics) and then, incubated overnight at 37°C or 48h at 28°C, respectively.

5.4.2. *Arabidopsis* transformation

Constitutively 35S::CaMV promoter driven *KMD1*, *KMD4* and *PAL2* over-expressers lines were established as follows: the full-length coding sequence of the above mentioned genes, was cloned with the Gateway system (see section 5.3. Cloning Methods) and the resulting construct was introduced into *A. tumefaciens* strain C58C1 cells, followed by floral dip transformation of *Arabidopsis* Col-0 ecotype (WT). For the flor dip method (Clough & Bent 1998), *Arabidopsis* plants were grown in soil during 20-25 days in long-day conditions before their transformation. Young inflorescences were infiltrated by inversion during 10 minutes with a suspension of *A. tumefaciens* carrying the construct of interest, in Murashige and Skoog (MS) medium (3.67g of MS from Duchefa Bochemie per 1.5L of bidistilled water) supplemented with 5% of sucrose and a 0.02% of the surfactant agent Silwet L77. T1 seeds were screened for hygromicine B resistance, by sowing the T1 seeds into Johnson medium supplemented with 50 µg/mL carbenicilin (used for excluding *A. tumefaciens* growth). Resistant T1 plants were transferred to soil to obtain T2 seeds for further homozygosity analysis.

Due to the nature of *Agrobacterium*-mediated transformation, neither the locus nor the number of given T-DNA insertions can be controlled. In the T1 generation the insertion locus will be in majority in hemizygous state, independently of the number of insertion loci in the genome. In following generations, the insertion will subsequently segregate, according to Mendel's first law, for each individual locus. Dependent on the number of independent functional insertions loci, this lead to plants with different copy number of the transgene. As a result, the transcript levels of transgene expression can vary, which was observed for the T2 over-expresser lines established during this research.

If not stated otherwise, all subsequent studies were performed using mutant or over-expresser T2 seeds.

5.4.3. Agroinfiltration of *N. benthamiana* leaves

N. benthamiana plants, provided by the CNB greenhouse service, grown during 3-4 weeks were infiltrated for various experiments. *A. tumefaciens* cells transformed with the different constructs were grown overnight and used for infiltration of *N. benthamiana* leaves according to (Sparkes *et al*., 2006). Leaves were co-infiltrated with p19, which suppresses gene silencing (Voinnet, 2003). After 3 days of infiltration, leaves were harvested or used for microscopic observations.

5.4.4. *S. cerevisae* transformation

S. cerevisae cells were transformed as it is described in Matchmaker Gal4 Two-Hybrid User Manual (CLONTECH Laboratories, Inc.).

5.4.5. Stablishment of doble and triple mutant plants and co-overexpressor lines

5.4.5.1. T-DNA mutant plants genotyping

To generate doble and triple *kmd* mutant plants, Arabidopsis *kmd1* (SALK_008497), *kmd2* (SALK_014388) and *kmd4* (SALK_080249) T-DNA insertion mutants in Col-0 ecotype were obtained from ABRC (Alonso, et al., 2003). Heterozygous plants were segregated to obtain single, double and triple homozygous mutant plants, which were identified by PCR using specific primers for the target gene and the T-DNA insertion (Table 9).

Table 9. Primers used for T-DNA insertion mutant plants genotyping.

MUTANT	AGI	SALK ID	NAME	SEQUENCE 5'- 3
kmd1	At1g80440	SALK_008497	LPSALK_008497	TGTTGCGGTTTAGGTTCAAAC
			RPSALK_008497	CTCCTCCTACCAACAGTTCCC
kmd2	At1g15670	SALK_014388	LPSALK_014388	AAATGATTGCCAAAAAGAAAATG
			RPSALK_014388	GGAGGAACAAGGGCAATTTAG
kmd4	At3g59940	SALK_080249	LPSALK_080249	TAAAATCTCCGGGGAATTCAG
			RPSALK_080249	AGCATCTCCTTCAGTGTCTC
T-DNA specific primer:			LBa1	TGGTTCACGTAGTGGGCCATCG

5.4.5.2. Cross-pollination of Arabidopsis

Arabidopsis plants were grown in a greenhouse in long-day conditions until the flowers were at a stage where they were not open, yet not closed. With fine forceps, all flower parts except the pistil were removed, and with pollen obtained from a donor plant this pistil was pollinated. Once siliques were dry, seeds were harvested and grown for selection.

Homozygous mutant plants were used to stablish the double mutants *kmd1/2* and *kmd1/4,* by the cross-pollination of *kmd1* with *kmd2* and *kmd4*, respectivelly. In the same manner, *kmd1/2* and *kmd1/4* homozygous mutant plants were cross-pollinated to stablish *kmd1/2/4* triple mutant plants.

Co-overexpressor oePAL2-GFP/oeKMD1-MYC transgenic plants, cross-pollination was carried using homozygous oeKMD1-MYC-8 and oeKMD1-MYC-10 pollen onto oePAL2-GFP-32 pistils. T1 seeds were collected and used for further analysis.

Triple mutant *pub27/28/29* was a kind gift of Prof. Salomé Prat (unpublished data).

Triple mutant *pub27/28/29* was generated as follows: *Arabidopsis pub28* T-DNA insertion mutant (At5g09800) in Col-0 ecotype (SALK_101434) was obtained from ABRC (Alonso *et al.*, 2003). *pub27* T-DNA insertion mutant (FLAG_104F05) in Ws ecotype (At5g64660) was obtained from INRA (Versailles; Dèrozier *et al.*, 2011). Homozygous FLAG_104F05 mutant plants were backcrossed 6 times to Col-0 to obtain *pub27* mutant in the Col-0 background. To obtain *pub27/28* double mutant, *pub 28* was crossed to *pub27* (backcrossed to Col-0) and double homozygous mutant plants were identified by PCR.

To obtain gene-specific silencing of *PUB29* (At3g18710), a 600 bp fragment from *PUB29* open reading frame was PCR amplified using primers RNAi *PUB29*-for (5´- CACCATGGGGAGAGATGAAACAGA -3´) and RNAi *PUB29*-rev (5´- TTAGCGTCGAAGGAGATCCAAT -3´) and cloned into pENTR/D-TOPO vector (Invitrogen). This fragment was then transferred into pH7GW1WG2(II) vector (Karimi *et al.*, 2002) using Gateway technology (invitrogen). Double mutant *pub27/28* plants were transformed with PUB29RNAi-pH7GW1WG2, using *Agrobacterium* strain GV 3101 and the floral dip method (Clough and Bent 1998), and transgenic plants were selected based on growth in hygromycin. Two different lines (12 and 24) with decreased expression of *PUB29* were identified by RT-qPCR (data not shown). Homozygous plants from *pub27/28* RNAi *PUB29* line 12 (*pub27/28/29*) were used in subsequent experiments.

5.5. NUCLEIC ACIDS TECHNOLOGY

5.5.1. DNA

5.5.1.1. Extraction of plasmid DNA from bacteria

To isolate plasmid DNA in the range of 20µg from a 5-10 ml bacterial culture, we used the QIAPrep Spin Miniprep kit (QIAGEN) in which DNA binds to silica gel membrane in a spin column.

5.5.1.2. Plant DNA isolation

Arabidopsis genomic DNA extraction was carried out following the method defined by (Doyle & Doyle, 1990).

5.5.1.3. Gel/PCR DNA fragments purification

DNA fragments separated by agarose gel electrophoresis or DNA amplified in a PCR, were purified using Qiaquick Gel Extraction Kit (QIAGEN).

5.5.1.4. Extraction of plasmid DNA from yeast

The methodology used to isolate plasmids from yeast is described in (Hoffman & Winston, 1987). Yeast plasmids were introduced into DH5α *E. coli* competent cells by electroporation in order to amplify the plasmid and subsequent sequencing.

5.5.1.5. Amplification of DNA

PCR has been used for selectively amplify target regions of DNA (Sambrook et al., 1989) by the activity of the thermostable polymerase Taq (Roche) for current amplifications, and the Pwo DNA polymerase (Roche) for high fidelity amplifications. Primers used were acquired at Sigma-Aldrich.

5.5.1.6. Gel electrophoresis of DNA

DNA fragments obtained by PCR or the total DNA obtained in extractions were visualized through agarose gel electrophoresis using ethidium bromide in 1x TAE buffer (50mM Tris-acetate, 1mM EDTA, pH 8), which intercalates with the DNA and fluoresces under UV light. Voltage range used has been 80-130 V.

5.5.1.7. Sequence analysis of DNA

DNA sequences were obtained at TAIR (http://www.arabidopsis.org). Macrogen and Secugen have provided sequencing service. Sequencing results were visualized using the software 4Peaks (http://www.mekentosj.com/science/4peaks) available online and aligned using GENOMATIX program alignment tool (http://www.genomatix.de/cgi-bin/dialign/dialign.pl).

5.5.2. RNA

5.5.2.1. RNA isolation

For RNA extraction, plant samples were homogenized using a Silamat S6 bead mill. RNA was extracted according to the Qiagen RNeasy kit protocol with these exceptions to the protocol: (I) the initial mixing of homogenized plant tissue with RLT lysis buffer was performed in the Silamat S6 bead mill instead of vortexing. (II) Before adding the plant sample/lysis buffer mix to the QIAshredder column, microcentrifuge tubes were briefly centrifuged to remove large cell debris. (III) Supernatant was loaded onto QIAshredder column and the pellet was discarded.

Following RNA isolation, RNA purity and concentration were examined by measuring absorption A260, A280 and A230 with a NanoDrop® ND-1000 UV-VIS spectrophotometer and only samples with concentrations higher than 150ng/µL, a lower 260/280 ratio than 1.9 and a higher 260/230 ratio higher than 1.5 were retained. For samples that did not meet these criteria, RNA isolation was repeated.

RNA samples were DNase digested to remove any co-precipitated genomic DNA. DNase digestion was performed using the Applied Biosystems TURBO DNA-free™ kit according to the manufacturer's protocol. A PCR reaction was performed to confirm removal of genomic DNA from the sample, using *Actin2* (At3g18780) primers (Table 10). A genomic DNA sample was included as a positive control.

5.5.2.2. cDNA synthesis

First strand cDNA synthesis was performed on DNase digested RNA samples, using SuperScript™ III reverse transcriptase (Invitrogen) according to the manufacturers protocol on 2µg of each of the DNase digested RNA samples.

The Quality of cDNA was examined by quantitative real-time PCR (qRT-PCR), using primer sets for housekeeping genes *UBQ10* (At4g05320) and *GAPDH* (At1g13440), the former using two primer sets, one for the 5' end of the gene and one for the 3' end. The ratio in threshold cycle value (CT value) between the 5' and the 3' end of *GAPDH* indicates to which level cDNA synthesis was completed for the full length of mRNA strands. Samples not showing a *UBQ10* CT value between 15 and 18, and showing a ratio of more than 1.5 for GAPDH3'/GAPDH5' or GAPDH5'/GAPDH3' were discarded. Primers for *UBQ10*, *GAPDH3'* and *GAPDH5'* are listed in Table 10.

5.5.2.3. Semi-quantitative PCR

Semi-quantitative PCR analysis was performed using cDNA as template and thermostable polymerase Taq (Roche). *ACT8* housekeeping gene primers and WT cDNA samples were included as a positive controls. Results were visualized by agarose gel electrophoresis (see section 5.5.1.6. Gel electrophoresis of DNA). Primers used are listed in Table 10.

5.5.2.4. Quantitative Real-Time PCR

qRT-PCR reactions were performed using the SYBR® Green JumpStart™ Taq ReadyMix™ (Sigma) or the TaqMan ®Universal ProbeLibrary System (UPL). All reactions were performed in two technical replicates. Analysis of qRT-PCR data and normalization was performed manually using the Excel software, and the results were obtained in the following ways:

- CT value: Cycle threshold value measuring when PCR amplification of the gene of interest is in linear exponential phase of amplification by setting a normalized fluorescence threshold for the reaction.

- ΔCT: The CT of the reference gene (*ACT8* for the UPL system and *UBQ10* for the SYBR® Green system) for the qRT-PCR, subtracted from the qRT-PCR reaction of interest. Serves to normalize Ct values to a housekeeping gene with a very constant expression level in plants in different conditions

- 40-ΔCT: The ΔCT value subtracted from the maximum cycle number in the qRT-PCR reaction (40 cycles). Serves to invert the data so that highly expressed genes have high values and low expressed genes have low values.

- ΔΔCt: The difference in ΔCt between two sample treatments.

- Foldchange: Equaling the fold change in expression, calculated as $2^{(-1*(\Delta\Delta CT))}$.

Primer pairs used in the qRT-PCR reactions are listed in Table 10.

Table 10. Primers used in RNA-based assays.

NAME	SEQUENCE 5'- 3	ASSAY
ACP5-qRT-LP	CAGTTTCTAACTAGTGGTGCTGGA	RT-qPCR
ACP5-qRT-RP	GCTTGGGATTGATGGTCACT	
ACT2-F	ACTTTCATCAGCCGTTTTGA	RNA and cDNA quality check
ACT2-R	ACGATTGGTTGAATATCATCAG	
ACT8-F	GACTCAGATCATGTTTGAGACCTTT	RT-qPCR
ACT8-R	CCAGAGTCCAACACAATACCG	
AT4-qRT-LP	TGGCCCCAAACACAAGAG	RT-qPCR
AT4-qRT-RP	CGAACATTCACAATCATAATCTCC	
GAPDH3'-F	TTGGTGACAACAGGTCAAGCA	cDNA quality check
GAPDH3'-R	AAACTTGTCGCTCAATGCAATC	
GAPDH5'-LP	CACACTCCACTTGGTCTTGCGT	cDNA quality check
GAPDH5'-LP	CGAAACCGTTGATTCCGATTC	
KMD1-LP1	CGTTGCTCGCGAGTGTCTCCTT	Semi-quantitative PCR
KMD1-RP	CTTGAACATGACCACCGTGTG	
KMD1-qRT-LP	TGTTACTTACGTAGCGGTGAGG	RT-qPCR
KMD1-qRT-RP	TATCCAGCCAACGCCTTC	
KMD2-LP	CGATGATGTCAGCTCTGGTG	Semi-quantitative PCR
KMD2-RP	GAACGTGGCCTTCATATTTATCATG	
KMD2-qRT-LP	CGATGATGTCAGCTCTGGTG	RT-qPCR
KMD2-qRT-RP	CCATATCCGGCAAGAAAGC	
KMD3-qRT-LP	TTCGATGACTATGGAAGTGTCG	RT-qPCR
KMD3-qRT-RP	CGGGAATCAATTCGTGACAT	
KMD4-LP	GAGATTTAATCCCAGGGTTACCAG	Semi-quantitative PCR
KMD4-RP	CCAGAGGGAGTGTTGACGTGGCT	
KMD4-qRT-LP	GATGGAAGGTGGTGAGATGAG	RT-qPCR
KMD4-qRT-RP	CTGCTGCGTCATCTGAGACT	
PAL1-qRT-LP	ATTAACGGGGCACACAAGAG	RT-qPCR
PAL1-qRT-RP	GTCTCCGCCGCATAACATAG	
PAL2-qRT-LP	GGAACGAAGTTGTTGACTGGA	RT-qPCR
PAL2-qRT-RP	CACATAGCAGTGAAGACCTTATCAA	
PAL3-qRT-LP	TCTCGTAGGAGGACTGACCAA	RT-qPCR
PAL3-qRT-RP	AATATCCCGGCGTTCAAATA	
PAL4-qRT-LP	GGTGAGACTTTGACGATTGGT	RT-qPCR
PAL4-qRT-RP	GCTAGCTCCACCGTAGATCCT	
PHF1- qRT-LP	TTTTGACCCCATTACTGCTTC	RT-qPCR
PHF1- qRT-RP	TCCTTAAGCGTGTGTGTTGC	
RNS1-qRT-LP	CCAAACCGCTCTTAACCTTAAAC	RT-qPCR
RNS1-qRT-RP	GATTAATCCCGGCTTTGGTT	
SQD1- qRT-LP	CATCCTCTAAACCAAAGCGTGT	RT-qPCR
SQD1- qRT-RP	AGTAGCCCAACCGCAATAAC	
UBQ10-qRT-F	CACACTCCACTTGGTCTTGCGT	RT-qPCR
UBQ10-qRT-R	TGGTCTTTCCGGTGAGAGTCTTCA	

5.6. PROTEIN TECHNOLOGY

5.6.1. Protein isolation

Plant material was harvested, frozen in liquid N_2 and then homogenized in native extraction buffer or immunoprecipitation buffer (IP buffer) (Table 11). The extracts were centrifuged twice at 4°C for 15 minutes at 13000rpm, and supernatants were recovered. Protein concentration in the supernatant was determined by Bradford assay (Bio-Rad).

5.6.2. Western blot analysis

Protein samples were boiled in 2xSDS loading buffer (0.125M Tris-HCl pH 6.8, 4% SDS, 20% Glycerol, 0.02% bromophenol blue, 1% β-mercaptoethanol) during 5 minutes, and 30µg of protein were loaded in SDS-PAGE gels (Sambrook et al., 1989). Two-layer gels were used, with a 4% acrilamid:bisacrilamid (29:1) (Biorad) stacking layer, and a 7.5-10% (depending on the protein fuisons size) resolving layer. Tris-Glycine buffer (25mM Tris, 192mM glycine, 0,1% SDS) was used during the protein separation by a dual amperage electrophoresis of 35mA for the stacking layer and 55mA for the resolving layer.

Gels were transferred to polyvinylidene difluoride (PVDF, Millipore) membranes with a pore size of 0.45µm, using a semidry (50mM Tris, 40mM glycine, 0.04% SDS and 20% methanol) transfer blot system under 110mA during 1.5h. The membranes were then saturated with 5% non-fat milk dissolved in PBS-T (PBS 1x and 0.1% Tween-20) during 1h at room temperature (RT), and incubated with the corresponding antibodies (Table 12). The immunoblot detection was carried out with ECL Plus Western Blotting Detection System (Amersham) or SuperSignal® West Femto Maximum Sensitivity Chemiluminescent Substrate (Thermo Scientific), according with the manufacture instructions.

5.6.3. Immunoprecipitation assays

5.6.3.1. Immunoprecipitation of tagged fusions

In order to test whether KMD1 and KMD4 can be detected in association with CUL1 *in planta*, immunoprecipitation (IP) assays were carried with total protein extracts in IP buffer (Table 11), from oeKMD1-GFP-82, oeKMD4-GFP-15 and oeKMD1-MYC-10 seedlings, grown during 9 days in +Pi solid Johnson media. 30µg of total protein were taken from the lysates and used as inputs. KMD1-GFP and KMD4-GFP, and KMD1-MYC fusions were

immunoprecipitated with a polyclonal anti-GFP antibody fused to the protein A-Sepharose® from *Staphylococcus aureus* (SIGMA-ALDRICH), and with EZviewTM Red Anti-c-Myc Affinity Gel (SIGMA-ALDRICH), respectively. Next, immunodetection of the immunoprecipitated KMD1-GFP, KMD4-GFP and KMD1-MYC, and the the co-immunoprecipitated endogenous CUL1, was performed with anti-GFP-HPR, anti-MYC and anti-CUL1 antibodies (Table 12).

Co-immunoprecipitation (Co-IP) of GFP-tagged PAL2 and MYC-tagged KMD1 proteins was performed in both (i) stable and (ii) transient expression systems.

(i) IP of PAL2-GFP fusions was performed using protein extracts in IP buffer (Table 11), prepared from 12-days-old seedlings corresponding to two independent T1 oePAL2-GFP-32/oeKMD1-MYC (-8 and-10) lines, and the two different oeKMD1-MYC parental lines (-8 and -10). 30µg of total protein were taken from the lysates and used as inputs. PAL2-GFP fusions were immunoprecipitated with a polyclonal anti-GFP antibody fused to the protein A-Sepharose® from *Staphylococcus aureus* (SIGMA-ALDRICH). Next, immunodetection of the immunoprecipitated PAL2-GFP, and the the co-immunoprecipitated KMD1-MYC, was performed with anti-GFP-HPR and anti-MYC antibodies (Table 12).

(ii) IP of KMD1-MYC fusions was performed using protein extracts in IP buffer (Table 11) from co-agroinfiltrated (35S::PAL2-GFP and 35S::KMD1-MYC) *N. benthamiana* leaves. 30µg of total protein were taken from the lysates and used as inputs. KMD1-MYC fusions were immunoprecipitated with EZviewTM Red Anti-c-Myc Affinity Gel (SIGMA-ALDRICH). As a negative control 35S::GFP and 35S::KMD1-MYC co-agroinfiltrated leaves were used. The inputs and outputs were incubated with anti-MYC and anti-GFP-HPR antibodies (table 12) to detect the immunoprecipitated KMD1-MYC fusion and the co-immunoprecipitated PAL2-GFP fusion, respectively.

Table 11. Total protein lysate buffers.

REAGENT	NATIVE EXTRACTION BUFFER	IP BUFFER
ATP	-	5µM
Dithiothreitol (DTT)	-	1µM
EDTA	-	1mM
Glycerol	-	10%
MG132	-	50µM
$MgCl_2$	10mM	-
NaCl	150mM	80mM
NP-40	0.1%	0.2%
Phenylmethylsulfonyl fluoride (PMSF)	1mM	1mM
Protease inhibitor cocktail (Roche)	1x	1x
Tris-HCl pH 7.5	50mM	50mM

5.6.3.2. Pull-down of Ub-conjugates

Pull-down assays of Ub-conjugates was carried out using 9 day-old oeKMD1-MYC seedlings and *N. benthamiana* leaves transiently overexpressing PAL2-GFP (35S::PAL2::GFP) (3 days post-*Agrobacterium*-infiltration). Total proteins were isolated in IP buffer (Table 11), as described previously (see 5.6.1. Protein isolation), and 30µg of total proteins were used as inputs.

Total ubiquitinated proteins were purified by incubation of total protein extracts with p62 agarose (p62) (Wilkinson et al., 2001) or with no-ubiquitin affinity agarose, during 4h at 4°C under constant rotation. The total ubiquitinated proteins (output) were eluted by boiling during 5 minutes in 2x loading buffer. Inputs and outputs were then used for Western blot analysis (see 5.6.2. Western blot analysis), and anti-Ub antibody (Table 12) was used to detect total ubiquitinated proteins. To detect the co-precipitated KMD1-MYC and PAL2-GFP fusions, anti-GFP-HRP and anti-MYC antibodies were used, as described in Table 12.

Table 12. Antibodies used for immunodetection of proteins.

ANTIBODY	INCUBATION	DETECTION	MANUFACTURE	SECONDARY
Anti-CUL1	1:500/Over night/4°C	Arabidopsis CUL1		Anti-rabbit
Anti-GFP-HRP	1:10000/1h/RT	KMD1-GFP KMD4-GFP PAL2-GFP SPX1-GFP	Milteny Biotec	-
Anti-MYC	1:1000/Over night/4°C	KMD1-MYC PHR1-MYC		Anti-mouse
Anti-RPT5	1:1000/Over night/4°C	Arabidopsis RPT5	Kwok et al., 1999	Anti-rabbit
Anti-Ub	1:1000/Over night/4°C	Arabidopsis Ub	Boston Biochem	Anti-rabbit

5.6.4. Yeast two-hybrid assays

Yeast two-hybrid (Y2H) approaches have been used in this work to study the interaction between two known proteins and to look for KMD1 interactors in a cDNA library. Y2H experiments were done with the Matchmaker GAL4 Two-Hybrid System (Clontech, Cat No. K1604-1, K1605-1, 630303), using the AH109 yeast strain (Clontech) for auxotrophy selection and the Y187 for β-galactidose activity. All the constructs used in the Y2H assays are listed in Table 8.

For direct Y2H experiments, proteins of interest were cloned into the Gateway compatible vectors, pGADT7 and pGBKT7 (Clontech) and co-transformed (see 5.4.4. *S. cerevisae* transformation) into AH109 yeast cells. Cells were selected in SD-WL medium for the presence of both pGADT7 and PGBKT7 plasmids, and then grown in the auxotrophic SD-WLH, SD-WLA and SD-WLHA media (see 5.2.2. Yeast culture methods), supplemented or not with 3-amino-1,2,4-triazole (3-AT), a competitive inhibitor of the product of the *HIS3* gene which is involved in histidine biosynthesis in *S. cerevisae*, to test for interaction. Yeast growth and handling was according to the Yeast Protocols Handbook (Clontech).

For the Y2H mating screening, full-length KMD1 was used as bait, and the cDNA library used was kindly provided by Dra. Maria Isabel Puga (Puga et al., 2014). Y2H screenings were done according to the Matchmaker Gal4 Two-Hybrid User Manual (Clontech). Interacting proteins obtained in these screenings were organized in functional classes using Mapman software (http://mapman.gabipd.org/web/guest/mapman).

5.7. MICROSCOPIC TECHNIQUES

Confocal images were obtained by Leica TCS SP2 and Leica TCS SP5 multispectral confocal microscopes (Leica Microsystems) with a 63x water-immersion objective, using photomultipliers for laser lines 405, 488, and 561 nm. LAS AF v.2.3.6 software was used for image acquisition. *Arabidopsis* seedlings visualised in confocal imaging were grown vertically for 4-6 days at 22°C with a 60% of humidity and 16-hours photoperiod with a fluorescent light of a 100 µmol m-2s-1 intensity. *Arabidopsis* root epidermal cells were visualised for the subcellular localization studies.

5.8. PHYSIOLOGICAL ASSAYS

5.8.1. Quantification of soluble Pi content

Shoot and root soluble Pi content was determined from 12 days-old seedlings grown under different Pi conditions, as it is described in (Ames, 1966). Roots were washed five times with bi-distilled water, in order to remove possible medium contamination that could alter subsequent quantification.

5.8.2. Quantification of anthocyanins content

Anthocyanin measurements were performed using a modified version of the protocol of (Swain & Hillis, 1959). Shoots were harvested and pooled in 2mL microcentrifuge tubes. 1mL of a 0,5N HCL, 80% v/v CH_3OH solution was added and samples were incubated at least 24h at 4°C in the dark, to fully extract anthocyanins from the plants tissue while avoiding photo bleaching of the anthocyanin. Samples were then thoroughly mixed and two aliquots of 100µL were added to separate spectrophotometer cubetes. To one cubete, a solution of 3N HCl, 1:5 CH_3OH was added, to the other cubete a bleaching solution containing 3N HCl, 1:5 CH_3OH and 1:9 H_2O_2 was added. Samples were incubated in the dark for 15 minutes and absorbance was measured at 540nm. Data was collected as ΔA540 values of bleached and non-bleached aliquots divided by the fresh weight (FW g).

5.8.3. Primary root length measurement: Pi, Suc and kinetin treatments

Seeds were plated on vertical complete Johnson medium (1mM Pi and 1% Suc) plates and were placed in a phytotron under long day conditions. After 4 days, seedlings were manually transfer to Johnson medium vertical plates with the different Pi (1mM Pi and -Pi), Suc (1% Suc and -Pi) and kinetin (100nM kinetin and -Kinetin) treatments. Measurement of primary root (PR) length was performed by using the ImageJ software (http://rsb.info.nih.gov/ij/, 11-12-2012) on pictures of vertical plates.

5.8.4. Cytokinins exogenous supply treatments

Seeds were plated on vertical complete Johnson medium (1mM Pi and 1% Suc) and were placed in a phytotron under long day conditions. After 4 days, seedlings were manually transfer to Johnson medium vertical plates with or without kinetin (100nM) or zeatin (100nM). Seedlings were harvested 7 days after treatment.

5.8.5. Metabolites quantification

Metabolites quatification was performed in collaboration with Prof. Joachim Kopka from the Max Planck Institute of Molecular Plant Physiology, Golm, Germany. Metabolite profiling was performed as detailed previously (Wagner *et al.*, 2003; Erban *et al.*, 2007) by gas chromatography coupled to electron impact ionization/time-of-flight mass spectrometry (GC-EI/TOF-MS) using an Agilent 6890N24 gas chromatograph (Agilent Technologies, Böblingen, Germany; http://www.agilent.com) with split and splitless injection onto a Factor Four VF-5ms capillary column, 30m length, 0.25mm inner diameter, 0.25µm film thickness (Varian-Agilent Technologies), which was

connected to a Pegasus III time-of-flight mass spectrometer (LECO Instrumente GmbH, Mönchengladbach, Germany; http://www.leco.de).

Metabolism of plant material was stopped by rapid sampling into liquid nitrogen under ambient light/environmental conditions. Frozen samples were stored at -80°C before they were pulverized under liquid nitrogen for metabolite extractions. Metabolites were extracted from 100 mg (fresh weight ±1 % tolerance) deep frozen powder of shoot with 360µl mixture of 300µl pre-cooled methanol, 30µl internal standard solution (2 mg/ml 13C6-sorbitol) and 30µl nonadecanoic acid methylester (2mg/ml stock in chloroform), was added, vortexed and incubated at 70°C for 15 minutes with shaking. 200µl chloroform was added and incubated at 37°C for 5 minutes with shaking. After adding 400µl water, the extract was vortexed and the polar phase was separated by centrifugation. Aliquots of 160 µl from the polar metabolite fraction were dried by vacuum concentration and stored dry under inert gas at -20°C until further processing.

Metabolites were methoxyaminated and trimethylsilylated manually prior to GC-EI/TOF-MS analysis (Fiehn *et al*., 2000; Roessner *et al*., 2000; Wagner *et al*., 2003; Lisec *et al*., 2006; Erban *et al*., 2007). Retention indices were calibrated by addition of a C10, C12, C15, C18, C19, C22, C28, C32, and C36 n-alkane mixture to each sample (Strehmel *et al*., 2008). GC-EI/TOF-MS chromatograms were acquired, visually controlled, baseline corrected and exported in NetCDF file format using ChromaTOF software (Version 4.22; LECO, St. Joseph, USA). GC-MS data processing into a standardized numerical data matrix and compound identification were performed using the TagFinder software (Luedemann *et al*., 2008; Allwood *et al*., 2009). Compounds were identified by mass spectral and retention time index matching to the reference collection of the Golm Metabolome Database (GMD, http://gmd.mpimpgolm.mpg.de/) (Kopka *et al*., 2005; Schauer *et al*., 2005; Hummel *et al*., 2010) and to the mass spectra of the NIST08 database (http://www.nist.gov/srd/mslist.htm).

Guidelines for manually supervised metabolite identification were the presence of at least three specific mass fragments per compound and a retention index deviation < 1.0% (Strehmel *et al*., 2008). All mass features of an experiment were normalized by sample FW, internal standard and maximum scaled. For quantification purposes all mass features were evaluated for best specific, selective and quantitative representation of observed analytes. Laboratory and reagent contaminations were evaluated by non-sample control experiments. Metabolites were routinely assessed by relative changes expressed as response ratios, i.e. x-fold factors in comparison to a control condition of each metabolite measure.

5.9. *IN SILICO* ANALYSIS

5.9.1. Protein aligments

KMD proteins alignments were performed using the Geneious software version 6.0.5 (http://www.geneious.com/). For pairwise comparisons, local alignments beased on the Smith-Waterman algorithm with a cost matrix Blosum62, were used. For multiple comparisons, global aligments based on Multiple Sequence Comparison by Log- Expectation (MUSCLE) algorithm, were used.

5.9.2. Tree reconstructions

Tree reconstructions were made using the Geneious software version 6.0.5 (http://www.geneious.com/). For the KMD proteins un-rooted tree reconstruction, the distance matrix was constructed with a global aligment with a cost matrix Blosum62, and the tree was built using the Jukes-Cantor genetic distance model with the Neighbor-joining (NJ) method. The tree reconstruction of the ASK proteins was made with a ClustalX global aligment, and the tree was built using the NJ method with 100 times bootstrap.

5.9.3. Protein secondary structure predictions

Protein secondary structure prediction was performed using the RaptorX software (Källberg *et al*., 2012) (http://raptorx.uchicago.edu/), over the full-length aa sequence of the KMD proteins, and the output is presented as the probability in % of the presence of one of the secondary structure elements, alpha helix, beta strand or loop structure, against the number of the corresponding aa (aa 1 being the N-terminal aa).

5.9.4. Protein terciary structure reconstructions

The prediction of the three-dimensional (3-D) structure of KMD proteins, as well as the *Arabidopsis* FBK proteins AFR (ATTENUATED FAR-RED RESPONSE) and FKF1 (FLAVIN-BINDING KELCH-REPEAT F-BOX1) (Harmon & Kay, 2003), was performed using the protein structure homology-modelling server SWISS-MODEL (Arnold *et al*. 2006; Guex *et al*., 2009; Kiefer *et al*. 2009; http://swissmodel.expasy.org/). KMD1, KMD2, KMD4 and AFR 3-D prediction was according to the crystal structure of a kelch protein from *Plasmodium falciparum* (template 4yy8.1), while the prediction for KMD2 and FKF1 was based on the Ta-TFP from *Thlaspi arvense* (templates 5a11.1/5a.10.1) (Gumz *et al*. 2015). The templates mentioned above were selected from the SwissModel Template Library (SMTL),

and displayed the highest Global Model Quality Estimation (GMQE). The structural elements are colored according to the QMEAN score. According to SWISS-MODEL, SMTL, GMQE and QMEAN are defined as follow:

- SMTL: SMTL is a large structural database of experimentally determined protein structures derived from the Protein Data Bank (Westbrook *et al*. in http://swissmodel.expasy.org/), and it serves as the main repository of structural information for the modelling pipeline, providing atomic coordinates of protein structures and maintaining sequence and profile databases which can be searched by BLAST and HHblits.
- GMQE: GMQE is a quality estimation which combines properties from the target-template alignment. The resulting GMQE score is expressed as a number between zero and one, reflecting the expected accuracy of a model built with that alignment and template. Higher numbers indicate higher reliability. Once a model is built, the GMQE gets updated for this specific case by also taking into account the QMEAN4 score of the obtained model in order to increase reliability of the quality estimation.
- QMEAN4: QMEAN4 (Benkert *et al*. in http://swissmodel.expasy.org/) is a composite scoring function for the estimation of the global and local model quality. QMEAN consisting of four structural descriptors: (i) the local geometry is analysed by a torsion angle potential over three consecutive amino acids; (ii) two pairwise distance-dependent potentials are used to assess all-atom and C-beta interactions; (iii) a solvation potential describes the burial status of the residues; (iv) the pseudo energies returned from the four structural descriptors. The final QMEAN4 score get directly related to what can be expect from high resolution X-ray structures of similar size using a Z-score scheme.
- Z-score: according to Zhang & Skolnick (1998) the Z-score of a protein is defined as the energy separation between the native fold and the average of an ensemble of misfolds in the units of the standard deviation of the ensemble. The Z-score is often used as a way of testing the knowledge-based potentials for their ability to recognize the native fold from other alternatives (Zhang & Skolnick, 1998).

5.9.5. Transcriptomic data retrival and analysis

*KMD*s gene expression data was retrieved from the public expression data collection stored at Genevestigator (Hruz *et al*. 2008; https://genevestigator.com/). Data stored under the *Anatomy*, *Development* and *Perturbations* conditions search tools under the compendium-wide analysis option, was used in this research. The data selected was from *Arabidopsis thaliana* samples used in Affymetrix *Arabidopsis* ATH1 genome arrays, and was

filtered based on WT genetic background. Only experiments with gene expression levels with $p<0.05$ were considered for further analysis.

The *KMD*s gene expression correlation analysis, and the hierarchical clusterings based on the eucidian distance, were performed using the Co-Expression and Hierarchical Clustering similarity search tools under the compendium-wide analysis option. The co-expression analysis performed with Genevestigator was based on the collection data under the *Perturbations* conditions search tools. A finer analysis was conducted selecting specific datasets for different types of perturbations, and co-expression analysis was conducted based on the Pearson's correlation coefficient using the Excel CORREL function that calculates the Pearson Product-Moment Correlation Coefficient for two sets of values (the syntax of the function is: CORREL(array1, array2)).

5.9.6. Over-representation analysis

The list of potential targets of KMD1 obtained in an Y2H mating screening, were used in an over-repressentation analysis performed with the MAPMAN over-representation analysis tool (Usadel *et al*., 2006; http://mapman.mpimp-golm.mpg.de/general/ora/ora.shtml). The output of the analysis presents the queries (KMD1 interactors) classified by hierarchical functional pathways or *BIN*s, with an associated *p*-value. In this work, a BIN was consider as over-represented when p-value<0.05.

5.10. STATISTICAL CONSIDERATIONS

In this thesis, unless otherwise noted, data presented with standard deviation and significance indicators represent the average of at least three biological replicates. Significance values were determined using the students T-test, and results are considered to be significant if p-value<0.05.

RESULTS

6. Results

6.1. PHOSPHATE CONTROLLED E3 UB LIGASES

The Pi starvation response in plants is complex and involves the coordinated action of a wide number of genes (Bustos *et al*. 2010) that produce a range of physiological, metabolic and developmental changes to cope with growth under Pi limiting conditions.

To evaluate the potential involvement of the UPS in the control of Pi starvation responses, the transcriptional behavior of different gene super-families that compose the UPS, in response to different Pi supplies, was analyzed. Bustos and collaborators (2010) performed a global comparative transcriptomic analysis, by hybridizing ATH1 Affymetrix microarrays with three independent biological replicates of RNA, from root and shoot of WT and *phr1/phl1* seedlings grown 7 days in +Pi and-Pi conditions. The results obtained (Bustos *et al*. 2010) were used in this research.

Probe sets corresponding to gene super-families that encode for E1, E2, E3 and DUB were identified in ATH1, therefore transcriptional behavior of genes behind the basic steps of the ubiquitination cascade could be analyzed using these arrays (Figure 9).

The different UPS components were analyzed grouped by an enzymatic distinction and by gene super-families: no substrate adaptors (E1, E2, CUL, ASK, DDB and DUB) and substrate adaptors (F-box, BTB, PHD, DCAF, HECT, U-box and RING). Thus, the different UPS elements can broadly be differentiated based on their ability/inability to physically recruit target proteins for ubiquitination. Genes that codify for elements that act as substrate adapters (as monomeric E3s or as multimeric E3 complex subunits) represent around the 94% of the total UPS genes in Arabidopsis, while the other 6% is shared by genes encoding the remaining functions within the UPS (Figure 9-A). Worth notice that, F-box (SCF E3 subunits) and RING (mostly monomeric E3s) super-families spanned 66% of all UPS elements known so far (Figure 9-A).

The representation of the gene super-families in ATH1 is heterogeneous and size-independent (Figure 9). Probe sets corresponding to more than 75% of the members of almost all gene super-families studied are represented, except for F-box (n= ~694) and HECT (n= ~8) families, whose representation was more limited (54.5% and 62.5%, respectively) (Figure 9-B). Super-families such as E1, E2, CUL, DDB and DUB had almost all their members represented (>90%) (Figure 9-B).

A

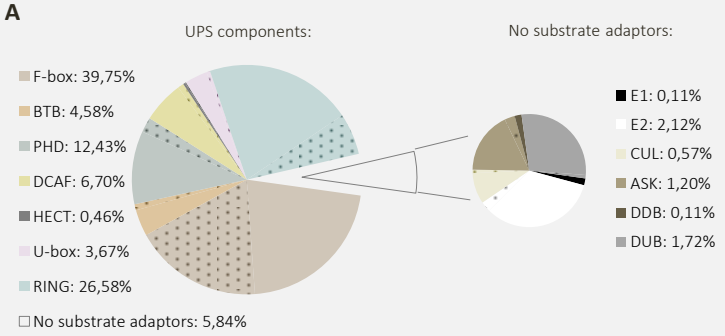

B

	Total	ATH1		No ATH1	
	n	n	%	n	%
F-box	694	378	54,47	316	45,53
BTB	80	65	81,25	15	18,75
PHD	217	180	82,95	37	17,05
DCAF	117	102	87,18	15	12,82
HECT	8	5	62,50	3	37,50
U-box	64	55	85,94	9	14,06
RING	464	362	78,02	102	21,98
E1	2	2	100,00	0	0,00
E2	37	34	91,89	3	8,11
CUL	10	9	90,00	1	10,00
ASK	21	18	85,71	3	14,29
DDB	2	2	100,00	0	0,00
DUB	30	29	96,67	1	3,33

Figure 9. UPS genes in the ATH1 Affymetrix microarray. (A) Distribution in genes super-families of the overall UPS components, including substrate adaptors (F-box, BTB, PHD, DCAF, HECT, U-box and RING) and no substrate adaptors super-families (E1, E2, CUL, ASK, DDB and DUB). Dots pattern fill represents the % of genes not represented in ATH1. Percentages are relative to the total number of UPS elements described (n = 1734). **(B)** Representation of the UPS gene super-families in the ATH1 Affymetrix microarray, in absolute (n) and percentage values (%). Percentages are relative to the total number of members reported for each super-family (www.plantsubq.genomics.purdue.edu).

Genes that were induced or repressed in response to-Pi, which fulfill an arbitrary selective criteria (Bustos, et al., 2010), were used for further analysis. Foldchange values of 2x and 1.5x, and FDR (False Discovery Rate) <0.05 and <0.1 (Benjamini & Hochberg, 1995), were the selection standards preferred for WT and *phr1/phl1* samples, respectively.

Following the criteria mentioned above, 9% and 3% of the UPS genes showed -Pi transcriptional responsiveness in the WT shoot and root, respectively, and slightly prone to the induction than to the repression (Figure 10-A-i-ii). By splitting the analysis in different gene families (Figure 10-B), it became remarkable the percentage of repressed DCAF (11%) genes in Pi starved shoots, and the 14% and 9% of induced U-box genes in-Pi shoots and roots, respectively (percentage relative to the number of genes represented in ATH1 for each gene family). In fact, a binomial distribution analysis made apparent an over-representation of up-regulated U-box genes, in response to Pi deficiency in the shoots (Figure 10-B). Families like E1, CUL and HECT showed no-Pi-responsive members (thus not represented in Figure 10-B).

In an attempt to explore the functionality of the overrepresentation of the shoot-Pi-inducible U-box genes in the context of Pi homeostasis, advantage was taken from a triple *pub27/28/29* knockdown line, kindly provided by Prof. Salomé Prat (National Center of Biotechnology CNB-CSIC). *pub27/28/29*, *phr1* and WT seedlings were grown for 7 days in low Pi (50 µM KH_2PO_4/K_2HPO_4) and +Pi (500 µM KH_2PO_4/K_2HPO_4) solid mediums, and total Pi

content was measured. In shoots, similar than in *phr1*, in *pub27/28/29* there was approximately 35% less Pi content than in the WT plants when grown under Pi sufficient conditions (Figure 10-C).

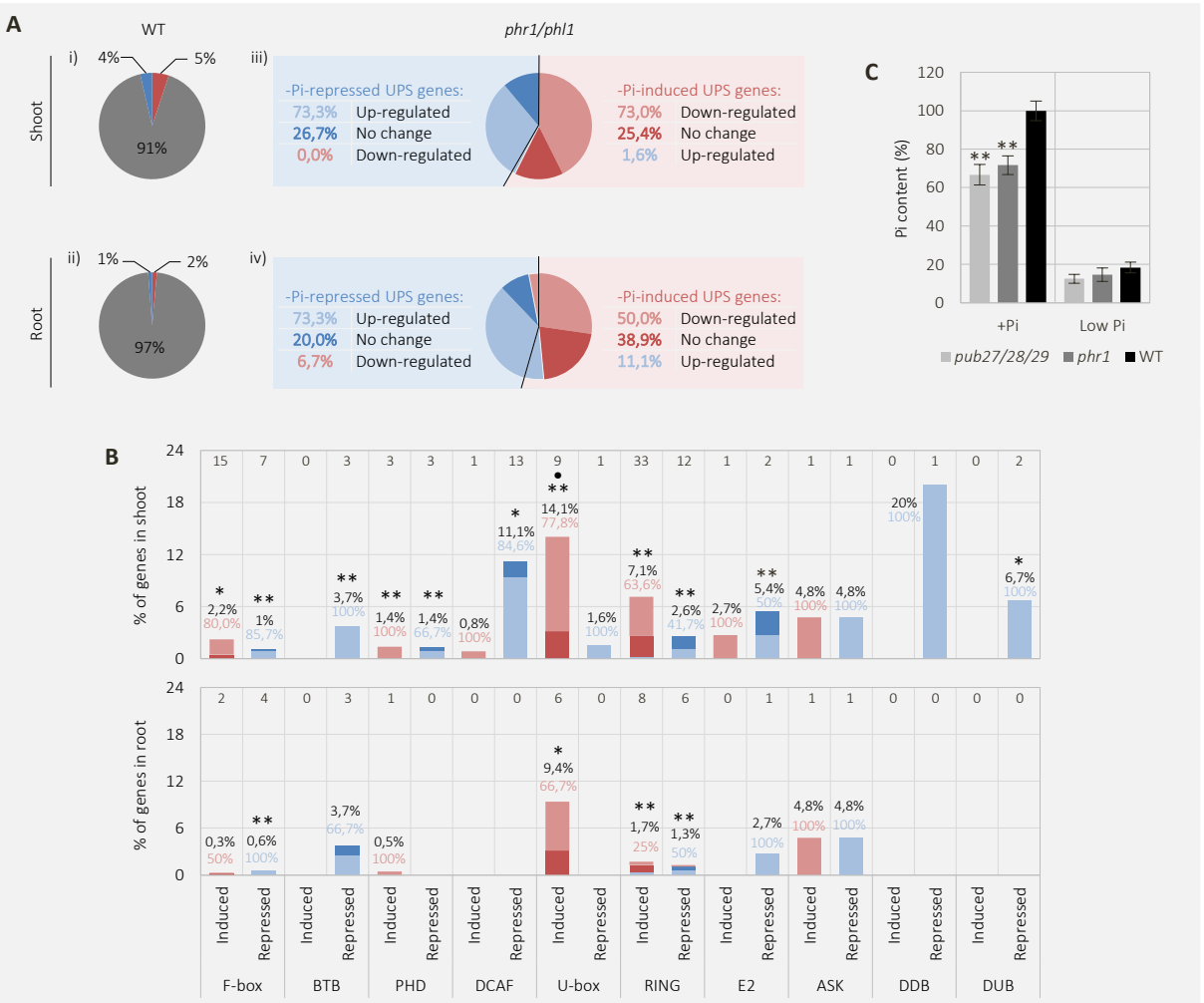

Figure 10. Phosphate Controlled E3 UB ligases. (A) Proportion illustrations of the Pi-starvation responsive UPS genes, that are induced (red slice) or repressed (blue slice) in response to –Pi, in (i and iii) wild-type (WT) and (ii and iv) *phr1/phl1* shoots (top) and roots (bottom). In ii and iv, changes in the transcriptional behavior due to *phr1/phl1* mutation are color-coded (see Conventions box), and percentages are relative to the number of induced or repressed UPS genes in WT in response to –Pi. **(B)** Percentages (%) of UPS genes, distributed in gene super-families, induced (red-scale bars) and repressed (blue-scale bars) in WT shoot and root, after 7 d of Pi-deficiency. Percentages are relative to the number of genes represented in the ATH1 array for each super-family (black % value). Absolute values on top. Changes in transcriptional behavior due to the double mutant *phr1/phl1* are represented in different colors (see Conventions box), and as percentages relative to the number of genes induced or repressed in WT in response to –Pi (red or blue % value) for each super-family. Two different cut-off values were used for WT and mutants (2× and FDR < 0.05 and 1.5× and FDR < 0.1 for WT and *phr1/phl1*, respectively). Data from Bustos *et al.*, 2010. **(C)** Pi content of shoots of 7-d-old seedlings grown in low Pi (50 µM KH_2PO_4/K_2HPO_4) and +Pi (500 µM KH_2PO_4/K_2HPO_4) solid Johnson media. Pi content is represented as percentage (%) relative to WT in +Pi. Color codes represent the three different genotypes used: *pub27/28/29*, *phr1* and Col-0. Values and error bars are means ± SD. Figure modified from Rojas-Triana *et al*. 2013. Statistical significance was determined by **(B)** binomial distribution analysis (•) (p<0,01) and by **(B-C)** t-test [(∗) (p<0,05); (**) (p<0,01)].

In assessing the transcriptional control of PHR/PHL1 TFs over the expression of -Pi-responsive UPS components, their transcript levels in the *phr1/phl1* mutant background were analyzed in comparison with those found in WT in response to -Pi. Changes on the transcriptional behavior of the -Pi-responsive UPS genes were extensively found in both shoot and root of *phr1/phl1* mutants. As exposed in Figure 10-A-iii-iv, in *phr1/phl1* more than 70% of the repressed-Pi-responsive UPS genes in both shoot and root, and 73% and 50% of the -Pi induced UPS genes in shoot and root, respectively, shown an inversion in their transcriptional behavior (from repression to up-regulation, and from induction to down-regulation).

By comparison of the overall transcriptional behavior of the -Pi-responsive members of each UPS gene super-families in *phr1/phl1* and WT lines, a significant control by PHR1/PHL1 TFs over Pi-starvation-responsiveness of the F-box, BTB, PHD, DCAF, U-box, E2 and DUB families, was found (Student's *t* test; Figure 10-B).

In order to further assess the relevance of the UPS system in the control of Pi signaling, weak *cul1–6* and *cul3*^{hyp} Arabidopsis mutant lines were used (Figure 11-A).

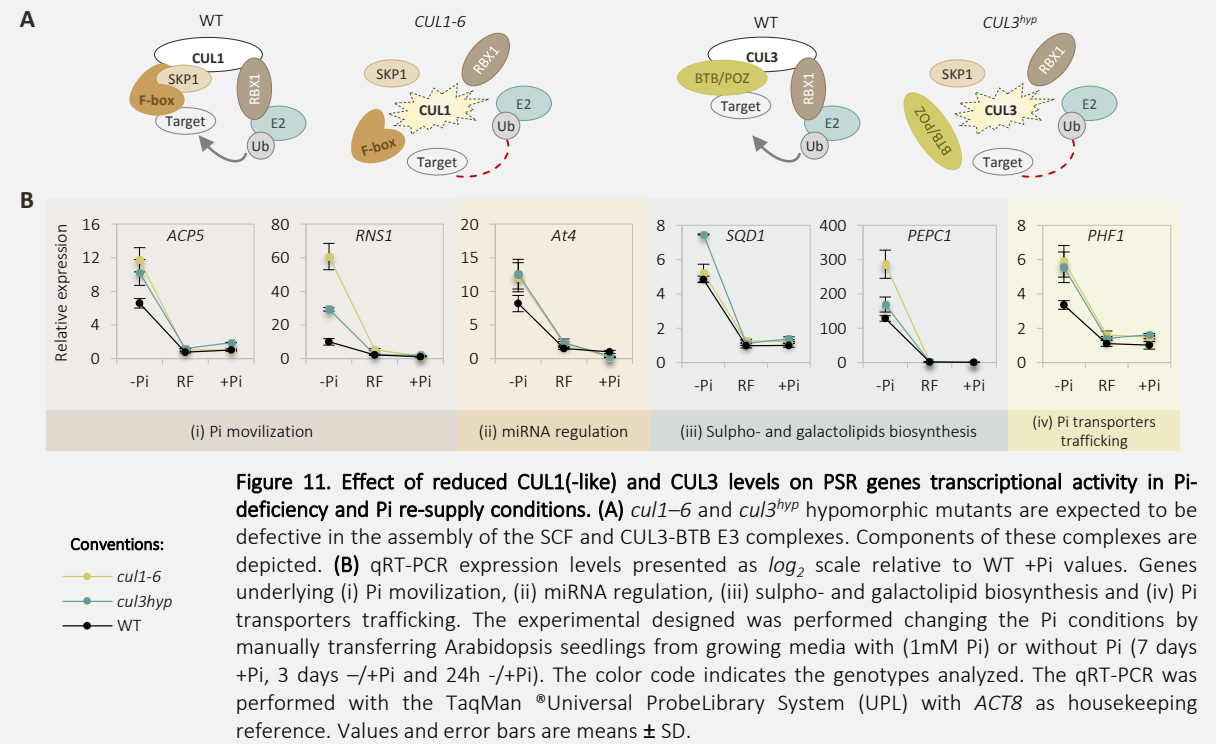

Figure 11. Effect of reduced CUL1(-like) and CUL3 levels on PSR genes transcriptional activity in Pi-deficiency and Pi re-supply conditions. (A) *cul1–6* and *cul3*^{hyp} hypomorphic mutants are expected to be defective in the assembly of the SCF and CUL3-BTB E3 complexes. Components of these complexes are depicted. **(B)** qRT-PCR expression levels presented as log_2 scale relative to WT +Pi values. Genes underlying (i) Pi movilization, (ii) miRNA regulation, (iii) sulpho- and galactolipid biosynthesis and (iv) Pi transporters trafficking. The experimental designed was performed changing the Pi conditions by manually transferring Arabidopsis seedlings from growing media with (1mM Pi) or without Pi (7 days +Pi, 3 days –/+Pi and 24h -/+Pi). The color code indicates the genotypes analyzed. The qRT-PCR was performed with the TaqMan ®Universal ProbeLibrary System (UPL) with *ACT8* as housekeeping reference. Values and error bars are means ± SD.

cul1–6, cul3^{hyp} and WT lines were grown during 7 days in +Pi (1mM KH_2PO_4/K_2HPO_4) and then transferred to +Pi/-Pi solid media. Three days after, a re-feeding treatment was performed for 24h to the Pi starved plants.

Using those seedlings, an analysis of transcript accumulation was conducted by qRT-PCR, monitoring highly-Pi-inducible genes (*PURPLE ACID PHOSPHATASE 17* or *ACP5*; *RIBONUCLEASE 1*, *RNS1*; *INDUCED BY PI STARVATION 2* or *AT4*, ; *SULFOQUINOVOSYLDIACYLGLYCEROL 1*, *SQD1*; *PHOSPHOETHANOLAMINE/PHOSPHOCHOLINE PHOSPHATASE 1*, *PEPC1*; *PHOSPHATE TRANSPORTER TRAFFIC FACILITATOR 1*, *PHF1*) involved in a pool of Pi limitation responses (Pi mobilization, miRNA regulation, sulpho- and galactolipids biosynthesis and Pi transporters trafficking; Figure 11-B). Both *cul1–6* and *cul3*^{hyp} hypomorphic mutants displayed higher transcript levels of PSR genes relative to WT seedlings under Pi-deficient conditions, but their responsiveness to Pi re-supply was as fast as in the WT (Figure 11-B).

6.1.1. KMD1-4 genes were selected for further analysis

A member of the F-box superfamily, At1g80440, was found to be down-regulated in response to Pi starvation in the root tissue, and to be tightly controlled by PHR1/PHR1 TFs. Thus, it act as repressor of Pi-starvation responses. At1g80440 transcript levels are repressed in the root tissue in-Pi and highly up-regulated in the double mutant *phr1/phl1*. Moreover, the close related genes At1g15670 and At3g59940 displayed a similar transcriptional behavior in response to Pi limiting conditions, so they were selected for further characterization. Following the nomenclature proposed by Kim and collaborators (2013) for the sub-family KISS ME DEADLY (KMD), At1g80440 was designated as KMD1 and its homologs At1g15670, At2g44130, and At3g59940 as KMD2, KMD3, and KMD4, respectively.

Table 3. *KMD1-4* transcriptional response to Pi starvation in WT and *phr1/phl1* lines according to an ATH1 Affymetrix microarray (Bustos *et al.*, 2010). Gene expression levels are represented as foldchange values relative to the +Pi levels.

		Shoot		Root	
AGI code	Name	WT	*phr1/phl1*	WT	*phr1/phl1*
At1g80440	*KMD1*	-1,18	3,73	-5,11	11,01
At1g15670	*KMD2*	1,18	-1,66	-3,58	3,02
At2g44130	*KMD3*	1,80	1,32	1,06	5,32
At3g59940	*KMD4*	1,15	1,16	-2,23	4,81

6.2. KMD1-4 ARE CONSERVED IN LAND PLANTS

In Arabidopsis, according with a phylogenetic reconstruction of the 694 potential F-box proteins reported by Gagne and collaborators (2002), KDM1-4 are located within the FKBs, and are forming a close subcluster with two main branches: (i) KMD1-2 and (ii) KMD3-4 (Figure 12-A). This inner subcluster linkage was confirmed by an un-rooted tree generated using the Jukes-Cantor genetic distance model and Neighbor-joining (NJ) tree build method (Figure 12-B). The percentages of identity in each branch were determined by local alignments based on the Smith-Waterman algorithm (cost matrix Blosum62): KMD1-2 shared 67% of identity, and KMD3-4 shared 62% of identity (Figure 12-B). The percentage of identity between the four members of the subcluster was determine using a multiple alignment based on the MUSCLE method (Multiple Sequence Comparison by Log-Expectation; Edgar, 2004; Supplemental Figure 1), and it was calculated close to a 35%.

On a wider scenario, insights on the evolution of KMDs in land plant species can be taken from a study presented by Schumann and collaborators (2011), in which a reconstruction of FBKs phylogeny was conducted, using the full-length aa sequences of FBKs from seven land plant species, including lower land plants like the bryophyte *Physcomitrella patens* (*P. patens*) and the lycophyte *Selaginella moellendorffii* (*S. moellendorffii*), the monocots *Oriza sativa* (*O. sativa*) and *Sorghum bicolor* (*S. bicolor*), and the eudicots *Arabidopsis thaliana* (*A. thaliana*), *Populus trichocarpa* (*P. trichocarpa*) and *Vitis vinifera* (*V. vinifera*). The reconstruction was based on neighbor-joining (NJ) methods, and was rooted with the only FBK identified in the single-celled green alga *Chlamydomonas reinhardtii* (*C. reinhardtii*) and with an unique human FBK (Sun *et al*., 2009). Noticeably, that there were no FBKs identified in the fresh water green algae Charophyceae family that is believed to represent the most recent common ancestor of land plants (Kenrick & Crane, 1997).

Inside the resulting phylogeny, KMD1-4 are grouped in a super-clade composed by one ancient and two stable clades, with no other Arabidopsis FKBs and with close putative orthologs within the eudicots *P. trichocarpa* and *V. vinifera*. Clear putative monocot orthologs grouped with KMDs, although KMD3-4 orthologs locate a little more distant than KMD1-2 orthologs. In the ancient clade, a putative KMD ortholog from the lower plant *S. moellendorffii* is found.

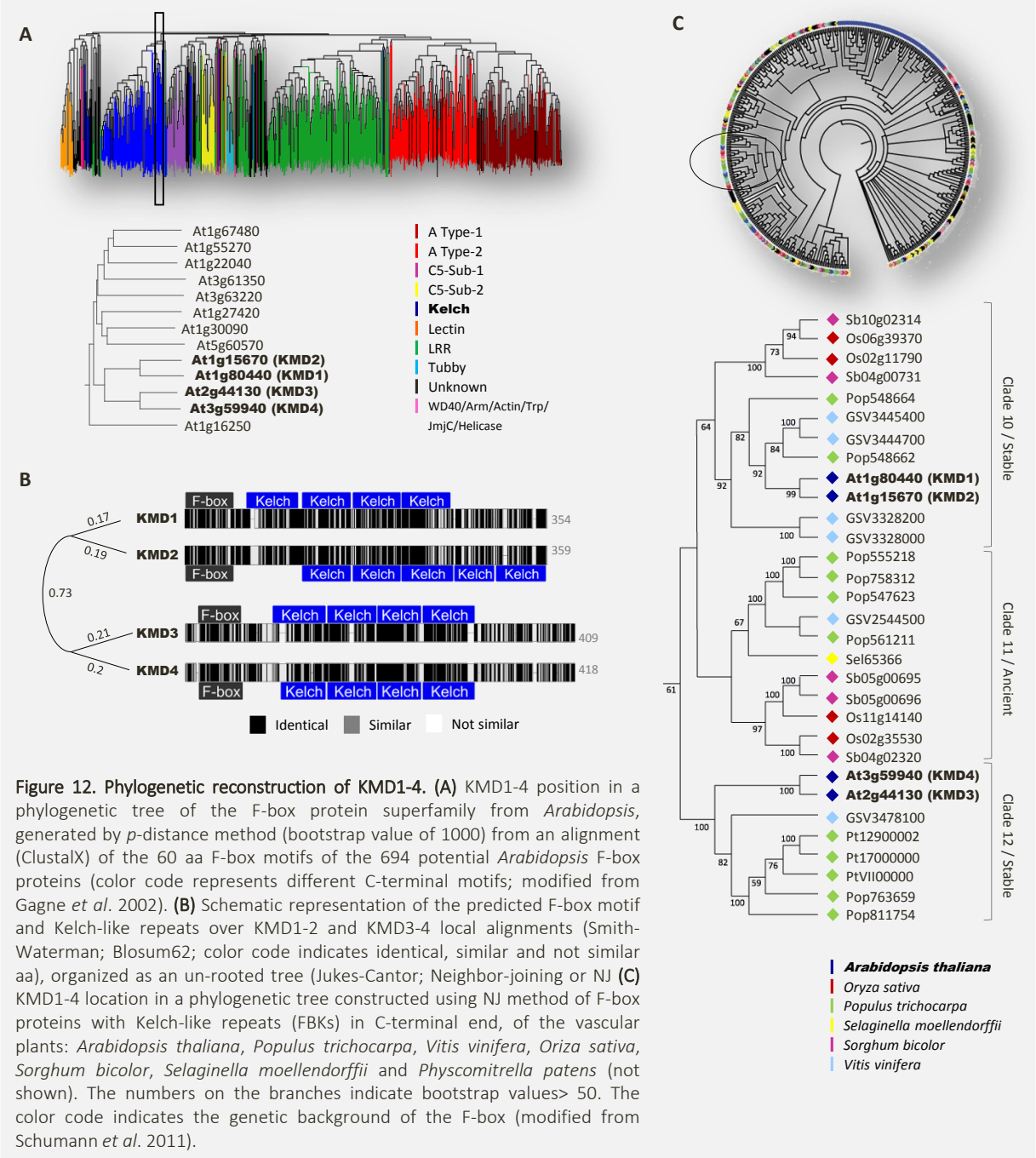

Figure 12. Phylogenetic reconstruction of KMD1-4. (A) KMD1-4 position in a phylogenetic tree of the F-box protein superfamily from *Arabidopsis*, generated by *p*-distance method (bootstrap value of 1000) from an alignment (ClustalX) of the 60 aa F-box motifs of the 694 potential *Arabidopsis* F-box proteins (color code represents different C-terminal motifs; modified from Gagne *et al*. 2002). **(B)** Schematic representation of the predicted F-box motif and Kelch-like repeats over KMD1-2 and KMD3-4 local alignments (Smith-Waterman; Blosum62; color code indicates identical, similar and not similar aa), organized as an un-rooted tree (Jukes-Cantor; Neighbor-joining or NJ **(C)** KMD1-4 location in a phylogenetic tree constructed using NJ method of F-box proteins with Kelch-like repeats (FBKs) in C-terminal end, of the vascular plants: *Arabidopsis thaliana*, *Populus trichocarpa*, *Vitis vinifera*, *Oriza sativa*, *Sorghum bicolor*, *Selaginella moellendorffii* and *Physcomitrella patens* (not shown). The numbers on the branches indicate bootstrap values> 50. The color code indicates the genetic background of the F-box (modified from Schumann *et al*. 2011).

Putative orthologs of *KMD1-4* genes have been annotated in a wide range of angiosperms, and examples can be mention from widely studied eudicots as grape (*V. vinifera*), medicago (*Medicago truncatula*) and soybean (*Glycine max*), and from monocots of high economic interest like maize (*Zea mays*) and rice (*O. sativa*) (Table 3).

Table 3. *KMD1-4* putative ortholog genes in grape (*Vitis vinifera*), maize (*Zea mays*), medicago (*Medicago truncatula*), rice (*Oriza sativa*) and soybean (*Glycine max*), according to the Database of Plants Ubiquitin Proteasome System (http://bioinformatics.cau.edu.cn/plantsUPS/). Gene models and % of identity are presented.

	GRAPE	MAIZE	MEDICAGO	POPLAR	RICE	SOYBEAN
KMD1	GSVIVP00034454001	AC200122.4_FG011	AC150706_11.4	eugene3.00011103	LOC_OS06G39370.1	GLYMA07G03860.1
	50.3%	39.7%	40.1%	49.7%	38.8%	52.1%
KMD2	GSVIVP00034454001	AC200122.4_FG011	AC150706_11.4	eugene3.00011103	LOC_OS06G39370.1	GLYMA07G03860.1
	48.9%	36.9%	34.9%	51.8%	39.7%	51.9%
KMD3	GSVIVP00034781001	AC183504.4_FG015	AC150706_11.4	fgenesh4_pg.C_LG_VII000004	LOC_OS11G14140.1	GLYMA05G28820.1
	42.4%	41.4%	39.2%	47.9%	40.1%	37.8%
KMD4	GSVIVP00034781001	AC183504.4_FG015	AC150706_11.4	fgenesh4_pg.C_LG_VII000004	LOC_OS11G14140.1	GLYMA05G28820.1
	41.6%	35.1%	34.1%	49.5%	34.7%	34.8%

For KMD1-4 aa primary structure, two main features are predicted: a F-box motif and Kelch repeats (Figure 12-B). The F-box motif is located at the N-terminal region, in between positions 2-49 for KMD1 and KMD2, 17-63 for KMD3, and 14-61 for KMD4 (Supplemental Figure 1). The *in silico* secondary structure prediction for this regions, performed with RaptorX (Kallberg et al. 2012; http://raptorx.uchicago.edu/), shows the presence of alpha helical secondary structures, with a high percentage probability value (Supplemental Figure 2).

The Kelch repeats are located at the C-terminus of the F-box motif. The primary structure of KMDs indicates that while KMD1, KMD3 and KMD4 contain four predicted Kelch repeats, KMD2 has an extra fifth Kelch repeat (Figure 12-A). Kelch repeats are covering a wide region between positions 63-263 for KMD1, 119-358 for KMD2, 98-300 for KMD3, and 104-314 for KMD4 (Supplemental Figure 1). This region, that spans most of KMDs protein sequence, displayed predicted consecutive beta strand secondary structures, according to high percentage probability values (Supplemental Figure 2). In concordance, the Kelch repeats domain in KMD1-4 more likely displays a tertiary β-propeller structure with the blades arranged around a central axis (Supplemental Figure 3). Regarding the KMD1-4 three-dimensional (3-D) structure prediction, performed with the protein structure homology-modelling server SWISS-MODEL (Arnold *et al.*, 2006; Guex *et al.*, 2009; Kiefer *et al.*, 2009; http://swissmodel.expasy.org/), it's worth noting that while KMD1, KMD3 and KMD4 showed higher GMQE (Global Model Quality Estimation; see 5.9.4. Protein terciary structure reconstructions) score values in reconstructions

according to the crystal structure of a Kelch protein from *Plasmodium falciparum* (template 4yy8.1). However, KMD2 reconstruction was more reliable when based on the crystal structure of a thiocyanate-forming protein (Ta-TFP) from *Thlaspi arvense* (field penny-cress; Brassicaceae), a Kelch protein Involved in glucosinolate breakdown (templates 5a11.1/5a.10.1; Gumz *et al*. 2015; Supplemental Figure 3).

6.3. *KMD1-4* SPATIO-TEMPORAL EXPRESSION PATTERNS

To evaluate whether potential sub-functionalization and/or partial functional redundancy exist between *KMD1-4*, *KMD1-4* transcriptional patterns and expression correlation were first analyzed.

For this, i*n silico* and own experimental data were obtained in order to determine *KMD1-4* transcript accumulation levels in different plant tissues and developmental stages, and in response to different abiotic perturbations.

6.3.1. *KMD1-4* gene expression correlation analysis

A co-expression analysis was performed taking advantage of the overall collection of gene expression data available on the Perturbations tool of the Genevestigator data base (https://genevestigator.com), using each of the four KMDs as queries (Figure 13-A). A pool of perturbations related with biotic and abiotic stimuli are grouped on the Perturbations category, including the following sub-categories: biotic, chemical, elicitor, hormone, light intensity, light quality, nutrient, other (callus formation, germination, CO_2 treatments, among others), photoperiod, stress, temperature and genetic background. When *KMD1*, *KMD3* and *KMD4* were used as queries, the other *KMD*s were found, with the exception of *KMD2*, on the top of the list of the most positively correlated genes (Figure 13-A). For *KMD1*, *KMD4* was found in position 7 and *KMD3* in position 12 (Figure 13-A-i), for *KMD3*, *KMD1* was found in position 1 and *KMD4* in position 3 (Figure 13-A-iii), and for *KMD4*, *KMD1* was found in position 3 and *KMD3* in position 28 (Figure 13-A-iv). In none of the above mentioned analysis *KMD2* was listed. Moreover, when *KMD2* was used as query, only *KMD1* was found in the distant position 60, with a low Pearson's correlation coefficient (*r*-value 0,45) (Figure 13-A-ii).

Keeping in mind the importance on the datasets selection to find co-expressed genes, a finer analysis was conducted selecting specific datasets for different types of perturbations, and co-expression analysis between the *KMD*s was conducted, based on the Pearson's correlation coefficient (Figure 13-B). For that, Genevestigator's experiments with *KMD*s gene expression values with *p*-values <0,05 were selected.

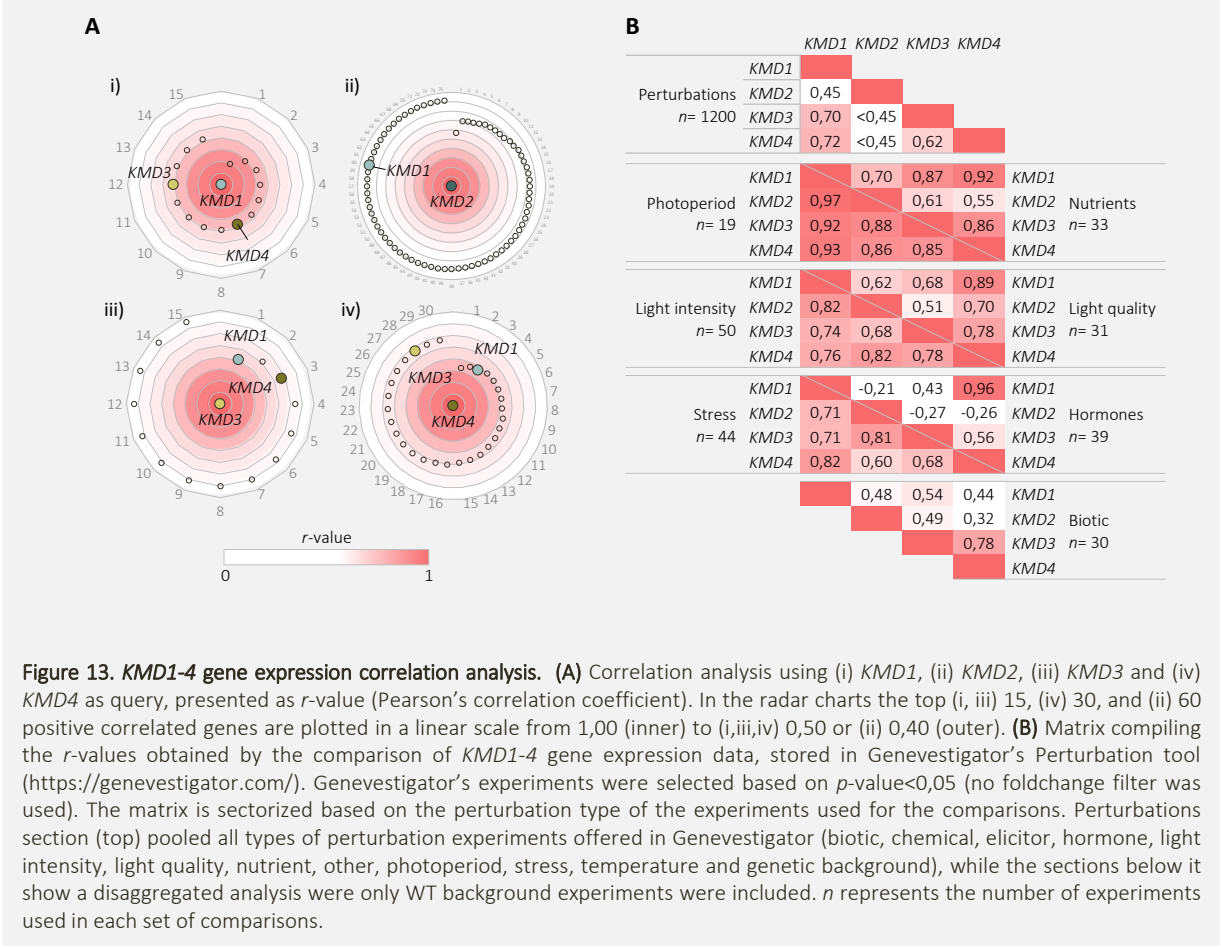

Figure 13. *KMD1-4* gene expression correlation analysis. **(A)** Correlation analysis using (i) *KMD1*, (ii) *KMD2*, (iii) *KMD3* and (iv) *KMD4* as query, presented as *r*-value (Pearson's correlation coefficient). In the radar charts the top (i, iii) 15, (iv) 30, and (ii) 60 positive correlated genes are plotted in a linear scale from 1,00 (inner) to (i,iii,iv) 0,50 or (ii) 0,40 (outer). **(B)** Matrix compiling the *r*-values obtained by the comparison of *KMD1-4* gene expression data, stored in Genevestigator's Perturbation tool (https://genevestigator.com/). Genevestigator's experiments were selected based on *p*-value<0,05 (no foldchange filter was used). The matrix is sectorized based on the perturbation type of the experiments used for the comparisons. Perturbations section (top) pooled all types of perturbation experiments offered in Genevestigator (biotic, chemical, elicitor, hormone, light intensity, light quality, nutrient, other, photoperiod, stress, temperature and genetic background), while the sections below it show a disaggregated analysis were only WT background experiments were included. *n* represents the number of experiments used in each set of comparisons.

KMD1-4 gene expression patterns highly correlated in response to photoperiod perturbations with *r*-values greater than 0.86, and *KMD1*, *KMD3* and *KMD4* patterns also highly correlated in response to different nutritional treatments (*r*-values > 0,85) (Figure 13-B).

Moreover, *KMD1* and *KMD4* shared a high Pearson's correlation coefficient of 0.96 in response to different phyto-hormone treatments, and that correlation seems to be specific for this two members of the *KMD*s cluster.

6.3.2. *KMD1-4* expression in different plant tissues

With the aim to analyze *KMD1-4* transcript accumulation in different plant tissues, WT plants were grown in full nutrition (FN) medium and *KMD1-4* gene expression was determined by RT-qPCR in shoot and root tissues. In addition, an *in silico* search using the Genevestigator Anatomy tool, provided *KMD1-4* levels of expression data as signal intensity values, in a collection of ATH1 Affymetrix microarrays hybridized with RNA samples from callus, seedling, inflorescence, shoot and root of WT plants (Figure 14-B). This data is congruent and, in consequence, supports the experimental results obtained.

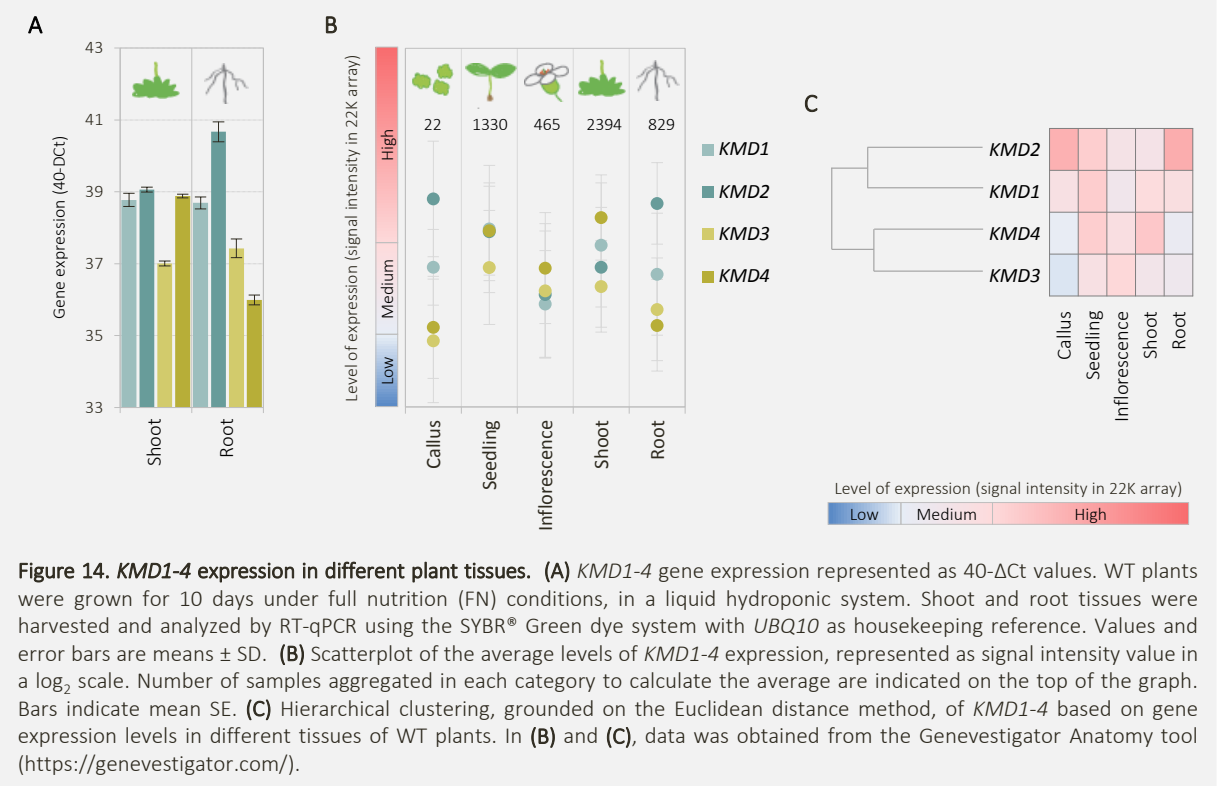

Figure 14. *KMD1-4* expression in different plant tissues. **(A)** *KMD1-4* gene expression represented as 40-ΔCt values. WT plants were grown for 10 days under full nutrition (FN) conditions, in a liquid hydroponic system. Shoot and root tissues were harvested and analyzed by RT-qPCR using the SYBR® Green dye system with *UBQ10* as housekeeping reference. Values and error bars are means ± SD. **(B)** Scatterplot of the average levels of *KMD1-4* expression, represented as signal intensity value in a $\log_2$ scale. Number of samples aggregated in each category to calculate the average are indicated on the top of the graph. Bars indicate mean SE. **(C)** Hierarchical clustering, grounded on the Euclidean distance method, of *KMD1-4* based on gene expression levels in different tissues of WT plants. In **(B)** and **(C)**, data was obtained from the Genevestigator Anatomy tool (https://genevestigator.com/).

KMD1-4 are constitutive expressed in both, root and shoot, but in a different extent (Figure 14-A-B). More in detail, the expression levels of the *KMD1-2* branch are higher in comparison to the *KMD3-4* branch (Figure 14-C), being particularly evident in the root tissue, where *KMD2*, and *KMD3-4* expression can be considered high and medium-low, respectively (Figure 14-A-B). While in the shoot the expression patterns are similar, with the exception of the low levels of *KMD3*, in the root *KMD1-4* expression patterns were heterogeneous (Figure 14-A-

B). Worth noting is that, while *KMD1* and *KMD3* transcript detection is similar between root and shoot, there is a clear differential transcript accumulation pattern between tissues for *KMD2* and *KMD*4. While *KMD2* transcripts are more abundant in the root tissue than in the shoot, the opposite is the case for *KMD4* transcripts that are more abundant in the shoot than in the root (Figure 14-A-B).

Interestingly, according to Genevestigation data, *KMD1-4* transcript accumulation in the callus, resembles the heterogeneous behavior and intensity of *KMD1-4* transcriptional expression in the root tissue (Figure 14-B).

6.3.3. *KMD1-4* expression in different developmental stages

With the porpoise of analyzing *KMD1-4* transcripts convergence during the development of the plant, advantage was taken from the Development tool of the Genevestigator database. *KMD1-4* gene expression signal intensity values were obtained from ATH1 Affymetrix microarrays hybridized with RNA samples from ten different developmental stages, comprised between 1 and > 50 days old, as follow: germinated seed (1-6 days), seedling (6-14 days), young rosette (14-18 days), developed rosette (18-21 days), bolting (21-25 days), young flower (25-29 days), developed flowers (29-36 days), flowers and siliques (36-45 days), mature siliques (45-50 days) and senescent plants (>50 days) (Figure 15).

KMD1-4 expression levels seems to be homogenous along the development of the plant until the development of the mature siliques, represented by similar signal intensity values along development for each gene (Figure 15-A), and a clear clustering of a the developmental stages in a single branch, as a result of a hierarchical clustering grounded on the Euclidean distance method (Figure 15-B). In this period, between day 1 and 50, *KMD1*, *KMD2* and *KMD4* displayed similar high signal intensity values, while *KMD3* appeared with lower absolute levels of expression into the medium range (Figure 15-A).

During the senescence of the plant, a striking heterogeneity is displayed at the transcriptional level by *KMD*s, characterized by a high peak of *KMD4* expression, and the lower signal intensity values during development for *KMD2* and *KMD3*. In consequence, the senescence stage is the unique distant outer branch in a combined hierarchical clustering, suggesting a putative functional diversification after day 50 of development for *KMD* genes (Figure 15-B).

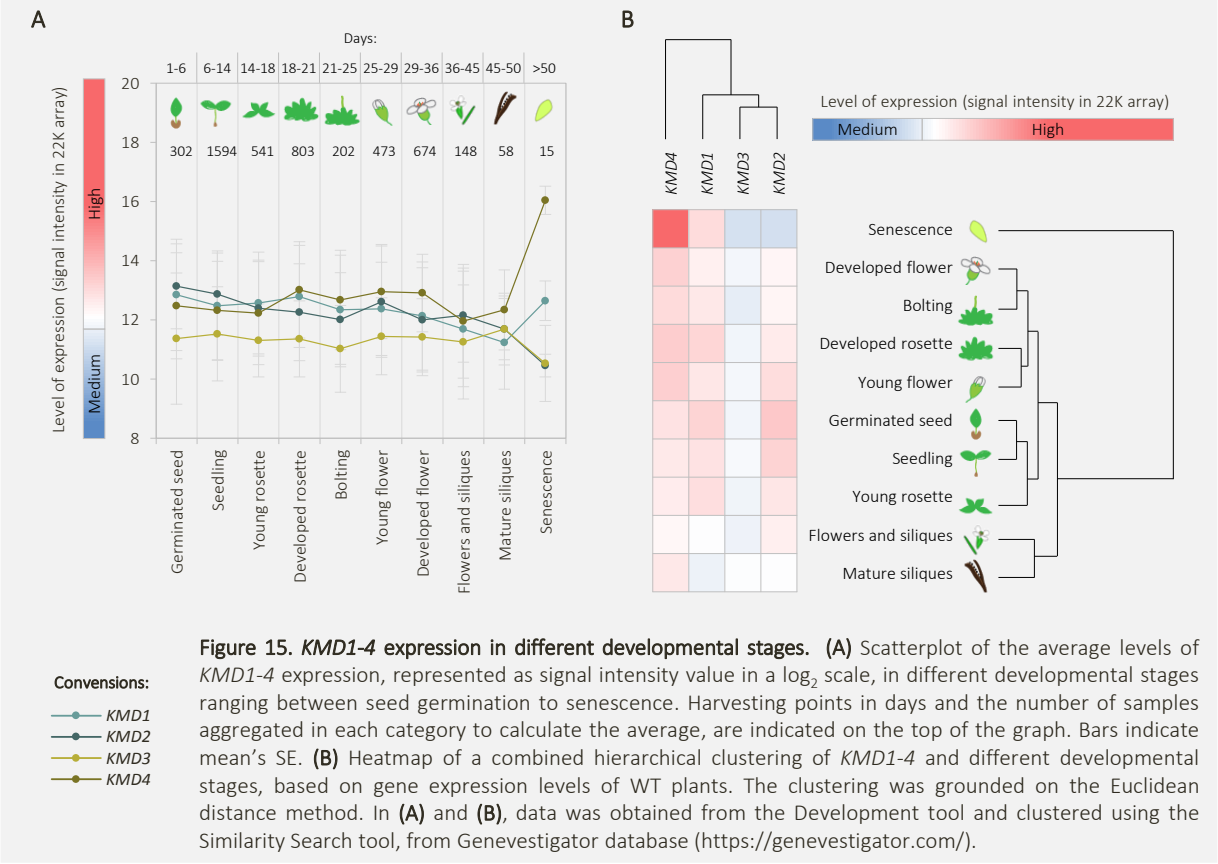

Figure 15. *KMD1-4* expression in different developmental stages. **(A)** Scatterplot of the average levels of *KMD1-4* expression, represented as signal intensity value in a $\log_2$ scale, in different developmental stages ranging between seed germination to senescence. Harvesting points in days and the number of samples aggregated in each category to calculate the average, are indicated on the top of the graph. Bars indicate mean's SE. **(B)** Heatmap of a combined hierarchical clustering of *KMD1-4* and different developmental stages, based on gene expression levels of WT plants. The clustering was grounded on the Euclidean distance method. In **(A)** and **(B)**, data was obtained from the Development tool and clustered using the Similarity Search tool, from Genevestigator database (https://genevestigator.com/).

6.3.4. *KMD1-4* expression in response to different nutritional stresses

In order to get insights about *KMD1-4* transcriptional response to Pi-related nutrients starvation, a nutrient deficiency experiment was carried out in a hydroponic system (Figure 16-A-B). For this, WT seedling were grown for seven days either in full nutrition (FN), low Pi or low nitrogen (N) conditions, and after the seedlings were treated for three days with-Pi,-N,-sucrose (-Suc) and FN mediums (experimental design on Figure 16-B). *KMD1-4* gene expression was determined by RT-qPCR in total seedling tissue.

Additionally, an *in silico* search using the nutrients dataset on the Genevestigator's Perturbations tool, provided *KMD1-4* gene expression as fold-change values relative to a control condition, in a collection of ATH1 Affymetrix microarrays hybridized with RNA samples from treatments with different nutrients like ion (Fe), potassium (K), Pi, sulfur (S) and the carbohidrates glucose (Glu) and Suc.

In this context, *KMD1-4* transcriptional response to nutritional stresses is not specific for Pi limitation (see 6.1. Phosphate Controlled E3 Ub Ligases) because, in fact, *KMD1*-4 mRNA levels of accumulation are positively responsive to Fe and Glu/Suc limitation treatments, and repressed by N starvation (Figure 16). When comparing the transcriptional responses between the *KMD*s, it is worth noting that *KMD1* displayed the stronger transcriptional response to nutrient perturbations, while *KMD2* seems to be the less responsive one (Figure 16-C).

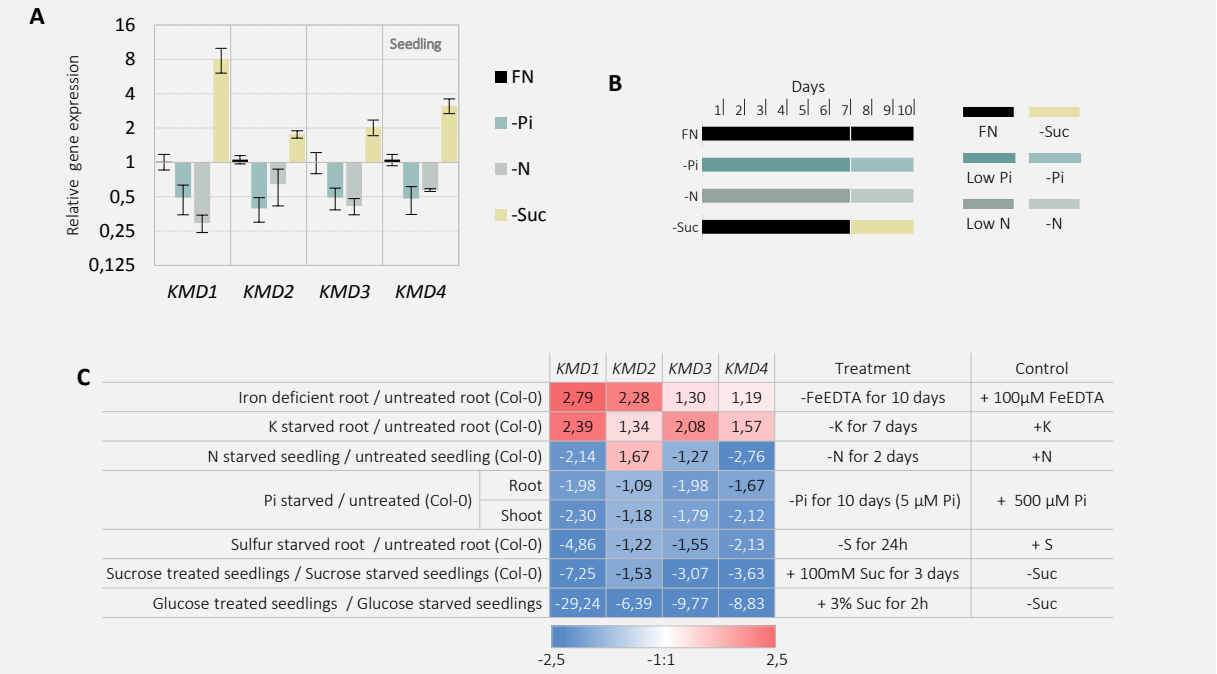

C

		KMD1	KMD2	KMD3	KMD4	Treatment	Control
Iron deficient root / untreated root (Col-0)		2,79	2,28	1,30	1,19	-FeEDTA for 10 days	+ 100µM FeEDTA
K starved root / untreated root (Col-0)		2,39	1,34	2,08	1,57	-K for 7 days	+K
N starved seedling / untreated seedling (Col-0)		-2,14	1,67	-1,27	-2,76	-N for 2 days	+N
Pi starved / untreated (Col-0)	Root	-1,98	-1,09	-1,98	-1,67	-Pi for 10 days (5 µM Pi)	+ 500 µM Pi
	Shoot	-2,30	-1,18	-1,79	-2,12		
Sulfur starved root / untreated root (Col-0)		-4,86	-1,22	-1,55	-2,13	-S for 24h	+ S
Sucrose treated seedlings / Sucrose starved seedlings (Col-0)		-7,25	-1,53	-3,07	-3,63	+ 100mM Suc for 3 days	-Suc
Glucose treated seedlings / Glucose starved seedlings		-29,24	-6,39	-9,77	-8,83	+ 3% Suc for 2h	-Suc

-2,5 -1:1 2,5

Figure 16. *KMD1-4* expression in response to different nutritional stresses. (A) *KMD1-4* relative gene expression represented in a $\log_2$ scale, obtained by RT-qPCR using the SYBR® Green dye system with *UBQ10* as housekeeping reference. WT seedlings were grown for 10 days in a liquid hydroponic system, following the experimental design in **(B)**. Values and error bars are means ± SD. **(C)** Heatmap of *KMD1-4* gene expression in response to different nutritional stresses, **represented as foldchange values. Representative example experiments are presented, and were chosen based on foldchange values of 2x and *p*-value<0,05, from the Genevestigator's Pertubations tool (https://genevestigator.com/). For detailed information on the experimental designs see Supplemental table 1.**

6.3.4.1. KMD1-4 transcriptional response to Pi starvation

Nutrient starvation affects the whole plant, but the various organs are differentially exposed to the given stress. Since Pi uptake occurs exclusively by the root system, this is the first organ to sense the lack of Pi in the rhizosphere. It was therefore interesting to investigate the expression levels of *KMD1-4* in roots and shoots of seedlings grown in Pi-sufficient and Pi-starvation conditions (Figure 17).

To investigate the transcriptional effect of the Pi starvation during time, time course experiments were performed (Figure 17-A-B). For this, plants were grown in low Pi medium (20µM Pi) for seven days, followed by three –Pi-medium treatment harvesting points: 24h, 3 days and 7 days (experimental design in Figure 17-B).

In the root tissue *KMD1-4* were gradually repressed in correspondence to the decreasing availability of Pi in the medium during 7 days of Pi starvation (Figure 17-A). However, the kinetic of the Pi starvation transcriptional response in the shoot differs of the one on the root.

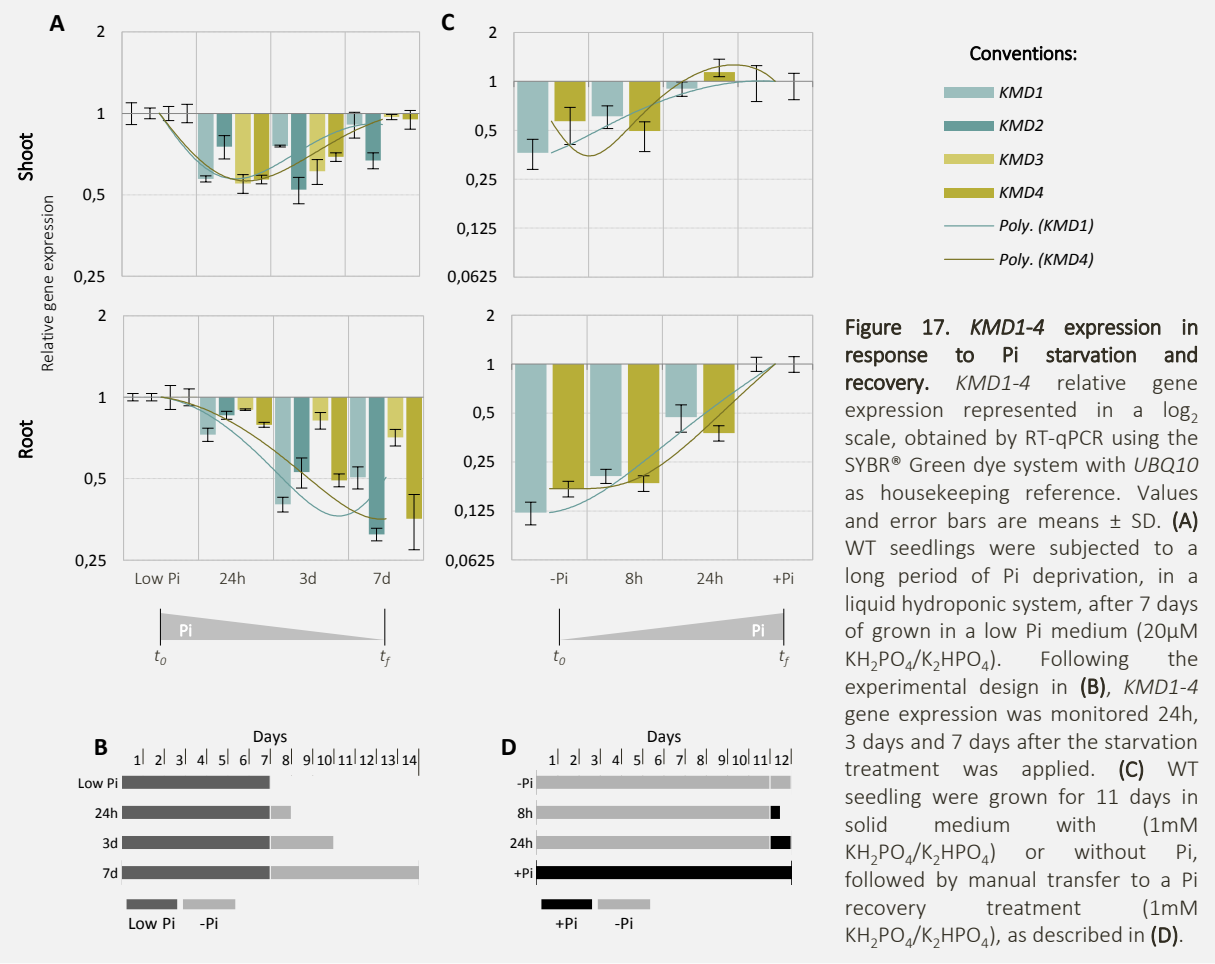

Figure 17. *KMD1-4* expression in response to Pi starvation and recovery. *KMD1-4* relative gene expression represented in a $\log_2$ scale, obtained by RT-qPCR using the SYBR® Green dye system with *UBQ10* as housekeeping reference. Values and error bars are means ± SD. **(A)** WT seedlings were subjected to a long period of Pi deprivation, in a liquid hydroponic system, after 7 days of grown in a low Pi medium (20µM KH_2PO_4/K_2HPO_4). Following the experimental design in **(B)**, *KMD1-4* gene expression was monitored 24h, 3 days and 7 days after the starvation treatment was applied. **(C)** WT seedling were grown for 11 days in solid medium with (1mM KH_2PO_4/K_2HPO_4) or without Pi, followed by manual transfer to a Pi recovery treatment (1mM KH_2PO_4/K_2HPO_4), as described in **(D)**.

In the shoot tissue, *KMD*s transcription is repressed after 24h of -Pi, followed by a reversal of the transcriptional repression between 24h and 3 days for *KMD1*, *KMD3* and *KMD4*, and after 3 days for *KMD2* (Figure 17-A). This result is indicating that after a long period of Pi starvation (7 days according to the proposed experimental design), *KMD1*-4 transcript levels in the shoot partially recover the abundance present during Pi

sufficient conditions of growth. Worth noting is that, after 24h of starvation the transcript levels in the shoot almost reached the minimum expression levels, indicating that it may play a role at an early stage of developing a Pi starvation response in the shoot. In contrast, the transcriptional response in the root tissue suggest that they may assume a role in persistent phosphate starvation in the root.

A fast recovery in the transcript levels after applying a reciprocal growth condition / treatment, indicates that the transcriptional control is condition / treatment specific or closely related.

In order to study the stimulus specificity of the *KMD*s transcriptional repression in response to Pi starvation, a re-feeding experiment was conducted (Figure 17-C-D). With this porpoise, plants were grown in –Pi solid medium for eleven days, followed by two Pi re-feeding treatment harvesting points: 8h and 24h (experimental design in Figure 17-D). *KMD1* and *KMD4* gene expression was determine, as representatives of the two main branches within the *KMD*s cluster.

Eight hours after Pi re-feeding, *KMD1* and *KMD4* transcript levels increased in both shoot and root. However, there is a delay of the recovery in the root compared with the shoot. After twenty four hours of Pi re-supply, while in the shoot *KMD1* and *KMD4* transcript levels fully recover the levels found in non-stress shoots, in the root the levels of gene expression are around half the levels found in the roots grown in full nutrition medium.

This findings are indicating that the transcriptional repression of *KMD*s is closely related to Pi starvation rather than to a general stress response, and are supporting the idea of a differential role of the *KMD*s transcript between the root and the shoot in the phosphate starvation response.

6.3.4.1.1. KMD1-4 are under the transcriptional control of the TFs PHR1/PHL1

The MYB transcriptional factors PHR1/PHL1 are required for the regulation of a mayor number of Pi-starvation responsive (PSR) genes. Due to the key role of PHR1/PHL1 in the regulation of the Pi starvation response regulation, it was decisive to examine its relationship to the *KMD*s.

phr1/phl1 and WT seedlings were grown 7 days in FN and low Pi liquid mediums, and then subject to FN and-Pi treatments during 3 more days (Figure 18-B-C). By qRT-PCR, *KMD1-4* transcript accumulation was analyzed. The Pi-starvation transcriptional effect over *KMD1*, *KMD3* and *KMD4* is still conserved in the *phr1/phl1*, as shown by lower levels of *KMD1/3/4* expression in mutant plants grown in-Pi in comparison with mutants grown in +Pi (Figure 18-A-i-iii-iv). The transcriptional effect of PHR1/PHL1 mutations over *KMD1*, *KMD3* and *KMD4* is

represented by an up-regulation in both +Pi and-Pi conditions, however in a different extend for the three of them, especially during Pi limitation (Figure 18-A-i-iii-iv). In *phr1/phl1* grown in-Pi, *KMD*1 levels were higher than in the WT grown in +Pi, indicating an opposite transcriptional behavior (from repression in the WT to induction in *phr1/phl1*) (Figure 18-A-i). In the same direction, *KMD3* levels were similar than in the WT grown in +Pi (Figure 18-A-iii) and, even if *KMD4* levels were still repressed compare with the WT grown in +Pi, they were higher than in the WT grown in-Pi (Figure 18-A-iv).

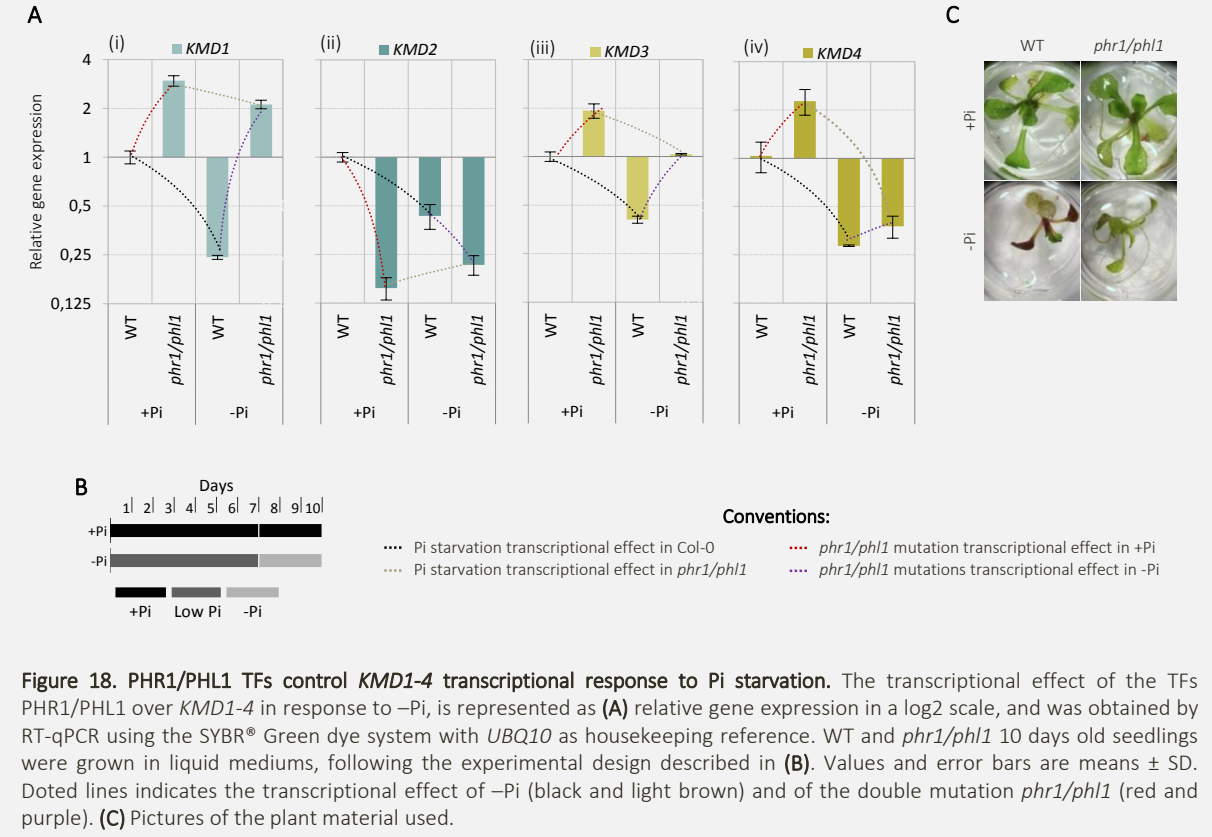

Figure 18. PHR1/PHL1 TFs control *KMD1-4* transcriptional response to Pi starvation. The transcriptional effect of the TFs PHR1/PHL1 over *KMD1-4* in response to –Pi, is represented as **(A)** relative gene expression in a log2 scale, and was obtained by RT-qPCR using the SYBR® Green dye system with *UBQ10* as housekeeping reference. WT and *phr1/phl1* 10 days old seedlings were grown in liquid mediums, following the experimental design described in **(B)**. Values and error bars are means ± SD. Doted lines indicates the transcriptional effect of –Pi (black and light brown) and of the double mutation *phr1/phl1* (red and purple). **(C)** Pictures of the plant material used.

In contrast, the Pi-starvation effect over *KMD2* transcription is disrupted in *phr1/phl1*. While *KMD2* is repressed in-Pi in WT background, in *phr1/phl1* plants, *KMD2* displayed higher levels of mRNA accumulation in-Pi than in +Pi, indicating a turning point in the transcriptional response to-Pi due to PHR1/PHL1 mutations. Moreover, PHR1/PHL1 transcriptional effect over *KMD2* is characterized by a down-regulation in both +Pi and-Pi conditions (Figure 18-A-ii).

The previous findings indicates that *KMD1-4* are downstream of the TFs PHR1/PHL1, and that PHR1/PHL1 has a differential regulatory effect over the *KMD*s. PHR1/PHL1 may be acting as negative transcriptional regulators of *KMD1*, *KMD3* and *KMD4*, and as a positive transcriptional regulator of *KMD2*. Furthermore, the clear transcriptional control over the *KMD*s by the -Pi regulation system exemplified by PHR1/PHL1 TFs, is making clear that *KMDs* transcriptional response to-Pi is involved in the adaptive response to Pi limitation, in detriment of been an unspecific stress response.

6.3.4.2. KMD1-4 transcriptional response to sucrose starvation

Given the facts that, the strongest transcriptional effect displayed by *KMD*s in response to a nutritional stress was found in sugars limitation (Glu and Suc), that there is a strong transcriptional correlation between the *KMD*s in photoperiod treatments close related with the carbohydrate availability, and that there is a positive bidirectional interaction between sugar and Pi starvation signaling (Franco-Zorrilla *et al*., 2005), a detailed characterization of *KMD1-4* expression in response to Suc starvation and recovery was conducted, as well as an *in silico* search of *KMD*s transcriptional response to different light/darkness treatments.

With that purpose, WT seedlings were grown for 11 days in a liquid hydroponic system, following the experimental design in Figure 19-B, and *KMD1-4* gene expression was analyzed by qRT-PCR on total seedlings tissue (Figure 19-A).

*KMD*s are induced during Suc starvation, however in a different extend between them. While *KMD1* displayed the strongest transcriptional response to-Suc, *KMD2* showed the weakest one. After applying a reciprocal growth condition, *KMD*s displayed a progressive transcriptional repression, until one hour after the Suc recovery treatment was applied. After that minimum expression value point, *KMD*s expression begins to increase. Even if *KMD2* mRNA levels of accumulation seem to recover faster than those of *KMD1/3/4*, the initial lower-Suc-induced *KMD2* levels should be taken in consideration (Figure 19-A).

The previous findings are indicating that KMDs are -Suc inducible genes that responded rapidly to a reciprocal treatment in a repressive manner that is sustain after 3h of the Suc re-supply. As well as in the Pi starvation context, the transcriptional response after 30 minutes of *KMD*s, suggest a transcriptional control close related to the carbohydrates availability.

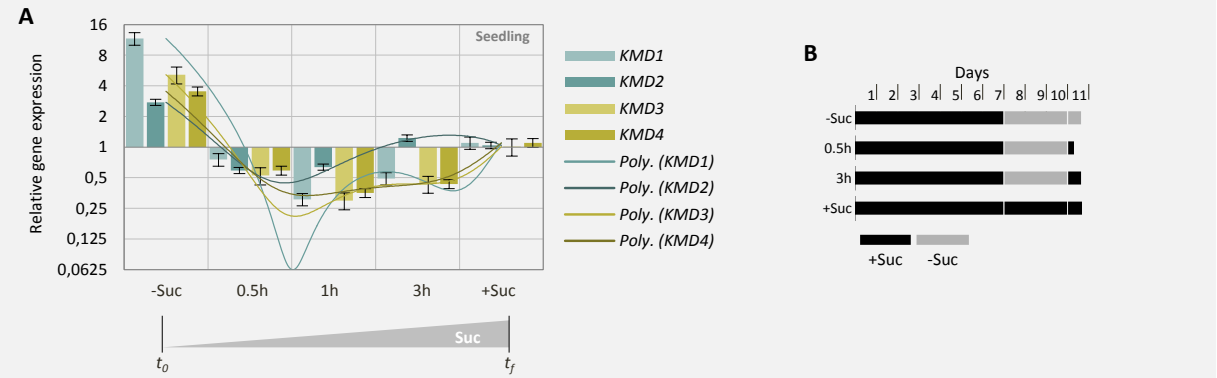

C

	KMD1	KMD2	KMD3	KMD4	Treatment	Control
Short day / long day grown seedlings (Col-0)	3,62	1,21	1,47	1,33	8h light / 16h dark	16h light / 8h dark
Long day / short day grown leafs (Col-0)	-10,96	-1,07	-4,57	-2,21	16h light / 8h dark	8h light / 16h dark
Night extension / untreated rosette (Col-0)	7,06	4,18	4,03	5,35	6 to 8h extended night	End of the night
Circadian clock: 18h dark / 6h dark shoots (Col-0)	4,98	4,31	4,09	4,21	18h darkness	6h darkness
Circadian clock: 17h dark+1h light / 18h dark shoots (Col-0)	-27,02	-8,94	-27,30	-10,44	17h darkness + 1h light	18h darkness

-2,5 -1:1 2,5

Figure 19. *KMD1-4* expression in response to sucrose starvation and recovery. (A) *KMD1-4* relative gene expression represented in a $\log_2$ scale, obtained by RT-qPCR using the SYBR® Green dye system with *UBQ10* as housekeeping reference. WT seedlings were grown for 11 days in a liquid hydroponic system, following the experimental design in **(B)**. Values and error bars are means ± SD. **(C)** Heatmap of *KMD1-4* gene expression in response to different photoperiod perturbations, represented as foldchange values. Representative example experiments are presented, and were chosen based on foldchange values of 2x and *p*-value<0,05, from the Genevestigator's Pertubations tool (https://genevestigator.com/). For detailed information on the experimental designs see Supplemental table 1.

Based on ATH1 Affymetrix microarray data from experiments designed with variable light/darkness conditions in WT background plants (Genevestigator database), *KMD1-4* transcript levels are up-regulated when light is not available for producing chemical energy, like in night extension or short day/long day treatments (Figure 19-C), which represents situations that mimics sugar limitation treatments. Consistent with the experimental results mentioned above, short light exposure after a long period of darkness and long day/ short day treatments, generate a fast repression of *KMD*s transcript levels (Figure 19-C), as is the output of the Suc re-feeding experiment (Figure 19-A).

6.3.5. KMD1-4 transcriptional response to different phytohormone exogenous supply

By means of studies on the cytokinin receptors, among others, is been establish a clear and intricate interconnection between cytokinin, sugar and Pi-starvation signaling (Franco-Zorrilla, *et al*., 2005). Considering the Pi- and Suc-starvation transcriptional responsiveness of *KMD*s, it was necessary to investigate the effect of cytokinins over *KMD*s gene expression. With that idea, WT plants were grown for 9 days under the two different adenine-type cytokinins kinetin and zeatin, and *KMD1-4* transcripts accumulation was analyzed by qRT-PCR (Figure 20-A).

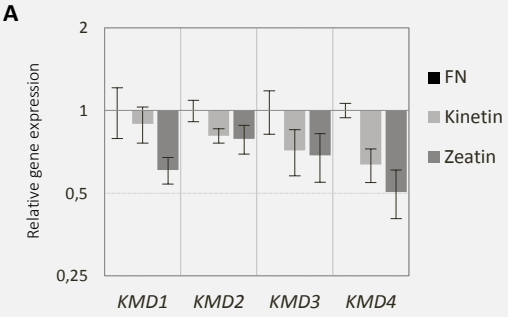

Figure 20. *KMD1-4* expression in response to different phytohormone exogenous supply. **(A)** *KMD1-4* relative gene expression represented in a $\log_2$ scale, obtained by RT-qPCR using the SYBR® Green dye system with *UBQ10* as housekeeping reference. WT seedlings were grown for 9 days in full nutrition (FN) solid medium without or with 100nM kinetin or zeatin. Plants grew in vertical position. Values and error bars are means ± SD. **(B)** Heatmap of *KMD1-4* gene expression in response to different phytohormone exogenous supplies, represented as foldchange values. Representative example experiments are presented, and were chosen based on foldchange values of 2x and *p*-value<0,05, from the Genevestigator's Pertubations tool (https://genevestigator.com/). For detailed information on the experimental designs see Supplemental table 1.

B

	KMD1	*KMD2*	*KMD3*	*KMD4*	Treatment	Control
BL treated cell culture / untreated cell culture	3,66	-15,14	2,84	2,04	+ 1µM BL for 6 days	Untreated
ABA treated guard cells / solvent treated guard cells (Col-0)	-3,83	-4,87	1,05	1,11	+ 50mM ABA for 3h	+ Ethanol for 3h
IAA treated seedlings / untreated seedling (Col-0)	-2,16	-1,27	-2,73	-2,91	+ 1µM IAA for 1h	Untreated
Zeatin treated seedlings / untreated seedlings (Col-0)	-2,48	-2,85	-2,18	-1,63	+ 20µM t-zeatin for 3h	Untreated

-2,5 -1:1 2,5

Expression of the four *KMD* genes are repressed in response to cytokinins enxogenous supply, however in a different extend between the different cytokinin forms tested (Figure 20-A). In this context, zeatin showed a stronger negative effect over the transcription of the *KMD*s in comparison with kinetin (Figure 20-A).

KMD1-4 are not exclusively responsive to cytokinins. According to a collection of transcriptomic experiments stored in the Genevestigator database, *KMD1-4* are also repressed by IAA exogenous supply. Interestingly, in response to ABA and brasinosteroids, there is a diversification of transcriptional responses within the *KMD*s. It is mainly represented by the ABA repression of *KMD1* and *KMD2*, and by the opposite transcriptional behavior among *KMD2* and *KMD1/3/4* in response to brassinolide exogenous supply (Figure 20-B).

6.4. EFFECT OF *KMD1*, *KMD2* AND *KMD4* ALTERED GENE EXPRESSION IN THE PHOSPHATE STARVATION PHYSIOLOGICAL RESPONSES

With the aim of identifying the effect of the altered expression of *KMD*s in some physiological responses to Pi limitation, and its link with sugars and cytokinins, mutants and over-expressor lines for *KMD*s were used as genetic tools.

Transfer DNA (T-DNA) insertion mutations were isolated for *KMD1*, *KMD2* and *KMD4* and homozygous T2 plants were obtained by segregation of T1 heterozygous parents obtained from the Salk collection (Figure 21-A-C). By cross-pollination, double *kmd1/2* and *kmd1/4* mutants were established and T2 homozygous lines were, in turn, cross-pollinated to generate *kmd1/2/4 triple* mutants. No full-length transcripts were detected for the respective *KMD*s in mutant alleles based on semiquantitative RT-PCR analysis (Figure 21-D-F), and no transcript amplicons displayed accumulation according to qRT-PCR analysis (Figure 21-G-I). These findings, plus the position of the T-DNA insertions (Figure 21-A-C), indicated that we have obtained null alleles. In the first instance, *kmd1/2*, *kmd1/4* and *kmd1/2/4* mutants showed no obvious changes in their overall appearance in comparison with WT plants (Figure 21-J).

As the main objective was to determine whether higher transcript levels of *KMD1* leads to differences compared to WT plants, over-expressor lines were selected on the basis of high transcript levels and further propagated through next generations. Two independent homozygous lines, oeKMD1-GFP-45 and oeKMD1-GFP-82, were selected for further characterization, based on the *KMD1* gene expression levels found by RT-qPCR in plants grown during 9 days in +Pi solid media (Figure 22-A). oeKMD1-GFP lines displayed *KMD1* transcript levels ranging from 10 (oeKMD1-GFP-45) to 20 (oeKMD1-GFP-82) times higher than the endogenous *KMD1* levels found in WT seedlings (Figure 22-A). oeKMD1-GFP-82 accumulates twice the amount of *KMD1* transcripts than oeKMD1-GFP-45, independently of the Pi and Suc availability in the growth media (Figure 22-A). This correlates with KMD1-GFP fusion accumulation levels, in both the shoot and the root tissues of these transgenic lines (Figure 22-B). In general terms, oeKMD1-GFP lines showed no obvious changes in their overall appearance in comparison with WT plants (Figure 22-C).

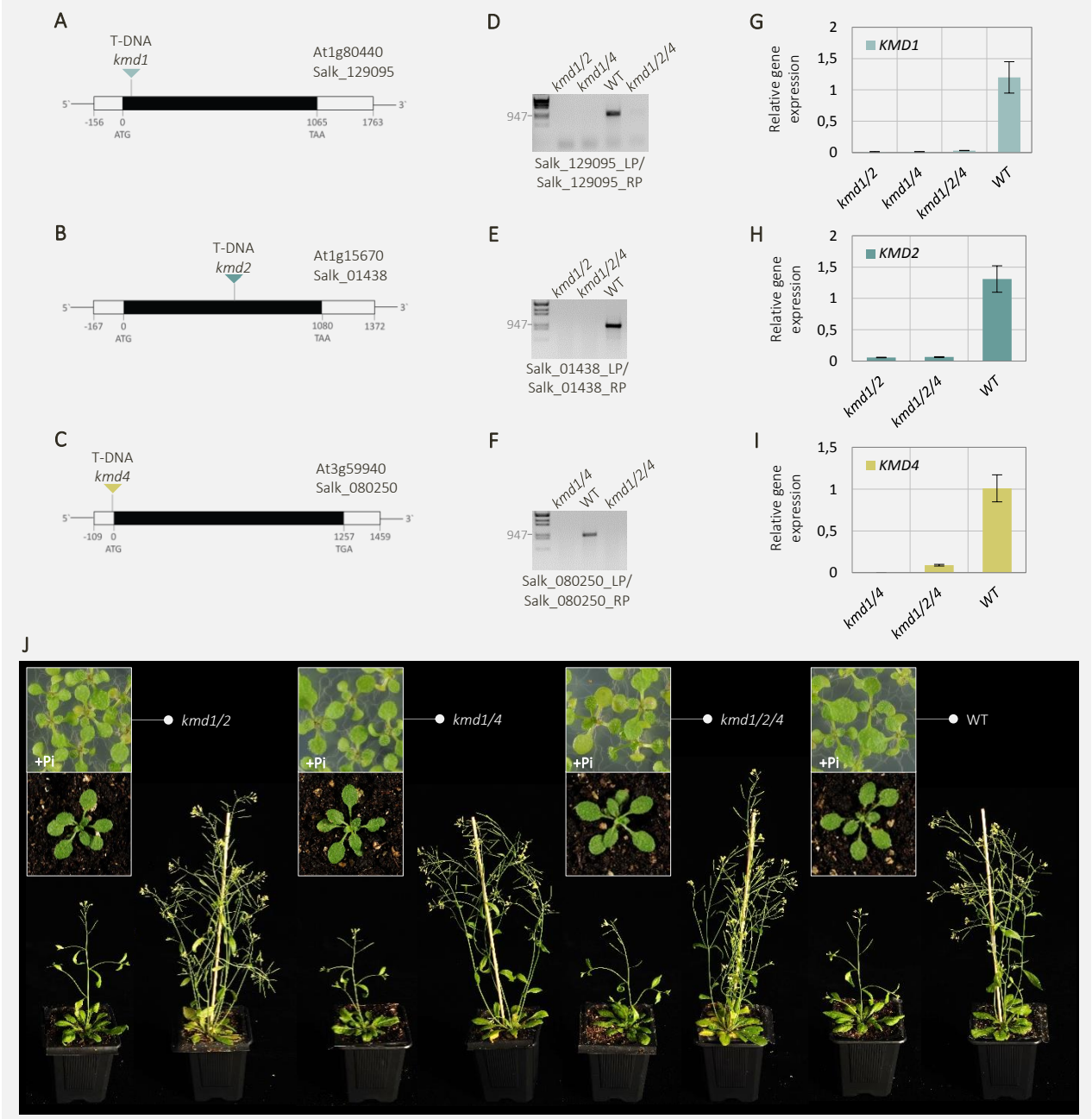

Figure 21. T-DNA knockout for *KMD*s mutant lines. T-DNA (from Transfer DNA) knockout in the Col-0 background lines, obtained from the SALK collection, were used for further physiological and molecular characterization. **(A-C)** Schematic representation of the T-DNA insertion position over *KMD1*, *KMD2* and *KMD4* exonic (black) or UTR (from Untranslated Region; grey) regions. **(D, G)** *KMD1*, **(E, H)** *KMD2* and **(F, I)** *KMD4* transcripts absence in the double mutants *kmd1/2* and *kmd1/4*, and in the triple mutant *kmd1/2/4*, by **(D-F)** semi-quantitative PCR and **(G-I)** RT-qPCR analysis. In **(D-F)** WT cDNA was used as positive control. Primers used are shown on the bottom of each panel. In **(G-I)** *KMD1*, *KMD2* and *KMD4* gene expression is shown as relative to WT in a linear scale, and it was performed with the TaqMan ®Universal ProbeLibrary System (UPL) with *ACT8* as housekeeping reference. Values and error bars are means ± SD. **(J)** *kmd1/2*, *kmd1/4*, *kmd1/2/4* and WT plants at different stages of development: seedling grown in +Pi medium, young rosette, bolting plant and mature plants.

In order to investigate whether *kmd1/2*, *kmd1/4* and *kmd1/2/4* mutants, and oeKMD1-GFP-82 lines are affected on the accumulation of Pi and anthocyanins, in response to combined Pi- and Suc-starvation treatments, the above mentioned lines were grown in a hydroponic system (Figure 23-A) during 9 days, following the experimental designed described in the Figure 23-B.

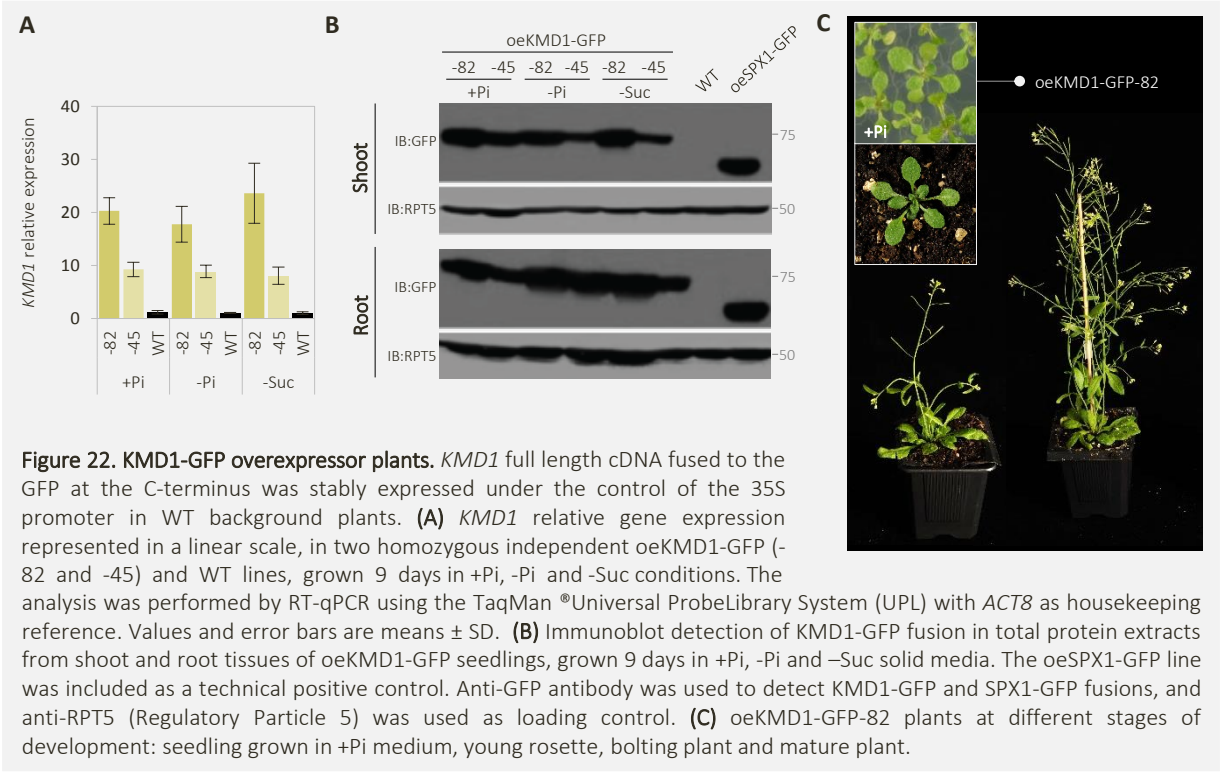

Figure 22. KMD1-GFP overexpressor plants. *KMD1* full length cDNA fused to the GFP at the C-terminus was stably expressed under the control of the 35S promoter in WT background plants. **(A)** *KMD1* relative gene expression represented in a linear scale, in two homozygous independent oeKMD1-GFP (-82 and -45) and WT lines, grown 9 days in +Pi, -Pi and -Suc conditions. The analysis was performed by RT-qPCR using the TaqMan ®Universal ProbeLibrary System (UPL) with *ACT8* as housekeeping reference. Values and error bars are means ± SD. **(B)** Immunoblot detection of KMD1-GFP fusion in total protein extracts from shoot and root tissues of oeKMD1-GFP seedlings, grown 9 days in +Pi, -Pi and –Suc solid media. The oeSPX1-GFP line was included as a technical positive control. Anti-GFP antibody was used to detect KMD1-GFP and SPX1-GFP fusions, and anti-RPT5 (Regulatory Particle 5) was used as loading control. **(C)** oeKMD1-GFP-82 plants at different stages of development: seedling grown in +Pi medium, young rosette, bolting plant and mature plant.

Neither *kmd1/2*, *kmd1/4* and *kmd1/2/4* mutants nor oeKMD1-GFP, displayed statistically significant differences in their total Pi content, compared to WT plants (Figure 23-C). However, Pi contents appeared to be slightly higher in oeKMD1-GFP-82 shoots and roots independently of Pi and Suc availability in the growth media, compared to WT plants, with the exception of the -Suc/-Pi treatment (Figure 23-C). In contrast, in the double and triple mutants, there was variation oin Pi content depending on the tissue, and both Pi and Suc exogenous supply. Thus, in the presence of Suc, there was a different Pi accumulation in roots and shoots of *kmd1/2*, *kmd1/4* and *kmd1/2/4* mutants, represented by slightly lower and higher levels in the shoot and the root, respectively (Figure 23-C). When Suc was the limiting factor, Pi levels in both shoot and root tissue, were lower than in WT tissues, with the exception of Pi levels found in the shoot under -Suc/-Pi conditions (Figure 23-C).

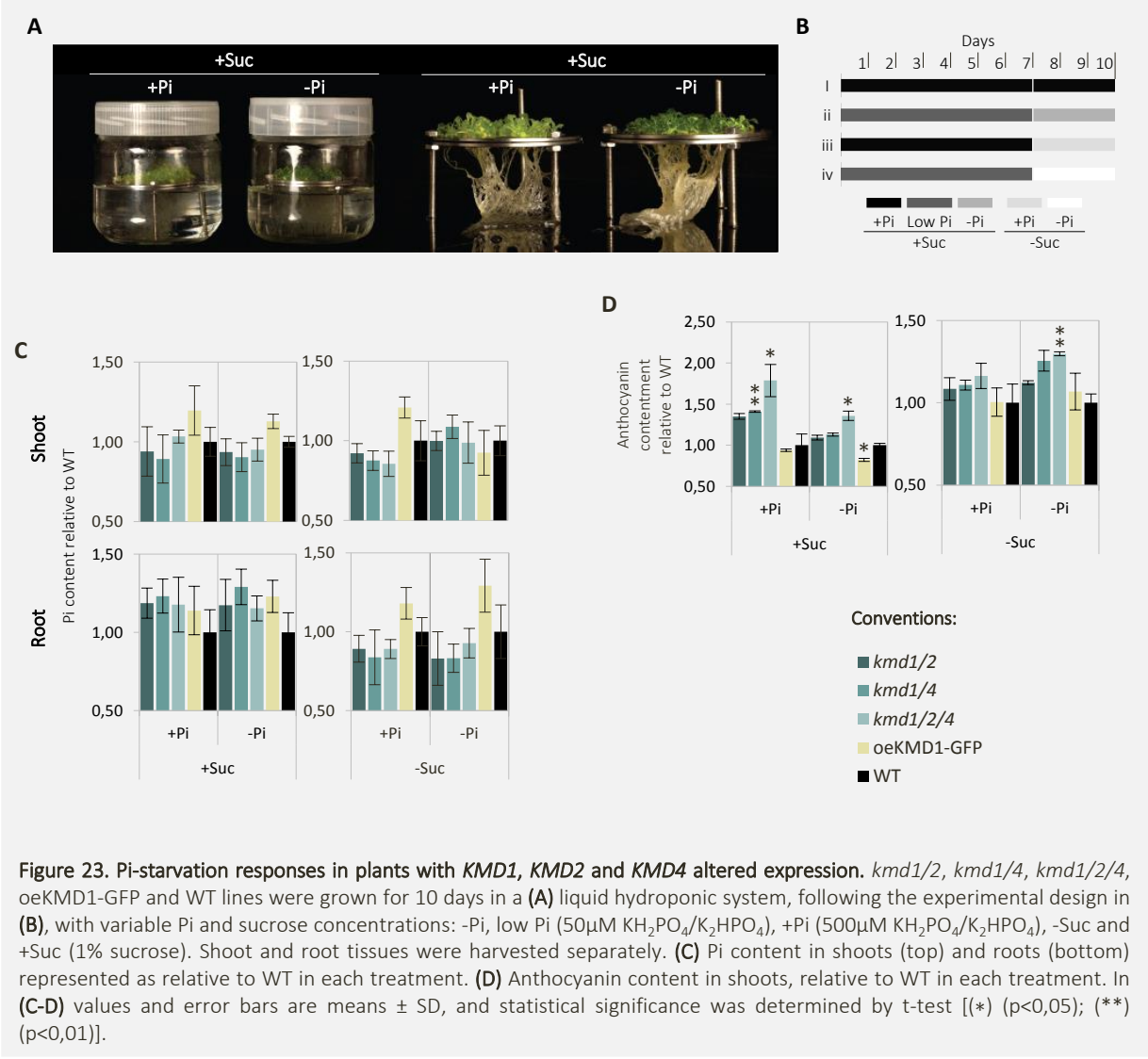

Figure 23. Pi-starvation responses in plants with *KMD1*, *KMD2* and *KMD4* altered expression. *kmd1/2*, *kmd1/4*, *kmd1/2/4*, oeKMD1-GFP and WT lines were grown for 10 days in a **(A)** liquid hydroponic system, following the experimental design in **(B)**, with variable Pi and sucrose concentrations: -Pi, low Pi (50µM KH_2PO_4/K_2HPO_4), +Pi (500µM KH_2PO_4/K_2HPO_4), -Suc and +Suc (1% sucrose). Shoot and root tissues were harvested separately. **(C)** Pi content in shoots (top) and roots (bottom) represented as relative to WT in each treatment. **(D)** Anthocyanin content in shoots, relative to WT in each treatment. In **(C-D)** values and error bars are means ± SD, and statistical significance was determined by t-test [(∗) ($p<0,05$); (**) ($p<0,01$)].

Slight differences in shoot coloration were observed in the double and triple *kmd* mutants, so the anthocyanin accumulations levels were measured in comparison with WT shoots (Figure 23-D). Independently of the Pi or Suc external supply, *kmd1/2*, *kmd1/4* and *kmd1/2/3* accumulated higher amounts of anthocyanins than the WT plants, with statistically significant differences found mainly in the case of *kmd1/2/4* (Figure 23-D). Conversely, oeKMD1-GFP-82 plants accumulated similar or lower levels of anthocyanins compared to WT plants (Figure 23-D).

6.4.1. Pi and sugar sensitivity of plants of *KMD*s altered expression

Based on the previously reported positive bidirectional interaction between Pi-starvation and sugars signaling (Franco-Zorrilla, et al., 2005), we investigated the involvement of *KMD*s in the Pi-sugar cross-talk. For this, *kmd1/2*, *kmd1/4*, *kmd1/2/4*, oeKMD1-GFP-82 and WT seedlings were grown during 10 days in Suc-sufficient (1%) solid media with different supply of Pi, as follow: 2mM, 10mM and 20mM KH_2PO_4/K_2HPO_4 (Figure 24).

As a result, *kmd1/2/4* plants were found to be hypersensitive to high concentrations of Pi (20mM KH_2PO_4/K_2HPO_4) in the growth media, represented by a statistically significant differences in their fresh weight (FW g/seedling) compared to WT controls (Figure 24-A and-D). Reciprocally, oeKMD1-GFP-82 displayed insensitivity to the 20mM Pi treatment relative to WT grown under the same conditions (Figure 24-A and-D).

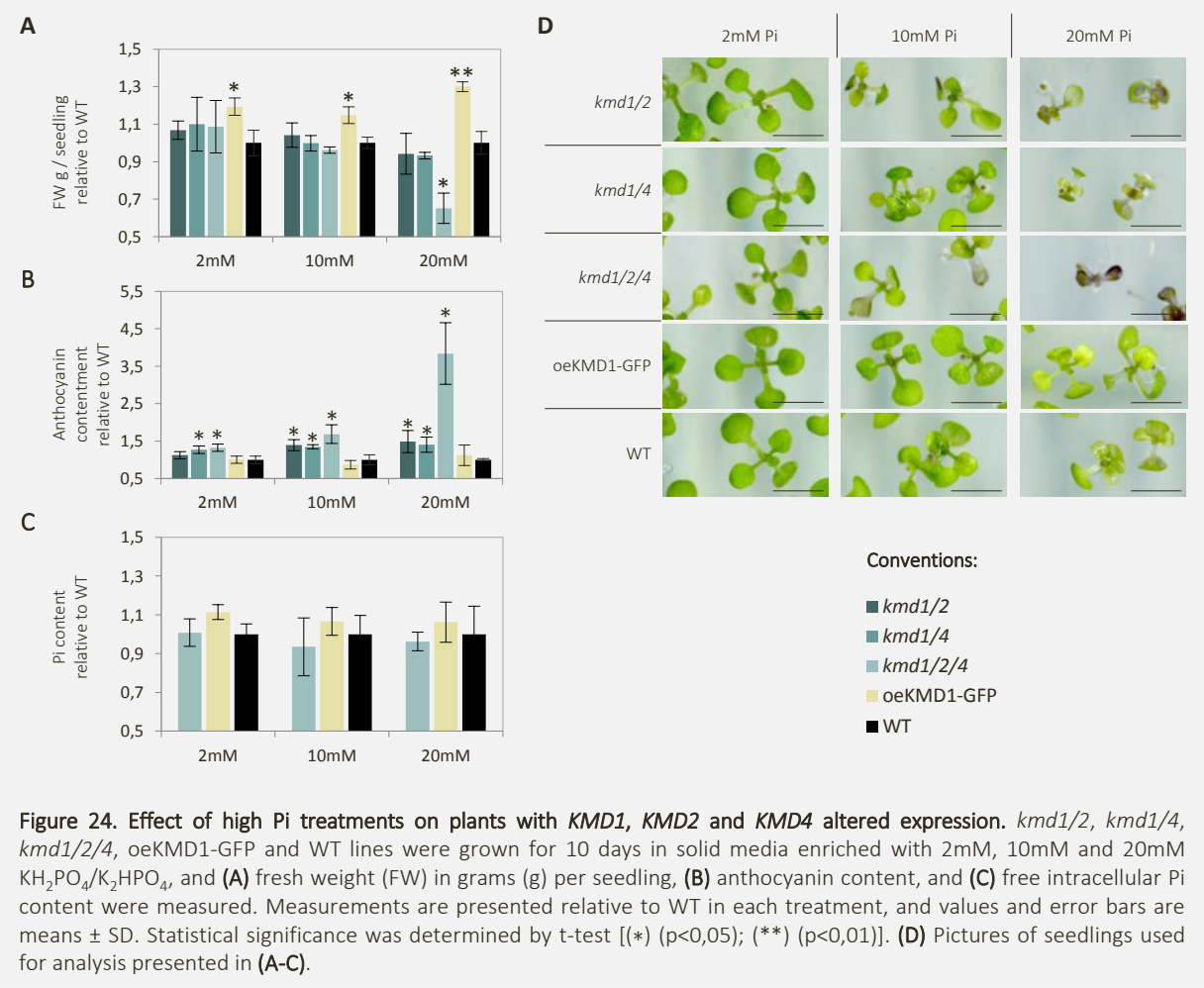

Figure 24. Effect of high Pi treatments on plants with *KMD1*, *KMD2* and *KMD4* altered expression. *kmd1/2*, *kmd1/4*, *kmd1/2/4*, oeKMD1-GFP and WT lines were grown for 10 days in solid media enriched with 2mM, 10mM and 20mM KH_2PO_4/K_2HPO_4, and **(A)** fresh weight (FW) in grams (g) per seedling, **(B)** anthocyanin content, and **(C)** free intracellular Pi content were measured. Measurements are presented relative to WT in each treatment, and values and error bars are means ± SD. Statistical significance was determined by t-test [(∗) ($p<0,05$); (**) ($p<0,01$)]. **(D)** Pictures of seedlings used for analysis presented in **(A-C)**.

Additionally, *KMD*s mutants showed higher anthocyanin content relative to the WT plants (Figure 24-B; see also Figure 23-D), which was particularly evident in *kmd1/2/4* plants under high Pi exogenous supply (20mM Pi treatments) (Figure 24-B). It is worth mentioning that, the previously described effects on Pi sensitivity and anthocyanin accumulation by the altered expression of the *KMD*s, seems to be independent of the Pi content, since no significant differences in the Pi content were found between all lines tested (Figure 24-C).

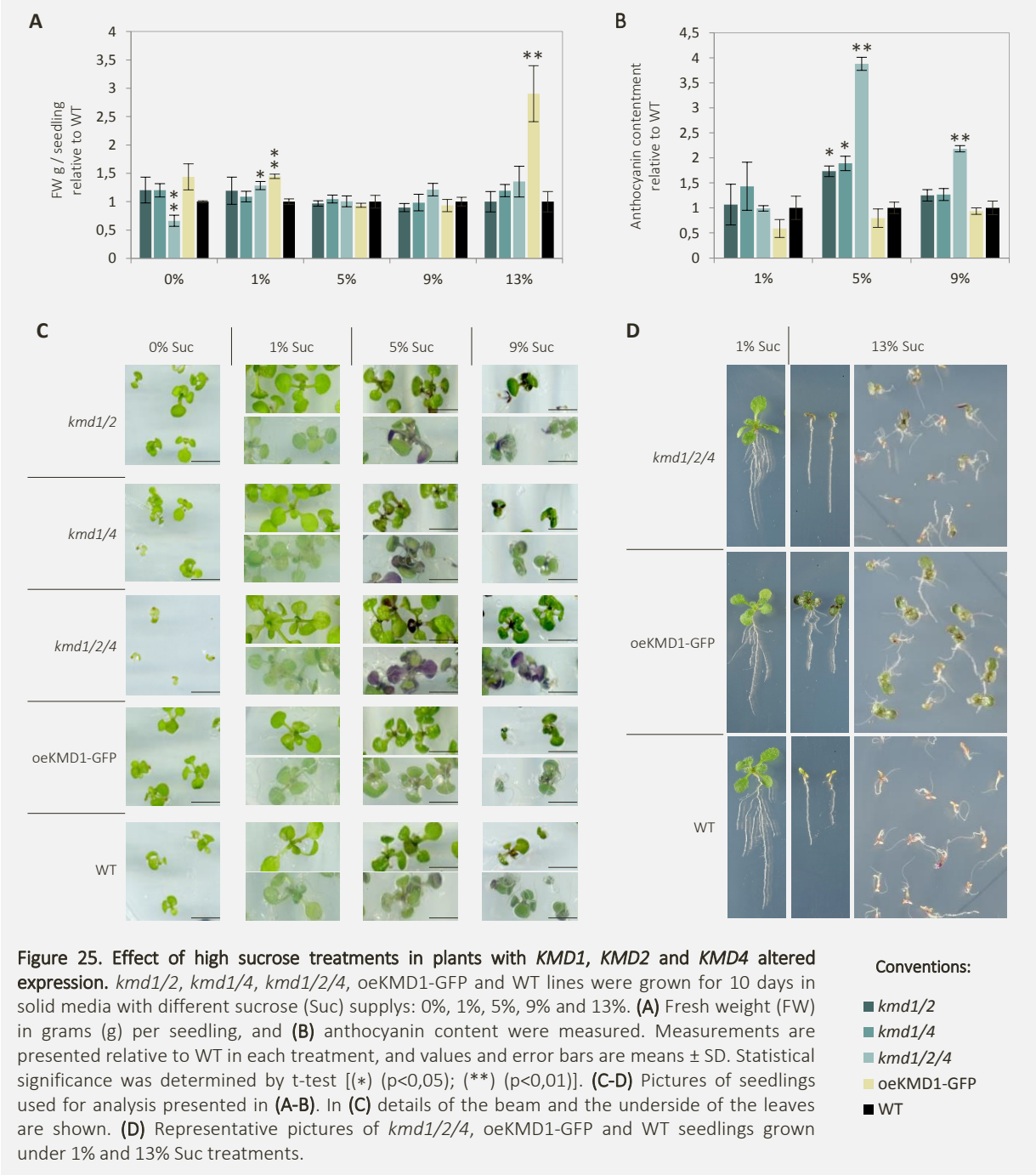

Figure 25. Effect of high sucrose treatments in plants with *KMD1*, *KMD2* and *KMD4* altered expression. *kmd1/2*, *kmd1/4*, *kmd1/2/4*, oeKMD1-GFP and WT lines were grown for 10 days in solid media with different sucrose (Suc) supplys: 0%, 1%, 5%, 9% and 13%. **(A)** Fresh weight (FW) in grams (g) per seedling, and **(B)** anthocyanin content were measured. Measurements are presented relative to WT in each treatment, and values and error bars are means ± SD. Statistical significance was determined by t-test [(∗) (p<0,05); (**) (p<0,01)]. **(C-D)** Pictures of seedlings used for analysis presented in **(A-B)**. In **(C)** details of the beam and the underside of the leaves are shown. **(D)** Representative pictures of *kmd1/2/4*, oeKMD1-GFP and WT seedlings grown under 1% and 13% Suc treatments.

Sugar sensitivity was evaluated in *kmd1/2*, *kmd1/4*, *kmd1/2/4* and oeKMD1-GFP plants. For that purpose, plants were germinated and grown for 10 days in Pi-complete (1mM Pi) solid media with increasing concentration of Suc, as follows: 0%, 1%, 5%, 9% and 13% (Figure 25).

Plants ectopically expressing *KMD1* were more resistant to high Suc concentrations than the WT controls, represented by statistically significant higher fresh weight per seedling (FW g/seedling) values, at 13% Suc treatments (Figure 25-A and-D). In addition, *kmd1/2/4* mutants displayed hypersensitivity to Suc starvation as the FW per seedling was significantly lower in comparison to WT seedlings grown under Suc limiting conditions (Figure 25-A and-C). Control experiments in which mannitol (150mM and 300mM) substituted Suc were carried out in parallel, and no difference between genotypes appearance and FW per seedling was observed (data not shown), excluding differences attributable to osmotic effects.

Notorious over accumulation of anthocyanins was observed in *kmd1/2*, *kmd1/4* and, especially, in *kmd1/2/4* mutants, compared to WT seedlings, at high Suc concentrations (Figure 15-B-C). It is worth noting that the higher difference was found between 5% and 7% Suc. At higuer Suc concentrations, such as 9%, a statistically significant difference was still found in *kmd1/2/4* relative to WT, however at a lower extent. This can be explained by increased anthocyanin accumulation in WT controls at 9% Suc.

6.4.2. Interaction of cytokinins with sugar- and Pi-starvation signaling pathways in plants with altered expression of *KMD*s

Taking in account the bidirectional antagonist interactions between cytokinin and both sugar and Pi-starvation signaling pathways (Franco-Zorrilla *et al*., 2005), we tested the effect of cytokinin treatments in the response of plants with altered expression of KMDs to -Pi and/or variation in Suc supply. For this, a root growth response assay was carried out, growing *kmd1/2/4*, oeKMD1-GFP-82 and WT seedlings in the presence or absence of Pi and Suc in combination with kinetin treatments (Figure 26).

In general, cytokinins exogenous supply has a negative effect on the primary root (PR) growth, mainly due to the negative effect over the root meristem size (Hwang *et al*., 2002). oeKMD1-GFP-82 exhibited insensitivity to kinetin treatments, enhanced by Suc starvation, represented by statistically significant higher PR length in comparison with the WT seedlings (Figure 26-B-C). Reciprocally, *kmd1/2/4* showed increased sensitivity to kinetin also exacerbated by the lack of Suc in the growth media (Figure 26-B-C). Moreover, even if Pi availability seems not

to determine the PR growth when Suc is available, in -Suc conditions Pi starvation decreased the kinetin-insensitivity displayed by oeKMD1-GFP, and has a negative effect on *kmd1/2/4* PR growth (Figure 26-B).

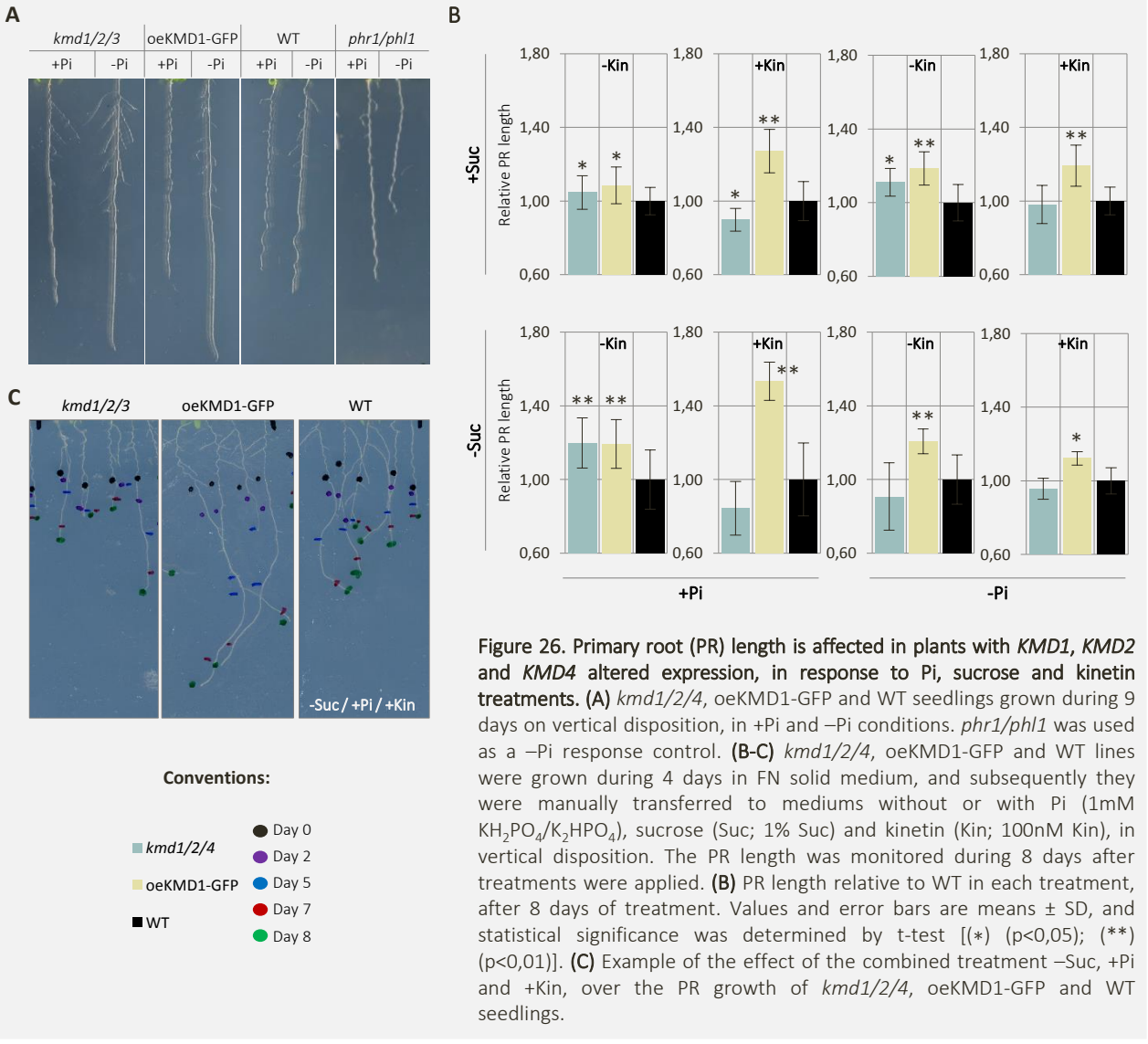

Figure 26. Primary root (PR) length is affected in plants with *KMD1*, *KMD2* and *KMD4* altered expression, in response to Pi, sucrose and kinetin treatments. (A) *kmd1/2/4*, oeKMD1-GFP and WT seedlings grown during 9 days on vertical disposition, in +Pi and –Pi conditions. *phr1/phl1* was used as a –Pi response control. **(B-C)** *kmd1/2/4*, oeKMD1-GFP and WT lines were grown during 4 days in FN solid medium, and subsequently they were manually transferred to mediums without or with Pi (1mM KH_2PO_4/K_2HPO_4), sucrose (Suc; 1% Suc) and kinetin (Kin; 100nM Kin), in vertical disposition. The PR length was monitored during 8 days after treatments were applied. **(B)** PR length relative to WT in each treatment, after 8 days of treatment. Values and error bars are means ± SD, and statistical significance was determined by t-test [(∗) ($p<0,05$); (**) ($p<0,01$)]. **(C)** Example of the effect of the combined treatment –Suc, +Pi and +Kin, over the PR growth of *kmd1/2/4*, oeKMD1-GFP and WT seedlings.

6.5. KMD1-4 HAVE CYTOPLASMIC AND NUCLEAR SUBCELLULAR LOCALIZATION

To examine the subcellular localization of the KMD proteins, KMD1 and KMD4 were used as representatives of each of the two main branches of the KMDs subcluster (KMD1-2 and KMD3-4).

In addition to the oeKMD1-GFP over-expressor lines described previously, stable transgenic plants expressing the full-length coding sequence of KMD4 fused to the GFP at the C-terminus (oeKMD4-GFP), under the control of the constitutive promoter 35S, were established in Col-0 background. Two independent homozygous lines, oeKMD4-GFP-12 and oeKMD4-GFP-15, were analyzed in greater detail. *KMD4* gene expression was determined by RT-qPCR, in plants grown during 9 days in +Pi solid mediums, and *KMD4* transcript levels in the oeKMD4-GFP lines were found to be almost 10 times higher than the levels of endogenous *KMD4* in WT seedlings (Figure 27-A-C). The immunoblot detection of KMD4-GFP fusion displayed the expected size, with higher accumulation of KMD4-GFP fusion in the root than in the shoot tissue (Figure 28-B).

oeKMD1-GFP-82 and oeKMD4-15 were grown for 5 days in +Pi,-Pi and-Suc conditions, after which they were examined by confocal laser scanning (Figure 28-D). In the root epidermal cells, KMD1-GFP and KMD4-GFP fusions localized in the cytosol and the nuclei. It is worth noting that, the stable constitutive expression of KMD4-GFP in Arabidopsis showed less extensive network-like cytosolic distribution and more nuclear/nuclear periphery localization, in comparison to KMD1-GFP. Moreover, the subcellular localization of KMD1-GFP and KMD4-GFP fusions seems to be Pi- and Suc-starvation independent. The common cytosolic and nuclear localization of KMD1-GFP and KMD4-GFP fusions supports their potential functional overlapping *in vivo*.

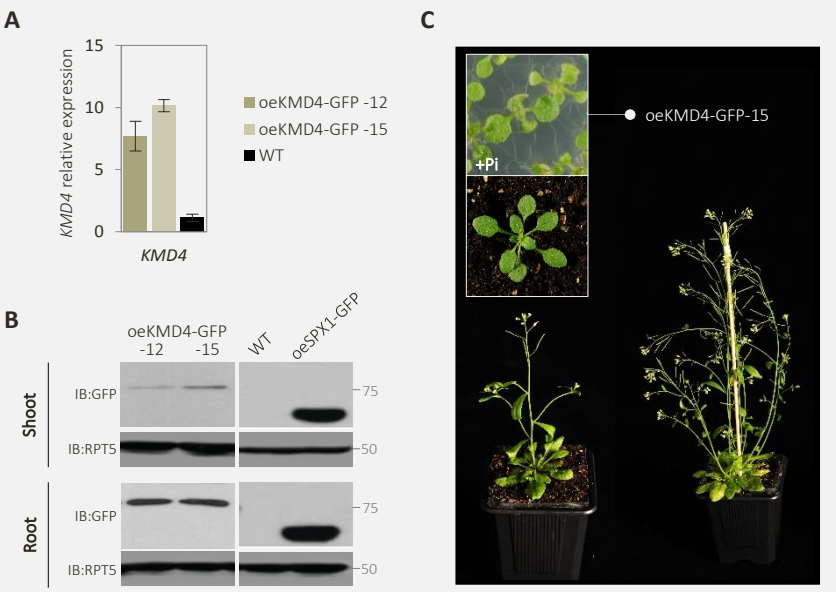

Figure 27. Cytosolic and nuclear localization of KMD1-GFP and KMD4-GFP fusions. KMD4-GFP overexpressor plants were stablished by the expression of *KMD4* full length cDNA fused to the GFP at the C-terminus, under the control of the 35S promoter in WT background plants. **(A)** *KMD4* relative gene expression represented in a linear scale, in two homozygous independent oeKMD4-GFP (-12 and -15) and WT lines, grown 9 days in +Pi conditions. The analysis was performed by RT-qPCR using the TaqMan ®Universal ProbeLibrary System (UPL) with *ACT8* as housekeeping reference. Values and error bars are means ± SD. **(B)** Immunoblot detection of KMD4-GFP fusion in total protein extracts from shoot and root tissues of oeKMD4-GFP seedlings, grown 9 days in +Pi solid mediums. oeSPX1-GFP line was included as a technical positive control. Anti-GFP antibody was used to detect KMD4-GFP and SPX1-GFP fusions, and anti-RPT5 (Regulatory Particle 5) was used as loading control. **(C)** oeKMD4-GFP-15 plants at different stages of development: seedling grown in +Pi medium, young rosette, bolting plant and mature plant. WT control plants are shown in Figure 21 and Supplemental Figure 4. **(D)** Root epidermal cells of 5 days old oeKMD1-GFP-82 and oeKMD4-GFP-15 seedlings, were observed by confocal laser scanning, using three different magnifications. Plants were grown in three different nutritional conditions: FN, -Pi and –Suc. Scale bars are 40µm.

6.6. KMD1-4 IN THE UBIQUITIN 26S PROTEASOME PATHWAY

The SCF complexes are formed by four sub-units: CUL1, ASK, RBX1 and an F-box protein. In Arabidopsis, close to 700 F-box proteins have been identified, including the KMDs. In this work, is reported that CUL1 co-immunoprecipitate with KMD1-GFP, KMD1-MYC and KMD4-GFP fusions *in planta*. Moreover, KMD1 and KMD4 physically interact with some ASKs proteins in a heterologous system, and KMD1-MYC fusion is detected in an Arabidopsis total ubiquitinated proteins pull-down assay. All the above findings support the idea that the KMDs are part of a SCF complex in Arabidopsis and that KMD1-MYC fusion stability seems to be ubiquitin/proteasome independent.

6.6.1. KMDs as a substrate adaptor subunits of SCF complexes in *Arabidopsis*

As putative substrate adaptor subunits of SCF complexes, KMD proteins are expected to be detected assorted to SCF core subunits CUL1 and ASKs. In order to test this hypothesis, KMD1 and KMD4 were used as representatives of each of the two main branches of the KMDs subcluster (KMD1-2 and KMD3-4).

In addition to the oeKMD1-GFP and oeKMD4-GFP over-expressor lines described previously, stable transgenic plants expressing the full-length coding sequence of KMD1 fused to the c-MYC tag at the C-terminus (oeKMD1-MYC), under the control of the constitutive promoter 35S, were established in WT Col-0 background. Two independent homozygous lines, oeKMD1-MYC-8 and oeKMD1-MYC-10, were selected for further characterization, based on the different levels of *KMD1* gene expression found by RT-qPCR, in plants grown during 9 days in +Pi solid mediums (Figure 28-A-C). oeKMD1-MYC lines displayed *KMD1* transcript levels between 8 (oeKMD1-MYC-8) and 20 (oeKMD1-MYC-10) times higher than endogenous *KMD1* levels found in WT seedlings (Figure 28-A). oeKMD1-MYC-10 accumulates twice the amount of *KMD1* transcripts than oeKMD1-MYC-8, and it correlated with KMD1-MYC protein levels, in both the shoot and the root tissues (Figure 28-B). This differential *KMD1* levels in the two oeKMD1-MYC lines selected, represented an useful tool for further biochemical analysis (see 6.8.4. PAL2 is ubiquitinated and degraded by the 26S proteasome).

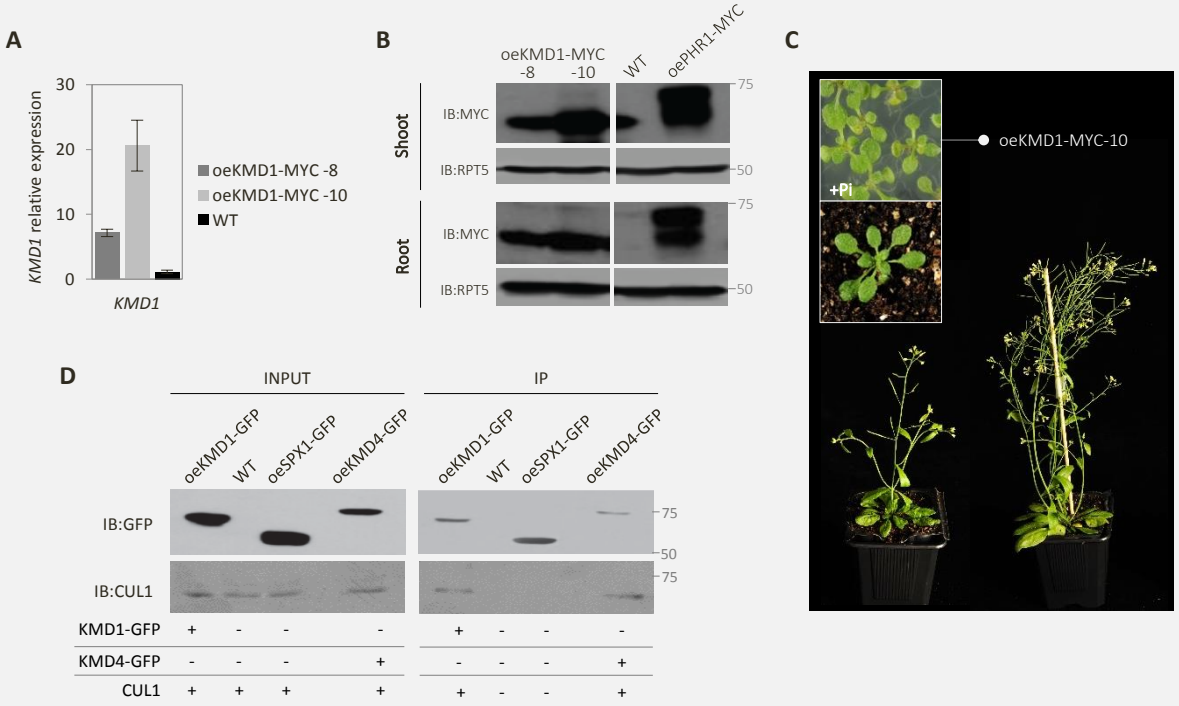

Figure 28. KMD1-GFP, KMD1-MYC and KMD4-GFP fusions physically interact with CUL1 *in planta*. KMD1-MYC overexpressor plants were established by the expression of *KMD1* full length cDNA fused to the c-MYC at the C-terminus, under the control of the 35S promoter in WT background plants. **(A)** *KMD1* relative gene expression represented in a linear scale, in two homozygous independent oeKMD1-MYC (-8 and -10) and WT lines, grown 9 days in +Pi conditions. The analysis was performed by RT-qPCR using the TaqMan ®Universal ProbeLibrary System (UPL) with *ACT8* as housekeeping reference. Values and error bars are means ± SD. **(B)** Immunoblot detection of KMD1-MYC fusion in total protein extracts from shoot and root tissues of oeKMD1-MYC seedlings, grown 9 days in +Pi solid mediums. oePHR1-MYC line was included as a technical positive control. Anti-RPT5 (Regulatory Particle 5) was used as loading control. **(C)** oeKMD1-MYC-10 plants at different stages of development: seedling grown in +Pi medium, young rosette, bolting plant and mature plant. WT control plants are shown in Figure 21 and Supplemental Figure 4. **(D-E)** Immunoblot detection of co-immunoprecipitated endogenous CUL1 after pulling down and **(D)** KMD1-GFP, KMD4-GFP and **(E)** KMD1-MYC fusions total protein extracts from constitutive overexpressor plants (oeKMD1-GFP-82, oeKMD4-GFP-15 and oeKMD1-MYC-10), grown during 9 days under +Pi conditions. The fusions **(D)** KMD1-GFP, KMD4-GFP, oeSPX1-GFP, and **(E)** KMD1-MYC were immunoprecipitated (top panels) with anti-GFP fused to protein A-Sepharose® from *Staphylococcus aureus* or with anti-Myc resin, respectively. The co-immunoprecipitated endogenous CUL1 (bottom panels) was detected using anti-CUL1. In **(D)** oeSPX1-GFP was used as a negative control, and KMD1-GFP, KMD4-GFP and SPX1-GFP fusions were detected using anti-GFP. In **(B)** and **(E)**, anti-MYC and anti-mouse antibodies were used to detect KMD1-MYC and PHR1-MYC fusions.

In order to test whether KMD1 and KMD4 can be detected in association with CUL1 *in planta*, immunoprecipitation assays were carried with total protein extracts from oeKMD1-GFP-82, oeKMD4-GFP-15 and oeKMD1-MYC-10 seedlings (see 5.6.3.1. Immunoprecipitation of tagged fusions). As a result, CUL1 was found to co-immunoprecipitate with KMD1-GFP, KMD1-MYC and KMD4-GFP fusions (Figure 28-D-E), indicating a positive association between KMDs and CUL1 *in planta*.

In Arabidopsis, the ASKs superfamily groupes 21 members (Risseeuw *et al*., 2003), divided in two main types: ASK1-19 (type I) which exhibit significant similarity within the H8 domain and are most closely related to the human SKP1 group of orthologs (Risseeuw *et al*., 2003), while ASK20-21 (type II) that are much larger than type I genes and encode chimeric proteins (Kong *et al*. 2007).

Considering the diversification of ASKs in Arabidopsis from a single ancestral copy in the most recent common ancestor (MRCA) of eudicots and monocots (Kong *et al*. 2007), and a recent study indicating that only a subset of ASK proteins participate in SCF activities (Kuroda *et al*., 2012), a phylogenetic reconstruction of the Arabidopsis ASKs was performed, in order to ensure the selection of representatives from different branches of the phylogeny, for further interaction studies with KMD1 and KMD4 in a heterologous system. The phylogenetic tree was constructed based on the full-length aa sequences, using ClustalX and the Neighbor-Joining (NJ) method with 100 times bootstrap (Figure 29).

Yeast AH109 strain was used to co-transform the full-length coding sequence of KMD1, KMD4 and 15 different ASK proteins, fused to the GAL4 DNA-binding domain (BD) and/or to the activation domain (AD). ASK1, ASK2, ASK6, ASK8, ASK10, ASK14 and ASK18 cloned into the pGAD were kindly provided by Dr. Juan Carlos del Pozo (Centro de Biotecnología y Genómica de Plantas UPM-INIA, Madrid, Spain). The co-transformed cells were subject to an auxotrophic complementation test in SD-WLA and SD-WLHA media, supplemented with an increasing range of 3-AT (Figure 29).

The results of the yeast co-transformation assays suggested that KMD1 and KMD4 weakly interactions with most of the different ASKs tested, preferentially with the closely related ASK1, ASK2 and ASK11, and with the distant ASK3 (Figure 29). This finding supports the KMD's putative role as substrate adaptors as part of SCF complexes.

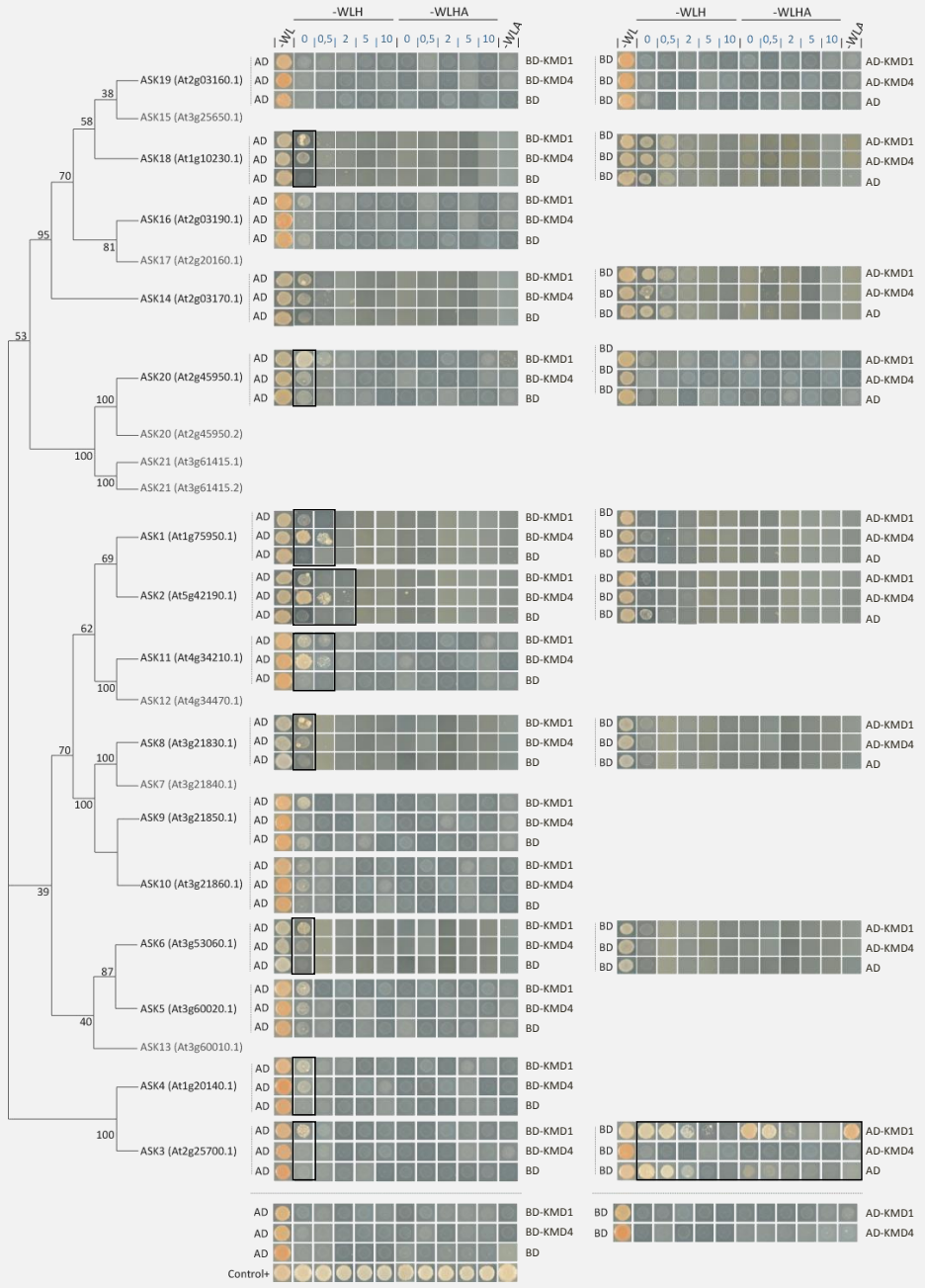

Figure 29. KMD1 and KMD4 interact with ASKs in a Y2H system. Y2H assays using full-length KMD1, KMD4 and a collection of ASKs. The figure composition is based on the ASKs phylogenetic reconstruction based on the full-length aa sequences, and performed using ClustalX and the Neighbor-Joining (NJ) method with 100 times bootstrap. Co-transformed yeast cells were subject to an auxotrophic complementation test in SD-WLA and SD-WLHA media supplemented with an increasing range of 3-amino-1,2,4-triazole (3-AT). Cells were co-transformed using KMD1 and KMD4 fused to BD or AD, and the corresponding complementation empty vector as a auto-activation control, and BD-PHR1/AD-SPX1 were used as positive control. Yeast cells were allowed to grow for 48h.

Since in a SCF complex, CUL1 brings the F-box and the Ub-E2 intermediate into close physical proximity to enable Ub transfer to a target protein (Zheng *et al*., 2002b), it is expected that Ub molecules and substrate adaptors can display a physical asociation due to an E2/E3 transient interaction. To determine whether such association, oeKMD1-MYC-10 seedlings were grown for 9 days under +Pi conditions, and total protein extracts were incubated with p62 agarose (p62) that displays high affinity for Ub molecules and binds them in a non-covalent manner. The pull-down output was used for the immunoblot detection of KMD1-MYC fusion, using anti-MYC antibody (Figure 30). KMD1-MYC fusion was clearly detected in the total ubiquitinated protein pulldown output, suggesting the presence of KMDs in SCF complexes *in planta* (Figure 30). However, KMD1-MYC fusion detection could be also interpreted as an evidence of KMD1 ubiquitination.

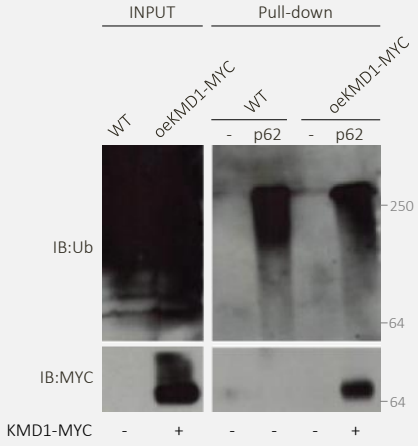

Figure 30. KMD1-MYC is detected in ubiquitinated proteins pull-down assay. Total ubiquitinated proteins were purified by incubation of total protein extracts of 9 days old oeKMD1-MYC-10 seedlings, with p62 resin (p62) or with no-ubiquitin affinity agarose (-). The total ubiquitinated proteins were detected with an anti-Ub antibody (top panel). KMD1-MYC fusion was detected using anti-MYC antibody (bottom panel).

It is widely accepted that the major meaning of the Ub labeling of a protein is the regulation of its stability by means of triggering degradation via the 26S proteasome. MG132 proteasome inhibitor is been widely used as a tool to unravel ubiquitin/proteasome-dependent destabilization of target proteins. Indeed, MG132 treatments inhibits the proteasome activity, resulting on the accumulation of proteins intended for degradation via the 26S proteasome. Accordingly, MG132 treatments were performed in both stable and transient systems to test whether KMD1 is the subject of Ub labeling itself.

oeKMD1-MYC-10 seedlings were grown for 9 days in +Pi conditions and then manually transferred to MS liquid medium supplemented with 50µM MG132 (Sigma-Aldrich) for 12h (Figure 31-A). In a similar way, agro-infiltrated *Nicotiana benthamiana* leaves transiently expressing 35S::KMD1-MYC, were sliced in squares and incubated following the previous description (Figure 31-B). Total protein extracts were used to detect KMD1-MYC fusion levels in MG132 treated and un-treated samples, and immuboblot detection was performed using anti-MYC antibody (Figure 31). KMD1-MYC fusion levels were not affected by MG132 treatments, indicating that the stability of KMD1-MYC fusion is independent of the ubiquitin/26S proteasome pathway. Therefore the Ub labeling of KMD1 seems unlikely.

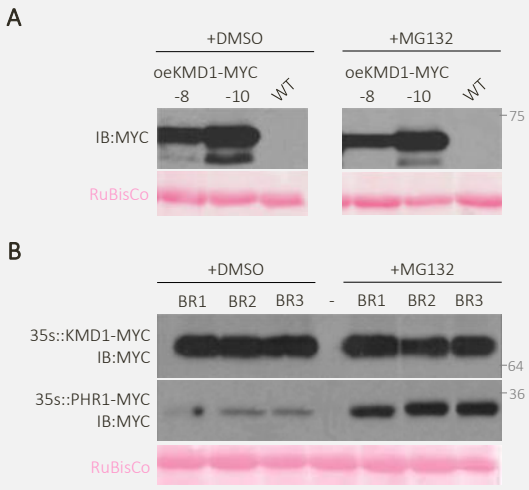

Figure 31. KMD1-MYC levels are unaffected by MG132 proteasome inhibitor treatments. Immunoblot detection of KMD1-MYC fusions in total protein extracts from **(A)** oeKMD1-MYC seedlings, and from **(B)** *Nicotiana benthamiana* leaves transiently expressing 35S::KMD1-MYC and 35S::PHR1-MYC. Seedlings and transfected leaves were treated with or without MG132 proteasome inhibitor. In **(B)**, PHR1-MYC was included as MG132 treatment positive control. In **(A)** and **(B)** KMD1-MYC and PHR1-MYC fusions were detected with anti-MYC and anti-mouse antibodies, and Ponceau staining was used as loading control.

6.6.2. Dimerization ability of *Arabidopsis* KMD proteins

In mammals, dimerization of F-box proteins has been described as a regulatory factor for substrate interactions (Welcker, et al., 2007). To get insight on KMD dimerization capacities, AH109 yeast strain was co-transformed with different combinatorial possibilities between the full-length coding sequences of KMD1, KMD2 and KMD4, fused to the GAL4 DNA-binding domain (BD) and to the activation domain (AD). Co-transformed cells were subjected to an auxotrophic complementation test in SD-WLA and SD-WLHA media, supplemented with an increasing range of 3-AT (Figure 32).

Results indicated that KMDs are able to dimerize, mainly as heterodimers. Thus, KMD1 and KMD2 displayed a positive but weak homodimerization capacity (Figure 32-A), the different combinatorial possibilities of heterodimetization showed clear yeast growth under SD-WLA with 3-AT for KMD1, KMD2 and KMD4 (Figure 32-B). Moreover, KMD1,2 had displayed strong ability to form heterodimers as show by growth of co-transformed cells in SD-WLHA (Figure 32-B).

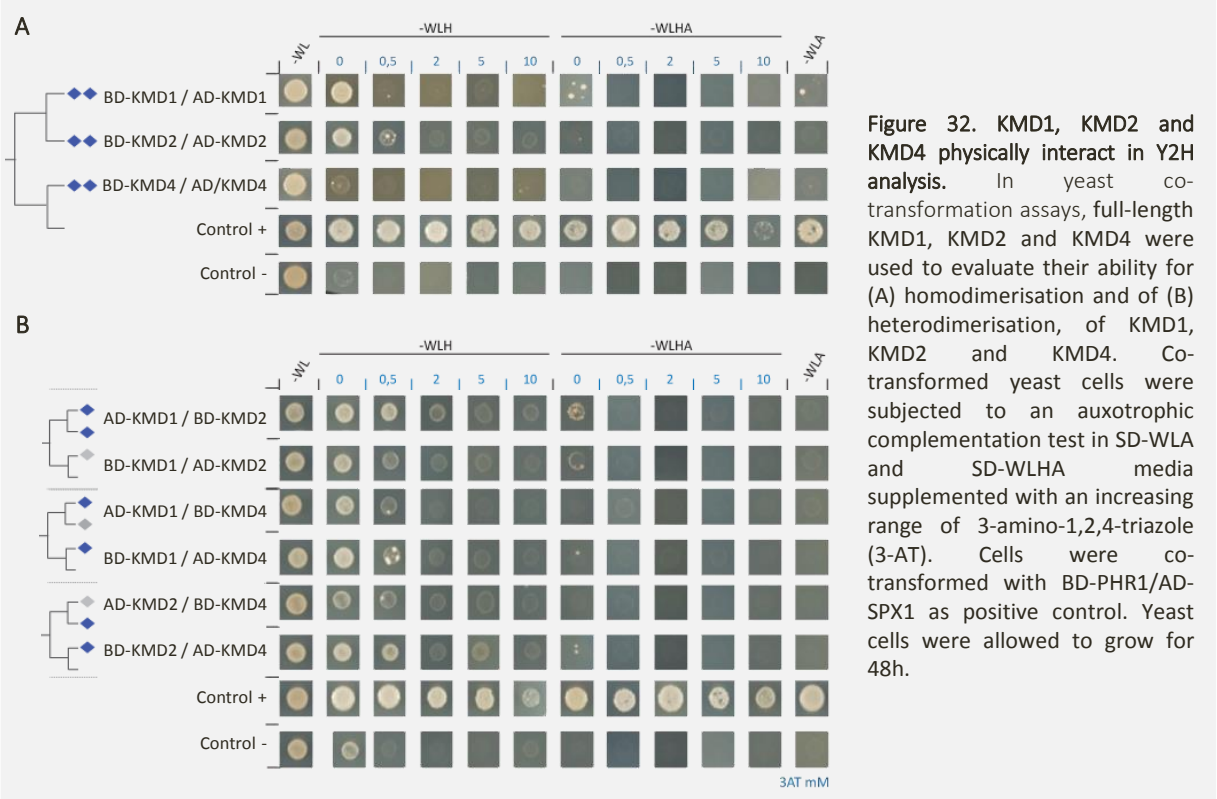

Figure 32. KMD1, KMD2 and KMD4 physically interact in Y2H analysis. In yeast co-transformation assays, full-length KMD1, KMD2 and KMD4 were used to evaluate their ability for (A) homodimerisation and of (B) heterodimerisation, of KMD1, KMD2 and KMD4. Co-transformed yeast cells were subjected to an auxotrophic complementation test in SD-WLA and SD-WLHA media supplemented with an increasing range of 3-amino-1,2,4-triazole (3-AT). Cells were co-transformed with BD-PHR1/AD-SPX1 as positive control. Yeast cells were allowed to grow for 48h.

6.7. ISOLATION OF POTENTIAL PROTEIN TARGETS OF KMD1

As part of SCF complexes, F-box domain-containing proteins physically interact with protein targets, recruiting them for further labeling with ubiquitin moieties and, thereby, determining the fate of the labeled proteins. At the beginning of this study, target proteins of SCF^{KMD} complexes in the context of the Pi starvation adaptive responses remained unknown, leaving an information gap about the molecular basis of KMD activity and the impact of post-translational regulation in the control of Pi signaling. To identify potential targets of KMD proteins with a role in Pi starvation responses, a Y2H mating screen was conducted using KMD1 as bait. The full-length coding sequence of KMD1 fused to the GAL4 DNA-binding domain (BD) was used to transform Y187 yeast cells and a bait self-activation test was performed (Figure 33).

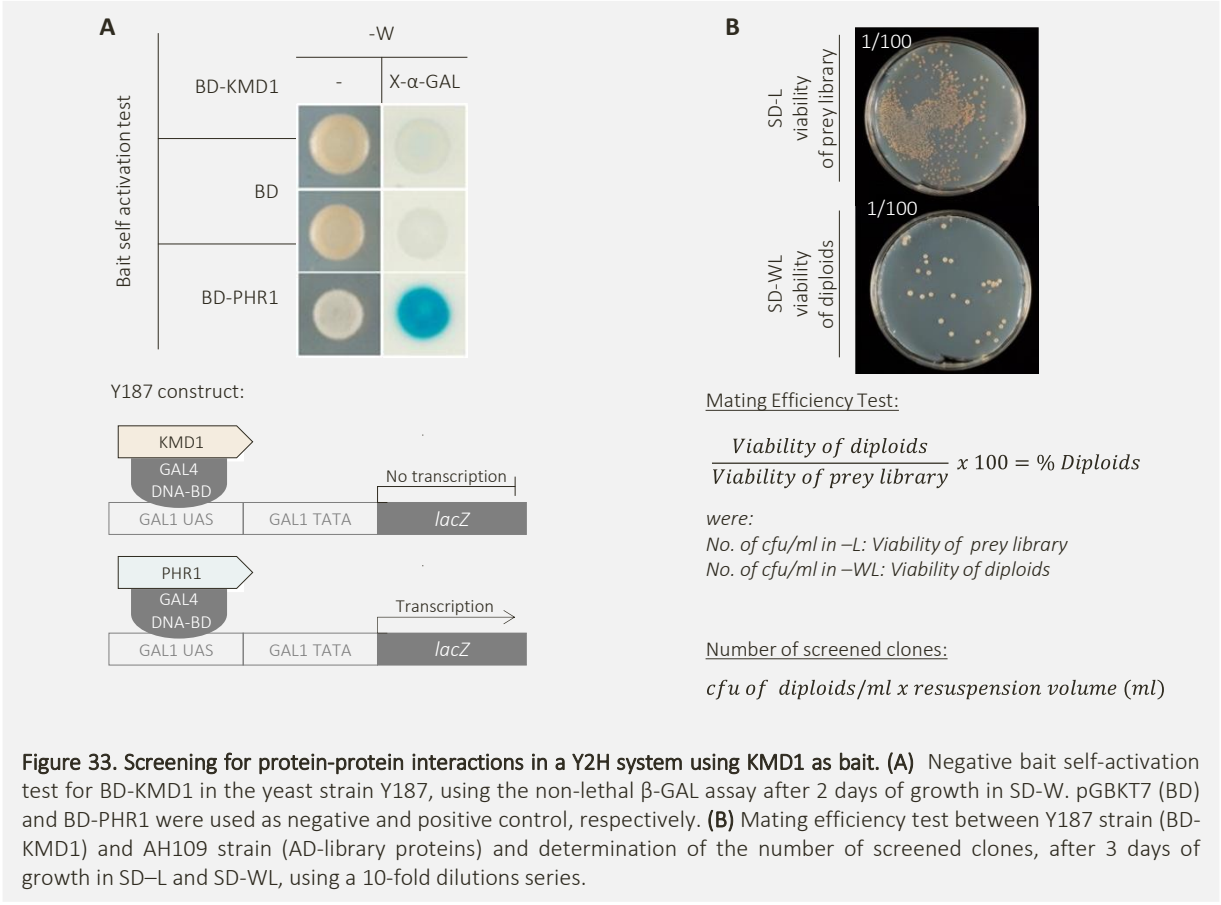

Figure 33. Screening for protein-protein interactions in a Y2H system using KMD1 as bait. (A) Negative bait self-activation test for BD-KMD1 in the yeast strain Y187, using the non-lethal β-GAL assay after 2 days of growth in SD-W. pGBKT7 (BD) and BD-PHR1 were used as negative and positive control, respectively. **(B)** Mating efficiency test between Y187 strain (BD-KMD1) and AH109 strain (AD-library proteins) and determination of the number of screened clones, after 3 days of growth in SD–L and SD-WL, using a 10-fold dilutions series.

As a result, we found that the BD-KMD1 fusion itself does not activate the transcription of the reporter gene lacZ being then suitable as bait in a Y2H mating screening (Figure 33). Next, a cDNA library (AH109 yeast strain) prepared with mRNAs purified from Pi-starved Arabidopsis seedlings (Puga *et al.*, 2014) was used to perform a Y2H mating screening using BD-KMD1 as bait. The conjugated yeast cells were spread on dropout media to test

the mating efficiency of the yeast strains AH109 and Y187 (SD-L and SD–WL) and to further select positive two-hybrid interactions (SD-WLH 0.5mM 3AT and SD–WLHA 0.5mM 3AT). After 4 days of incubation, the mating efficiency was represented by approximately 1.9% of diploid clones (Figure 33-B) and, from a total of ~12 million clones screened, 289 primary diploid colony-forming units (*cfu*) were selected and replicated (SD-WL) for further analysis (data not shown).

To analyze the viability and strength of the protein-protein interactions present in the primary diploid clones, yeast auxotrophy test and non-lethal β-galactosidase assays were conducted on 247 yeast clones that were successfully recovered after 2 days of *cfu* growth in dropout medium SD–WL (example in Supplementary Table 3). Among them, 99 clones were selected for gene identification by plasmid sequencing, following a selection criteria based on a wide coverage of protein-protein interaction strengths, from weak to strong interactions (e.g. clones 4 and 46 in Supplementary Table 3, respectively).

Yeast plasmids from selected clones (99) were transformed back into *E. coli*, so as to facilitate the sequencing process. Sequence data was analyzed based on the presence of open reading frames and searched against public Arabidopsis databases. Correct reading frames with the two lysine codons (AAA AAA) found in the attL1 recombination site, was established in 89 cases. Prey identity search of these 89 nucleotide sequences was conducted using a BLASTX search (nucleotide (nt) query, aa database (db)) against the TAIR10 Proteins dataset. A total of 63 Arabidopsis Gene Initiative (AGI) gene index numbers were identified, representing genes coding for potential KMD1 protein targets (Supplemental Table 3).

An overview of the list of KMD1 interactors indicates that it covers a broad range of functional pathways (BINs), according to the MapMan Ontology tool (a set of 34 tree-structured BINs, describing the central metabolism as well as other cellular processes from *Arabidopsis*), were the high-level BINs Photosystem, Reduction-Oxidation (Redox), Sulfur-assimilation (S-assimilation), Fermentation, DNA and Secondary metabolism are over-represented with a p-value<0.05 (Figure 34-A).

Moreover, 7 high-level BINs grouped a total of 12 AGIs with multiple entries in the KMD1 interactors list (Figure 34-B). Multiple entries of an AGI in the preys list of a Y2H mating screening constitutes an indirect evidence of the quality of a specific protein-protein interaction (independent diploids with the same AGI identity ≥2).

Thus, preys that are both grouped in an over-represented BIN and represented by multiple entries, are high-confidence outputs from a Y2H mating screening. According to this criteria, KMD1 potential targets for ubiquitination were: i) Secondary metabolism-related protein Phenylalanine Ammonia-Lyase 2 (PAL2; first enzyme of the phenylpropanoid pathway) (Bate *et al.*, 1994); ii) photosystem-related proteins Proton Gradient Regulator 1

(PGR1), Ribulose Bisphosphate Carboxylase Small Chain 1A (RBCS1A) and Fructose-bisphosphate Aldolase 2 (FBA2), involved in light reactions and the Calvin cycle; and iii) Redox-related thioredoxin proteins like the product of At2g04700 and the chloroplast-localized Thioredoxin M2 (ATHM2).

A

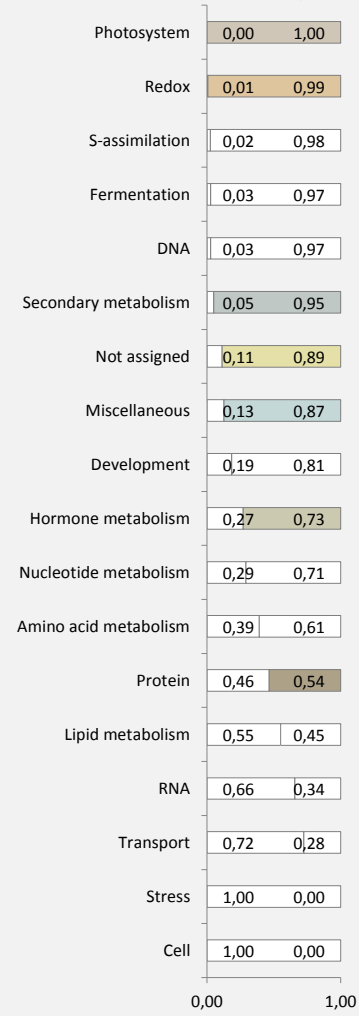

B

BINs	AGI	Name/Description		No.	Clones ID
Light reaction	At4g03280	PGR1 PETC	Proton Gradient Regulator 1 Photosynthetic Electron Transfer C	5	9, 29, 63, 168, 194
Calvin cycle	At1g67090	RBCS1A	Ribulose Bisphosphate Carboxylase Small Chain 1A	2	64, 163
	At4g38970	FBA2	Fructose-bisphosphate Aldolase 2	2	6, 119
Thioredoxin	At2g04700	Ferredoxin thioredoxin reductase catalytic beta chain family protein		2	26, 59
	At4g03520	ATHM2, TRXM2	Thioredoxin M2 Redox activated co-chaperone localized in the chloroplast	6	33, 35, 38, 120, 141, 257
Phenylpropanoids	At3g53260	PAL2	Phenylalanine Ammonia-Lyase 2	5	4, 18, 117, 199, 285
Unknown	At4g32020	Unknown protein		2	201, 222
Peroxidases	At3g32980	Peroxidase superfamily protein		2	114, 212
	At3g49120	PRXCB PRX34	Peroxidase CB Peroxidase 34	3	71, 85, 88
Auxin	At3g47620	TCP14	Teosinte Branched Cycloidea and PCF 14	2	81, 121
Postranslational modification	At4g25130	PMSR4	Peptide Met Sulfoxide Reductase 4	5	28, 40, 49, 80, 261
Folding	At2g44650	CPN10	Choroplast Chaperonin 10	2	42, 116

Figure 34. Over-representation analysis of KMD1 Y2H interactors grouped by BINs. A) BINs with *p-value*<0.05 are over-represented in the list of potential KMD1 interactors according to the MAPMAN tool (Usadel *et al*. 2006), using TAIR8 genes as control group. The bar represents *p-value* + (1 – *p-value*) = 1. **(B)** Proteins identified by Y2H mating analysis as interactors of KMD1 represented by two or more than two independent yeast clones. The list includes the yeast clone ID (Clones ID), the number of independent yeast clones representing each potential KMD1 prey (Clones No.), the AGI code, the protein name and description (TAIR8), and the BINs according to MAPMAN tool (Usadel *et al*. 2006). In **(A)** (1 – *p-value*) and **(B)** the color code differentiates between BINs that are grouping preys represented by two or more independent yeast clones.

6.8. KMD PROTEINS FACILITATE PAL2 DEGRADATION BY THE 26S PROTEASOME

To cope with varying degrees of Pi stress, plants have evolved a number of adaptive mechanisms that involve developmental, physiological and metabolic changes. During Pi starvation, the secondary metabolism plays a key role improving plant survival, especially by means of the accumulation of anthocyanin pigments that protect the shoots against free radicals released during photoinhibition, which takes place when nutrients like Pi or N are limiting (Trull *et al.*, 1997; Nilsson *et al.*, 2007).

Anthocyanins are flavonoid pigments synthesized via the phenylpropanoid pathway. Phenylalanine ammonia lyase (PAL) mediates the first and committed step in the phenylpropanoid pathway, catalyzing the conversion of L-phenylalanine to ammonia and trans-cinnamic acid. In Arabidopsis, PAL is encoded by four genes, one of which codifies for a well-supported KMD1 prey in our Y2H mating screening, PAL2.

In the context of Pi starvation, *PAL2* (At3g53260) transcript levels increase in the shoot of WT plants under Pi-limiting conditions, while *PAL2* transcription is down-regulated in *phr1/phl1* double mutants, indicating a role for PHR1/PHL1 in the regulation of *PAL2* expression (Supplemental Table 3: clones 4, 18, 117, 199 and 285) (Bustos *et al.*, 2010).

In order to determine whether SCF^{KMD} controls PAL2 activity at the posttranslational level, we first analyzed the ability of KMD1/2/4 to interact with PAL2 both in Y2H assays and *in planta*.

6.8.1. Y2H analysis of KMD1/2/4 and PAL2 interaction

Targeted Y2H assays were used to further validate the physical interaction between KMD1 and PAL2 proteins (Figure 35), and to evaluate a potential functional redundancy between KMD1/2/4 proteins towards PAL2. For this, the full-length coding sequence of the three KMD proteins and PAL2 were amplified and fused to BD and AD, and co-transformed into AH109 yeast cells. BD-KMD1/2/4 and PAL2-AD fusions did not self-activate the transcription of the reporter genes in the presence of empty AD and BD constructs, respectively, being appropriate for Y2H testing of protein-protein interactions (Figure 35-B).

Yeast co-transformations were performed using both BD-KMD1/2/4 and PAL2-AD constructs and 12 independent diploid clones were selected from each construct combination, to test yeast auxotrophy activity.

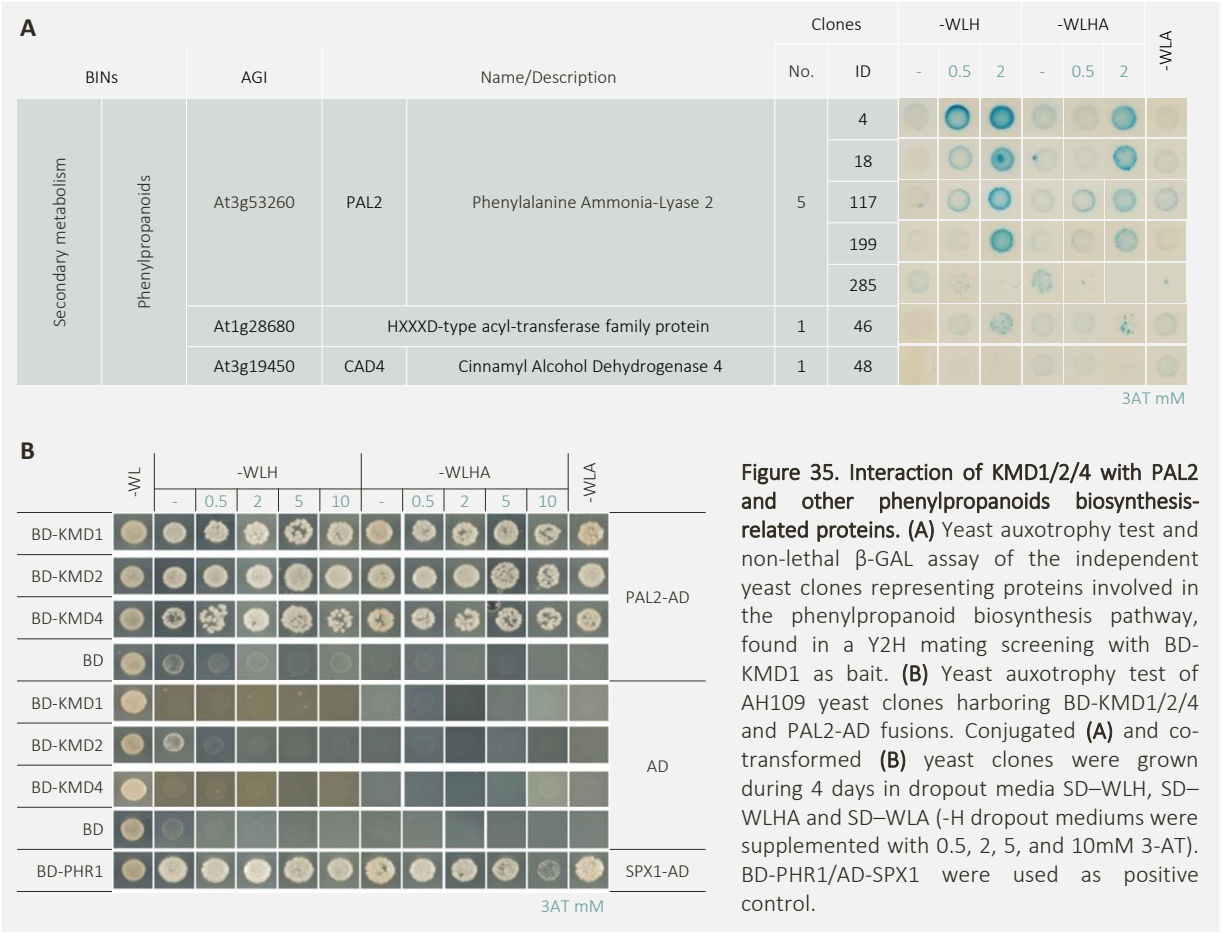

Figure 35. Interaction of KMD1/2/4 with PAL2 and other phenylpropanoids biosynthesis-related proteins. (A) Yeast auxotrophy test and non-lethal β-GAL assay of the independent yeast clones representing proteins involved in the phenylpropanoid biosynthesis pathway, found in a Y2H mating screening with BD-KMD1 as bait. **(B)** Yeast auxotrophy test of AH109 yeast clones harboring BD-KMD1/2/4 and PAL2-AD fusions. Conjugated **(A)** and co-transformed **(B)** yeast clones were grown during 4 days in dropout media SD–WLH, SD–WLHA and SD–WLA (-H dropout mediums were supplemented with 0.5, 2, 5, and 10mM 3-AT). BD-PHR1/AD-SPX1 were used as positive control.

The yeast auxotrophy test showed that all three KMDs interact with PAL2 in a strong manner, although differences in the strength of each interaction could be observed. Thus, KMD1 and KMD2 diploid clones showed an intense proliferation in highly restrictive dropout media, whereas KMD4 showed a less intense growth, indicating that KMD1 and KMD2 interaction with PAL2 is slightly stronger than that of KMD4 (Figure 35-B).

6.8.2. Establishment and characterization of transgenic Arabidopsis plants constitutively over-expressing PAL2

In order to determine if the physical and functional interaction between KMD1/2/4 and PAL2 is taking place *in planta* and whether this interaction leads to PAL2 ubiquitination and degradation by the 26S proteasome, the constitutive 35S promoter was used to drive the expression of *PAL2* full-length coding sequence fused to the GFP at the C-terminus, in both transient and stable expression systems. For the last one, Col-0 background plants were used to establish stable transgenic oePAL2-GFP lines. Two independent T2 homozygous lines, oePAL2-GFP-32 and oePAL2-GFP-42, were selected for further characterization, based on the different levels of *PAL2* gene expression found by RT-qPCR in plants grown during 12 days in +Pi solid media (Figure 36-A). oePAL2-GFP-32 and oePAL2-GFP-42 transgenic lines exhibited *PAL2* mRNA levels 10-fold and 20-fold higher, respectively, than the endogenous *PAL2* levels found in WT plants (Figure 36-A).

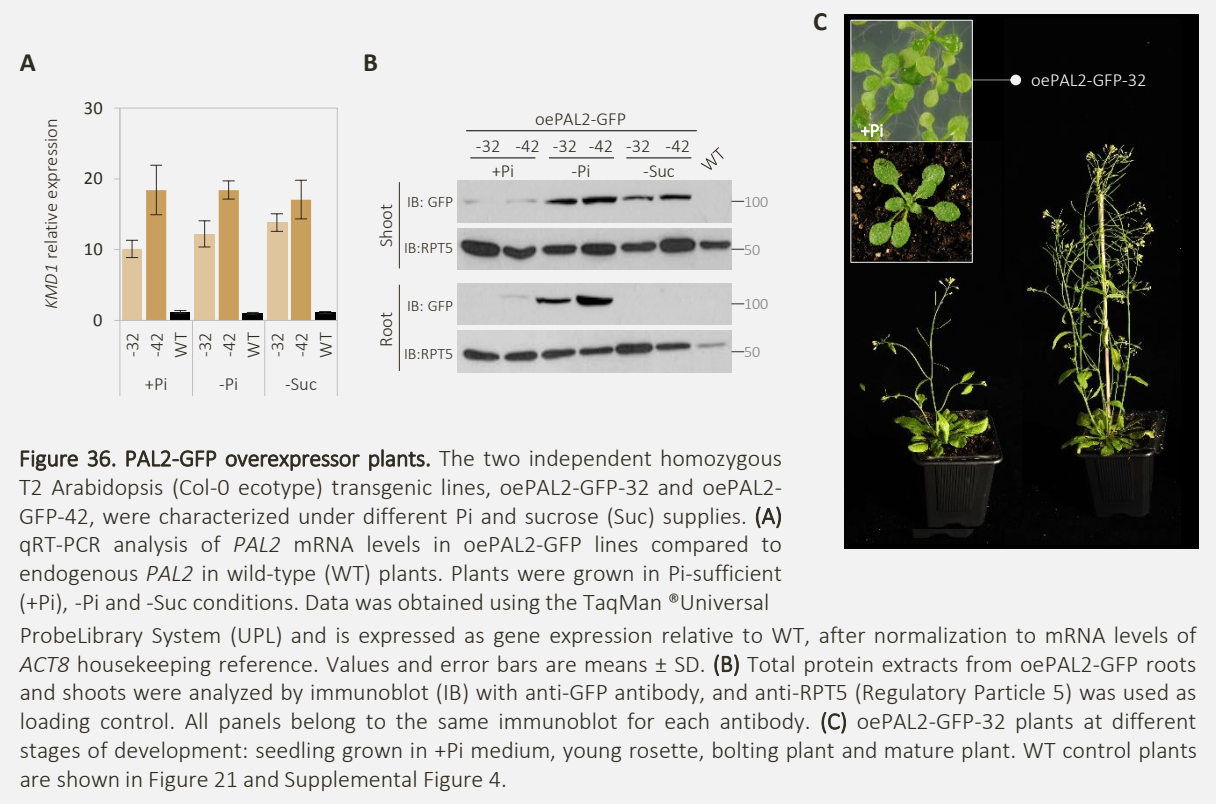

Figure 36. PAL2-GFP overexpressor plants. The two independent homozygous T2 Arabidopsis (Col-0 ecotype) transgenic lines, oePAL2-GFP-32 and oePAL2-GFP-42, were characterized under different Pi and sucrose (Suc) supplies. **(A)** qRT-PCR analysis of *PAL2* mRNA levels in oePAL2-GFP lines compared to endogenous *PAL2* in wild-type (WT) plants. Plants were grown in Pi-sufficient (+Pi), -Pi and -Suc conditions. Data was obtained using the TaqMan ®Universal ProbeLibrary System (UPL) and is expressed as gene expression relative to WT, after normalization to mRNA levels of *ACT8* housekeeping reference. Values and error bars are means ± SD. **(B)** Total protein extracts from oePAL2-GFP roots and shoots were analyzed by immunoblot (IB) with anti-GFP antibody, and anti-RPT5 (Regulatory Particle 5) was used as loading control. All panels belong to the same immunoblot for each antibody. **(C)** oePAL2-GFP-32 plants at different stages of development: seedling grown in +Pi medium, young rosette, bolting plant and mature plant. WT control plants are shown in Figure 21 and Supplemental Figure 4.

Despite the constitutive character of PAL2-GFP overexpression in oePAL2-GFP-32 and oePAL2-GFP-42, posttranslational regulation of PAL2 occurs in response to Pi and Suc availability in the growth media, in both shoot and root tissues, where accumulation of PAL2-GFP fusion mainly occurs in –Pi (Figure 36-A-B).

Since PAL proteins enable the flux of primary metabolites into the phenylpropanoid pathway (Bate et al., 1994; Cochrane et al., 2004), the functionality of the PAL2-GFP fusion, was determined by measuring the anthocyanins levels in oePAL2-GFP lines. In a first instance, oePAL2-GFP overexpressor lines showed no apparent change in their overall appearance in comparison with the WT plants (Figure 36-C).

Anthocyanins levels were 3-fold higher than in the WT under low Pi conditions (30µM), in both oePAL2-GFP-32 and oePAL2-GFP-42 lines, as well as in 100µM Pi, although at lesser extent (Figure 37-A-B). A difference in the anthocyanin phenotype was found between oePAL2-GFP-32 and oe-PAL2-GFP-42 lines in response to –Pi (Figure 37). Thus, whereas oePAL2-GFP-32 plants exhibited similar anthocyanin accumulation as in the WT, after 11 days of groth in the total absence of Pi, the levels displayed by oePAL2-GFP-42 plants were almost 2-fold lower than in the WT (Figure 37-A).

The defect in anthocyanin accumulation found in oePAL2-GFP-42 plants in-Pi maybe related with their higher *PAL2* overexpression levels (Figure 36-A), because both PAL activity and *PAL* gene transcription are negatively regulated by biosynthetic intermediates (Zhang, et al., 2015). Interestingly, *KMD1-4* were up-regulated in oePAL2-GFP-32 but not in oePAL2-GFP-42 in +Pi and-Pi conditions (Figure 37-C), which may be also related with overexpression level of *PAL2*. Due to the negative regulation that seems to be taking place on PAL function in the oeKMD2-GFP-42 line, oePAL2-GFP-32 line was selected for further analyses.

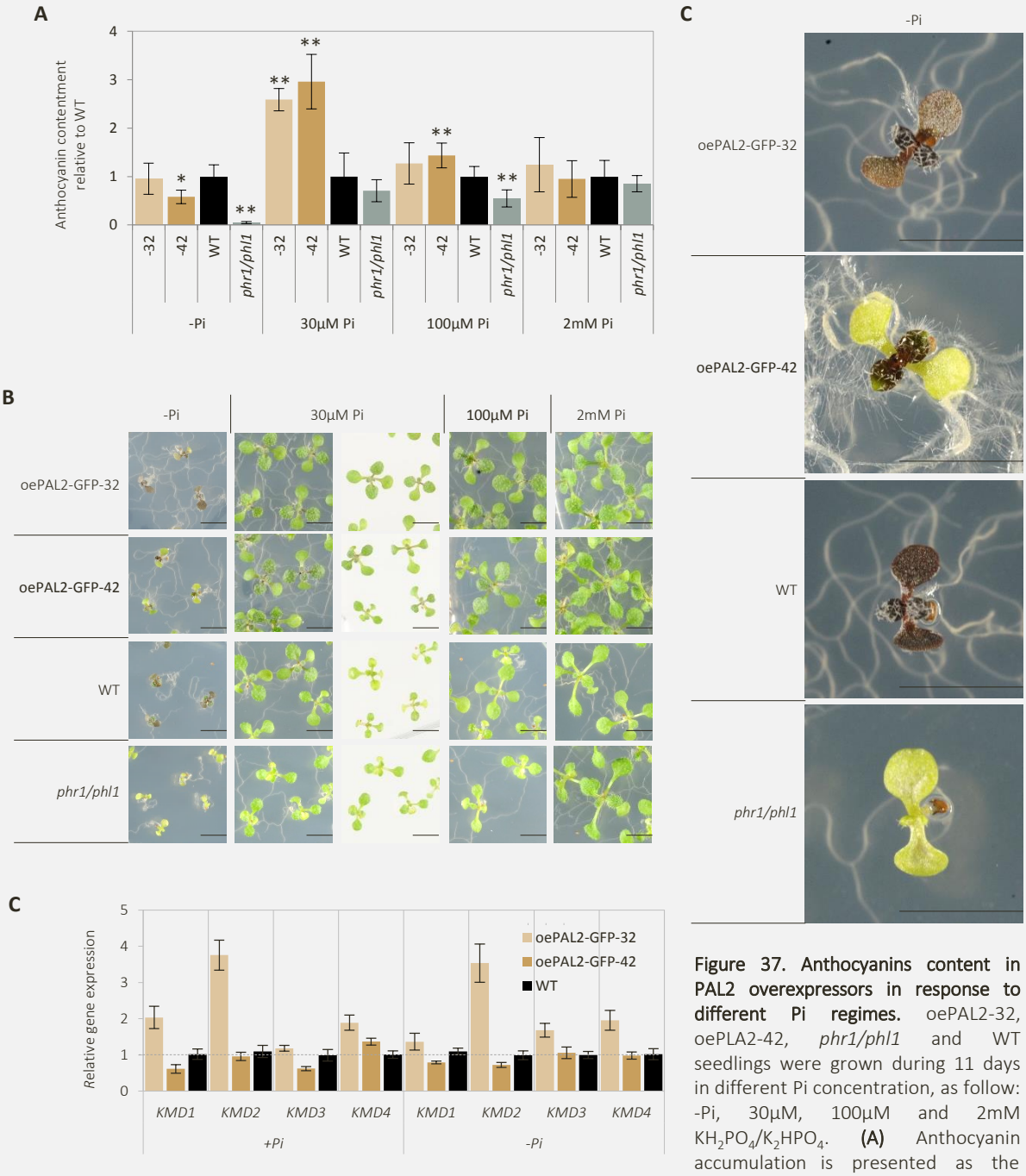

Figure 37. Anthocyanins content in PAL2 overexpressors in response to different Pi regimes. oePAL2-32, oePLA2-42, *phr1/phl1* and WT seedlings were grown during 11 days in different Pi concentration, as follow: -Pi, 30µM, 100µM and 2mM KH_2PO_4/K_2HPO_4. **(A)** Anthocyanin accumulation is presented as the average of six biological replicates (n=6), relative to WT in each treatment, ± SD. **(B)** Pictures of seedlings used for analysis presented in **(A)**. **(C)** *KMD1-4* relative gene expression analysis was performed by RT-qPCR using the SYBR® Green dye system with *UBQ10* as housekeeping reference. Values and error bars are means ± SD. **(D)** Detailed pictures of oePAL2-GFP-32, oePAL2-GFP-42, *phr1/phl1* and WT seedlings grown under -Pi. *phr1/phl1* mutant was included as a control. Pictures bar scale = 5mm. Statistical significance was determined by t-test [(*) (p<0,05); (**) (p<0,01)].

To examine the localization of the PAL2-GFP fusion in response to Pi and Suc availability, 5-days-old oePAL2-GFP-32 roots were observed under the confocal microscope and an invariable cytosolic localization was found under +Pi,-Pi and –Suc conditions (Figure 38).

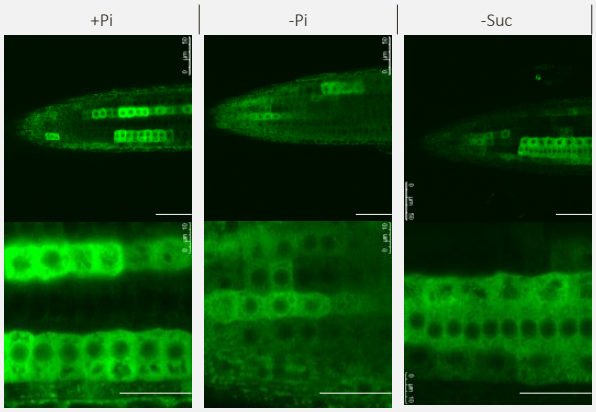

Figure 38. Cytosolic localization of PAL2-GFP fusion. Root epidermal cells of 5 days old oePAL2-GFP-32 seedlings, were observed by confocal laser scanning, using three different magnifications. Plants were grown in three different nutritional conditions: +Pi, -Pi and –Suc. Scale bars are 40µm.

6.8.3. KMD1 and PAL2 physically interact *in planta*

To determine whether KMD1 and PAL2 interact *in planta*, stable and transient expression systems were used to co-express KMD1-MYC and PAL2-GFP fusions.

Thus, Arabidopsis transgenic lines overexpressing both PAL2-GFP and KMD1-MYC (oePAL2-GFP-32/oeKMD1-MYC-8 and oePAL2-GFP-32/oeKMD1-MYC-10) were established by cross-pollination using oeKMD1-MYC-8 and oeKMD1-MYC-10 pollen onto oePAL2-GFP-32 pistils. T1 seeds were collected and used for further analysis. The heterozygous state of each insertion loci, KMD1-MYC and PAL2-GFP, in the T1 generation was overcome by increasing the size of the population under analysis (n≥60 seedlings in each biological replicate). In the other hand, *N. benthamiana* leaves were co-agroinfiltrated with *A. tumefaciens* clones harboring the 35S::KMD1::MYC and 35S::PAL2::GFP constructs, in the presence of the P19 suppressor of gene-silencing protein.

In both systems, KMD1-MYC and PAL2-GFP were found to co-immunoprecipitate independently on the partner used in the initial immunoprecipitation (IP). Therefore, as shown in the Figure 39-A, KMD1-MYC was

detected by immunoblotting in PAL2-GFP immunoprecipitates. Likewise, PAL2-GFP was detected after immunoprecipitating KMD1-MYC from crude lysates of *N. benthamiana* leaves (Figure 39-B).

These results indicate that PAL2 and KMD1 proteins physically interact *in planta* and, therefore, that PAL2 is a potential target of ubiquitination mediated by SCF^{KMD} complexes.

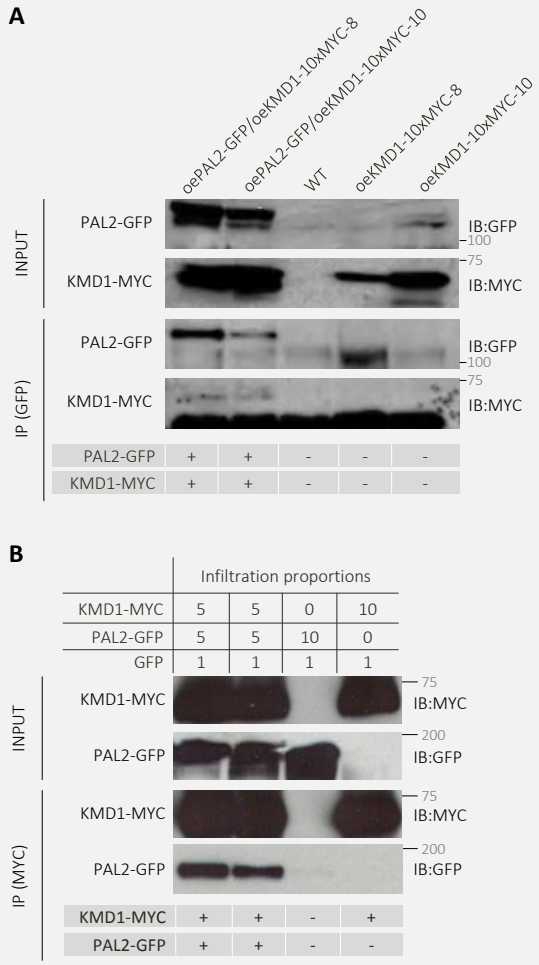

Figure 39. PAL2 interacts with KMD1 *in planta*. **(A-B)** Co-immunoprecipitation (Co-IP) of GFP-tagged PAL2 and MYC-tagged KMD1 proteins in both **(A)** stable and **(B)** transient expression systems. **(A)** Immunoprecipitation (IP) of PAL2-GFP fusions was performed using soluble protein extracts prepared from 12-days-old seedlings corresponding to oePAL2-GFP-32 and two independent T1 oePAL2-GFP/oeKMD1-MYC (-8 and -10) lines. Total extracts (INPUT) and IPs were subjected to immunoblot (IB) analysis with anti-GFP and anti-MYC antibodies to detect PAL2-GFP and co-immunoprecipitated KMD1-MYC, respectively. **(B)** IP of KMD1-MYC fusion from total native extracts of co-agroinfiltrated (35S::PAL2::GFP and 35S::KMD1::MYC) *N. benthamiana* leaves. The lysates (INPUT) were incubated with anti-c-MYC agarose bead. As a negative control 35S::GFP and 35S::KMD1::MYC co-agroinfiltrated leaves were used. Anti-MYC antibody was used to detect KMD1-MYC (IP upper panel) and anti-GFP antibody was used to detect co-immunoprecipitated PAL2-GFP (IP lower panel). In **(A-B)** tables at the bottom indicate the presence/absence (+/-) of each fusion in the final IPs.

6.8.4. PAL2 is ubiquitinated and degraded by the 26S proteasome

The fact that PAL2 interacts physically with KMD1/2/4 components of SCF E3 complexes, opens up the possibility that PAL2 is a substrate of the UPS pathway. To test this possibility, the above-mentioned transient and stable expression systems were used along with ubiquitinated-protein affinity purification assays and 26S proteasome degradation experiments, respectively.

To detect Ub modifications on PAL2, Ub-conjugated proteins were purified in bulk from *N. benthamiana* leaves transiently overexpressing PAL2-GFP, using commercially available p62 resin that has an affinity for Ub and binds it in a non-covalently manner (Figure 40). PAL2-GFP was detected, by immunoblotting with an anti-GFP antibody, in the purified pool of ubiquitinated proteins but not when an empty resin was used (Figure 40), indicating that PAL2 enzyme is post-translationally modified by labeling with Ub moieties.

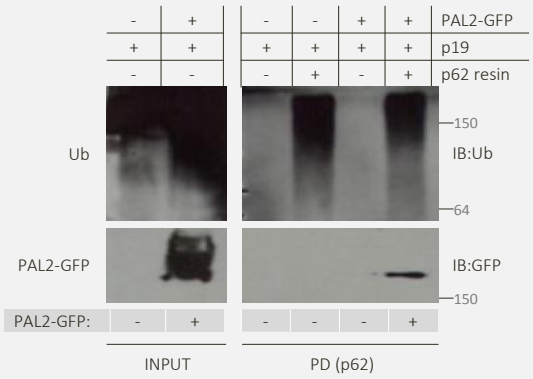

Figure 40. PAL2 is an ubiquitin target. Affinity purification of ubiquitinated PAL2-GFP from native extracts of *N. benthamiana* leaves transiently overexpressing PAL2-GFP (35S::PAL2::GFP) (3 days post-*Agrobacterium*-infiltration). Protein extracts were incubated with ubiquitin (Ub) binding-p62 resin or with empty agarose resin (negative control). Anti-Ub antibody was used to detect total ubiquitinated proteins (upper panel). Anti-GFP antibody allowed the detection of the pulled down (PD) PAL2-GFP (lower panel). Extracts from leaves infiltrated with P19 gene silencing suppressor (p19) were used as immunoblot (IB) controls. The lower table indicates the presence/absence (+/-) of PAL2-GFP in each lane.

Consequently, in order to assess if PAL2 is degraded at the 26S proteasome in Arabidopsis and weather KMD proteins are regulating such process, oePAL2-GFP-32/oeKMD1-MYC-8 and oePAL2-GFP-32/oeKMD1-MYC-10 plants, as well as the parental lines oePAL2-GFP-32, oeKMD1-MYC-8 and oeKMD1-MYC-10 (Figure 41-A), were treated with proteasome inhibitor MG132 and analyzed by immunoblot with anti-GFP (Figure 41-B) and anti-MYC (Figure 41-C) antibodies.

Upon proteasome inhibition, PAL2-GFP levels increased in both oePAL2-GFP/oeKMD1-MYC lines and in the oePAL2-GFP-32 parental line, compared with DMSO-treated controls (Figure 41-B), indicating that PAL2 is degraded via the ubiquitin-26S proteasome pathway. In contrast, that was not the case for KMD1-MYC because KMD1-MYC fusion accumulation was not altered by MG132 treatments (Figure 41-C).

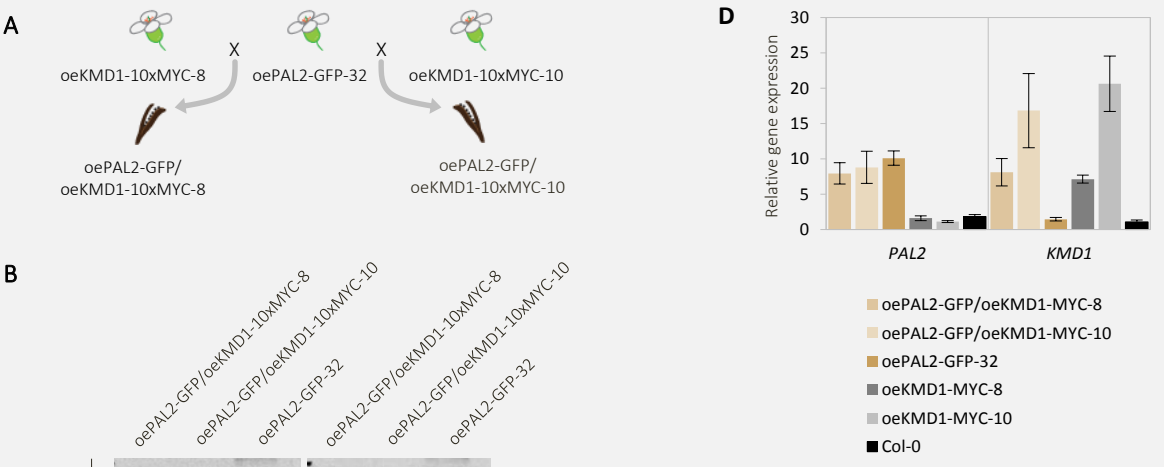

Figure 41. KMD1 overexpression promotes PAL2 protein degradation through the Ub proteasome system. Two independent T1 co-overexpressor lines (oePAL2-GFP-32/oeKMD1-MYC-8 and oePAL2-GFP-32/oeKMD1-MYC-10) were established and used for **(B-C)** immunoblot (IB) and **(D)** qRT-PCR analysis. **A)** The T1 co-overexpressor lines shared the oePAL2-GFP genotype (oePAL2-GFP-32) and differ in the oeKMD1-MYC contribution (oeKMD1-MYC-8 and oeKMD1-MYC-10). **(B-C)** IB analysis of **(B)** PAL2-GFP and **(C)** KMD1-MYC levels in 10-days-old **(B-C)** co-overexpressor lines oePAL2-GFP-32/oeKMD1-MYC-8 and oePAL2-GFP-32/oeKMD1-MYC-10 and in the parental lines **(B)** oePAL2-GFP-32, **(C)** oeKMD1-MYC-8 and oeKMD1-10, treated or not (DMSO) during 8h with the proteaosome inhibitor MG132 (50µM). In **(B-C)** the lower panel shows Ponceau staining of RuBisCO as loading control. **(D)** qRT-PCR analysis for the expression of *PAL2* and *KMD1* in 12-days-old co-overexpressor lines oePAL2-GFP-32/oeKMD1-MYC-8 and oePAL2-GFP-32/oeKMD1-MYC-10, and the parental lines oePAL2-32, oeKMD1-MYC-8 and oeKMD1-MYC-10, grown in FN conditions. Analysis was performed using the TaqMan ®Universal ProbeLibrary System (UPL) with ACT8 as housekeeping reference. Values are means ±SD, and are represented in a linear scale.

Immunoblot analyses using both oePAL2-GFP/oeKMD1-MYC and parental lines showed a clear reduction in PAL2-GFP fusion levels when it was co-expressed with KMD1-MYC fusion in Arabidopsis (Figure 41-B). Moreover, the levels of PAL2-GFP appeared to be inversely proportional to those of KMD1-MYC, as evidenced by lower levels of PAL2-GFP in oePAL2-GFP/oeKMD1-MYC-10 plants, where KMD1-MYC levels are higher than in oePAL2-GFP/oeKMD1-MYC-8 (Figure 41-C). By analyzing the transcript levels of *PAL2* and *KMD1* in the above-mentioned lines, co-suppression effects due to transgene overexpression could be discarded (Figure 41-D).

6.8.4.1. KMDs altered expression impairs the biosynthesis of phenylpropanoids

To assess the function of the KMDs in regulating phenylpropanoid biosynthesis by the regulation of PAL2 stability (Figure 41), the content of different metabolites was examined using GC-MS technology on shoots from *kmd1/2*, *kmd1/4*, oeKMD1-GFP-82 and WT seedlings grown during 11 days in +Pi solid medium.

Two intermediates from the phenylpropanoids biosynthesis pathway that are down-stream PAL2, were detected using GC-MS: ferulic acid and sinapic acid (detailed Phenylpropanoids biosynthesis pathway map in Supplemental Figure 5). Biosynthesis of ferulic acid is catalyzed by the caffeic acid 3-O-methyltransferase (COMT; Figure 6) from caffeic acid (Supplemental Figure 5) and it is an intermediate in the synthesis of lignans, and of monolignols, i. e., the monomers of lignin. Sinapic acid is biosynthesized by COMT as well, from the precursor 5-hydroxyferulic acid methyl ester (Supplemental Figure 5), which in turn is produced by the ferulate 5-hydroxylase (F5H; Figure 6).

A statistically significant increase in the ferulic and sinapic acids in both *kmd1/2* and *kmd1/4* was found relative to the endogenous levels in WT (Figure 43-A). In contrast, clear decrease was found in oeKMD1-GFP-82, although without statistical significance (Figure 42-A).

The content of intermediates from the phenylalanine, tyrosine and tryptophan biosynthesis, mainly represented by the shikimate pathway (Supplemental Figure 6) were analyzed to examine whether altered accumulation of metabolites in plants with *KMD*s altered expression also occurred up-stream of PAL2 activity. Shikimic acid (more commonly known as its anionic form shikimate) accumulation was not affected either in the double mutants or in oeKMD1-GFP-82 plants (Figure 42-B). Interestingly, the aa phenylalanine that is a final product of the shikimate pathway, showed a significantly lower content in *kmd1/2* and *kmd1/4* in comparison with WT (Figure 42-B), however other amino acids involved in the biosynthesis of plant secondary metabolites (Supplemental Figure 7), like aspartic acid and alanine were not affected (Figure 42-C) excluding a general defect on amino acids biosynthesis. Moreover, metabolites from relatively distant metabolic pathways were measured in order to establish the specificity of *KMD*s altered expression effect. As an example, intermediates from the ascorbate and aldarate metabolism (Supplemental Figure 8), like the lyxonic and saccharid acid were found not to be affected in *kmd1/2*, *kmd1/4* and oeKMD1-GFP-82 plants (Figure 42-C).

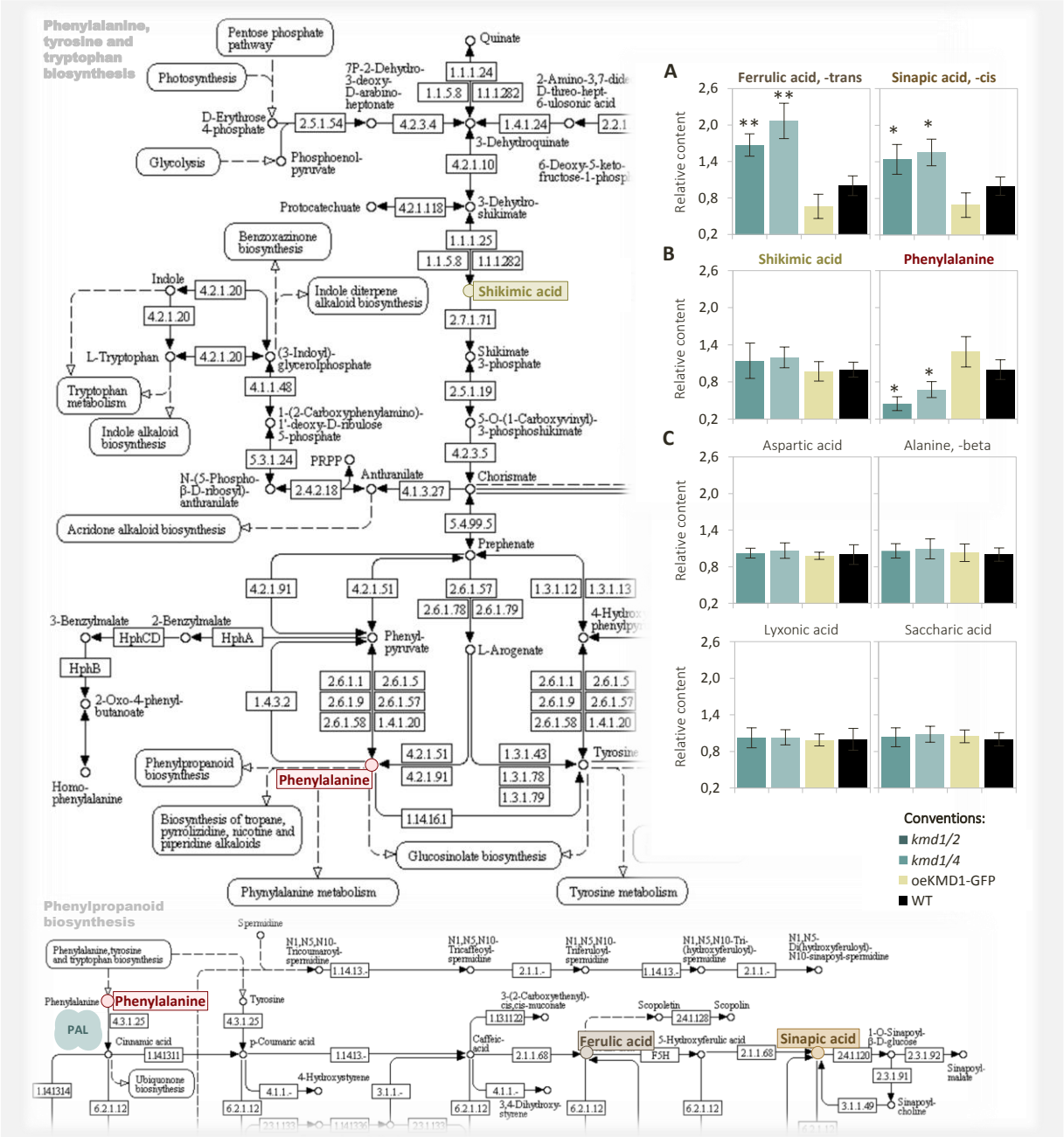

Figure 42. Phenylpropanoid intermediates in plants with *KMD*s altered expression. Levels of accumulation of intermediates from pathways related and partially unrelated with the phenylpropanoids biosynthesis, in shoots of *kmd1/2*, *kmd1/4*, oeKMD1-GFP-82 and WT seedlings, grown 11 days in +Pi conditions. In **(A)** the phenylpropanoids biosynthesis intermediates ferulic acid and sinapic acid. In **(B)** the intermediate shikimic acid and the product phenylalanine, from the so called phenylalanine, tyrosine and tryptophan byosinthesis pathway. In **(C)** the aminoacids aspartic acid, alanine, and the intermediates lyxonic acid and saccharic acid. Values are presented as relative to WT, and are means of 5 biological replicates ± SD. Statistical significance was determined by t-test [(∗) (p<0,05); (**) (p<0,01)]. Metabolites were detected by GC-MS technology. Pathway maps were taken from KEGG PATHWAY database (http://www.genome.jp/kegg/), and used as background. Complete pathway maps in Supplemental Figure 5 and Supplemental Figure 6.

Noteworthy, the decreased content of the phenylpropanoids intermediates ferulic and sinapic acids were not due to altered transcription of *PAL* genes, since *PAL1-4* gene expression was up-regulated relative to the endogenous levels in WT seedlings (Figure 43) reflecting a positive feedback regulation of *PAL* expression in response to PAL turnover. *PAL1-4* up-regulation was also observed in the *KMD4* overexpressor line oeKMD4-15 (Figure 43), suggesting that, similar to *KMD1* overexpression, *KMD4* altered expression also affects PAL stability/activity *in planta*.

The higher levels of phenylpropanoids intermediates in the double mutants, despite the lower levels of the precursor phenylalanine, suggests that *KMD*s expression directly influences the turnover of PAL *in planta*, and therefore its activity.

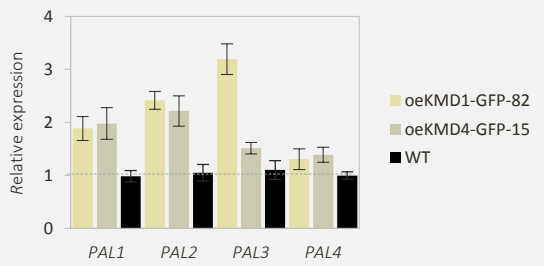

Figure 43. *PAL1-4* gene expression in *KMD*s overexpressor transgenic plants. qRT-PCR analysis of *PAL1-4* mRNA levels in the overexpressor lines oeKMD1-GFP-82 and oeKMD4-GFP-15. Seedlings were grown during 11 days in +Pi solid medium. Data was obtained using the SYBR® Green dye system with *UBQ10* as housekeeping reference. Values and error bars are means ± SD.

DISCUSSION

7. DISCUSSION

7.1. PHOSPHATE RESPONSIVE UPS COMPONENTS

The involvement of the UPS in Pi-signaling clearly goes beyond the previously described ubiquitin-mediated modulation of Pi starvation responses (3.2.2.2.4. Ubiquitin-mediated modulation of Pi starvation responses). The transcriptional effect of long term Pi starvation and of the double mutation *PHR1/PHL1* over different UPS gene super-families was analyzed, taking advantage from ATH1 Affymetrix data obtained by Bustos and collaborators (2010). It should be kept in mind that, in this analysis, inherent limitations in the expression arrays, such as incomplete representation of gene families and the loss of information derived from unspecific probe sets, and/or low gene expression levels, represent challenges to reliable measurements (Benjamini & Hochberg, 1995). Even if the representation of the gene super-families is heterogeneous in the ATH1 microarray, they are broadly represented. Thus, probe sets were found corresponding to more than 75% of the members of almost all gene super-families studied, except for HECT and F-box super-families. Thus, there is an information gap derived from more than 300 F-boxes without corresponding ATH1 probe sets, which needs to be examined by alternative expression profiling techniques.

The transcriptional behavior of the overall UPS components in response to Pi starvation differed from that found in the global ATH1 probe sets. Indeed, Pi-responsive UPS components were, in general, slightly underrepresented. This is in agreement with the lack of overrepresentation of PHR1 binding sites in the promoter sequences of the UPS component genes (data not shown). However, by splitting the analysis in different gene families, over-representation of up-regulated genes in response to Pi deficiency in shoots became apparent in the case of the U-box family (binomial distribution analysis). This over-representation seems to be functionally relevant in the context of Pi homeostasis, as shown by analysis of a triple *pub27/28/29* knockdown line which accumulated less Pi under different Pi conditions, similar to *phr1* mutants (Rubio *et al*., 2001)). Interestingly, increased *PUB28* gene expression in response to low Pi is controlled by *PHR1/PHL*1 genes (Bustos *et al*., 2010), supporting the implication of this single-unit E3 family in the regulation of adaptive Pi-deficiency responses in Arabidopsis. In assessing the transcriptional effects of the double mutant *phr1phl1* on the expression of UPS components, it is evident that the post-transcriptional regulatory processes that involve the UPS in Pi-deficiency responses are mainly under the control of PHR1(-like) TFs. Thus, most of the Pi-responsive UPS components exhibited reduced expression in the double mutant *phr1phl1*, both in shoots and in roots, and displayed concordant dynamic ranges (Bustos, *et al*., 2010). This transcriptional effect was independent of the representation of deregulated genes in each family. However, by comparing the overall transcriptional behavior of each gene super-family in *phr1phl*1 and WT lines, it became evident that PHR1/PHL1 largely influences the expression of genes encoding substrate

receptors (both E3 complex components and monomeric E3 enzymes. Thus, PHR1/PHL1 was observed to significantly control Pi starvation-responsiveness of the F-box, BTB, PHD, DCAF, U-box and E2 families. PHR1/PHL1 TFs also regulated expression of DUBs in Arabidopsis shoots, indicating that Ub deconjugation from specific protein targets and Ub recycling may play regulatory roles in the control of Pi starvation responses at the whole-plant level, and not specifically in roots as shown for UBP14 (Li *et al*., 2010).

The relevance of the UPS system in the control of Pi signaling, was analyzed using weak *cul1–6* and *cul3*^{hyp} Arabidopsis mutant lines (note that null mutants are embryo-lethal), which partially affect the assembly and function of two different E3s: the SCF and CUL3- BTB complexes, respectively (Moon *et al*., 2007; Thomann *et al*., 2009). Partial lack of CUL1 and CUL3 function should yield a reduction in the function of F-box and BTB proteins, including those that respond to Pi supply variations. The up-regulation of PSR genes in *cul1–6* and *cul3*^{hyp} hypomorphic mutants, suggest that specific SCF and CUL3-BTB complexes, which are only partly active in the aforementioned mutants, control the abundance of positive regulators of PSR gene transcription. The identification of specific substrate adaptors with the capacity to recruit regulators of the-Pi responses, as well as these targeted-regulators will be of utmost importance.

Within the F-box super-family, the *FBK* genes *KMD1-4* were found to be -Pi-repressed genes and tightly controlled by PHR1/PHL1 TFs (Bustos *et al*., 2010), while being forming a close sub-cluster within the phylogeny of the Arabidopsis F-box proteins (Gagne *et al*., 2002). Thus, *KMD*s represented good candidates as hypothetical repressors of the Pi-starvation responses.

7.2. *KMD1-4*: GENE EXPRESSION PATTERNS AND PROTEIN FEATURES IN AN EVOLUTIONARY CONTEXT

KMD1-4 are classic FBK multidomain proteins. While the F-box connects the protein via a restricted set of ASK adaptor proteins to the rest of the SCF complex, the C-terminal kelch repeats domain most likely recruit target proteins destined for Ub labelling. Even though *FBK*s are widespread in land plant genomes, there is hardly any experimental evidence addressing the function of the vast majority of these genes. However, their patterns of evolution are strongly suggestive, according with the phylogenetic reconstruction of the land plants FBKs, performed by Schumann and collaborators (2011). Unlike the work presented by Gagne and collaborators (2002), were only the 60-aa F-box motifs were used to build a phylogenetic reconstruction of the Arabidopsis F-box protein superfamily, in Schuman and collaborators the full length aa sequences of the FBKs found in seven different land plant species were used, allowing to turn the focus from the F-box domain to the Kelch repeats protein-protein interaction domain and, as a consequence, to the target recruiting function. In this manner, Schumann and

collaborators (2011) reconstruction provided evolutionary insights as well as it represented a scaffold for functional analysis, of this large family of F-box proteins.

For the evolutionary classification, Schumann and collaborators (2011) adopted the "stable/unstable" terminology proposed by Thomas (2006) and extended it with "super-stable" and "ancient" categories. Unstable genes are lineage specific without clear orthologs in the other species analyzed. Stable genes are conserved across species with orthologs in at least one additional species. Super-stable genes have orthologs in all analyzed species and, therefore, exhibit the highest degree of evolutionary conservation, and ancient genes has orthologs in at least one lower plant, one monocot and one eudicots species. Meaningfully, a distinction between plant stable and super-stable genes cannot be directly translated into the evolutionary age of the gene due to the possibility of gene losses in the individual species analyzed by Schumann and collaborators (2011). Based on the location of *KMD1-4* in a super-clade composed by one ancient and two stable clades, it is conceivable that KMDs most likely became devoted to specific endogenous substrates long ago, as hypothesized by Thomas (2006) for stable F-box genes from three species of the nematode genus *Caenorhabditis*. Accordingly, strong evidence was found for purifying selection in the C-terminal substrate-binding domains of stable F-box genes in *Caenorhabditis* (Thomas, 2006) as well as in Arabidopsis (Schumann *et al*., 2011). In Arabidopsis unstable genes, numerous regions located C-terminal to the F-box domain seemed to be under strong positive selection, and while in most cases the F-box domain is rather conserved, it is the substrate-recruiting Kelch domain that seems to be positively selected for. Hence, Kelch repeats evolve in a manner that supports the constant development of novel substrate specificities, and therefore responsible for the functional redundancy or sub-functionalization in regards to target specificity.

Even if it was argued that most of the F-box proteins of Arabidopsis do not have obvious functional paralogs based on direct sequence aligments between members of the same clade (Gagne *et al*., 2002), at least partial functional redundancy could be shown for the auxin receptors (Dharmasiri *et al*., 2005), the ethylene signaling components EIN3-BINDING F-BOX PROTEIN1-2 (An *et al*., 2010) and EIN2-TARGETING PROTEIN1/2 (Qiao *et al*., 2009), the root development regulators VIER F-BOX PROTEINE1-4 (Schwager *et al*., 2007), and more importantly for the FBKs ZTL, FKF1, and LKP2 (Baudry *et al*., 2010). Indeed, full genetic redundancy is evolutionary instable (Thomas, 1993) because the duplication of a gene lowers the selective pressure on both the new copy and the original gene (Hughes, 1994). In the context of the *FBK*s, their rapid gene superfamily expansion suggests scenarios wherein natural selection favors additional copies for an increased repertoire of molecular tools via sub-functionalization (Demuth & Hahn, 2009). The latter is supported by clear differences in transcriptional regulation within Arabidopsis *FBK*s phylogenetic subclades (Schumann *et al*., 2011).

The molecular characterization of *KMD*s indicates conservation of protein features such as subcellular localization, ability to associate with CUL1 and partially ASK-binding patterns (see 6.3. KMDs as substrate adaptor subunits of SCF complexes that control PAL stability in Arabidopsis). This indicates that KMDs may be able to integrate into the same SCF complexes and act in the same cellular compartments. Therefore, as well as indicated for others FBK sub-clades (Schumann *et al*., 2011), it is attractive to hypothesize that two genetic mechanism can mainly contribute to potential partial sub-functionalization, if applicable, of *KMD*s in Arabidopsis: (i) positive selection acting primarily on the Kelch repeats domain that can result in modified substrate specificities, and (ii) different transcriptional regulation.

In one hand, according to the crystal structure of proteins containing kelch repeats, these modules form a β-propeller (Ito *et al*., 1994; Bork *et al*., 1994; Gumz *et al*. 2015), which contains multiple potential protein-protein contact sites (Andrade *et al*., 2001). Based on the molecular modelling of the kelch repeats of the galactose oxidase (GAO) crystal structure from the fungus *Dactylium dendroides* (Ito *et al*., 1994), it was establish that Arabidopsis FBK kelch repeats form a potential protein-protein interaction domain (Andrade *et al*., 2001) that, therefore, defines their biological function.

3-D reconstruction predicted that KMDs adopt the stereotypical topology of a β-propeller. Typically, five to seven Kelch repeats form a β-propeller with the blades arranged around a central axis, with intrablade and interblade loops of varying lengths that can protrude above, below, or at the sides of the β-sheets, contributing with the variability of the binding properties (Fulop & Jones, 1991; Jawad & Paoli, 2002; Prag & Adams, 2003). With the exception of the Arabidopsis AFR, all functionally characterized kelch proteins in plants contain a minimum of five kelch repeats, as well as KMD2. Therefore, KMD2 match the prerequisites to form a closed propeller structure with stabilized interactions between the first and last blade. However, KMD1, KMD3 and KMD4, contain four kelch repeats. This is in concordance with the vast majority of plant FBKs that contain less than three kelch repeats (Schumann *et al*., 2011). It is questionable therefore, whether functional β-propellers can be form in KMD1, KMD3 and KMD4. However, it is unlikely that the kelch repeats in KMD1, KMD3 and KMD4, as well as in the vast majority of FBKs, are nonfunctional, so some hypothetical scenarios are attractive. It is conceivable that KMD proteins with less than 5 kelch repeats dimerize to achieve a full set of propeller blades. Also, due to the poor sequence conservation of the kelch motif, the missing repeats are present but not recognized in protein databases like Pfam (http://pfam.xfam.org/). Actually, other motif recognition algorithms/databases such as Interpro (http://www.ebi.ac.uk/interpro/) recognize a complete galactose oxidase β-propeller domain (IPR015916) in the four KMDs.

In mammals, dimerization of F-box proteins has been described as a regulatory factor for substrate interactions (Welcker *et al*., 2007). However, in most cases the *in vivo* effect of F-box protein dimerization on substrate selection and ubiquitination remains unclear (Li *et al*., 2010; Yen *et al*., 2012; Suzuki *et al*., 2000; Hao *et al*., 2007; Welcker *et al*., 2007). This opens the possibility that plant F-box proteins, including the FBKs, also displays similar dimerization abilities. In fact, size exclusion chromatography and small-angle X-ray scattering (SAXS) of a recombinant FKF1-LOV polypeptide, from the Arabidopsis FBK protein FKF1, indicates a dimeric association (Nakasako *et al*., 2005). Moreover, the only Kelch repeat-containing protein from the plant kingdom which has its crystal structure characterized, the thiocyanate-forming protein (TFP) from *Thlaspi arvense* (field penny-cress; Brassicaceae), crystallized as homodimer (Gumz *et al*., 2015). In concordance, KMD1, KMD2 and KMD4 have the ability to form dimers in a heterologous system. This finding allow to hypothesize that they can achieve a tertiary structure suitable for the interaction with target proteins, with combinatorial possibilities that can have an effect on the diversity and/or specificity of the recruiting substrates. Moreover, the putative convergence of different KMDs in the same SCF complex is an indicator of its involvement in common biological processes. However, a detailed study of KMDs dimerization abilities and its effects on target recruiting *in planta* is yet to be done.

In the other hand, differential gene regulation indeed contributes to functional diversification, as it was reported on the auxin receptors, members of the F-box LRR subfamily (Dharmasiri *et al*., 2005; Parry *et al*., 2009). In this context, transcriptional co-regulation can be positively related with functional conservation. Even if the transcriptional co-expression does not necessarily means transcriptional co-regulation, the study of the correlation between the expression patterns of *KMD1-4* is a starting point to get insights on its spatio-temporal transcripts convergence. According to the results, differential correlation can be found between *KMD1-3-4* and *KMD2* gene expression patterns, depending on the datasets selected. While *KMD1-4* are clearly co-express in response to photoperiod, and in a less extend to light intensity and stress experiments, *KMD2* appeared with lower and even negative Pearson's correlation coefficient in the analysis for other stimuli like nutrients and hormones, respectively. For example according with Genevestigator's data, *KMD2* seems to be less responsive to some nutritional stresses (Figure 16-C) and divergent in response to some phytohormone exogenous supply treatments like BL (Figure 20-B).

Unlike unstable *FBK* genes, *KMD1-4* displayed medium-high levels of expression in different tissues and developmental stages (Figures 14-15) as it is the case for most *Arabidopsis* stable *FBK* genes, supporting the idea that they perform functions in developmental and/or physiological processes conserved in all land plant species. Indeed, the few *FBK*s biologically characterized are ancient genes with conserved function in essential physiological processes such as the regulation of light responses and circadian rhythms, like *AFR*, *ZTL*, *FKF1* and *LKP2* that have

orthologs in several species. Nevertheless, differences between *KMD*s levels of expression in the tissues callus and root, and during senescence support the idea of a partial sub-functionalization between the KMDs.

Altogether indicates that *KMD*s are genes conserved in land plants that may have roles in relevant physiological processes. These roles can be performed by KMDs through the physical interaction with target proteins via the kelch repeats protein-protein interaction domain, which has a predicted β-propeller tertiary structure that can be accomplish by the four KMDs as monomers and probably as dimers. Based on the hypothetical mechanisms driving putative sub-functionalization discussed previously, correlation in the *KMD*s gene expression patterns indicates that *KMD*s may have redundant functions in some biological functions. At the same time, specific transcriptional behavior/intensity in response to determine stimuli, and in few selected tissues and stages of development argued that *KMD*s partially sub-functionalized. Mainly, *KMD2* seems to be most likely subject to sub-functionalization because it exhibits a higher number of kelch repeats that can result in modified substrate specificities, and seems to be under a partially different transcriptional regulation.

7.3. KMDs AS SUBSTRATE ADAPTOR SUBUNITS OF SCF COMPLEXES WITH PUTATIVE MULTIPLE FUNCTIONS

KMDs function as canonical F-box substrate adaptors, based on their interactions with known components of the Arabidopsis SCF complex. Myc-tagged KMD1 and GFP-tagged KMD1 and KMD4 co-immunoprecipitated with CUL1 *in planta*, consistent with the KMD proteins functioning within a SCF complex in plant cells. In the same direction, KMD1 and KMD4, which were selected as representatives of the two branches of the KMDs sub-cluster, interacted with ASKs in a heterologous system. Both KMD1 and KMD4 interact with ASK1, ASK2 and ASK11, while a strong interaction was found between KMD1 and ASK3. This finding is in concordance with a large scale yeast-2-hybrid interaction study, tested assembly of 341 F-box proteins with 19 ASK family members, where seven ASK proteins (ASK1-3 and ASK11-14) were each able to interact with more than 40 different F-box proteins (Kuroda *et al*., 2012). KMD1 and KMD4 also interact with ASKs that displayed higher specificity, as suggested for ASK4-6 that were reported to interact with less than five of the 341 F-box tested by Kuroda and collaborators (2012). Interestingly, ASK8 and ASK18, and ASK20 were found to also activate the Y2H system when co-transformed with KMD1 and KMD4, and with KMD1, respectively, indicating that KMDs can interact with ASKs rarely involved in SCF complexes or that require secondary modifications to accomplish the assembling of the SCF core (Kuroda *et al*., 2012; Choi *et al*., 2014). Moreover, KMD1-MYC fusion was found to be associated with Ub molecules. Since KMD1-MYC fusion is not subject to degradation via the 26S proteasome either in stable or transient systems, KMD1-MYC detection in a total ubiquitinated proteins pull-down assay is in concordance with the fact that Ub molecules and substrate adaptors can display a physical association due to an E2/E3 transient interaction, because in a SCF

complex CUL1 brings the F-box and the Ub-E2 intermediate into close physical proximity to enable Ub transfer to a target protein (Zheng *et al*., 2002b).

SCF^{KMD} complexes in Arabidopsis plant cells are demonstrated based on KMDs ability to physically interact (i) with CUL1 *in planta*, (ii) with ASK proteins in a heterologous systems, and (iii) by the *in vivo* physical association with Ub molecules in a 26S-proteasome independent manner.

KMD proteins may function as substrate recruiters in the cytoplasm as well as in the nucleus, as suggested by KMD1, KMD2 (data not shown), and KMD4 subcellular localization. Consistently, KMD1, as part of SCF complexes, seems to be involved in multiple aspects of the cell biology, as suggested by the diversity of interactors found in the Y2H mating screening. Most likely, KMD1 play crucial roles in BINs like (i) Photosystem, through the light reactions and the Calvin cycle; (ii) Redox, through thioredoxines; (iii) S-assimilation, through the adenosine-5'-phosphosulfate reductases; (iv) Fermentation, through aldehyde dehydrogenases; (v) DNA repair; (vi) Secondary metabolism, through the biosynthesis of phenylpropanoids. However, a detailed study of KMD1 function(s) in these last processes is yet to be done, with the exception of the biosynthesis of the phenylpropanoids (see 7.4. KMDs mediate PAL stability with consequences in the phenylpropanoids biosynthesis).

7.4. KMDs MEDIATE PAL STABILITY WITH CONSEQUENCES IN THE PHENYLPROPANOIDS BIOSYNTHESIS

Synthesis and accumulation of anthocyanins are stimulated by different abiotic stresses (Tsukaya *et al*., 1991). However, responses common to several different stresses may be controlled by signaling pathways specific to each stress type, as it is the case of-Pi-induced anthocyanin accumulation in Arabidopsis (Rubio *et al*., 2001). By means of the discovery and characterization of *phr1*, it was possible to establish that anthocyanin accumulation is a primary response to Pi limitation (Rubio *et al*., 2001), rather than a secondary side effect controlled by a shared mechanism, as suspected previously (Trull *et al*., 1997).

Two main arguments sustained the study of KMDs as putative substrate adaptors that recruit PAL for Ub labeling: (i) anthocyanins are water-soluble vacuolar flavonoids, synthesized via the phenylpropanoid pathway that has as the entry-point the enzyme PAL, which catalyzes the non-oxidative elimination of ammonia from L-Phe to yield *t*-CA (Cochrane *et al*., 2004); (ii) numerous independent diploid yeasts clones harboring PAL2 were found in a mating using KMD1 as bait. Indeed, four of the five independent clones associated with PAL2 represented strong interactions with KMD1.

Different lines of evidence in this study revealed that KMD1 physically interact with PAL2, like the genome-wide Y2H screening using a cDNA library prepared with mRNAs purified from Pi-starved Arabidopsis seedlings,

followed by pairwise Y2H validation extended with KMD2 and KMD4, and the co-IP of KMD1 with PAL2 in a transient system and, more importantly, in two independent co-overexpressor lines oePAL2-GFP/oeKMD1-MYC. The inmmunodetection of PAL2 in the co-IP assay is not due to the artificial interaction with the GFP tag, since the GFP alone is not detected in the co-IP output when co-expressed with KMD1-MYC, indicating that the co-immunoprecipitation only occurs when PAL2 is fused to the GFP tag.

KMD proteins most likely dominates the substrate specificity of SCF^{KMD} complex, leading to ubiquitination and degradation of PAL2. In fact, KMD1 and PAL2 co-overexpression in a stable system resulted in an obvious decrease of PAL stability. PAL2-GFP levels of detection in oePAL2-GFP/oeKMD1-MYC co-overexpresor lines was discernible attenuated in comparison with the oePAL2-GFP-32 parental line. Indeed, in the co-overexpressor lines, PAL2-GFP fusion levels were inversely proportional to the KMD1-MYC contribution, as evidenced by the strongest reduction on PAL2-GFP levels on oPAL2-GFP/oeKMD1-MYC-10 than in oePAL2-GFP/oeKMD1-MYC-8. Reduction on PAL2-GFP levels in the co-overexpressor lines due to co-suppression effects can be discarded because no significant difference on *PAL2* expression levels were found between the oePAL2-GFP/oeKMD1-MYC lines and oePAL2-GFP-32 parental line.

It is worth noting that, the recognized control of PAL can occur through several mechanisms like product inhibition and metabolite feedback regulation, among others (Zhang *et al*., 2015). oePAL2-GFP-32 selection as the parental line for cross-pollination and subsequent generation of oePAL2-GFP/oeKMD1-MYC co-overexpressor lines, was made having in consideration PAL and phenylpropanoid biosynthesis feedback regulation, which may introduced an extra level of complexity in the study of the post-transcriptional regulation of PAL via KMDs. By means of the anthocyanin accumulation levels, the functionality of the over-expressed *PAL2* was evaluated in oePAL2-GFP plants and, based on that criteria, in oePAL2-GFP-32 line PAL2-GFP and/or phenylpropanoids biosynthesis was found to not been under a detectable negative regulation. However, levels of *PAL2* overexpression higher than those found in oePAL2-GFP-32 seems to be sufficient to trigger a negative feedback regulation. oePAL2-GFP-42 showed a significant reduction on the anthocyanin accumulation in response to -Pi in the cotyledons, but not in the presence of Pi in the growing medium. This phenomena can be explain based on a combinatorial effect of the high levels of *PAL2* over-expression and the reported strong -Pi-induction of the MYB TFs *PAP1* (*PRODUCTION OF ANTHOCYANIN PIGMENT 1*) and its close homolog *PAP2* (*PRODUCTION OF ANTHOCYANIN PIGMENT 2*) (Scheible *et al*., 2004; Morcuende *et al*., 2007). PAP1 is a key positive regulator of genes that encode for anthocyanin synthesis enzymes like PAL, CHS, and DFR (Tohge *et al*., 2013). Under -Pi, the constitutive high levels of PAL2 plus the -Pi-induced levels of CHS, DFR and GST, may result in high levels of the immediate product of PAL (*t*-CA), and of intermediates from, at least, the flavonoid biosynthesis pathway, since CHS is the first committed enzyme of it

(Durbin *et al*., 2000; Tuteja *et al*., 2004). *t*-CA has long been proposed as a signal molecule, regulating flux into the pathway (Lamb, 1979; Bolwell, *et al*., 1986), by negatively regulating PAL activity and transcription, either via exogenous supply or by a limiting down-stream enzymatic activity (Lamb 1979; Bolwell *et al*., 1986; Mavandad *et al*., 1990; Blount *et al*., 2000).

In the same direction, negative feedback regulation can be triggered by intermediates from branch pathways like the aforementioned flavonoid biosynthesis. In Arabidopsis, PAL activity and *PAL1*, *PAL2* and *CHS* are repressed in response to a deficiency on the 3-O-glycosilation of flavonols, found in a double mutant deficient in *AtUGT78D1-2* (Olsen *et al*., 2008), so repressing flavonol synthesis itself. Interestingly, *KMD*s transcript levels are up-regulated in oePAL2-GFP-32 plants but not in oePAL2-GFP-42, indicating that the negative feedback regulation proposed for oePAL2-GFP-42 involves also post-transcriptional regulatory elements like the *KMD*s.

In addition, PAL2 was found to be ubiquitinated *in vivo*, as revealed by the detection of PAL2-GFP fusion in the purified pool of ubiquitinated proteins from *N. benthamiana* leaves transiently overexpressing PAL2-GFP. Supporting this finding, ubiquitin-PAL conjugates were found in a tandem affinity purification and mass spectrometric analysis of ubiquitinated proteins in Arabidopsis (Saracco *et al*., 2009).

Ub labelling of PAL2 seems to be regulating its degradation via the 26S proteasome system because PAL2-GFP fusion accumulation levels were sensitive to MG132 treatments. In the presence of the specific 26S proteasome inhibitor MG132, PAL2-GFP fusions appeared to be stabilized in *N. benthamiana* leaves transiently overexpressing PAL2-GFP.

This effect on PAL2 stability driven by SCF^{KMD} was evidenced in plants with *KMD*s altered expression, by changes on the levels of accumulation of precursors, intermediates and products of the phenylpropanoids biosynthesis pathway. The levels of the phenylpropanoids precursor (i) L-Phe, the intermediates (ii) ferulic and sinapic acids, and the product (iii) anthocyanins, were reciprocally affected by the silencing and overexpression of *KMDs*. L-Phe levels were found to be significantly lower in both *kmd1/2* and *kmd1/4* double mutants, consistent with a higher rate of catalysis of L-Phe into *t*-CA by PAL, in the absence of functional KMD1/2/4. Reciprocally, L-Phe levels in oeKMD1-GFP were higher than in WT plants, indicating lower carbon flux into the phenylpropanoids biosynthesis when *KMD1* is overexpressed. Consistent with a KMDs-mediated turnover of PAL, higher and lower levels of the intermediates ferulic and sinapic acids, located down-stream PAL in the biosynthesis of the phenylpropanoids, were found in the double mutants and in oeKMD1-GFP lines, respectively. In the same direction, anthocyanins that are one of the final products of the phenylpropanoids biosynthesis pathway, were found to accumulate in a higher extent in *kmd1/2*, *kmd1/4* and *kmd1/2/4* in comparison with WT seedlings, mainly in the presence of sugars. Actually, this effect can answer to a combinatorial effect of the KMDs-mediated post-

transcriptional regulation of PAL, and the reported induction of anthocyanins by high carbon source or the related sugar signaling (Tsukaya *et al*., 1991; 2005; Solfanell, *et al*., 2006).

The genetic and metabolic evidence discussed above strongly suggest that KMDs, as substrate adaptors of SCF^{KMD} complexes, act as basic post-transcriptional regulators of carbon flux toward phenylpropanoids secondary metabolites by controlling the stability of the entry-point enzyme of the general phenylpropanoids pathway, PAL. During the development of this document, similar results were published that are supporting our findings (Zhang *et al*. 2013).

7.5. KMDs AS AN INTERPLAY NODE BETWEEN Pi, SUGAR AND CYTOKININ SIGNALING

Based on our findings, KMDs act as an integrator node of the previously reported (i) bidirectional antagonistic interactions between cytokinin and both sugar and Pi-starvation signaling (Franco-Zorrilla *et al*., 2005), as well and more importantly in the focus of this research, of the (ii) positive bidirectional interaction between sugar and Pi-starvation signaling (Franco-Zorrilla *et al*., 2005; Karthikeyan *et al*., 2007; Lei *et al*., 2011) by means of the post-transcriptional regulation of PAL stability (Figure 44).

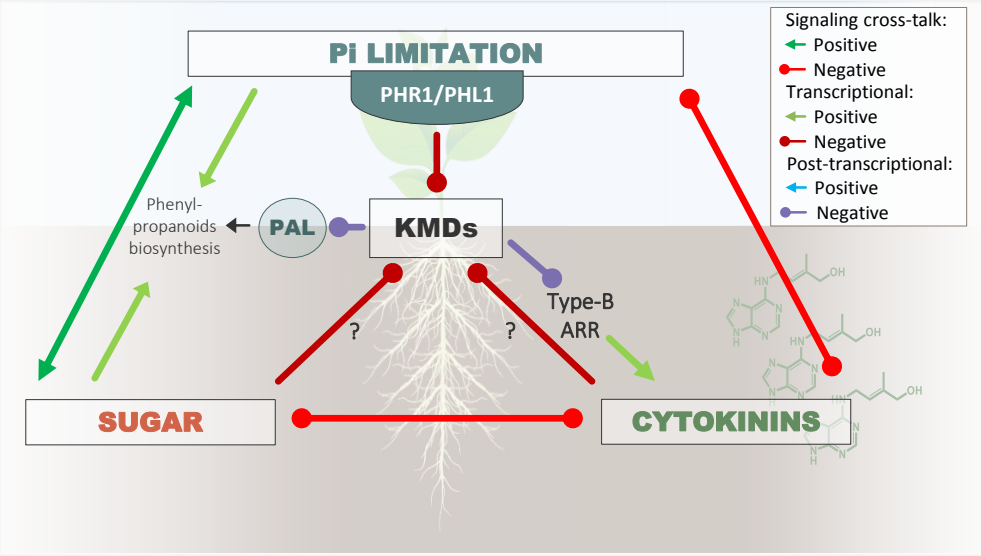

Figure 44. KMDs as integrators of the interplay between cytokinin, sugar and Pi signaling. KMDs act as an integrator node of the bidirectional antagonistic interactions between cytokinin and both sugar and Pi-starvation signaling, as well of the positive bidirectional interaction between sugar and Pi-starvation signaling, by means of the post-transcriptional regulation of PAL and type-B ARR stability.

KMDs integrates evidence on the intricate interconnections between cytokinin, sugar and Pi-starvation signaling. Kinetin treatments revealed that the high level mutant *kmd1/2/*4 and the oeKMD1-GFP line exhibit enhanced and reduced response to exogenous kinetin supply, respectively, with a striking cytokinin-insensitive PR

growth displayed by oeKMD1-GFP seedlings under sufficient Pi and Suc conditions. The PR growth response assay in the presence or absence of Pi and Suc in combination with kinetin treatments, indicates that oeKMD1-GFP insensitivity to kinetin is Pi dependent and Suc independent, although it is exacerbated by the lack of Suc in the growth medium. Moreover, the almost unaffected response to kinetin found in both *kmd1/2/4* and oeKMD1-GFP under the combined-Pi and-Suc treatment, relates with a high place of Pi-starvation signaling in the regulatory hierarchy controlling plant metabolism and development in harmony with the physiological importance of Pi (Franco-Zorrilla *et al*., 2005). Such a hierarchical organization, allows development (i. e. root growth) to be adjusted to Pi status. For instance, low Pi will reduce cytokinin signaling, thereby increasing the root-to-shoot growth ratio and concomitantly the soil Pi scavenging potential, as well accelerating senescence, which is a Pi-mobilizing process (Franco-Zorrilla *et al*., 2005). Interestingly, during the development of this research, KMDs-mediated regulation of cytokinin signaling in Arabidopsis was reported (Kim *et al*., 2013). SCF^{KMD} complexes are negatively regulating the cytokinin responses by the post-transcriptional control of the type-B ARR (Arabidopsis Response Regulators) TFs levels, whose action is regulating the transcriptional response to cytokinins in Arabidopsis (Kim *et al*., 2013). KMDs are directly interacting with the type-B ARR TFs and targeting them for degradation (Kim *et al*., 2013). This cytokinin-regulatory role of KMDs may be partially explaining the marked heterogeneity in the *KMD*s gene expression and, in particular, the high *KMD2* transcriptional activity found in the tissues callus and root. In this context, future studies should address the identification of TFs regulating *KMD*s transcriptional activity in response to cytokinins and, more importantly, to sugar fluctuations.

In the context of this research, we had focus con KMDs role in the positive bidirectional interaction between sugar and Pi-starvation signaling. The sugar metabolism is close linked to Pi status, linkage that is a primary determinant of metabolic adaptations in plants (Franco-Zorrilla *et al*., 2005). Pi plays a key role in the coupling of light and dark reactions in photosynthesis and in the export of trioses from the chloroplast. Pi is also a substrate or a product in many reactions of sugar metabolism and an effector of key enzymes of starch and Suc synthesis. Paralleling this close metabolic link, it is well known that Pi starvation induced the expression of Suc-responsive genes (Sadka *et al*., 1994; Nielsen *et al*., 1998; Ciereszko *et al*., 2001; Ciereszko & Kleczkowski, 2001; Karthikeyan *et al*., 2007), while the expression of most if not all the Pi starvation-induced genes is enhanced by Suc (Franco-Zorrilla *et al*., 2005; Karthikeyan *et al*., 2007; Lei *et al*., 2011). Although sugar input appears to be down-stream of initial Pi sensing (Karthikeyan *et al*., 2007), it is absolutely required for the completion of the PSI signaling pathway (Karthikeyan *et al*., 2007), and studies on the *SUC2* (*SUCROSE TRANSPORTER2*) had demonstrated that it is the level of Suc, rather than a particular Suc transporter, that affects the magnitude of plant responses to Pi starvation (Lei *et al*., 2011). In this direction, the highest expression of sugar and Pi starvation-responsive genes when Pi-starvation and high sugar conditions are combined (Franco-Zorrilla *et al*., 2005), can be explained as that these

genes are actually Pi starvation responsive and that high sugar further reduces cellular Pi levels by increasing the levels of sugar Pi (Sadka *et al*., 1994). However, this metabolic interpretation based on a stoichiometric balance between Pi and sugars is insufficient alone because even if the elevate Suc levels is sufficient to induce or enhance the expression of many PSI genes in Pi-sufficient conditions, the degree of induction is much lower compared with that induced by Pi starvation (Lei *et al*., 2011). This observation, enforce the idea that Suc needs to interact with other factors under Pi starvation conditions to orchestrate the wide range of PSR.

We propose that KMDs contribute in sugar and Pi-starvation signaling interaction acting as integrators of the two pathways, by controlling the stability of the common effector PAL, which alters the carbon flux directed to the phenylpropanoids biosynthesis and, in consequence, the fine-tuned balance between Pi and sugar status. Indeed, PAL-mediated carbon flux into the phenylpropanoid pathway affects the homeostasis of carbohydrate metabolism (Rohde *et al*., 2004). This impact is due that PAL is the major drain of the carbon fixed in the primary metabolism that is pumped into the shikimate pathway, by consuming L-Phe. Under normal conditions, 20% of all fixed carbon in a plant is pumped into the shikimate pathway (Hermann, 1995), and PAL directs up to 30% of that source to the synthesis of different phenolics (Rohde *et al*., 2004). Thus, in the context of PAL as a common effector of the positively-linked signaling pathways sugar and Pi-starvation, depending on the Pi and sugar balance in the plant different scenarios involving KMDs are possible, as resume in Figure 45, as follow: (i) Pi-limitation, (ii) high Suc availability, (iii) high Pi supply, and (iv) Suc starvation.

Due to the positive bidirectional interaction between sugar and Pi-starvation, under (i) Pi limitation and (ii) high Suc treatments, there is a transcriptional repression of *KMD*s that will limit KMDs-mediated PAL removal, thereby promoting the carbon flux to the synthesis of phenolic compounds (Figure 45-A-B). It is in concordance with the higher levels of anthocyanins accumulation found in *kmd1/2/4* in response to-Pi and high Suc treatments. Considering the important amount of carbon pumped into the phenylpropanoids pathway by PAL, most likely it will contribute to normalize the perception of the ratio sugar:Pi, by the reduction of sugar Pi hence increasing the levels of Pi in the system (Figure 45-A-B). A different yet consistent output is taking place when the sugar:Pi balance turn to (iii) high Pi and (iv) Suc starvation (Figure 45-C-D). As long as there is sugar available in the system, under high Pi treatments extra Pi will be available for the production of sugar Pi, therefore routing the perception towards Suc limitation that, in turn, strongly induce *KMD*s transcription and further PAL-mediated reduction of carbon flux towards phenylpropanoids biosynthesis (Figure 45-C). In this way, KMDs are contributing to buffer the Pi-excess effect over the sugar:Pi balance (Figure 45-C). Indeed, *kmd1/2/4* plants respond to high Pi treatments by over accumulating anthocyanin pigments, indicating that despite the high Pi-mediated Suc limitation perception, *KMD*s silencing is sufficient to maintain a drain of fixed carbon from the shikimate pathway (Figure 45-C). A similar

scenario, however with a different output, is taking place when no sugar is available in the system. Under-Suc conditions there is a lack of substrate to produce sugar Pi hence increasing the perception of Pi availability (Figure 45-D), situation that favors a remarkable induction of *KMD*s transcription and KMDs-mediated PAL degradation via the 26S proteasome. However, the absence of anthocyanins in the higher order *kmd* triple mutant in-Suc is indicating that KMDs-mediated flux of fixed carbon into the phenylpropanoids biosynthesis is Suc dependent.

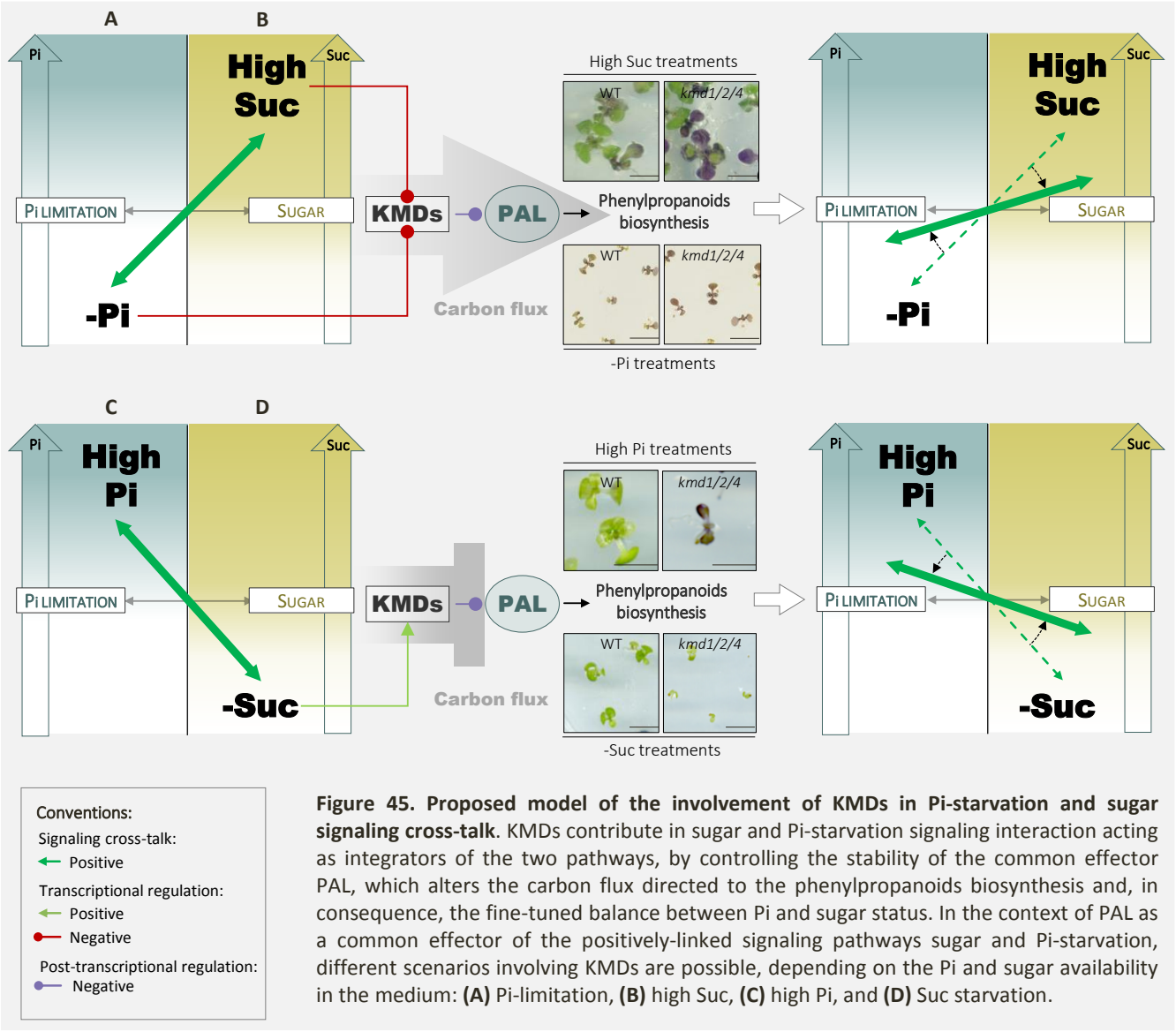

Figure 45. Proposed model of the involvement of KMDs in Pi-starvation and sugar signaling cross-talk. KMDs contribute in sugar and Pi-starvation signaling interaction acting as integrators of the two pathways, by controlling the stability of the common effector PAL, which alters the carbon flux directed to the phenylpropanoids biosynthesis and, in consequence, the fine-tuned balance between Pi and sugar status. In the context of PAL as a common effector of the positively-linked signaling pathways sugar and Pi-starvation, different scenarios involving KMDs are possible, depending on the Pi and sugar availability in the medium: **(A)** Pi-limitation, **(B)** high Suc, **(C)** high Pi, and **(D)** Suc starvation.

Altogether, our model give an idea on the fine regulation of the energetic balance and growth, depending on the available Pi and sugars. KMDs contribution to it, can have far-reaching consequences in the metabolic adaptations of plants. Actually, perturbations in PAL function seems to lead to adjustments in carbon fixation and carbohydrate metabolism (Rohde *et al*., 2004). In the Arabidopsis double mutant *pal1/pal2*, that should be

resemble by an overexpression of *KMD*s, Rubisco (RIBULOSA-1,5-BIPHOSPHATE CARBOXYLASE/OXYGENASE) is upregulated, as well as Rubisco activase in *pal1,* and both enzymes are central parts of CO_2 fixation into organic carbon (Rohde *et al*., 2004). In addition, *pal* mutants have upregulation in the transcriptional activity of genes encoding other enzymes of the carbohydrate metabolism, such as phosphoglycerate kinase and triose phosphate isomerase that metabolize the phosphoglycerate generated by Rubisco; the trehalose 6-phosphate synthase, that generates trehalose 6-phosphate that, in turn, has an important function in controlling the flux into glycolysis in yeast and controls carbohydrate use in plants (Eastmond & Graham, 2003; Schluepmann *et al*., 2003). Therefore, is tempting to thing that KMDs may not only contribute with the regulation of the phenylpropanoids biosynthesis and, thereby, with the fine-tuned sugar:Pi balance, but also be affecting CO_2 fixation and starch usage, so producing general changes in the energetic metabolism of the plant and in the cellular homeostasis. In this context, it will be very interesting to study whether *KMD*s overexpression have an effect on the carbon fixation rates. Also, it will be relevant to answer why oeKMD1-GFP mitigate the harmful effect of high sucrose treatments, insensitivity that can't be explained by a higher CO2 fixation by PAL mediated by KMDs. This outlook hypothesis open new questions about KMDs novel roles on sugar sensing in the plant.

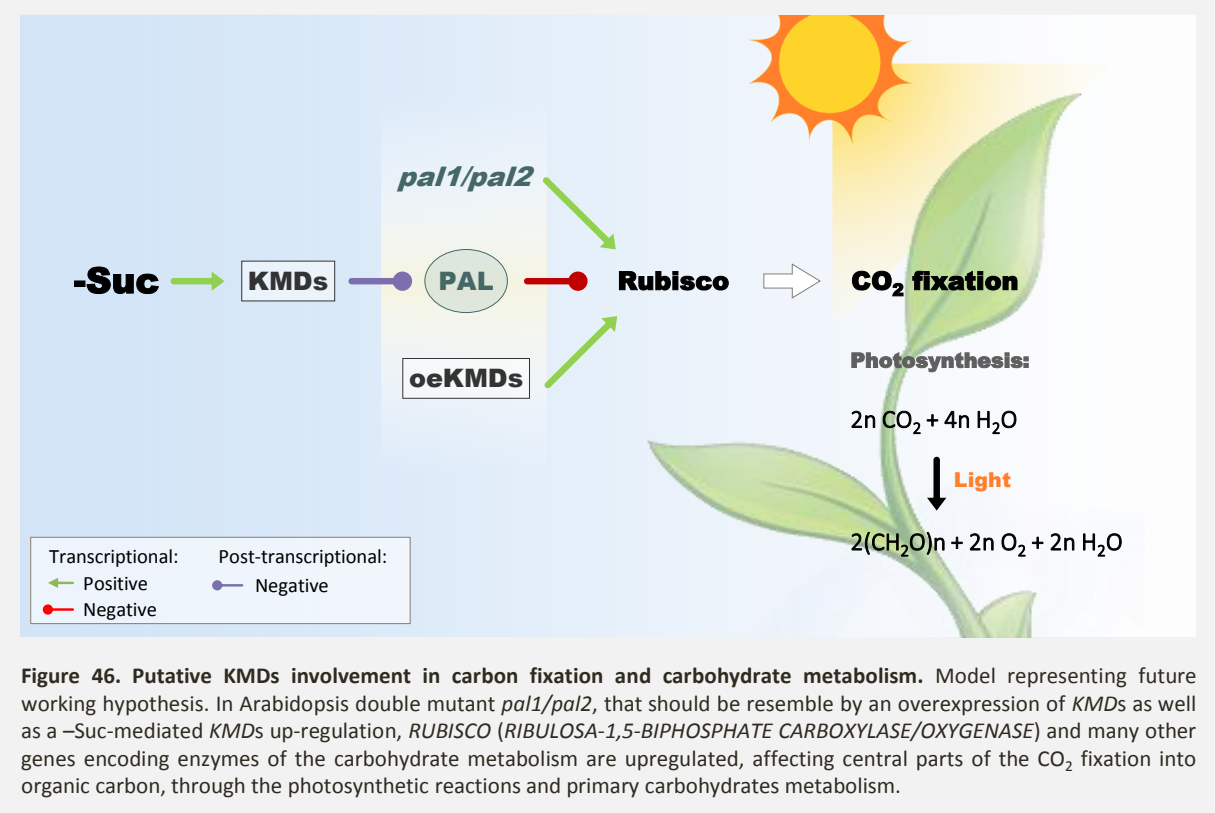

Figure 46. Putative KMDs involvement in carbon fixation and carbohydrate metabolism. Model representing future working hypothesis. In Arabidopsis double mutant *pal1/pal2*, that should be resemble by an overexpression of *KMD*s as well as a –Suc-mediated *KMD*s up-regulation, *RUBISCO* (*RIBULOSA-1,5-BIPHOSPHATE CARBOXYLASE/OXYGENASE*) and many other genes encoding enzymes of the carbohydrate metabolism are upregulated, affecting central parts of the CO_2 fixation into organic carbon, through the photosynthetic reactions and primary carbohydrates metabolism.

CONCLUSIONS

8. CONCLUSIONS

1. KMD protein are substrate adaptors in SCF E3 complexes in Arabidopsis.

2. KMD proteins regulates PAL2 stability at the post-transcriptional level.

3. KMD proteins regulates the biosynthesis of the phenylpropanoids in Arabidopsis.

4. KMD proteins participate as a negative post-traductional regulators of CKs signaling in Arabidopsis.

5. KMD proteins are an integrator node of the antagonic bidirectional crosstalk between CKs and Pi-starvation and sugar signaling in Arabidopsis.

6. KMD proteins are integrator elements of the crosstalk between Pi-starvation and sugar signaling in Arabidopsis, by the post-traductional control of the common effector PAL in Arabidopsis.

CONCLUSIONES

9. CONCLUSIONES

1. Las proteínas KMD son adaptadores de substrato en complejos E3 ubiquitin ligasa del tipo SCF.

2. Las proteínas KMD regulan la estabilidad de la enzima PAL a nivel post-traduccional.

3. Las proteínas KMD regulan la biosíntesis de fenilpropanoides en Arabidopsis.

4. Las proteínas KMD participan como reguladores post-traduccionales negativos de la señalización de citoquininas en Arabidopsis.

5. Las proteínas KMD son un nodo integrador de la relación antagónica bidireccional entre las citoquininas y las rutas de señalización del ayuno de Pi y de azúcares.

6. Las proteínas KMD son un elemento integrador en la relación bidireccional positive entre las rutas de señalización al ayuno de Pi y de azucares, mediante en control post-traduccional del efector común PAL en Arabidopsis.

SUPPLEMENTAL DATA

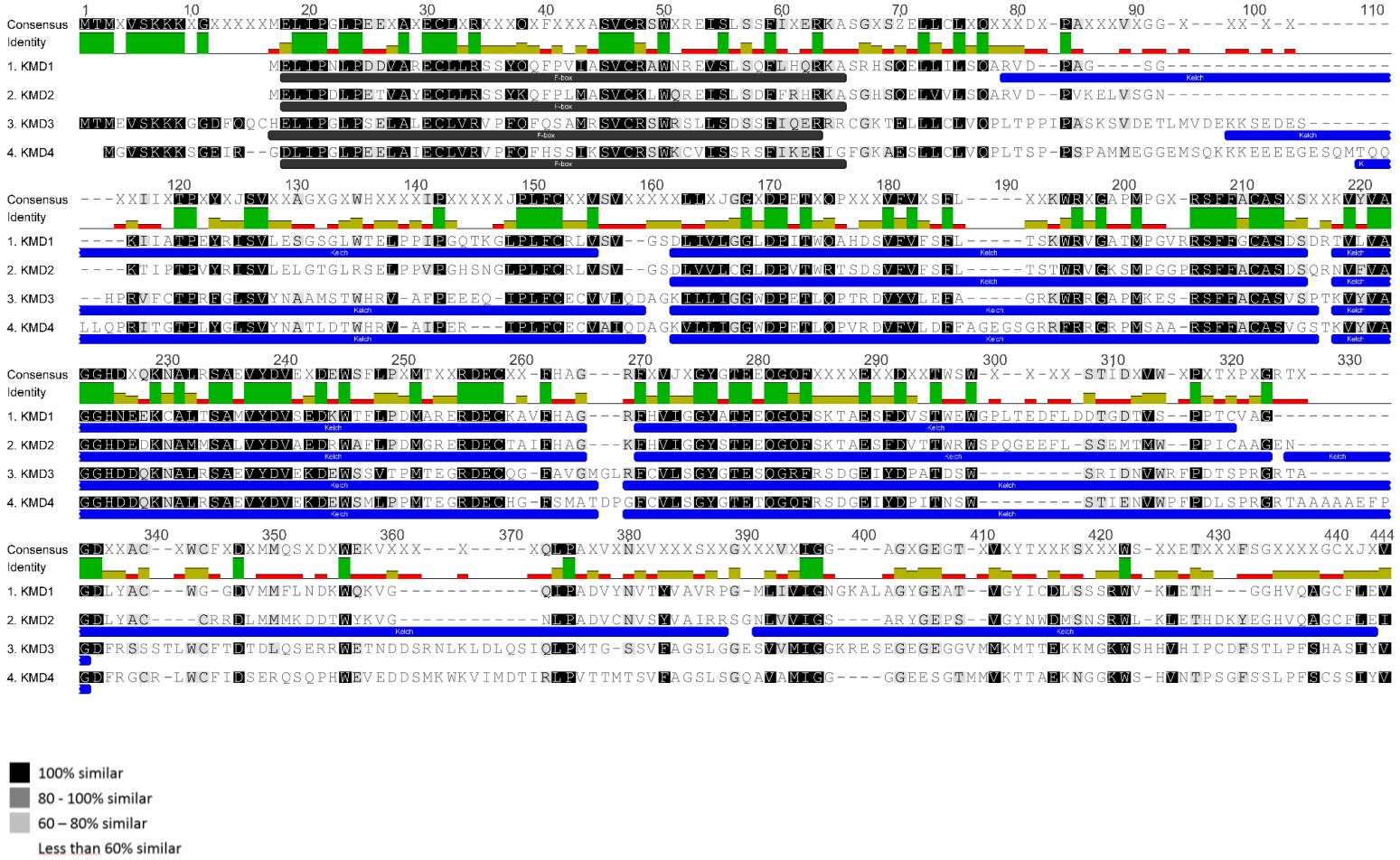

Supplemental Figure 1. Multiple alignment of primary protein structure of KMD1-4 by MUSCLE. Graphical representation of a multiple alignment of the primary structure of KMD1-4, performed using the MUSCLE algorithm (Geneious software version 8.1.7; http://www.geneious.com/). Annotated F-box motif (dark grey) and Kelch repeats (blue) for KMD1-4 are noted along the alignment representation. The color code over the amino acids (aa) indicates the similarity between sequences. A consensus sequence is presented above the alignment, as well as and an identity graph that is green when the sequence do not differ, yellow when there is a partial similarity, and red when there are no aa coincidence.

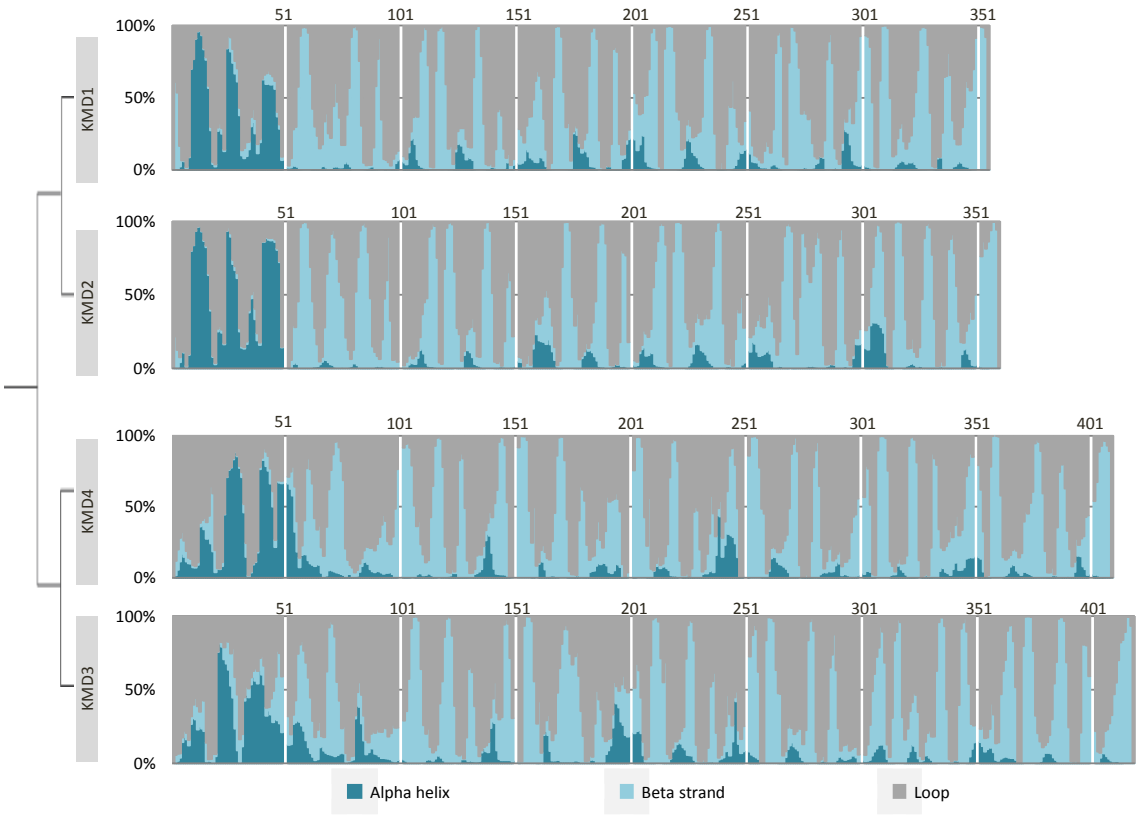

Supplemental Figure 2. *In silico* prediction of secondary protein structure of KMD1-4 by RaptorX. Stacked bar-chart representation of *in silico* predictions of the secondary structures of Arabidopsis KMD1-4. The secondary structure prediction is represented as the probability in % of the presence of one of the secondary structure elements, alpha helix, beta strand or loop structure, against the number of the corresponding amino acid (aa) (aa 1 being the N-terminal aa). The probability of an alpha helical, beta strand and loop secondary structure is presented in dark blue, light blue and grey, respectively. Secondary structure prediction was performed in RaptorX (Kallberg *et al*. 2012; http://raptorx.uchicago.edu/), using protein sequences obtained from TAIR version 8 (http://arabidopsis.org).

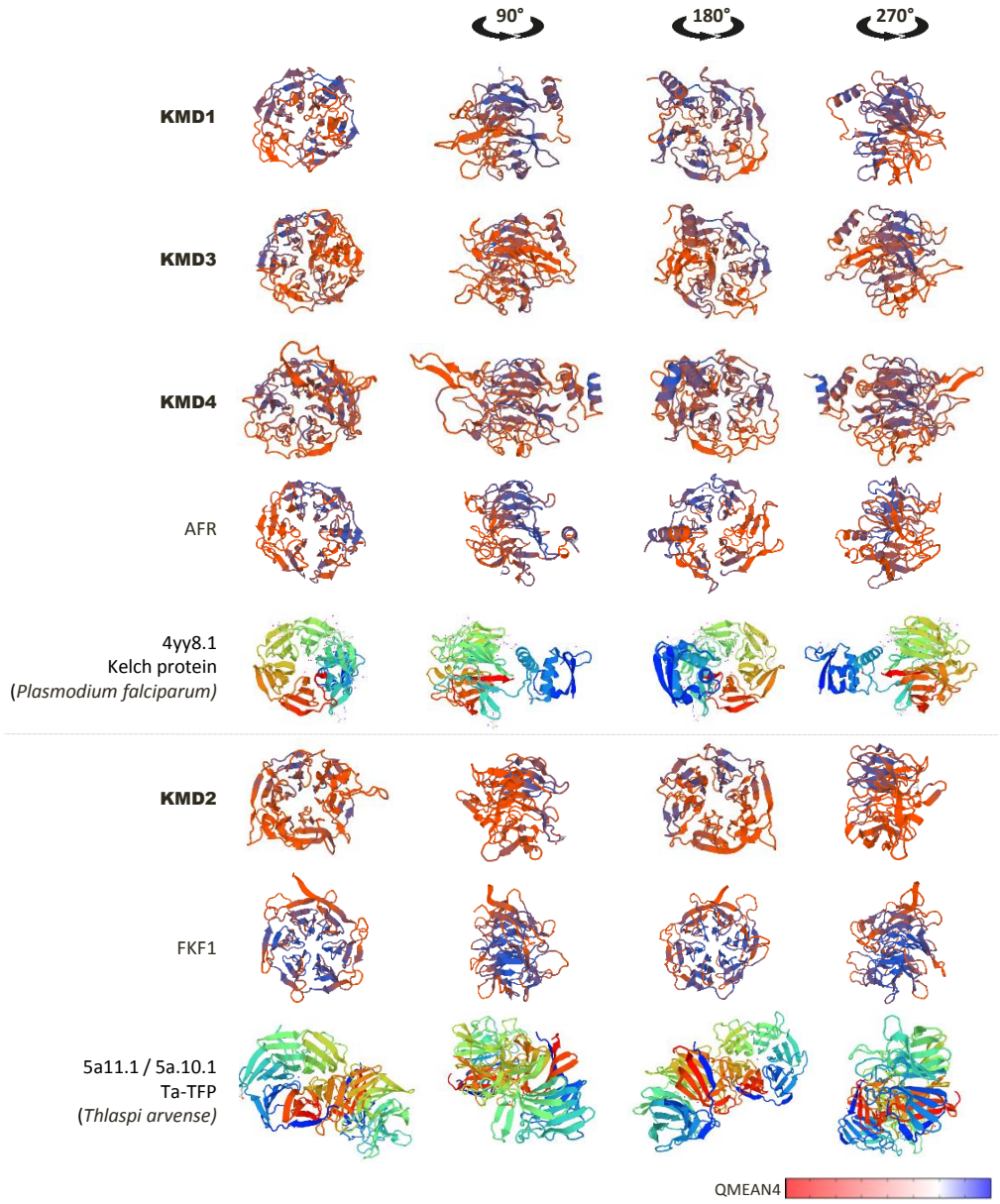

Supplemental Figure 3. KMD1-4 predicted three-dimensional structure. Predicted three-dimensional (3-D) structure of KMD1-4 proteins, performed using the protein structure homology-modelling server SWISS-MODEL (Arnold *et al*. 2006; Guex *et al*., 2009; Kiefer *et al*. 2009; Biasini *et al*., 2014; http://swissmodel.expasy.org/). The previously described FBKs from Arabidopsis, AFR (ATTENUATED FAR-RED RESPONSE) and FKF1 (FLAVIN-BINDING KELCH-REPEAT F-BOX1) (Harmon and Kay, 2003), were included, as well as the best match templates. The 3-D predictions were according to the crystal structure of a kelch protein from *Plasmodium falciparum* (template 4yy8.1) and a Ta-TFP from *Thlaspi arvense* (templates 5a11.1/5a.10.1) (Gumz *et al*. 2015), for KMD1, KMD3, KMD4 and AFR, and for KMD2 and FKF1, respectively. The arrows represent the β-strands. The structural elements are colored according to the QMEAN4 score. QMEN is a composite scoring function for the estimation of the global and local model quality, describing the expected similarity to the native structure (template). Blue and red color indicate higher and lower reliability, respectively (see color bar; Benkert *et al*., 2009; Benkert *et al*., 2011).

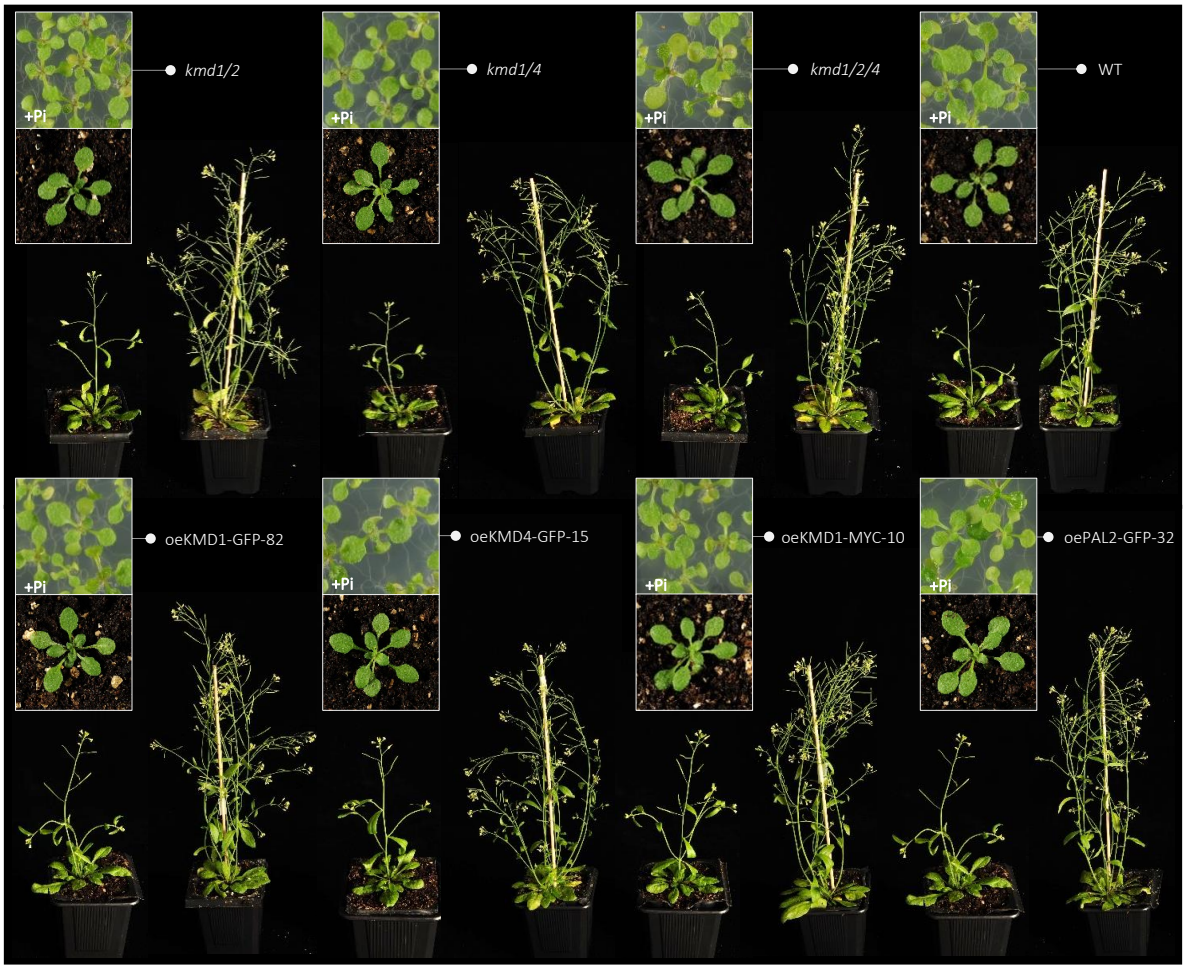

Supplemental Figure 4. Plants with altered KMDs expression. *kmd1/2*, *kmd1/4*, *kmd1/2/4*, WT, oeKMD1-GFP-82, oeKMD4-GFP-15, oeKMD1-MYC-10 and oePAL2-GFP-32 plants at different stages of development: seedling grown in +Pi medium, young rosette, bolting plant and mature plant.

Phenylpropanoid biosynthesis

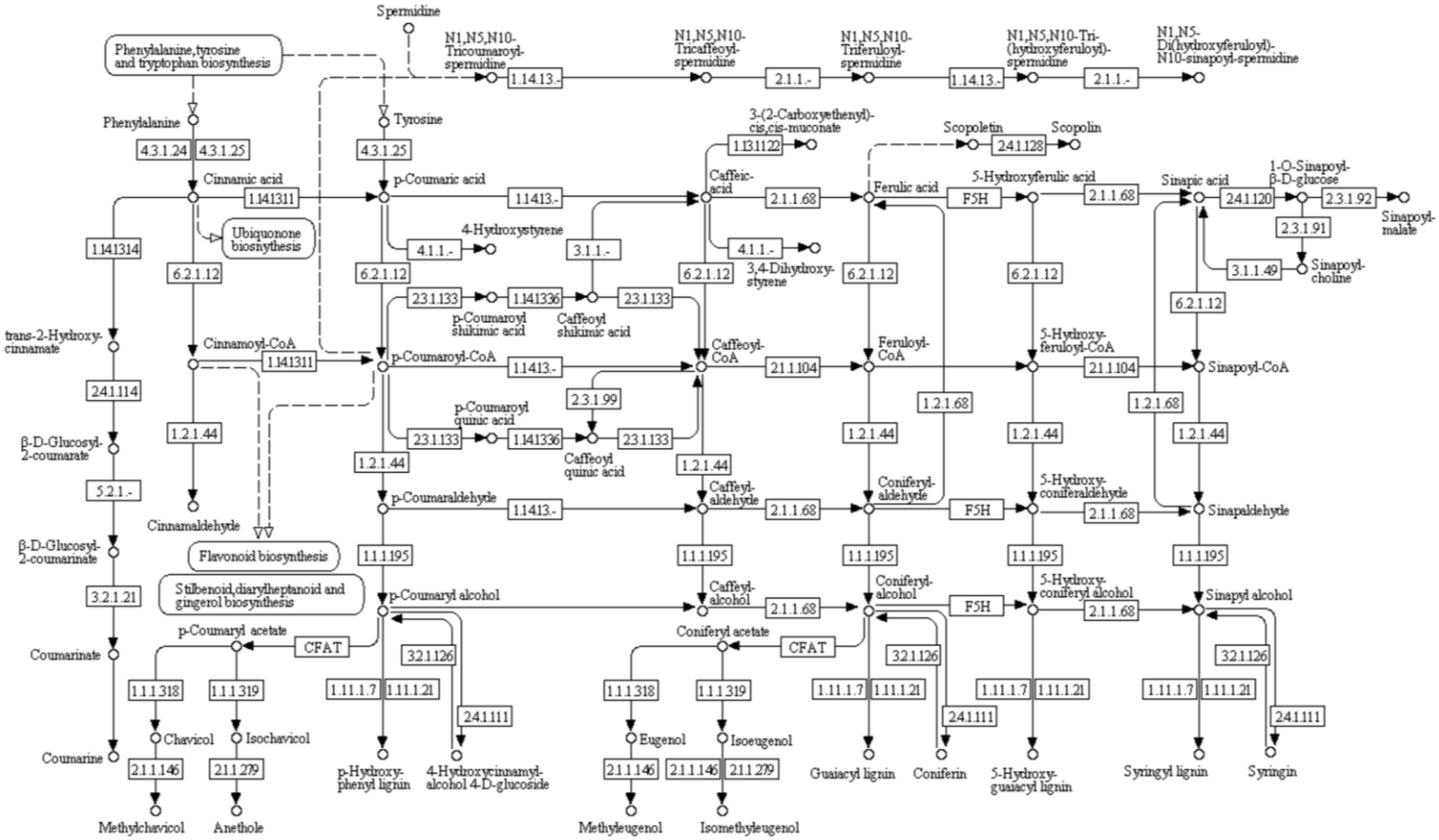

Supplemental Figure 5. Phenylpropanoids biosynthesis pathway. Map of the phenylpropanoids biosynthesis pathway, taken from KEGG PATHWAY database (http://www.genome.jp/kegg/).

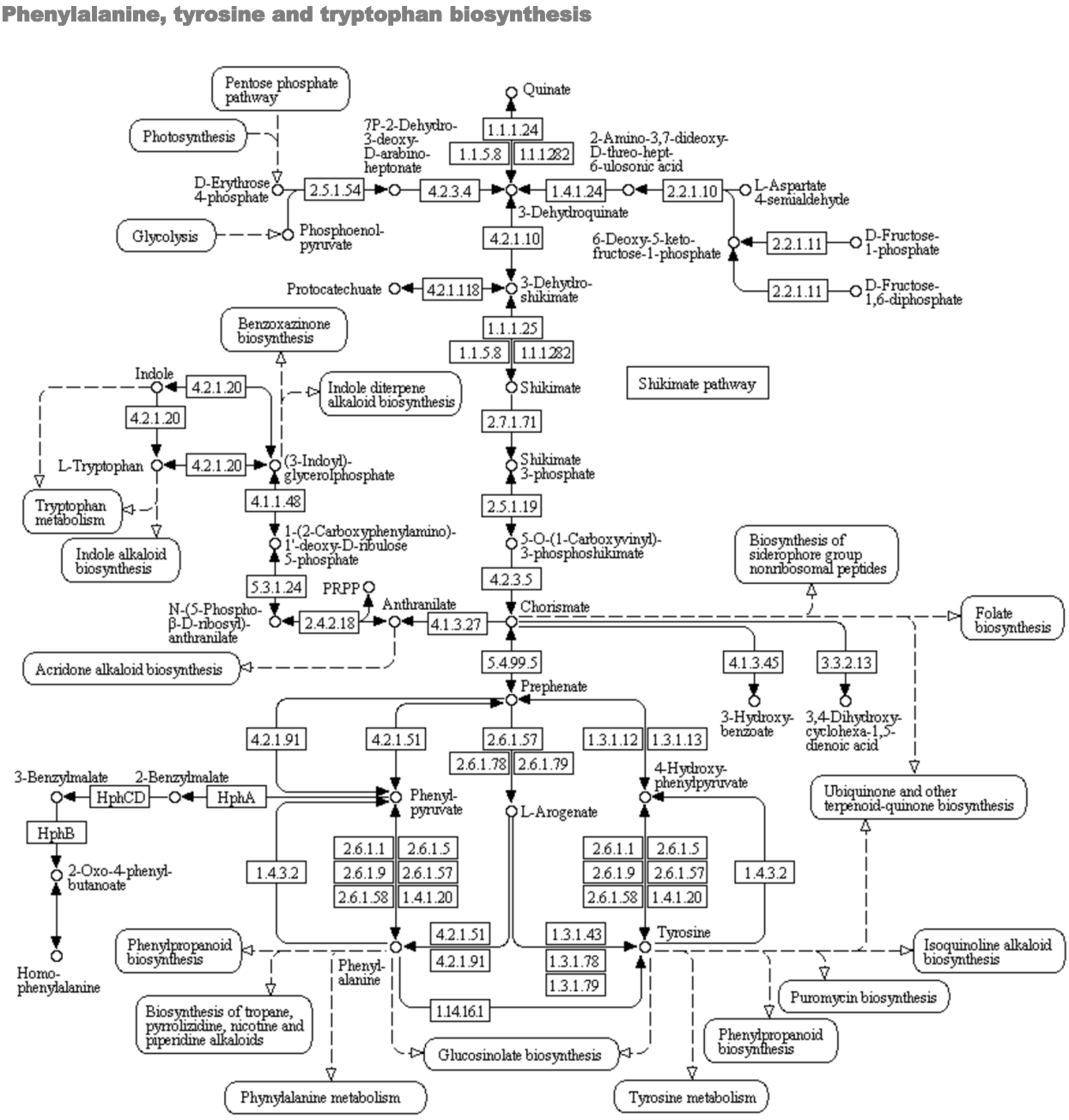

Supplemental Figure 6. Phenylalanine, tyrosine and tryptophan byosinthesis pathway. Map of the phenylalanine, tyrosine and tryptophan byosinthesis pathway, taken from KEGG PATHWAY database (http://www.genome.jp/kegg/).

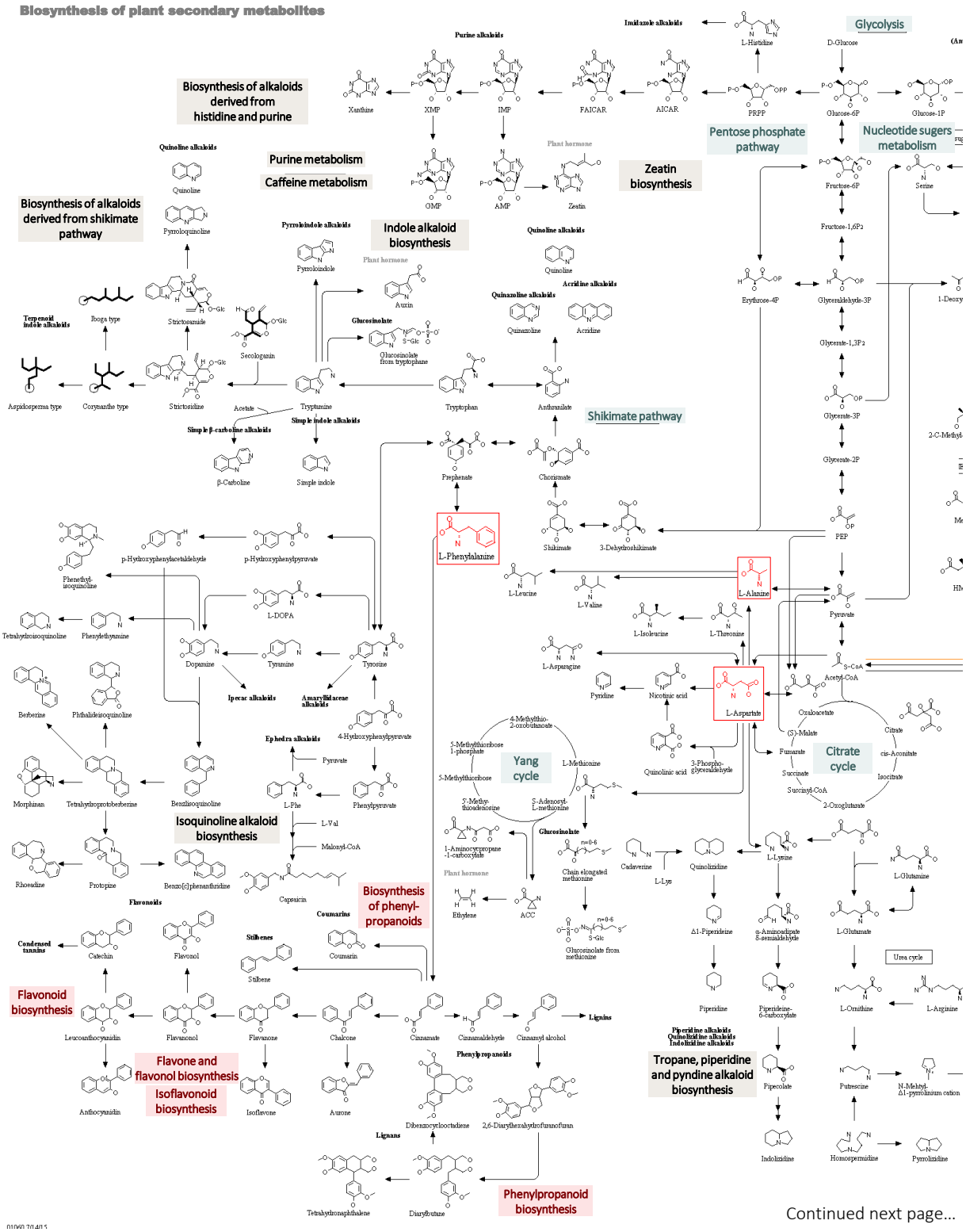

Continued next page...

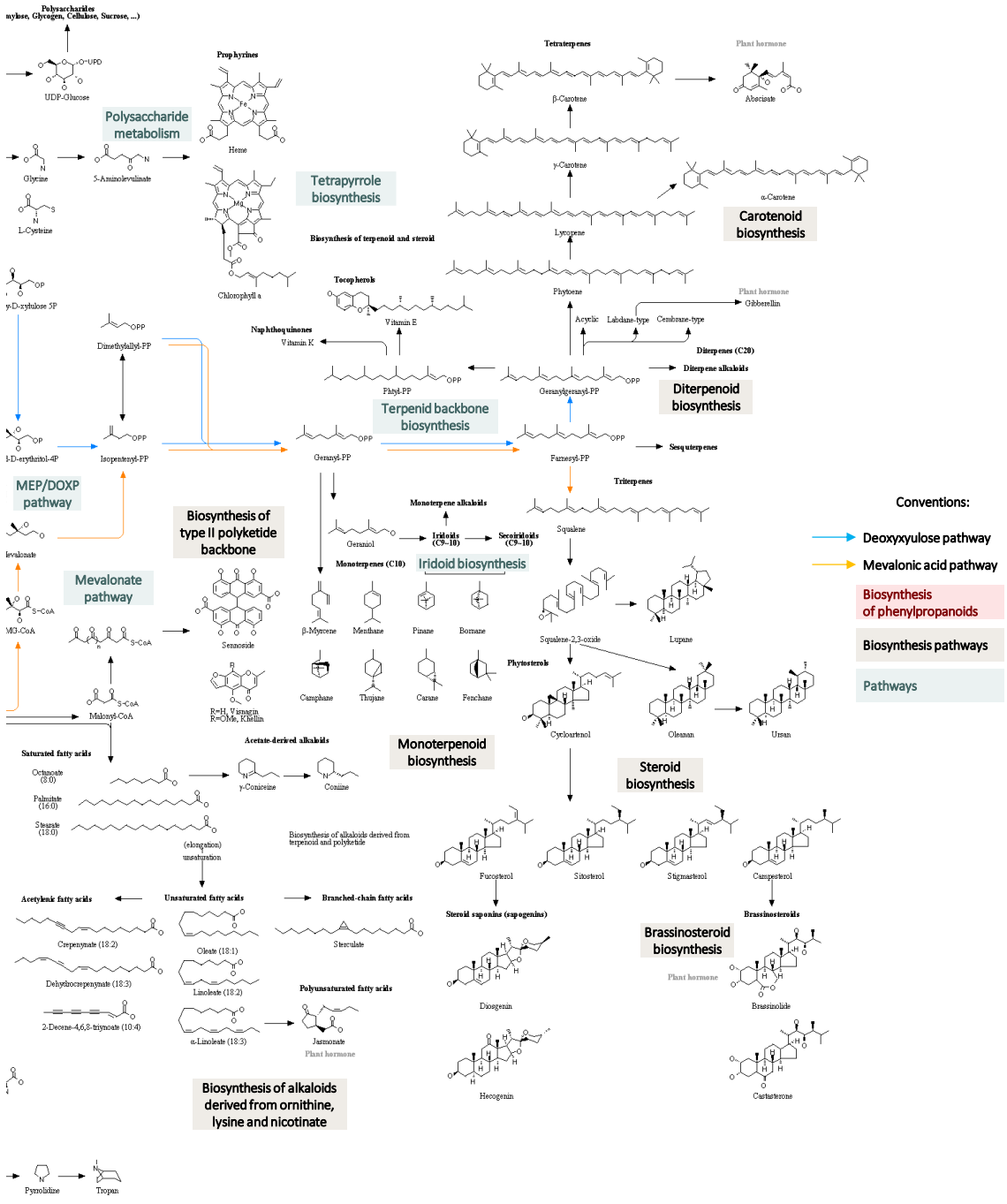

Supplemental Figure 7. Biosynthesis of plant secondary metabolites. Map of the biosynthesis pathways of plant secondary metabolites, taken from KEGG PATHWAY database (http://www.genome.jp/kegg/). Phenylalanine, aspartic acid and alanine amino acids are highlighted in red.

Ascorbate and aldarate metabolism

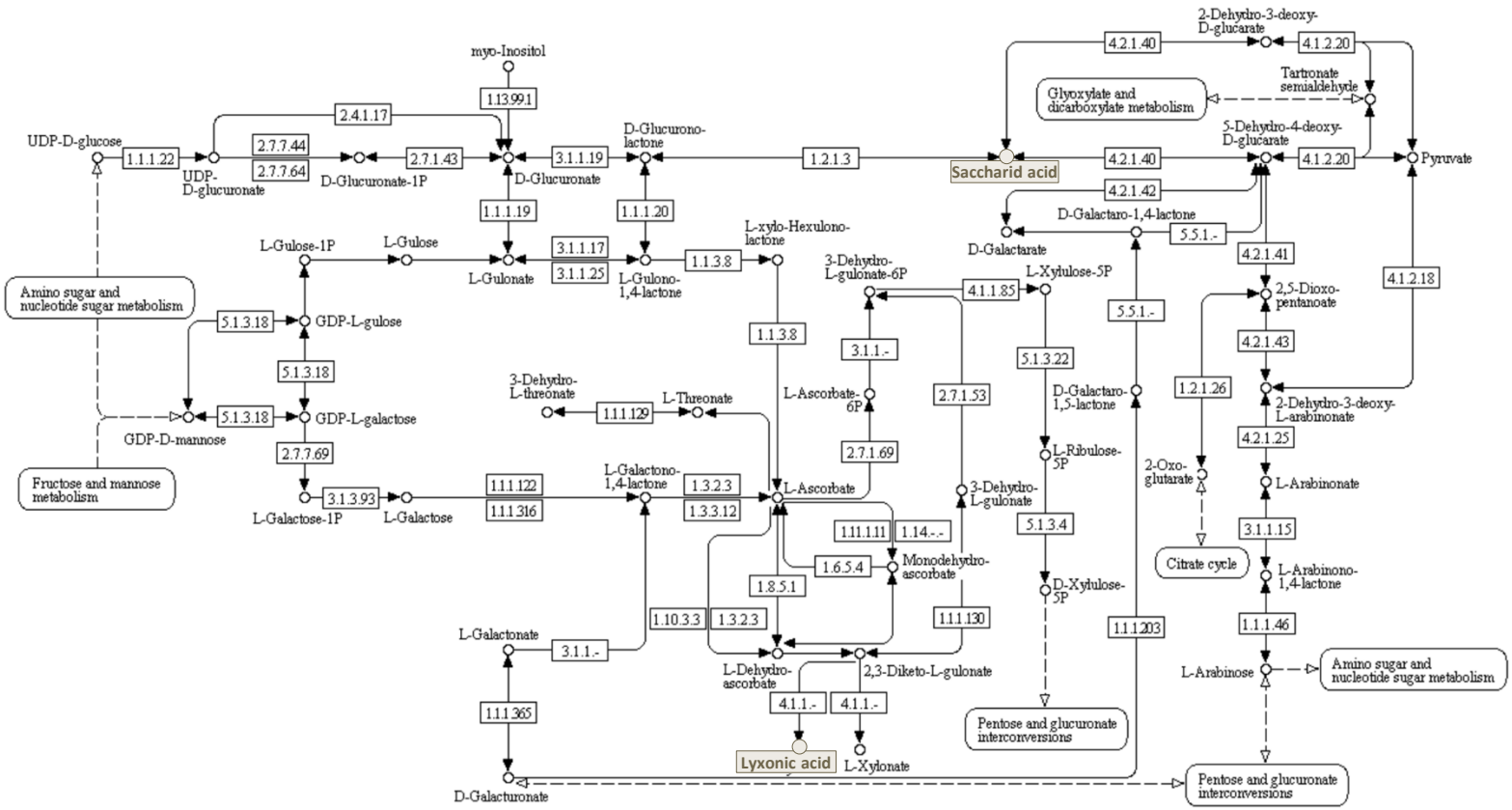

Supplemental Figure 8. Ascorbate and aldarate metabolism, Map of the ascorbate and aldarate metabolism, taken from KEGG PATHWAY database (http://www.genome.jp/kegg/). Lyxonic acid and saccharid acid are highlighted in light brown boxes. Lyxonic acid is also known as L-Lyxonate, and saccharid acid is also known as D-Glucarate.

Supplemental table 1. Detailed description of the experiments selected from the Genevestigator's Perturbations tool, presented in the Figures 16, 19 and 20. Data modified from Genevestigator (https://genevestigator.com/).

	TREATMENT	CONTROL	DESCRIPTION / DESIGN
Nutrients:			
Iron deficient root / untreated root (Col-0)	-FeEDTA for 10 days	+ 100µM FeEDTA	Root samples of Col-0 grown for 10 days on vertical plates containing solid half-strength Murashige and Skoog medium (pH 5.7) , with 1% sucrose; 21°C, 16h light / 8h darkness.
K starved root / untreated root (Col-0)	-K for 10 days	+K	Root samples of Col-0 plants which were initially grown on agar containing 1/10 MS salts and which were then transferred on agar containing 1/10 MS nutrient solution with or wothout K for seven days.
N starved seedling / untreated seedling (Col-0)	-N for 2 days	+N	Seedling samples of Col-0 grown in sterile liquid medium with 4mM KNO3 (N-replete condition) for 7 days and then for 2 days in medium with or without N.
Pi starved root or shoot / untreated root or shoot (Col-0)	-Pi for 10 days (5 µM Pi)	+ 500 µM Pi	Surface-sterilized seeds were sown in square Petri dishes on Murashige and Skoog (MS) 1/10 medium, 0.5% sucrose, 0.8% agar, and supplemented with 5 or 500µM Pi; plants were grown vertically and leaves and roots were harvested 10 days after.
Sulfur starved root / untreated root (Col-0)	-S for 24h	+ S	Whole root samples of Col-0 seedlings grown for 5 days on sulfur-sufficient medium (1x Murashige and Skoog salt mixture, 0.05% MES, 1% sucrose, 1% agar; pH 5.7), then transferred for 24h to sulfur-deficient or sulfur sufficient medium.
Sucrose treated seedlings / Sucrose starved seedlings (Col-0)	+ 100mM Suc for 3 days	-Suc	Col-0 seedling samples, grown on agar plates with or without sucrose for 3 days.
Glucose treated seedlings / Glucose starved seedlings	+ 3% Suc for 2h	-Suc	Seedlings were grown in liquid culture for 7 days on MS medium containing 0.5% glucose in constant light. After 7days growth, seedlings were treated with medium with or without glucose for 24 hrs.
Photoperiod:			
Shortday / long day grown seedlings (Col-0)	8h light / 16h dark	16h light / 8h dark	Arabidopsis seedlings were grown in a photoperiod of 8 h light / 16 h dark (treatment) and 16h light / 8h dark (control.
Long day / short day grown leafs (Col-0)	16h light / 8h dark	8h light / 16h dark	Leaf samples of plants grown on soil (supplemented with Hoagland medium) under long (16h light / 8h darknes) and short (8h light / 16h darkness) day conditions for 21 and 35 days, respectivelly. In both: 120 -160µmol photons m-2 s-1 at 20°C / 8h darkness at 18°C.
Night extension / untreated rosette (Col-0)	6 to 8h extended night	End of the night	Gene expression data from Arabidopsis rosettes at the end of the night (control) and 6h to 8h into an extended night (treatment).
18h dark / 6h dark shoots (Col-0)	18h darkness	6h darkness	Shoot samples of plants grown for 13.5 days on soil under 12h light / 12h dark cycles at 22°C, then, starting at the beginning of the dark period on day 14, kept for (i) 18h in darkness, (ii) 6h in darkness, and 17h in darkness and (iii) 1h on light.
17h dark+1h light / 18h dark shoots (Col-0)	17h darkness + 1h light	18h darkness	

Supplemental table 1. (Continued)

	TREATMENT	CONTROL	DESCRIPTION / DESIGN
Hormones:			
BL treated cell culture / untreated cell culture	+ 1µM BL for 6 days	Untreated	Cells were transferred into medium with or without brassinolide (1µM) for 6d.
ABA treated guard cells / solvent treated guard cells (Col-0)	+ 50mM ABA for 3h	+ Ethanol for 3h	Isolated guard cell samples of 5 weeks old WT plants, treated with 50mM ABA or ethanol for 3h.
IAA treated seedlings / untreated seedling (Col-0)	+ 1µM IAA for 1h	Untreated	Seedling samples of WT grown for 7 days in liquid ATS medium (22°C, constant white fluorescent light) and then treated with or without 1µM IAA for 1h.
Zeatin streated seedlings / untreated seedlings (Col-0)	+ 20µM t-zeatin for 3h	Untreated	Whole plant samples of 21 days old WT plants were treated with or without 20µM t-zeatin for 3h.

Supplemental table 2. Collection of *KMD1-4* gene expression data in response to a wide range of abiotic stimuli, taken from the Genevestigator database Perturbations tool (https://genevestigator.com/). Gene expression represented as foldchange relative to the control condition. Experiments performed on WT background samples and with 2x foldchange values, were grouped in photoperiod, light intensity, light quality, hormones and nutrients.

		KMD1	*KMD2*	*KMD3*	*KMD4*
Photoperiod: WT background					
Long day	Long day (Col-0) / short day (Col-0)	-10.97	-1.07	-4.58	-2.21
Circadian clock	Circadian clock (5h dark+1h light) / circadian clock (6h dark)	-11.30	-4.67	-5.68	-2.44
	Circadian clock (17h dark+1h light) / circadian clock (18h dark)	-27.04	-8.94	-27.34	-10.44
	Circadian clock (17h dark+1h light) / circadian clock (5h dark+1h light)	2.08	2.25	-1.18	-1.02
	Circadian clock (18h dark) / circadian clock (6h dark)	4.98	4.31	4.10	4.21
Night extension	Night extension (early) / untreated rosette samples	5.59	4.14	3.91	3.81
	Night extension (intermediate) / untreated rosette samples	7.06	4.18	4.03	5.35
	Night extension (late) / untreated rosette samples	7.02	4.75	3.86	4.64
Short day	Short day / long day grown seedlings	3.62	1.21	1.47	1.33
Shift SD to LD	Shift SD to LD (Col-0) / short day (Col-0)	1.19	2.75	1.05	-1.03
	Shift SD to LD (5d) / short day shoot apex samples at 16°C (Col-0)	-1.23	2.80	1.06	-1.31
	Shift SD to LD (9d) / short day shoot apex samples at 16°C (Col-0)	-1.15	2.68	-1.07	-1.35
Light intensity: WT backgrounds					
High light	High light (Col-0) / untreated leaf samples (Col-0)	-7.44	-3.01	-5.58	-6.33
	High light (15min) / untreated shoot apical meristem samples (15min)	-2.54	-1.15	-1.88	-3.40
	High light (45min) / untreated shoot apical meristem samples (45min)	-7.14	-2.01	-4.01	-4.89
	High light (3h) / untreated leaf samples (Col-4)	-2.54	-2.50	-2.18	-1.14
	High light (8h) / untreated leaf samples (Col-4)	-7.23	-1.17	-2.27	-3.37
	High light (exposed) / low light grown leaf samples	-5.72	-1.81	-3.59	-2.76
	High light (distal) / low light grown leaf samples	-5.17	3.13	-3.43	-1.66
	High light (Col-0) / low light grown seedlings (Col-0)	-6.43	-1.17	-1.73	-1.78
	High light / 21°C (60-120min) / moderate light / 21°C (60-120min)	-3.60	-1.56	-1.68	-1.90
	High light / 21°C (140-200min) / moderate light / 21°C (140-200min)	-5.06	-2.14	-2.43	-2.76
	High light / 21°C (220-280min) / moderate light / 21°C (220-280min)	-3.14	-1.60	-1.52	-1.82
	High light / 21°C (300-360min) / moderate light / 21°C (300-360min)	-2.59	-1.18	-1.48	-1.83
Light / low CO_2	Light / low CO_2 / dark / low CO_2	-1.30	-2.03	-2.25	-1.35
Light	Light / dark grown Col-0 seedlings	-2.39	-2.11	-1.84	-1.56
	Light / dark grown Ler-0 seedlings	-2.16	-3.84	-2.21	-1.91
	Light (Col-0) / dark grown seedlings (Col-0)	-3.41	1.10	-3.79	-1.33
Low light	Low light / 4°C (60-120min) / low light / 21°C (60-120min)	-2.26	-1.43	-1.74	-2.17
	Low light / 4°C (140-200min) / low light / 21°C (140-200min)	-3.85	-1.13	-2.94	-2.47
	Low light / 4°C (220-280min) / low light / 21°C (220-280min)	-4.67	-1.07	-4.33	-2.51
	Low light / 4°C (300-360min) / low light / 21°C (300-360min)	-3.51	-1.03	-3.59	-1.65

Supplemental table 2. (Continued)

		KMD1	*KMD2*	*KMD3*	*KMD4*
Low light	Low light / 4°C (640 and 1280min) / low light / 21°C (640 and 1280min)	-1.75	-1.16	-1.49	-2.41
	Low light / 21°C (5-40min) / moderate light / 21°C (5-40min)	2.13	1.18	1.38	1.13
	Low light / 21°C (60-120min) / moderate light / 21°C (60-120min)	2.08	2.03	1.55	1.18
	Low light / 21°C (220-280min) / moderate light / 21°C (220-280min)	2.00	1.61	1.70	1.29
	Low light / 21°C (300-360min) / moderate light / 21°C (300-360min)	2.81	1.70	1.80	1.21
	Low light / 21°C (640 and 1280min) / moderate light / 21°C (640 and 1280min)	2.16	1.26	1.18	-1.00
	Low light (4h) / ambient CO_2 / ambient light developing leaf samples (4h)	2.14	1.18	1.47	1.50
	Low light (12h) / ambient CO_2 / ambient light developing leaf samples (12h)	2.98	1.36	1.86	1.76
	Low light (24h) / ambient CO_2 / ambient light mature leaf samples (24h)	4.98	1.60	2.43	1.91
	Low light + DBMIB (0.5h) / low light (6h)	3.96	2.00	22.05	2.83
	Low light + DBMIB (2h) / low light (6h)	2.46	1.32	5.52	-1.39
	Low light (Col-0) / standard light (Col-0)	8.17	4.06	9.81	2.88
Dark	Dark / 21°C (5-40min) / moderate light / 21°C (5-40min)	3.00	1.45	1.93	1.39
	Dark / 21°C (60-120min) / moderate light / 21°C (60-120min)	3.91	7.38	2.57	1.55
	Dark / 21°C (140-200min) / moderate light / 21°C (140-200min)	2.58	5.20	1.74	1.20
	Dark / 21°C (220-280min) / moderate light / 21°C (220-280min)	4.64	4.70	3.73	1.72
	Dark / 21°C (300-360min) / moderate light / 21°C (300-360min)	8.96	4.60	5.40	2.36
	Dark / 21°C (640 and 1280min) / moderate light / 21°C (640 and 1280min)	33.04	5.80	8.11	3.72
	Dark / 32°C (300-360min) / dark / 21°C (300-360min)	1.20	2.08	-1.02	1.39
	Dark / 4°C (60-120min) / dark / 21°C (60-120min)	1.08	-4.10	-1.17	-1.16
	Dark / 4°C (220-280min) / dark / 21°C (220-280min)	-2.67	1.31	-5.71	-1.72
	Dark / 4°C (300-360min) / dark / 21°C (300-360min)	-2.64	1.98	-6.76	-1.71
Light quality: WT backgrounds					
Blue	Blue / low light grown seedlings (Col-0)	-5.45	-1.43	-2.77	-3.40
	Blue / dark grown Col-0 seedlings	-1.64	-2.21	-1.47	-1.45
Red	Red (1h) / dark grown seedlings (Col-0)	-2.65	-1.74	-1.55	-2.12
	Red (45h) / dark grown seedlings (Col-0)	-1.07	-2.35	1.13	1.13
Far red	Far red preconditioning (Col-0) / not pre-conditioned Col-0 seedlings	-1.23	1.45	-2.37	1.00
	White + far-red (Col-0) / white (Col-0)	-1.14	1.31	-2.00	-1.18
	White + far-red (Col-0) / white (Col-0)	2.44	2.11	-1.06	2.04
UV	Shift UV filtered WG345 to WG305 (Col-0) / UV filtered WG345 (Col-0)	-2.20	-1.06	-3.06	-1.57
	UV filtered WG295 (1h) / seedlings irradiated with 327nm cut-off (1h)	3.99	-1.30	1.20	1.02
	UV filtered WG295 (6h) / seedlings irradiated with 327nm cut-off (6h)	2.87	-1.09	1.11	2.69
	UV unfiltered max-310nm (1h) / seedlings irradiated with 327nm cut-off (1h)	7.00	-1.01	1.60	1.52
	UV unfiltered max-310nm (6h) / seedlings irradiated with 327nm cut-off (6h)	7.01	1.58	1.61	1.92
Low R/FR	Low R/FR + MeJA (2h) / high R/FR + MeJA (2h)	1.01	2.31	1.47	-1.06
	Low R/FR + MeJA (2h) / low R/FR (2h)	2.27	1.85	1.73	1.54
	LowR-FR (late) / continuous high R/FR treated seedlings	2.31	1.49	1.39	1.13

Supplemental table 2. (Continued)

		KMD1	*KMD2*	*KMD3*	*KMD4*
Hormones: WT backgrounds					
Abscisic acid	ABA (30min) / mock treated seedlings (30min)	-1.79	-2.26	-1.04	-1.56
	ABA (Col-0) / untreated seed samples	-3.12	1.23	-2.52	-2.83
	ABA / untreated embryo endosperm samples	-1.69	-2.51	-1.70	1.33
	ABA (Col-0) / untreated plant samples (Col-0)	-1.01	-2.12	1.18	1.60
	ABA (Col-0) / solvent treated seedling samples (Col-0)	-1.68	-1.97	1.63	2.26
	ABA (Col-0) / solvent treated guard cell samples (Col-0)	-3.83	-4.87	1.05	1.11
	ABA (Col-0) / untreated plant samples (Col-0)	1.48	-1.20	1.57	2.24
	DFPM + ABA (Col-0) / solvent treated seedling samples (Col-0)	1.48	-1.25	4.09	3.28
Salicylic acid	Salicylic acid (4d) / mock treated Col-0 rosette leaf samples (4d)	1.77	3.88	-1.15	-1.45
	Salicylic acid (Col-0) / mock treated leaf samples (Col-0)	-1.21	3.76	-1.10	-1.65
	Salicylic acid / mock treated seedlings	-1.08	3.18	-2.48	-1.36
	Salicylic acid / mock treated seedlings	-1.26	1.47	-1.50	-2.00
Jasmonic acid	MeJa (30min) / mock treated seedlings (30min)	-2.47	1.19	-1.04	-2.22
	MeJa (1h) / mock treated seedlings (1h)	-2.06	1.25	-1.00	-3.18
Brassinosteroids	24-eBL + glucose (dark) / 24-eBL (dark)	-32.16	-2.13	-13.51	-17.72
	24-eBL + glucose (dark) / mock treated seedling samples	-27.74	-1.83	-10.21	-14.67
	BL/H_3BO_3 (2d) / untreated cell culture samples	-1.52	-15.20	-1.08	1.13
	BL/H_3BO_3 (4d) / untreated cell culture samples	3.10	-29.10	1.56	1.58
	BL/H_3BO_3 (6d) / untreated cell culture samples	3.66	-15.15	2.84	2.04
	BL/H_3BO_3 (8d) / untreated cell culture samples	2.63	-21.75	1.56	1.63
	BL/H_3BO_3 (10d) / untreated cell culture samples	3.11	-15.65	1.34	1.54
Auxin	IAA (Col) / mock treated seedlings (Col)	1.12	1.33	-2.67	1.11
	IAA (1h) / mock treated root samples (1h)	2.21	2.60	-1.58	1.91
	IAA (2h) / mock treated root samples (2h)	1.34	2.14	-2.15	1.35
	IAA (4h) / mock treated root samples (4h)	1.49	2.85	-2.20	-1.03
	NAA (2d) / mock treated inflorescence stem starch sheath cell samples (2d)	3.93	1.48	-1.14	1.41
	NAA (5d) / mock treated inflorescence stem starch sheath cell samples (5d)	-1.58	1.19	1.02	-7.03
	NAA (5d) / untreated inflorescence stem internode cell samples	-1.65	1.88	-2.69	-2.70
	Shift NPA to NAA (2h) / NPA	-1.88	1.33	-9.77	-4.87
	IAA (Col-0) / untreated seedling samples (Col-0)	-2.23	-1.74	-3.60	-2.68
	IAA (Col-0) / untreated seedling samples (Col-0)	-2.16	-1.27	-2.73	-2.91
	IAA (Col-0) / untreated seedling samples (Col-0)	-2.79	-1.28	-2.63	-1.90
Auxin and Brassinosteroids	NAA + FLG22 (1h) / untreated leaf disc samples (Col-0)	-1.55	1.08	-1.13	-3.91
	NAA + FLG22 (2h) / untreated leaf disc samples (Col-0)	-1.49	1.19	-1.67	-2.74
RALF	RALF (30min) / mock treated seedling samples (30min)	1.08	-1.65	-1.81	-2.73
Gibberellins	GA (1h) / untreated leaf disc samples (Ler-0)	-1.45	-1.55	-1.21	-2.01
Cytokinins	Zeatin (1h) / mock treated seedlings (1h)	-1.30	-1.35	-1.62	-2.16
	Zeatin (Col-0) / solvent treated aerial parts (Col-0)	-1.40	-1.06	-2.73	-1.11
	Zeatin (Col-0) / untreated whole plant samples (Col-0)	-2.48	-2.85	-2.18	-1.63

Supplemental table 2. (Continued)

		KMD1	*KMD2*	*KMD3*	*KMD4*
Nutrients: WT backgrounds					
Iron	Iron deficiency (intermediate) / mock treated root samples	1.04	-2.02	1.03	-1.36
	Iron deficiency (late) / mock treated root samples	1.74	-1.08	2.37	-1.26
	Iron deficiency (Col-0) / untreated root samples (Col-0)	2.54	1.30	1.61	1.14
	Iron deficiency (Col-0) / untreated Col-0 root samples	2.79	2.28	1.30	1.19
Potassium	K^+ starvation (root) / untreated root samples	2.39	1.34	2.08	1.57
	KNO_3 / $(NH_4)_2SO_4$	3.13	2.03	1.92	1.75
	KNO_3 / NH_4NO_3 (Col-0)	2.16	1.43	1.54	1.22
	KNO_3 (15min) / mock treated root samples (15min)	2.35	1.15	1.89	1.15
	KNO_3 (root) / mock treated root samples (Col-0)	3.66	1.19	-1.09	-1.07
	KNO_3 / NH_4NO_3 / light (Col-0) / mock treated Col-0 plant samples (light)	2.40	-1.46	-1.09	1.36
Mannitol	Mannitol (2h) / untreated seedlings	1.31	-1.00	2.22	1.22
	Mannitol (Col-0) / mock treated Col-0 guard cell samples	1.38	1.05	3.27	2.51
Nitrogen	$(NH_4)_2SO_4$ (1.5h) / N depletion	2.89	1.61	1.13	2.22
	Ample NH_4NO_3: elevated CO_2 (midnight) / elevated CO_2 (midday)	1.75	2.75	1.24	-1.29
	Midday: limiting NH_4NO_3 / elevated CO_2 / ample NH_4NO_3 / ambient CO_2	1.14	2.32	-1.54	-1.18
	Low nitrogen / high nitrogen treated rosette samples	1.06	3.02	-1.28	1.08
	Nitrate (Col-0) / untreated root tissue samples (Col-0)	3.27	1.15	-1.30	-1.00
	N depletion (Col-0) / Seedlings grown under N-replete condition (Col-0)	-2.14	1.67	-1.27	-2.76
	Nitrate starvation / untreated seedlings	-4.61	-1.18	-2.04	-7.68
Nitrogen and Sucrose	Nitrate(45mM) / sucrose(90mM) / root samples (N-free/suc-free)	-1.71	-1.14	2.10	-1.41
	Nitrate(0mM) / sucrose(30mM) / root samples (N-free/suc-free)	-3.52	-3.29	1.11	-1.44
Sucrose	Sucrose (dark) / dark	-1.52	1.34	-3.28	-3.03
	Sucrose / untreated seedlings	-1.79	-1.03	-2.51	-2.25
	Sucrose (Col-0) / mock treated Col-0 guard cell samples	-3.61	-1.30	-2.88	-3.04
Glucose	Glucose (2h) / untreated seedlings	-29.26	-6.39	-9.79	-8.84
	Glucose (4h) / untreated seedlings	-17.74	-3.72	-6.20	-7.13
	Glucose + estradiol (Col-0) / estradiol (Col-0)	-10.50	-2.18	-4.75	-3.63
	Glucose (dark) / mock treated seedling samples	-41.47	-1.85	-13.14	-24.86
Sulfur	Sulfur deficiency (3h) / mock treated root samples	-19.89	-2.57	-2.21	-10.08
	Sulfur deficiency (12h) / mock treated root samples	-13.08	-1.44	-1.97	-4.91
	Sulfur deficiency (24h) / mock treated root samples	-4.86	-1.22	-1.55	-2.13
	Sulfur deficiency (48h) / mock treated root samples	-3.34	-1.27	-1.17	-1.86
	Sulfur deficiency (72h) / mock treated root samples	-4.11	-1.40	-2.11	-2.19
Phosphate	Pi deficiency (leaf) / Pi supplemented leaf samples	-2.30	-1.18	-1.79	-2.12
	Pi deficiency (root) / mock treated Col-0 root samples	-1.15	-1.14	-1.25	-2.03
	Pi deficiency (late) / high Pi treated whole plant samples (late)	-1.22	1.17	3.85	1.05
	Pi deficiency (shoot) / mock treated Col-0 shoot samples	1.60	1.00	2.30	1.32
	Shift 5µM Pi to 1mM Pi / Pi deficiency (5µM Pi)	1.16	1.13	1.19	2.01

Supplemental Table 3. Proteins identified by Y2H mating analysis as interactors of KMD1 and it transcriptional response to –Pi. The list includes the yeast clone ID (Clon ID), the Arabidopsis Gene Initiative (AGI) gene index number, the protein name or description (TAIR8), a qualitative characterization of yeast clones growth under different auxotrophic conditions (presence(+)/absence(-)) and fold changes in mRNA levels in response to -Pi conditions (–Pi vs +Pi) in WT and *phr1/phl1* (Bustos *et al*. 2010) plants. The table is accompanied by the non-lethal β-GAL assay over the yeast clones grown in –WLH 2mM 3-AT.

			Presence/Absence of yeast growth							Gene expression: fold change value (-Pi/+Pi)			
			-WLH			-WLHA			-WLA	WT		*phr1/phl1*	
Clon ID	AGI	Names/Description	-3-AT	0.5mM 3-AT	2mM 3-AT	-3-AT	0.5mM 3-AT	2mM 3-AT		Shoot	Root	Shoot	Root
1	At5g23240	DNAJ heat shock N-terminal domain-containing protein	+	+	+	+	+	+	+	-15.16	1.45	2.78	1.08
3	At5g16070	TCP-1/cpn60 chaperonin family protein	+	+	+	+	+	-	+	-2.10	-1.30	3.93	-1.06
4	At3g53260	(ATPAL2);PHENYLALANINE AMMONIA-LYASE 2 (PAL2)	+	+	+	+	+	+	+	2.24	-1.88	-3.02	-1.06
6	At4g38970	FRUCTOSE-BISPHOSPHATE ALDOLASE 2 (FBA2); (ATFBA2)	+	+	+	+	+	-	-	1.09	-2.83	1.14	9.89
7	At4g12060	Double Clp-N motif protein	+	+	+	+	+	+	+	-2.10	1.18	1.21	-1.02
8	At1g62640	3-KETOACYL-ACYL CARRIER PROTEIN SYNTHASE III (KAS III)	+	+	+	+	+	+	+	-2.04	-1.09	1.10	-1.08
9	At4g03280	PROTON GRADIENT REGULATION 1 (PGR1);PHOTOSYNTHETIC ELECTRON TRANSFER C (PETC)	+	+	+	+	+	+	+	-1.44	-2.36	1.56	5.67
12	At2g46735	Unknown protein	+	+	+	+	+	-	+	1.34	1.31	-1.15	-1.11
16	At1g72160	Sec14p-like phosphatidylinositol transfer family protein	+	+	+	+	+	+	+	-1.70	-1.15	-1.42	-1.38
18	At3g53260	(ATPAL2);PHENYLALANINE AMMONIA-LYASE 2 (PAL2)	+	+	+	+	+	+	+	2.24	-1.88	-3.02	-1.06
21	At2g41710	Integrase-type DNA-binding superfamily protein	+	+	+	+	+	+	+	-1.01	-1.38	1.47	1.29
24	At5g14470	GHMP kinase family protein	+	+	+	+	+	+	+	1.04	1.04	1.05	1.39
26	At2g04700	Ferredoxin thioredoxin reductase catalytic beta chain family protein	+	+	-	+	+	+	+	-1.50	-1.24	1.32	1.32
28	At4g25130	PEPTIDE MET SULFOXIDE REDUCTASE 4 (PMSR4)	+	+	+	+	+	+	+	-1.10	1.08	-1.26	1.19
29	At4g03280	PROTON GRADIENT REGULATION 1 (PGR1);PHOTOSYNTHETIC ELECTRON TRANSFER C (PETC)	+	`	+	+	-	+	+	-1.44	-2.36	1.56	5.67
31	At3g07670	Rubisco methyltransferase family protein	+	+	+	-	-	+	-	-3.04	-1.50	2.15	1.89
32	At5g11530	EMBRYONIC FLOWER 1 (EMF1)	+	+	+	+	+	+	+	-1.15	-1.18	1.14	-1.02
33	At4g03520	(ATHM2)	+	+	+	+	+	+	+	-1.07	1.05	1.28	1.34
35	At4g03520	(ATHM2)	+	+	+	+	+	+	+	-1.07	1.05	1.28	1.34
38	At4g03520	(ATHM2)	+	+	+	+	+	+	+	-1.07	1.05	1.28	1.34
40	At4g25130	PEPTIDE MET SULFOXIDE REDUCTASE 4 (PMSR4)	+	+	+	+	+	+	+	-1.10	1.08	-1.26	1.19
41	At5g42850	Thioredoxin superfamily protein	+	+	+	+	+	+	+	2.37	1.16	-2.14	1.06
42	At2g44650	CHLOROPLAST CHAPERONIN 10 (CPN10);CHLOROPLAST CHAPERONIN 10 (CHL-CPN10)	+	+	+	+	+	+	+	-2.83	-1.21	2.01	1.57
46	At1g28680	HXXXD-type acyl-transferase family protein	+	+	+	+	+	+	+	2.20	1.03	-4.14	-1.41
48	At3g19450	CINNAMYL ALCOHOL DEHYDROGENASE 4 (CAD4); (CAD-C); (CAD); (ATCAD4)	+	+	+	+	+	+	+	1.16	1.09	-1.31	-1.15
49	At4g25130	PEPTIDE MET SULFOXIDE REDUCTASE 4 (PMSR4)	+	+	+	+	+	+	+	-1.10	1.08	-1.26	1.19

Supplemental Table 3. (Continued)

			Presence/Absence of yeast growth							Gene expression: fold change value (-Pi/+Pi)			
			-WLH			-WLHA			-WLA	WT		*phr1/phl1*	
Clon ID	AGI	Names/Description	-3-AT	0.5mM 3-AT	2mM 3-AT	-3-AT	0.5mM 3-AT	2mM 3-AT		Shoot	Root	Shoot	Root
56	At5g26690	Heavy metal transport/detoxification superfamily protein	+	+	+	+	+	+	+	-	-	-	-
57	At1g27100	Actin cross-linking protein	+	+	+	+	+	-	+	-1.01	1.30	1.41	1.35
59	At2g04700	Ferredoxin thioredoxin reductase catalytic beta chain family protein	+	+	+	+	+	-	+	-1.50	-1.24	1.32	1.32
61	At1g58100	TCP DOMAIN PROTEIN 8 (TCP8)	+	+	+	+	+	-	+	1.21	1.01	1.36	1.11
62	At2g20260	PHOTOSYSTEM I SUBUNIT E-2 (PSAE-2)	+	+	+	+	+	-	+	-1.38	-1.96	-1.07	4.43
63	At4g03280	PROTON GRADIENT REGULATION 1 (PGR1);PHOTOSYNTHETIC ELECTRON TRANSFER C (PETC)	+	+	+	+	+	+	+	-1.44	-2.36	1.56	5.67
64	At1g67090	RIBULOSE BISPHOSPHATE CARBOXYLASE SMALL CHAIN 1A (RBCS1A)	+	+	+	+	+	-	+	-1.16	-2.07	1.01	9.99
68	At4g37470	KARRIKIN INSENSITIVE 2 (KAI2)	+	+	+	+	+	+	+	1.54	1.20	-1.77	-1.06
71	At3g49120	PEROXIDASE CB (PRXCB);PEROXIDASE 34 (PRX34);ARABIDOPSIS THALIANA PEROXIDASE CB (ATPCB);PEROXIDASE 34 (PERX34); (ATPERX34)	+	+	+	+	+	+	+	2.01	1.16	-1.39	1.55
72	At4g20760	NAD(P)-binding Rossmann-fold superfamily protein	+	+	+	+	+	+	+	-1.04	1.30	1.39	-1.15
77	At3g20820	Leucine-rich repeat (LRR) family protein	+	+	+	+	+	+	+	-1.36	-1.18	1.12	2.78
78	At3g48000	ALDEHYDE DEHYDROGENASE 2B4 (ALDH2B4);ALDEHYDE DEHYDROGENASE 2 (ALDH2);ALDEHYDE DEHYDROGENASE 2A (ALDH2A)	+	+	+	+	-	+	+	1.49	1.12	-1.19	1.45
79	At1g13470	Unknown protein	+	+	+	+	+	+	+	-1.24	1.04	1.15	-1.12
80	At4g25130	PEPTIDE MET SULFOXIDE REDUCTASE 4 (PMSR4)	+	+	+	+	+	+	+	-1.10	1.08	-1.26	1.19
81	At3g47620	TEOSINTE BRANCHED, CYCLOIDEA AND PCF (TCP) 14 (AtTCP14);TEOSINTE BRANCHED, CYCLOIDEA AND PCF (TCP) 14 (TCP14)	+	+	+	+	+	+	+	1.13	-1.75	2.00	2.56
82	At1g60670	Unknown protein	-	+	+	+	+	+	+	1.01	-1.11	1.19	-1.08
84	At1g01490	Heavy metal transport/detoxification superfamily protein	-	+	-	+	+	+	+	-1.96	-1.36	1.03	1.24
85	At3g49120	PEROXIDASE CB (PRXCB);PEROXIDASE 34 (PRX34);ARABIDOPSIS THALIANA PEROXIDASE CB (ATPCB);PEROXIDASE 34 (PERX34); (ATPERX34)	+	+	+	+	+	+	+	2.01	1.16	-1.39	1.55
86	At2g15570	ARABIDOPSIS THIOREDOXIN M-TYPE 3 (ATM3); (ATHM3);GFP ARRESTED TRAFFICKING 1 (GAT1);THIOREDOXIN-M3 (TRX-M3)	-	+	+	+	+	-	+	1.59	1.31	-2.52	1.00
88	At3g49120	PEROXIDASE CB (PRXCB);PEROXIDASE 34 (PRX34);ARABIDOPSIS THALIANA PEROXIDASE CB (ATPCB);PEROXIDASE 34 (PERX34); (ATPERX34)	-	+	+	+	+	+	+	2.01	1.16	-1.39	1.55
93	At5g07940	Dentin sialophosphoprotein-related	+	-	+	-	+	+	+	-1.41	-1.37	1.24	1.01

Supplemental Table 3. (Continued)

			Presence/Absence of yeast growth							Gene expression: fold change value (-Pi/+Pi)			
			-WLH			-WLHA			-WLA	WT		*phr1/phl1*	
Clon ID	AGI	Names/Description	-3-AT	0.5mM 3-AT	2mM 3-AT	-3-AT	0.5mM 3-AT	2mM 3-AT		Shoot	Root	Shoot	Root
97	At4g18020	PSEUDO-RESPONSE REGULATOR 2 (PRR2); (APRR2)	+	+	+	+	+	+	+	-1.27	-1.22	-1.46	1.03
114	At3g32980	Peroxidase superfamily protein	-	+	+	+	+	+	+	-	-	-	-
115	At5g42000	ORMDL family protein	-	+	+	+	+	+	+	-1.44	1.02	1.35	-1.02
116	At2g44650	CHLOROPLAST CHAPERONIN 10 (CPN10);CHLOROPLAST CHAPERONIN 10 (CHL-CPN10)	-	+	+	-	-	+	+	-2.83	-1.21	2.01	1.57
117	At3g53260	(ATPAL2);PHENYLALANINE AMMONIA-LYASE 2 (PAL2)	+	+	+	+	+	+	+	2.24	-1.88	-3.02	-1.06
119	At4g38970	FRUCTOSE-BISPHOSPHATE ALDOLASE 2 (FBA2); (ATFBA2)	+	+	+	+	+	+	+	1.09	-2.83	1.14	9.89
120	At4g03520	(ATHM2)	-	+	+	+	+	+	+	-1.07	1.05	1.28	1.34
121	At3g47620	TEOSINTE BRANCHED, CYCLOIDEA AND PCF (TCP) 14 (AtTCP14);TEOSINTE BRANCHED, CYCLOIDEA AND PCF (TCP) 14 (TCP14)	-	+	+	+	+	+	+	1.13	-1.75	2.00	2.56
125	At5g14660	(ATDEF2);PEPTIDE DEFORMYLASE 1B (PDF1B); (DEF2)	-	+	+	-	-	-	-	-1.83	-1.30	1.09	1.30
126	At1g33811	GDSL-like Lipase/Acylhydrolase superfamily protein	+	+	+	+	+	+	+	-1.20	1.03	-2.30	1.06
141	At4g03520	(ATHM2)	+	+	+	+	+	+	+	-1.07	1.05	1.28	1.34
142	At2g45190	ABNORMAL FLORAL ORGANS (AFO);YABBY1 (YAB1);FILAMENTOUS FLOWER (FIL)	+	+	+	+	+	+	+	-1.34	1.20	1.44	1.42
148	At4g21860	METHIONINE SULFOXIDE REDUCTASE B 2 (MSRB2)	+	+	+	+	+	+	+	1.29	-1.24	-1.10	1.77
150	At3g30370	Transposase	+	+	+	+	+	+	+	-1.03	1.10	-1.01	-1.03
151	At1g17530	TRANSLOCASE OF INNER MITOCHONDRIAL MEMBRANE 23 (TIM23-1);TRANSLOCASE OF INNER MITOCHONDRIAL MEMBRANE 23 (ATTIM23-1)	+	+	-	+	+	+	+	2.01	-1.05	1.31	1.29
153	At2g39420	Alpha/beta-Hydrolases superfamily protein	+	+	+	+	+	+	+	2.87	1.37	-2.93	-1.40
154	At5g39830	(DEG8);DEG PROTEASE 8 (DEGP8)	+	+	+	+	+	+	+	-1.98	-1.09	1.51	1.25
163	At1g67090	RIBULOSE BISPHOSPHATE CARBOXYLASE SMALL CHAIN 1A (RBCS1A)	+	+	-	+	+	+	+	-1.16	-2.07	1.01	9.99
165	At1g21500	Unknown protein	+	+	+	+	+	+	+	-1.25	-1.29	1.06	1.76
168	At4g03280	PROTON GRADIENT REGULATION 1 (PGR1);PHOTOSYNTHETIC ELECTRON TRANSFER C (PETC)	+	+	+	+	+	+	+	-1.44	-2.36	1.56	5.67
174	At1g33990	METHYL ESTERASE 14 (MES14);METHYL ESTERASE 14 (ATMES14)	+	+	+	+	+	+	+	1.10	-1.04	1.02	-1.04
186	At5g03370	Acylphosphatase family	+	+	+	+	-	+	+	1.30	1.15	1.10	1.14
191	At3g26080	plastid-lipid associated protein PAP / fibrillin family protein	+	+	+	+	+	+	+	-	-	-	-
194	At4g03280	PROTON GRADIENT REGULATION 1 (PGR1);PHOTOSYNTHETIC ELECTRON TRANSFER C (PETC)	+	+	+	+	+	-	+	-1.44	-2.36	1.56	5.67
199	At3g53260	(ATPAL2);PHENYLALANINE AMMONIA-LYASE 2 (PAL2)	+	+	+	+	+	+	+	2.24	-1.88	-3.02	-1.06
201	At4g32020	Unknown protein	+	+	+	+	+	+	+	2.06	-1.04	-2.56	1.04

Supplemental Table 3. (Continued)

			Presence/Absence of yeast growth							Gene expression: fold change value (-Pi/+Pi)			
			-WLH			-WLHA				WT		*phr1/phl1*	
Clon ID	AGI	Names/Description	-3-AT	0.5mM 3-AT	2mM 3-AT	-3-AT	0.5mM 3-AT	2mM 3-AT	-WLA	Shoot	Root	Shoot	Root
210	At2g26230	Uricase / urate oxidase / nodulin 35, putative	+	+	-	+	+	+	+	1.27	1.23	-1.64	-1.04
212	At3g32980	Peroxidase superfamily protein	+	+	+	+	+	+	+	-	-	-	-
213	At4g26910	Dihydrolipoamide succinyltransferase	+	+	+	+	+	+	+	-1.25	1.08	1.12	-1.02
222	At4g32020	Unknown protein	+	+	+	+	+	+	+	2.06	-1.04	-2.56	1.04
233	At4g27130	Translation initiation factor SUI1 family protein	+	+	+	+	+	+	+	1.03	-1.25	2.17	1.31
233	At5g54760	Translation initiation factor SUI1 family protein	+	+	+	+	+	+	+	-1.01	-1.00	-1.52	-1.10
257	At4g03520	(ATHM2)	+	+	+	+	+	+	+	-1.07	1.05	1.28	1.34
258	At2g05230	DNAJ heat shock N-terminal domain-containing protein	+	+	+	+	+	+	+	1.19	-1.06	-1.04	-1.03
261	At4g25130	PEPTIDE MET SULFOXIDE REDUCTASE 4 (PMSR4)	+	+	+	+	+	+	+	-1.10	1.08	-1.26	1.19
267	At1g62180	5'ADENYLYLPHOSPHOSULFATE REDUCTASE 2 (APR2);ADENOSINE-5'-PHOSPHOSULFATE REDUCTASE (APSR)	+	+	+	+	+	+	+	2.32	-1.09	-5.46	-1.63
271	At1g75330	ORNITHINE CARBAMOYLTRANSFERASE (OTC)	+	+	+	+	+	+	+	1.28	-1.03	-1.24	-1.01
275	At5g07680	NAC DOMAIN CONTAINING PROTEIN 80 (ANAC080); (ATNAC4);ARABIDOPSIS NAC DOMAIN CONTAINING PROTEIN 79 (ANAC079)	+	+	+	+	+	+	+	-1.29	-1.87	1.55	3.64
276	At5g64040	(PSAN)	+	+	+	+	+	-	+	-1.01	-1.17	1.02	3.51
283	At2g06050	OXOPHYTODIENOATE-REDUCTASE 3 (OPR3); (AtOPR3)	+	+	+	+	+	-	+	6.40	1.76	-6.10	-1.48
285	At3g53260	(ATPAL2);PHENYLALANINE AMMONIA-LYASE 2 (PAL2)	+	+	+	+	+	+	+	2.24	-1.88	-3.02	-1.06
287	At4g30690	Translation initiation factor 3 protein	+	+	+	+	+	-	+	-3.47	-1.31	2.60	1.84

Non-lethal β-galactosidase assay in –WLH 2mM 3-AT

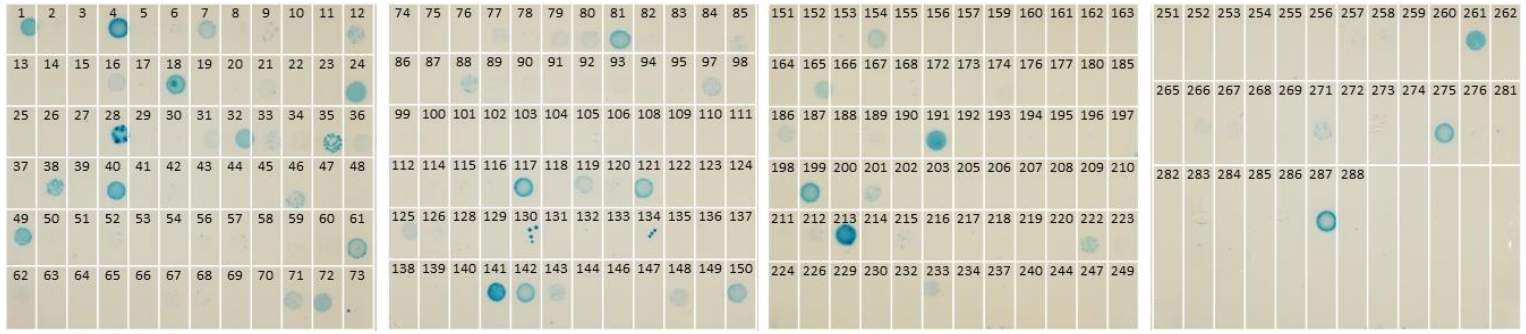

BIBLIOGRAPHY

11. BIBLIOGRAPHY

Akiyama, K, Matsuzaki, K-i, and Hayashi, H (2005) Plant sesquiterpenes induce hyphal branching in arbuscular mycorrhizal fungi. Nature 435, 824-827.

Allen, E, Xie, Z, Gustafson, AM, and Carrington, JC (2005). microRNA-Directed Phasing during Trans-Acting siRNA Biogenesis in Plants. Cell 121, 207-221.

Alonso, JM, Hirayama, T, Roman, G, Nourizadeh, S, and Ecker, JR (1999) EIN2, a bifunctional transducer of ethylene and stress responses in Arabidopsis. Science 284, 2148-2152.

Alonso J, Stepanova A, Leisse TJ, Kim CJ, Chen H, Shinn P, Stevenson DK, Zimmerman J, Barajas P, Cheuk R, Gadrinab C, Heller C, Jeske A, Koesema E, Meyers CC, Parker H, Prednis L, Ansari Y, Choy N, Deen H, Geralt M, Hazari N, Hom E, Karnes M, Mulholland C, Ndubaku R, Schmidt I, Guzman P, Aguilar-Henonin L, Schmid M, Weigel D, Carter DE, Marchand T, Risseeuw E, Brogden D, Zeko A, Crosby WL, Berry CC, Ecker JR (2003) Genome-wide insertional mutagenesis of Arabidopsis thaliana. Science. 1;301(5633):653-7.

Allwood J.W., Erban A., de Koning S., Dunn W.B., Luedemann A., Lommen A., . . . Goodacre R. (2009) Inter-laboratory reproducibility of fast gas chromatography-electron impact-time of flight mass spectrometry (GC-EITOF/MS) based plant metabolomics. Metabolomics: Official Journal of the Metabolomic Society 5, 479–496.

Ames BN (1966) Assay of inorganic phosphate, total phosphate and phosphatases. Methods of Enzimol. 8, 115-118.

An F, Zhao Q, Ji Y, Li W, Jiang Z, Yu X, Zhang C, Han Y, He W, Liu Y, et al (2010) Ethylene-induced stabilization of ETHYLENE INSENSITIVE3 and EIN3-LIKE1 is mediated by proteasomal degradation of EIN3 binding F-box 1 and 2 that requires EIN2 in Arabidopsis. Plant Cell 22: 2384–2401

Andrade, M A, Gonzalez-Guzman, M, Serrano, R & Rodriguez, P L (2001) A combination of the F-box motif and kelch repeats defines a large Arabidopsis family of F-box proteins. Plant Mol. Biol. 46, 603–614.

Angers, S, Li, T, Yi, X, MacCoss, MJ, Moon, RT, and Zheng, N (2006) Molecular architecture and assembly of the DDB1-CUL4A ubiquitin ligase machinery. Nature 443, 590-593.

Anterola, AM, Jeon, JH, Davin, LB, and Lewis, NG (2002) Transcriptional control of monolignol biosynthesis in Pinus taeda: factors affecting monolignol ratios and carbon allocation in phenylpropanoid metabolism. J. Biol. Chem. 277:18272–18280.

Appert, C, Logemann, E, Hahlbrock, K, Schmid, J, and Amrhein, N (1994) Structural and catalytic properties of the four phenylalanine ammonia-lyase isoenzymes from parsley (Petroselinum crispum Nym.). Eur. J. Biochem. 225:491–499.

Ariizumi, T, Lawrence, PK, and Steber, CM (2011) The role of two f-box proteins, SLEEPY1 and SNEEZY, in Arabidopsis gibberellin signaling. Plant Physiol. 155, 765-775.

Arnold K, Bordoli L, Kopp J, and Schwede T (2006). The SWISS-MODEL Workspace: A web-based environment for protein structure homology modelling. Bioinformatics.,22,195-201.

Arpat AB, Magliano P, Wege S, Rouached H, Stefanovic A, Poirier Y (2012) Functional expression of PHO1 to the Golgi and transGolgi network and its role in export of inorganic phosphate. Plant J. 71, 479–491.

Aung K, Lin SI, Wu CC, Huang YT, Su CL, Chiou TJ (2006) pho2, a phosphate overaccumulator, is caused by a nonsense mutation in a microRNA399 target gene. Plant Physiol. 141, 1000–1011.

Austin, MJ, Muskett, P, Kahn, K, Feys, BJ, Jones, JD, and Parker, JE (2002) Regulatory role of SGT1 in early R gene-mediated plant defenses. Science 295, 2077-2080.

Azevedo, C, Sadanandom, A, Kitagawa, K, Freialdenhoven, A, Shirasu, K, and Schulze-Lefert, P (2002) The RAR1 interactor SGT1, an essential component of R gene-triggered disease resistance. Science 295, 2073-2076.

Bachmair A, Novatchkova M, Potuschak T, Eisenhaber F (2001) Ubiquitylation in plants: A post-genomic look at a post-translational modification. Trends Plant Sci. 6, 463–470.

Baek D, Kim MC, Chun HJ, Kang S, Park HC, Shin G, Park J, Shen,M, Hong H, Kim WY, *et al.* (2013) Regulation of miR399f Transcription by AtMYB2 Affects Phosphate Starvation Responses in Arabidopsis. Plant Physiology 161, 362-373

Bari R, Datt Pant B, Stitt M, Scheible WR (2006) PHO2, microRNA399, and PHR1 define a phosphate-signaling pathway in plants. Plant Physiol. 141, 988–999.

Bariola PA, Howard CJ, Taylor CB, Verburg MT, Jaglan VD, Green PJ (1994) The Arabidopsis ribonuclease gene RNS1 is tightly controlled in response to phosphate limitation. Plant J. 6, 673–685.

Bartke T, Pohl C, Pyrowolakis G, Jentsch S (2004) Dual role of BRUCE as an antiapoptotic IAP and a chimeric E2/E3 ubiquitin ligase. Mol. Cell 14, 801–811.

Bate, NJ, Orr, J, Ni, W, Meroni, A, Nadler-Hassar, T, Doerner, PW, Dixon, RA, Lamb, CJ, and Elkind, Y (1994) Quantitative relationship between phenylalanine ammonia-lyase levels and phenylpropanoid accumulation in transgenic tobacco identifies a rate determining step in natural product synthesis. Proc. Natl. Acad. Sci. U S A 91:7608–7612.

Bates TR, Lynch P (1996) Stimulation of root hair elongation in Arabidopsis thaliana by low phosphorus availability. Plant Cell Environ. 19, 529–538.

Bates PW, Vierstra RD (1999) UPL1 and 2, two 405kDa ubiquitin–protein ligases from Arabidopsis thaliana related to the HECT-domain protein family. Plant J. 20, 183–195.

Bates, R, and Lynch, JP (2001) Root hairs confer a competitive advantage under low phosphate availability. Plant and Soil 236, 243-250.

Baudry A, Ito S, Song YH, Strait AA, Kiba T, Lu S, Henriques R, PrunedaPaz JL, Chua NH, Tobin EM, et al (2010) F-box proteins FKF1 and LKP2 act in concert with ZEITLUPE to control Arabidopsis clock progression. Plant Cell 22: 606–622

Bayle V, Arrighi JF, Creff A, Nespoulous C, Vialaret J, Rossignol M, Gonzalez E, Paz-Ares J, Nussaume L (2011) Arabidopsis thaliana high-affinity phosphate transporters exhibit multiple levels of posttranslational regulation. Plant Cell 23, 1523–1535.

Benjamini Y, Hochberg Y (1995) Controlling the false discovery rate: A practical and powerful approach to multiple testing. J. Roy. Statist. Soc. 57, 289–300.

Berleth ES, Pickart CM (1996) Mechanism of ubiquitin conjugating enzyme E2–230K: Catalysis involving a thiol relay? Biochemistry 35, 1664–1671.

Bernhardt, A, Lechner, E, Hano, P, Schade, V, Dieterle, M, Anders, M, Dubin, MJ, Benvenuto, G, Bowler, C, Genschik, P, and Hellmann, H (2006) CUL4 associates with DDB1 and DET1 and its downregulation affects diverse aspects of development in Arabidopsis thaliana. Plant J. 47, 591-603.

Besserer, A, Puech-Pagès, V, Kiefer, P, Gomez-Roldan, V, Jauneau, A, Roy, S, Portais, J-C, Roux, C, Bécard, G, and Séjalon-Delmas, N (2006) Strigolactones Stimulate Arbuscular Mycorrhizal Fungi by Activating Mitochondria. PLoS Biol 4, 1239-1247.

Biedermann, S, and Hellmann, H (2010) The DDB1a interacting proteins ATCSA-1 and DDB2 are critical factors for UV-B tolerance and genomic integrity in Arabidopsis thaliana. Plant J.62, 404-415.

Biedermann, S, and Hellmann, H (2011) WD40 and CUL4-based E3 ligases: lubricating all aspects of life. Trends Plant Sci. 16, 38-46.

Binder, BM, Walker, JM, Gagne, JM, Emborg, TJ, Hemmann, G, Bleecker, AB, and Vierstra, RD (2007) The Arabidopsis EIN3 binding F-Box proteins EBF1 and EBF2 have distinct but overlapping roles in ethylene signaling. Plant Cell 19, 509-523.

Blilou, I, Frugier, F, Folmer, S, Serralbo, O, Willemsen, V, Wolkenfelt, H, Eloy, NB, Ferreira, PC, Weisbeek, P, and Scheres, B (2002) The Arabidopsis HOBBIT gene encodes a CDC27 homolog that links the plant cell cycle to progression of cell differentiation. Genes Dev. 16, 2566-2575.

Blount, J.W., Korth, K.L., Masoud, S.A., Rasmussen, S., Lamb, C., and Dixon, R.A. (2000). Altering expression of cinnamic acid 4-hydroxylase in transgenic plants provides evidence for a feedback loop at the entry point into the phenylpropanoid pathway. Plant Physiol. 122:107–116.

Bolwell, G.P., Cramer, C.L., Lamb, C.J., Schuch, W., and Dixon, R.A. (1986). L-Phenylalanine ammonia-lyase from Phaseolus vulgaris. Modulation of the levels of active enzyme by trans-cinnamic acid. Planta 169:97–107.

Borch, K, Bouma, TJ, Lynch, JP, and Brown, KM (1999) Ethylene: a regulator of root architectural responses to soil phosphorus availability. Plant, Cell & Environment 22, 425-431.

Borden, KL (2000) RING domains: master builders of molecular scaffolds? J. Mol. Biol. 295, 1103–1112.

Bork, P. and Doolittle, R.F. (1994). Drosophila kelch motif is derived from a common enzyme fold. J. Mol. Biol. 236: 1277–1282.

Branscheid, A, Sieh, D, Pant, BD, May, P, Devers, EA, Elkrog, A, Schauser, L, Scheible, W-R, and Krajinski, F (2010) Expression Pattern Suggests a Role of MiR399 in the Regulation of the Cellular Response to Local Pi Increase During Arbuscular Mycorrhizal Symbiosis. Molecular Plant-Microbe Interactions 23, 915-926.

Brodersen P, Sakvarelidze-Achard L, Bruun-Rasmussen M, Dunoyer P, Yamamoto YY, Sieburth L, Voinnet O (2008) Widespread Translational Inhibition by Plant miRNAs and siRNAs. Science 320, 1185-1190.

Bu, Q, Lv, T, Shen, H, Luong, P, Wang, J, Wang, Z, Huang, Z, Xiao, L, Engineer, C, Kim, TH, Schroeder, JI, and Huq, E (2014) Regulation of drought tolerance by the F-box protein MAX2 in arabidopsis. Plant Physiol. 164, 424-439.

Bubna, GA, Lima, RB, Zanardo, DY, Dos Santos, WD, Ferrarese Mde, L, and Ferrarese-Filho, O (2011) Exogenous caffeic acid inhibits the growth and enhances the lignification of the roots of soybean (Glycine max). J. Plant Physiol. 168:1627–1633.

Bucher, M (2007) Functional biology of plant phosphate uptake at root and mycorrhiza interfaces. New Phytologist 173, 11-26.

Bustos R, Castrillo G, Linhares F, Puga MI, Rubio V, Perez-Pérez J, Solano R, Leyva A, Paz-Ares J (2010) A central regulatory system largely controls transcriptional activation and repression responses to phosphate starvation in Arabidopsis. PLoS Genet. 6, 1–15.

Calabrese, JC, Jordan, DB, Boodhoo, A, Sariaslani, S, and Vannelli, T (2004) Crystal structure of phenylalanine ammonia lyase: multiple helix dipoles implicated in catalysis. Biochemistry 43: 11403–11416.

Callis J, Carpenter T, Sun CW, Vierstra RD (1995) Structure and evolution of genes encoding polyubiquitin and ubiquitin-like proteins in *Arabidopsis thaliana* ecotype Columbia. Genetics 139:921–39.

Capron, A, Okresz, L, and Genschik, P (2003a) First glance at the plant APC/C, a highly conserved ubiquitin-protein ligase. Trends Plant Sci. 8, 83-89.

Capron, A, Serralbo, O, Fulop, K, Frugier, F, Parmentier, Y, Dong, A, Lecureuil, A, Guerche, P, Kondorosi, E, Scheres, B, and Genschik, P (2003b) The Arabidopsis anaphase-promoting complex or cyclosome: molecular and genetic characterization of the APC2 subunit. Plant Cell 15, 2370-2382.

Chae, E, Tan, QK, Hill, TA, and Irish, VF (2008) An Arabidopsis Fbox protein acts as a transcriptional co-factor to regulate floral development. Development 135, 1235-1245.

Chandrika NNP, Sundaravelpandian K, Yu SM, Schmidt W (2013) ALFIN-LIKE 6 is involved in root hair elongation during phosphate deficiency in Arabidopsis. New Phytologist 198, 709-720.

Chang, A, Lim, MH, Lee, SW, Robb, EJ, and Nazar, RN (2008) Tomato phenylalanine ammonia-lyase gene family, highly redundant but strongly underutilized. J. Biol. Chem. 283:33591–33601.

Chapin, FS, and Bieleski, RL (1982) Mild phosphorus stress in barley and a related low-phosphorus-adapted barleygrass: Phosphorus fractions and phosphate absorption in relation to growth. Physiologia Plantarum 54, 309-317.

Chassy, B. M. & Flickinger, J. L. (1987) Transformation of Lactobacillus casei by electroporation. . FEMS Microbiology Letters. 44, 173-177.

Chen ZH, Nimmo GA, Jenkins GI, Nimmo HG (2007) BHLH32 modulates several biochemical and morphological processes that respond to Pi starvation in Arabidopsis. Biochem. J. 405, 191– 198.

Chen, H, Huang, X, Gusmaroli, G, Terzaghi, W, Lau, OS, Yanagawa, Y, Zhang, Y, Li, J, Lee, JH, Zhu, D, and Deng, XW (2010) Arabidopsis CULLIN4-damaged DNA binding protein 1 interacts with CONSTITUTIVELY PHOTOMORPHOGENIC1-SUPPRESSOR OF PHYA complexes to regulate photomorphogenesis and flowering time. Plant Cell 22, 108-123.

Chen ZH, Jenkins GI, Nimmo HG (2008) Identification of an F-Box protein that negatively regulates Pi starvation responses. Plant Cell Physiol. 49, 1902–1906.

Chen, L, Lee, JH, Weber, H, Tohge, T, Witt, S, Roje, S, Fernie, AR, and Hellmann, H (2013) Arabidopsis BPM proteins function as substrate adaptors to a cullin3-based E3 ligase to affect fatty acid metabolism in plants. Plant Cell 25, 2253-2264.

Chen L, Hellmann H (2013) Plant E3 Ligases: Flexible Enzymes in a Sessile World. Molecular Plant. 6, 1388–1404.

Chen YF, Li LQ, Xu Q, Kong YH, Wang H, Wu WH (2009) The WRKY6 Transcription Factor Modulates PHOSPHATE1 Expression in Response to Low Pi Stress in Arabidopsis. The Plant Cell Online 21, 3554-3566.

Cheng MC, Hsieh EJ, Chen JH, Chen HY, Lin TP (2012) Arabidopsis RGLG2, functioning as a RING E3 ligase, interacts with AtERF53 and negatively regulates the plant drought stress response. Plant Physiol. 158, 363–375.

Chevalier F, Rossignol M (2011) Proteomic analysis of Arabidopsis thaliana ecotypes with contrasted root architecture in response to phosphate deficiency. J. Plant Physiol. 168, 1885–1890.

Chevalier, F, Pata, M, Nacry, P, Doumas, P, and Rossignol, M (2003) Effects of phosphate availability on the root system architecture: large-scale analysis of the natural variation between Arabidopsis accessions. Plant, Cell & Environment 26, 1839-1850.

Chiou TJ, Aung K, Lin SI, Wu CC, Chiang SF, Su CL (2006) Regulation of phosphate homeostasis by MicroRNA in Arabidopsis. Plant Cell 18, 412–421.

Chiou TJ, Lin SI (2011) Signaling network in sensing phosphate availability in plants. Annu. Rev. Plant Biol. 62,185–206.

Choi C M, Gray WM, Mooney S, Hellmann H (2014) Composition, roles, and regulation of cullin-based ubiquitin e3 ligases. The Arabidopsis book / American Society of Plant Biologists 12, e0175, doi:10.1199/tab.0175.

Christians, MJ, Gingerich, DJ, Hansen, M, Binder, BM, Kieber, JJ, and Vierstra, RD (2009) The BTB ubiquitin ligases ETO1, EOL1 and EOL2 act collectively to regulate ethylene biosynthesis in Arabidopsis by controlling type-2 ACC synthase levels. Plant J. 57, 332-345.

Ciereszko I, Johansson H, Hurry V, Kleczkowski LA (2001) Phosphate status aVects the gene expression, protein content and enzymatic activity of UDP-glucose pyrophosphorylase in wild-type and pho mutants of Arabidopsis. Planta 212:598–605

Cochrane, FC, Davin, LB, and Lewis, NG (2004) The Arabidopsis phenylalanine ammonia lyase gene family: kinetic characterization of the four PAL isoforms. Phytochemistry 65:1557–1564.

Cordell, D, Schmid-Neset, T, White, S, and Drangert, J-O (2009). Preferred future phosphorus scenarios: a framework for meeting long-term phosphorus needs for global food demand. International Conference on Nutrient Recovery from Wastewater Streams, 23-43.

Craig, KL, and Tyers, M (1999) The F-box: a new motif for ubiquitin dependent proteolysis in cell cycle regulation and signal transduction. Prog. Biophys. Mol. Biol. 72, 299–328.

Czarnecki, O, Yang, J, Weston, D, Tuskan, G, and Chen, J-G (2013) A Dual Role of Strigolactones in Phosphate Acquisition and Utilization in Plants. International Journal of Molecular Sciences 14, 7681-7701.

da Fonseca, PC, Kong, EH, Zhang, Z, Schreiber, A, Williams, MA, Morris, EP, and Barford, D (2011) Structures of APC/C(Cdh1) with substrates identify Cdh1 and Apc10 as the D-box co-receptor. Nature 470, 274-278.

Dai X, Wang Y, Yang A, Zhang WH (2012) OsMYB2P-1, an R2R3 MYB Transcription Factor, Is Involved in the Regulation of Phosphate-Starvation Responses and Root Architecture in Rice. Plant Physiology 159, 169-183.

Deb, S, Sankaranarayanan, S, Wewala, G, Widdup, EE, and Samuel, M (2014) The S-domain Receptor Kinase AtARK2 and the U-box/ARM-repeat-Containing E3 Ubiquitin Ligase AtPUB9 Module Mediates Lateral Root Development Under Phosphate Starvation in Arabidopsis. Plant Physiology 165, 1647-1656.

del Pozo, JC, Boniotti, MB, and Gutierrez, C (2002a) Arabidopsis E2Fc functions in cell division and is degraded by the ubiquitinSCF(AtSKP2) pathway in response to light. Plant Cell 14, 3057-3071.

del Pozo J C, Allona I, Rubio V, Leyva A, de la Pena A, Aragoncillo C, Paz-Ares J (1999) A type 5 acid phosphatase gene from Arabidopsis thaliana is induced by phosphate starvation and by some other types of phosphate mobilizing/ oxidative stress conditions. Plant J. 19, 579–589.

del Pozo, JC, Dharmasiri, S, Hellmann, H, Walker, L, Gray, WM, and Estelle, M (2002b) AXR1-ECR1-dependent conjugation of RUB1 to the Arabidopsis Cullin AtCUL1 is required for auxin response. Plant Cell 14, 421-433.

Delhaize E, Randall PJ (1995) Characterization of a phosphateaccumulator mutant of Arabidopsis thaliana. Plant Physiol. 107, 207–213.

Demuth JP, Hahn MW (2009) The life and death of gene families. Bioessays 31: 29–39

Deshaies RJ, Joazeiro CA (2009) RING domain E3 ubiquitin ligases. Annu. Rev. Biochem. 78, 399–434.

Deshaies, R (1999) SCF and Cullin/RING H2-based Ubiquitin ligases. Annu. Rev. Cell Dev. Biol. 15, 435-467.

Devaiah BN, Karthikeyan AS, Raghothama KG (2007a) WRKY75 transcription factor is a modulator of phosphate acquisition and root development in Arabidopsis. Plant Physiol. 143, 1789–1801.

Devaiah BN, Nagarajan VK, Raghothama KG (2007b) Phosphate homeostasis and root development in Arabidopsis are synchronized by the zinc finger transcription factor ZAT6. Plant Physiol. 145, 147– 159.

Devaiah BN, Madhuvanthi R, Karthikeyan AS, Raghothama KG (2009) Phosphate Starvation Responses and Gibberellic Acid Biosynthesis Are Regulated by the MYB62 Transcription Factor in Arabidopsis. Molecular Plant 2, 43-58.

Dharmasiri, N, Dharmasiri, S, Weijers, D, Lechner, E, Yamada, M, Hobbie, L, Ehrismann, JS, Jurgens, G, and Estelle, M (2005b) Plant development is regulated by a family of auxin receptor F box proteins. Dev. Cell 9, 109-119.

Dharmasiri N, Dharmasiri S, Estelle M (2005a) The F-box protein TIR1 is an auxin receptor. Nature 435, 441–445.

Dharmasiri, N, Dharmasiri, S, Weijers, D, Karunarathna, N, Jurgens, G, and Estelle, M (2007) AXL and AXR1 have redundant functions in RUB conjugation and growth and development in Arabidopsis. Plant J. 52, 114-123.

Dieterle, M, Zhou, YC, Schafer, E, Funk, M, and Kretsch, T (2001) EID1, an F-box protein involved in phytochrome A-specific light signaling. Genes Dev. 15, 939-944.

Dieterle, M, Thomann, A, Renou, JP, Parmentier, Y, Cognat, V, Lemonnier, G, Muller, R, Shen, WH, Kretsch, T, and Genschik, P (2005). Molecular and functional characterization of Arabidopsis Cullin 3A. Plant J. 41, 386-399

Dinkelaker B, Hengeler C, Marschner H (1995) Distribution and function of proteoid roots and other root clusters. Acta Bot. 108, 183–200.

Dixon, RA, and Paiva, NL (1995) Stress-induced phenylpropanoid metabolism. Plant Cell 7:1085–1097.

Doelling JH, Yan N, Kurepa J, Walker J, Vierstra RD (2001) The ubiquitin-specific protease UBP14 is essential for earlyembryo development in Arabidopsis thaliana. Plant J. 27, 393–405.

Doerner P (2008) Phosphate starvation signaling: A threesome controls systemic Pi homeostasis. Curr. Opin. Plant Biol. 11, 536–540.

Dohmann, EM, Kuhnle, C, and Schwechheimer, C (2005) Loss of the CONSTITUTIVE PHOTOMORPHOGENIC9 signalosome subunit 5 is sufficient to cause the cop/det/fus mutant phenotype in Arabidopsis. Plant Cell. 17, 1967–1978.

Dong B, Rengel Z, Delhaize E (1998) Uptake and translocation of phosphate by pho2 mutant and wild-type seedlings of Arabidopsis thaliana. Planta 205, 251–256.

Downes BP, Stupar RM, Gingerich DJ, Vierstra RD (2003) The HECT ubiquitinprotein ligase (UPL) family in Arabidopsis: UPL3 has a specific role in trichome development. Plant J. 35:729–42.

Doyle, J. J. & Doyle, J. L. (1990) Isolation of plant DNA from fresh tissue. Focus. 12., 13-15.

Duda, DM, Scott, DC, Calabrese, MF, Zimmerman, ES, Zheng, n, and Schulman, BA (2011) Structural regulation of cullin–RING ubiquitin ligase complexes. Curr. Opin. Struct. Biol. 21, 257–264.

Duff SMG, Moorhead GBG, Lefebvre DD, Plaxton WC (1989) Phosphate starvation inducible bypasses of adenylate and phosphate dependent glycolytic enzymes in Brassica nigra suspension cells. Plant Physiol. 90, 1275–1278.

Durbin, M. L., McCaig, B. & Clegg, M. T. (2000) Molecular evolution of the chalcone synthase multigene family in the morning glory genome. Pl. Molec. Biol. 42, 79–92.

Essigmann B, Guler S, Narang RA, Linke D, Benning C (1998) Phosphate availability affects the thylakoid lipid composition and the expression of SQD1, a gene required for sulfolipid biosynthesis in Arabidopsis thaliana. Proc. Natl. Acad. Sci. USA 95, 1950– 1955.

Eastmond, P.J., and Graham, I.A. (2003). Trehalose metabolism: A regulatory role for trehalose-6-phosphate? Curr. Opin. Plant Biol. 6, 231–235.

Erban A., Schauer N., Fernie A.R. & Kopka J. (2007) Non-supervised construction and application of mass spectral and retention time index libraries from time-of-flight GC-MS metabolite profiles. Methods in Molecular Biology 358, 19–38.

Eulgem T, Rushton PJ, Robatzek S, Somssich IE (2000) The WRKY superfamily of plant transcription factors. Trends Plant Sci. 5, 199– 206.

Feys, B, Benedetti, CE, Penfold, CN, and Turner, JG (1994) Arabidopsis Mutants Selected for Resistance to the Phytotoxin Coronatine Are Male Sterile, Insensitive to Methyl Jasmonate, and Resistant to a Bacterial Pathogen. Plant Cell 6, 751-759.

Fiehn O., Kopka J., Dörmann P., Altmann T., Trethewey R.N. & Willmitzer L. (2000) Metabolite profiling for plant functional genomics. Nature Biotechnology 18, 1157–1161.

Figueroa, P, Gusmaroli, G, Serino, G, Habashi, J, Ma, L, Shen, Y, Feng, S, Bostick, M, Callis, J, Hellmann, H, and Deng, XW (2005) Arabidopsis has two redundant Cullin3 proteins that are essential for embryo development and that interact with RBX1 and BTB proteins to form multisubunit E3 ubiquitin ligase complexes in vivo. Plant Cell 17, 1180-1195.

Fixen, PE, and Johnston, AM (2012) World fertilizer nutrient reserves: a view to the future. J Sci Food Agric 92, 1001-1005

Fragoso, S, Espindola, L, Paez-Valencia, J, Gamboa, A, Camacho, Y, Martinez-Barajas, E, and Coello, P (2009) SnRK1 isoforms AKIN10 and AKIN11 are differentially regulated in Arabidopsis plants under phosphate starvation. Plant Physiol. 149, 1906-1916.

Franco-Zorrilla JM, Gonzalez E, Bustos R, Linhares F, Leyva A, Paz-Ares J (2004) The transcriptional control of plant responses to phosphate limitation. J. Exp. Bot. 55, 285–293.

Franco-Zorrilla JM1, Martín AC, Leyva A, Paz-Ares J. (2005) Interaction between phosphate-starvation, sugar, and cytokinin signaling in Arabidopsis and the roles of cytokinin receptors CRE1/AHK4 and AHK3. Plant Physiol. 138(2):847-57.

Franco-Zorrilla JM, Valli A, Todesco M, Mateos I, Puga MI, Rubio Somoza I, Leyva A, Weigel D, García JA, Paz-Ares J (2007) Target mimicry provides a new mechanism for regulation of microRNA activity. Nat. Genet. 39, 1033–1037.

Fraser, CM, and Chapple, C (2011) The phenylpropanoid pathway in Arabidopsis. Arabidopsis Book 9:e0152.

Fredeen, AL, Rao, IM, and Terry, N (1989) Influence of Phosphorus Nutrition on Growth and Carbon Partitioning in Glycine max. Plant Physiology 89, 225-230

Fu H, Doelling JH, Rubin DM, Vierstra RD (1999) Structural and functional analysis of the six regulatory particle AAAATPase subunits from the Arabidopsis 26S proteasome. Plant J. 18:529–39.

Fu, ZQ, Yan, S, Saleh, A, Wang, W, Ruble, J, Oka, N, Mohan, R, Spoel, SH, Tada, Y, Zheng, N, and Dong, X (2012) NPR3 and NPR4 are receptors for the immune signal salicylic acid in plants. Nature 486, 228-232

Fujii H, Chiou TJ, Lin SI, Aung K, Zhu JK (2005) A miRNA involved in phosphate-starvation response in Arabidopsis. Curr. Biol. 15, 2038– 2043.

Fulop, K, Tarayre, S, Kelemen, Z, Horvath, G, Kevei, Z, Nikovics, K, Bako, L, Brown, S, Kondorosi, A, and Kondorosi, E (2005) Arabidopsis anaphase-promoting complexes: multiple activators and wide range of substrates might keep APC perpetually busy. Cell Cycle 4, 1084-1092

Fulop V, Jones DT (1999) Beta propellers: structural rigidity and functional diversity. Curr Opin Struct Biol 9: 715–721

Gagne JM, Downes BP, Shiu S-H, Durski AM, Vierstra RD (2002) The F-Box subunit of the SCF E3 complex is encoded by a diverse superfamily of genes in *Arabidopsis*. Proc. Natl. Acad. Sci. USA 99:11519–24.

Gieffers, C, Dube, P, Harris, JR, Stark, H, and Peters, JM (2001) Three-dimensional structure of the anaphase-promoting complex. Mol. Cell 7, 907-913.

Gingerich, dJ, Gagne, JM, Salter, dW, Hellmann, H, Estelle, M, Ma, L, and Vierstra, Rd (2005) Cullins 3a and 3b assemble with members of the broad complex/tramtrack/bric-a-brac (BTB) protein family to form essential ubiquitin–protein ligases (E3s) in Arabidopsis. J. Biol. Chem. 280, 18810–18821.

Gomez-Roldan, V, Fermas, S, Brewer, PB, Puech-Pages, V, Dun, EA, Pillot, J-P, Letisse, F, Matusova, R, Danoun, S, Portais, J-C, *et al* (2008) Strigolactone inhibition of shoot branching. Nature 455, 189-194

Gonzalez E, Solano R, Rubio V, Leyva A, Paz-Ares J (2005) PHOSPHATE TRANSPORTER TRAFFIC FACILITATOR1 is a plant-specific SEC12-related protein that enables the endoplasmic reticulum exit of a high-affinity phosphate transporter in Arabidopsis. Plant Cell 17, 3500–3512.

Gray WM, Kepinski S, Rouse D, Leyser O, Estelle M (2001) Auxin regulates SCFTIR1-dependent degradation of AUX/IAA proteins. Nature 414, 271–276.

Gray, WM, Hellmann, H, dharmasiri, S, and Estelle, M (2002) Role of the Arabidopsis RING–H2 protein RBX1 in RUB modification and SCF function. Plant Cell. 14, 2137–2144

Gray, WM, Muskett, PR, Chuang, HW, and Parker, JE (2003) Arabidopsis SGT1b is required for SCF(TIR1)-mediated auxin response. Plant Cell 15, 1310-1319.

Gray, WM, del Pozo, JC, Walker, L, Hobbie, L, Risseeuw, E, Banks, T, Crosby, WL, Yang, M, Ma, H, and Estelle, M (1999) Identification of an SCF ubiquitin-ligase complex required for auxin response in Arabidopsis thaliana. Genes Dev. 13, 1678-1691.

Greenham, K, Santner, A, Castillejo, C, Mooney, S, Sairanen, I, Ljung, K, and Estelle, M (2011) The AFB4 auxin receptor is a negative regulator of auxin signaling in seedlings. Curr. Biol. 21, 520-525.

Guex, N. and Peitsch, M.C. (1997) SWISS-MODEL and the Swiss-PdbViewer: an environment for comparative protein modeling. Electrophoresis, 18, 2714-2723.

Gumz F, Krausze J, Eisenschmidt D, Backenko A, Barleben L, Brandt W, Wittstock U (2015) The crystal structure of the thiocyanate-forming protein from Thlaspi arvense, a kelch protein involved in glucosinolate breakdown. Plant Mol Biol. 89:67–81. DOI 10.1007/s11103-015-0351-9.

Gusti, A, Baumberger, N, Nowack, M, Pusch, S, Eisler, H, Potuschak, T, De Veylder, L, Schnittger, A, and Genschik, P (2009) The Arabidopsis thaliana F-box protein FBL17 is essential for progression through the second mitosis during pollen development. PloS One 4, e4780.

Hackenberg M, Shi BJ, Gustafso P, Langridge P (2013a) Characterization of phosphorus-regulated miR399 and miR827 and their isomirs in barley under phosphorus-sufficient and phosphorus-deficient conditions. BMC Plant Biology 13, 1-17.

Hamburger D, Rezzonico E, MacDonald-Comber Petetot J, Somerville C, Poirier Y (2002) Identification and characterization of the Arabidopsis PHO1 gene involved in phosphate loading to the xylem. Plant Cell 14, 889–902.

Hamilton KS, Ellison MJ, Barber KR, Williams RS, Huzil JT, *et al*. (2001) Structure of a conjugating enzyme-ubiquitin thiolester intermediate reveals a novel role for the ubiquitin tail. Structure 9:897–904.

Hammond JP, Bennett MJ, Bowen HC, Broadley MR, Eastwood DC, May ST, Rahn C, Swarup R, Woolaway KE, White PJ (2003) Changes in gene expression in Arabidopsis shoots during phosphate starvation and the potential for developing smart plants. Plant Physiol. 132, 578–596.

Hammond, JP, and White, PJ (2008) Sucrose transport in the phloem: integrating root responses to phosphorus starvation. Journal of Experimental Botany 59, 93-109.

Harmon FG, Kay SA (2003) The F box protein AFR is a positive regulator of phytochrome A-mediated light signaling. Curr Biol 13: 2091–2096

Hartmann-Petersen R, Seeger M, Gordon C (2003) Transferring substrates to the 26S proteasome. Trends Biochem. Sci. 28:26–31.

Hao Y, Sekine K, Kawabata A, Nakamura H, Ishioka T, Ohata H, Katayama R, Hashimoto C, Zhang X, Noda T, Tsuruo T, Naito M (2004) Apollon ubiquitinates SMAC and caspase-9, and has an essential cytoprotection function. Nat. Cell Biol. 6, 849–857.

Hao B, et al. (2007) Structure of a Fbw7-Skp1-cyclin E complex: multisite-phosphorylated substrate recognition by SCF ubiquitin ligases. Mol. Cell. 26:131–143

Harrison MJ (2005) Signaling in the arbuscular mycorrhizal symbiosis. Annu. Rev. Microbiol. 59, 19–42.

Hauser HP, Bardroff M, Pyrowolakis G, Jentsch S (1998) A giant ubiquitin-conjugating enzyme related to IAP apoptosis inhibitors. J. Cell Biol. 141, 1415–1422.

Havir, EA, and Hanson, KR (1973) L-Phenylalanine ammonia-lyase (maize and potato). Evidence that the enzyme is composed of four subunits. Biochemistry 12:1583–1591

Hatfield PM, Gosink MM, Carpenter TB, Vierstra RD (1997) The ubiquitinactivating enzyme (E1) gene family in Arabidopsis thaliana. Plant J. 11:213–26.

He, C-J, Morgan, PW, and Drew, MC (1992) Enhanced Sensitivity to Ethylene in Nitrogen- or Phosphate-Starved Roots of Zea mays L. during Aerenchyma Formation. Plant Physiology 98, 137-142.

Helmstaedt, K, Schwier, Eu, Christmann, M, nahlik, K, Westermann, M, Harting, R, Grond, S, Busch, S, and Braus, GH (2011) Recruitment of the inhibitor Cand1 to the cullin substrate adaptor site mediates interaction to the neddylation site. Mol. Biol. Cell. 22, 153–164.

Herrmann, K.M. (1995). The shikimate pathway: Early steps in the biosynthesis of aromatic compounds. Plant Cell 7, 907–919.

Hershko A, Ciechanover A, Heller H, Haas AL, Rose IA (1980) Proposed role of ATP in protein breakdown: conjugation of protein with multiple chains of the polypeptide of ATP-dependent proteolysis. Proceedings of the National Academy of Sciences of the United States of America 77, 1783-1786.

Hershko A, Ciechanover A (1982) Mechanisms of intracellular protein breakdown. Annual review of biochemistry 51, 335-364, doi:10.1146/annurev.bi.51.070182.002003.

Hershko A, Ciechanover A (1998) The ubiquitin system. Annu. Rev. Biochem. 67, 425–479.

Hewitt, MM, Carr, JM, Williamson, CL, and Slocum, RD (2005) Effects of phosphate limitation on expression of genes involved in pyrimidine synthesis and salvaging in Arabidopsis. Plant Physiology and Biochemistry 43, 91-99.

Hoffman, C. S. & Winston, F. A (1987) ten-minute DNA preparation from yeast efficiently releases autonomous plasmids for transformation of Escherichia coli. Gene 57, 267-272.

Holford ICR (1997) Soil phosphorus: Its measurement, and its uptake by plants. Aust. J. Soil Res. 35, 227–239.

Horgan, JM, and Wareing, PF (1980) Cytokinins and the Growth Responses of Seedlings of Betula pendula Roth. and Acer pseudoplatanus L. to Nitrogen and Phosphorus Deficiency. Journal of Experimental Botany 31, 525-532.

Hsieh LC, Lin SI, Shi, AC, Chen JW, Lin W-, Tseng CY, Li WH, Chiou TJ (2009) Uncovering Small RNA-Mediated Responses to Phosphate Deficiency in Arabidopsis by Deep Sequencing. Plant Physiology 151, 2120-2132.

Huang, X, Ouyang, X, Yang, P, Lau, OS, Chen, L, Wei, N, and Deng, XW (2013b) Conversion from CUL4-based COP1-SPA E3 apparatus to UVR8-COP1-SPA complexes underlies a distinct biochemical function of COP1 under UV-B. Proc. Natl. Acad. Sci. 110, 16669-16674.

Hummel J., Strehmel N., Selbig J., Walther D. & Kopka J. (2010) Decision tree supported substructure prediction of metabolites from GC-MS profiles. Metabolomics: Official Journal of the Metabolomic Society 6, 322–333.

Hwang I, Chen HC, Sheen J (2002) Two-component signal transduction pathways in Arabidopsis. Plant Physiol 129: 500–515

Hughes AL. (1994). The Evolution of Functionally Novel Proteins after Gene Duplication. Proceedings: Biological Sciences 256, 119–124.

Huibregtse JM, Scheffner M, Beaudenon S, and Howley PM (1995) A family of proteins structurally and functionally related to the E6-AP ubiquitin–protein ligase. Proc. Natl Acad. Sci. U S A. 92, 5249.

Hurley, BA, Tran, HT, Marty, NJ, Park, J, Snedden, WA, Mullen, RT, and Plaxton, WC (2010) The dual-targeted purple acid phosphatase isozyme AtPAP26 is essential for efficient acclimation of Arabidopsis to nutritional phosphate deprivation. Plant physiology 153, 1112-1122.

Iglesias, J, Trigueros, M, Rojas-Triana, M, Fernández, M, Albar, JP, Bustos, R, Paz-Ares, J, and Rubio, V (2013) Proteomics identifies ubiquitin–proteasome targets and new roles for chromatin-remodeling in the Arabidopsis response to phosphate starvation. Journal of Proteomics 94, 1-22.

Israel, DW, Rufty, TW, and Cure, JD (1990) Nitrogen and phosphorus nutritional interactions in a CO2 enriched environment. Journal of Plant Nutrition 13, 1419-1433.

Ito, S, Song, YH, and Imaizumi, T (2012) LOV domain-containing Fbox proteins: light-dependent protein degradation modules in Arabidopsis. Mol. Plant 5, 573-582.

Ito, N., Phillips, S.E., Yadav, K.D. and Knowles, P.F. (1994). Crystal structure of a free radical enzyme, galactose oxidase. J. Mol. Biol. 238: 794–814.

Jain A, Poling MD, Karthikeyan AS, Blakeslee JJ, Peer WA, Titapiwatanakun B, Murphy AS, Raghothama KG (2007) Differential effects of sucrose and auxin on localized phosphate deficiencyinduced modulation of different traits of root system architecture in Arabidopsis. Plant Physiol. 144, 232–247.

Jang, S, Marchal, V, Panigrahi, KC, Wenkel, S, Soppe, W, Deng, XW, Valverde, F, and Coupland, G (2008) Arabidopsis COP1 shapes the temporal pattern of CO accumulation conferring a photoperiodic flowering response. EMBO J.27, 1277-1288.

Jawad Z, Paoli M (2002) Novel sequences propel familiar folds. Structure 10: 447–454

Jiang, C, Gao, X, Liao, L, Harberd, NP, and Fu, X (2007) Phosphate Starvation Root Architecture and Anthocyanin Accumulation Responses Are Modulated by the Gibberellin-DELLA Signaling Pathway in Arabidopsis. Plant Physiology 145, 1460-1470.

Jiang, J, and Clouse, SD (2001) Expression of a plant gene with sequence similarity to animal TGF-beta receptor interacting protein is regulated by brassinosteroids and required for normal plant development. Plant J. 26, 35-45.

Johnson CM, Stout PR, Broker TC, Carlton AB (1957) Comparative chlorine reuirements of different plats species. Palnt and soil. 8, 337-353.

Jurado, S, Diaz-Trivino, S, Abraham, Z, Manzano, C, Gutierrez, C, and del Pozo, C (2008) SKP2A, an F-box protein that regulates cell division, is degraded via the ubiquitin pathway. Plant J. 53, 828-841.

Källberg, M., Wang, H., Wang, S., Peng, J., Wang, Z., Lu, H., and Xu, J. (2012). "Template-based protein structure modeling using the RaptorX web server." Nat. Protocols, 7(8), 1511-1522.

Kant S, Peng M, Rothstein SJ (2011) Genetic regulation by NLA and microRNA827 for maintaining nitrate-dependent phosphate homeostasis in Arabidopsis. PLoS Genet. 3, e1002021.

Karthikeyan AS, Varadarajan DK, Jain A, Held MA, Carpita NC, Raghothama KG (2007) Phosphate starvation responses are mediated by sugar signaling in Arabidopsis. Planta. 225(4):907-18.

Kawaoka, A, Kaothien, P, Yoshida, K, Endo, S, Yamada, K, and Ebinuma, H (2000) Functional analysis of tobacco LIM protein Ntlim1 involved in lignin biosynthesis. Plant J. 22:289–301.

Kawaoka, A, and Ebinuma, H (2001) Transcriptional control of lignin biosynthesis by tobacco LIM protein. Phytochemistry 57:1149–1157.

Kenrick P, Crane PR (1997) The origin and early evolution of plants on land. Nature 389: 33–39

Kepinski S, Leyser O (2005) The Arabidopsis F-box protein TIR1 is an auxin receptor. Nature 435, 446–451.

Kevei, Z, Baloban, M, Da Ines, O, Tiricz, H, Kroll, A, Regulski, K, Mergaert, P, and Kondorosi, E (2011) Conserved CDC20 cell cycle functions are carried out by two of the five isoforms in Arabidopsis thaliana. PloS One 6, e20618.

Kiba, T, Henriques, R, Sakakibara, H, and Chua, NH (2007) Targeted degradation of PSEUDO-RESPONSE REGULATOR5 by an SCFZTL complex regulates clock function and photomorphogenesis in Arabidopsis thaliana. Plant Cell 19, 2516-2530.

Kiefer F, Arnold K, Künzli M, Bordoli L, Schwede T (2009). The SWISS-MODEL Repository and associated resources. Nucleic Acids Res. 37, D387-D392.

Kim, H-J, Lynch, JP, and Brown, KM (2008) Ethylene insensitivity impedes a subset of responses to phosphorus deficiency in tomato and petunia. Plant, Cell & Environment 31, 1744-1755.

Kim, HJ, Oh, SA, Brownfield, L, Hong, SH, Ryu, H, Hwang, I, Twell, D, and Nam, HG (2008) Control of plant germline proliferation by SCF(FBL17) degradation of cell cycle inhibitors. Nature 455, 1134-1137.

Kim JH, Park KC, Chung SS, Bang O, Chung CH (2003) Deubiquitinating enzymes as cellular regulators. J. Biochem. 134, 9–18.

Kim, S, Choi, HI, Ryu, HJ, Park, JH, Kim, MD, and Kim, SY (2004) ARIA, an Arabidopsis arm repeat protein interacting with a transcriptional regulator of abscisic acid-responsive gene expression, is a novel abscisic acid signaling component. Plant Physiol. 136, 3639- 3648

Kim H, Chianga Y, Kieberb J, Schallera G (2013) SCFKMD controls cytokinin signaling by regulating the degradation of type-B response regulators. PNAS. 110; 24, 10028–10033

Kobayashi K, Masuda T, Takamiya K-i, Ohta H (2006) Membrane lipid alteration during phosphate starvation is regulated by phosphate signaling and auxin/cytokinin cross-talk. Plant J. 47, 238–248.

Kong, H., Landherr, L.L., Frohlich, M.W., Leebens-Mack, J., Ma, H., and dePamphilis, C.W. (2007). Patterns of gene duplication in the plant SKP1 gene family in angiosperms: evidence for multiple mechanisms of rapid gene birth. Plant J. 50, 873-885

Koops, P, Pelser, S, Ignatz, M, Klose, C, Marrocco-Selden, K, and Kretsch, T (2011) EDL3 is an F-box protein involved in the regulation of abscisic acid signalling in Arabidopsis thaliana. J. Exp. Bot. 62, 5547-5560.

Kopka J., Schauer N., Krueger S., Birkemeyer C., Usadel B., Bergmüller E., . . . Steinhauser D. (2005) GMD@CSB.DB: the Golm Metabolome database. Bioinformatics (Oxford, England) 21, 1635–1638

Kuroda, H., Yanagawa, Y., Takahashi, N., Horii, Y., and Matsui, M. (2012). A comprehensive analysis of interaction and localization of Arabidopsis SKP1-like (ASK) and F-box (FBX) proteins. PloS One 7, e50009.

Kraft E, Stone SL, Ma L, Su N, Gao Y, Lau OS, Deng XW, Callis J (2005) Genome analysis and functional characterization of the E2 and RING-type E3 ligase ubiquitination enzymes of Arabidopsis. Plant Physiol. 139, 1597–1611.

Kuiper, D, Schuit, J, and Kuiper, PC (1988) Effects of internal and external cytokinin concentrations on root growth and shoot to root ratio ofPlantago major sspPleiosperma at different nutrient conditions. Plant and Soil 111, 231-236.

Lamb, C.J. (1979). Regulation of enzyme levels in phenylpropanoid biosynthesis: characterization of the modulation by light and pathway intermediates. Arch. Biochem. Biophys. 192:311–317.

Lambers, H, Finnegan, PM, Laliberte, E, Pearse, SJ, Ryan, MH, Shane, MW, and Veneklaas, EJ (2011) Update on phosphorus nutrition in Proteaceae. Phosphorus nutrition of proteaceae in severely phosphorus-impoverished soils: are there lessons to be learned for future crops? Plant physiology 156, 1058-1066.

Lammens, T, Boudolf, V, Kheibarshekan, L, Zalmas, LP, Gaamouche, T, Maes, S, Vanstraelen, M, Kondorosi, E, La Thangue, NB, Govaerts, W, Inze, D, and De Veylder, L (2008). Atypical E2F activity restrains APC/CCCS52A2 function obligatory for endocycle onset. Proc. Natl. Acad. Sci. 105, 14721-14726.

Lan P, Li W, Schmidt W (2012) Complementary proteome and transcriptome profiling in phosphate-deficient Arabidopsis roots reveals multiple levels of gene regulation. Mol. Cell. Proteomics. doi: 10.1074/mcp.M112.020461.

Lau, OS, and Deng, XW (2009) Effect of Arabidopsis COP10 ubiquitin E2 enhancement activity across E2 families and functional conservation among its canonical homologues. Biochem. J. 418, 683-690.

Lee HK, Cho SK, Son O, Xu Z, Hwang I, Kim WT (2009a) Drought stress-induced Rma1H1, a RING membraneanchor E3 ubiquitin ligase homolog, regulates aquaporin levels via ubiquitination in transgenic Arabidopsis plants. Plant Cell. 21, 622–641.

Lee, SJ, Cho, DI, Kang, JY, and Kim, SY (2009b) An ARIA-interacting AP2 domain protein is a novel component of ABA signaling. Mol. Cells 27, 409-416.

Lee, JH, Terzaghi, W, Gusmaroli, G, Charron, JB, Yoon, HJ, Chen, H, He, YJ, Xiong, Y, and Deng, XW (2008) Characterization of Arabidopsis and rice DWD proteins and their roles as substrate receptors for CUL4-RING E3 ubiquitin ligases. Plant Cell 20, 152-167.

Lee, JH, Yoon, HJ, Terzaghi, W, Martinez, C, Dai, M, Li, J, Byun, MO, and Deng, XW (2010) DWA1 and DWA2, two Arabidopsis DWD protein components of CUL4-based E3 ligases, act together as negative regulators in ABA signal transduction. Plant Cell 22, 1716-1732.

Lee, JH, Terzaghi, W, and Deng, XW (2011) DWA3, an Arabidopsis DWD protein, acts as a negative regulator in ABA signal transduction. Plant Science 180, 352-357.

Lei, M, Zhu, C, Liu, Y, Karthikeyan, AS, Bressan, RA, Raghothama, KG, and Liu, D (2011a) Ethylene signalling is involved in regulation of phosphate starvation-induced gene expression and production of acid phosphatases and anthocyanin in Arabidopsis. New Phytologist 189, 1084-1095.

Leung KC, Li HY, Mishra G, Chye ML (2004) ACBP4 and ACBP5, novel Arabidopsis acyl-CoA-binding proteins with kelch motifs that bind oleoyl-CoA. Plant Mol Biol 55: 297–309

Levin, JZ, and Meyerowitz, EM (1995) UFO: an Arabidopsis gene involved in both floral meristem and floral organ development. Plant Cell 7, 529-548.

Li K, Xu C, Zhang K, Yang A, Zhang J (2007) Proteomic analysis of roots growth and metabolic changes under phosphorus deficit in maize (Zea mays L.) plants. Proteomics 7, 1501–1512.

Li, D, Zhu, H, Liu, K, Liu, X, Leggewie, G, Udvardi, M, and Wang, D (2002) Purple acid phosphatases of Arabidopsis thaliana. Comparative analysis and differential regulation by phosphate deprivation. The Journal of biological chemistry 277, 27772-27781.

Li X, Zhang D, Hannink M, Beamer LJ (2004) Crystal structure of the kelch domain of human Keap1. J Biol Chem 279: 54750–54758

Li W, Dai L, Wang GL (2012) PUB13, a U-box/ARM E3 ligase, regulates plant defense, cell death, and flowering time. Plant Signal Behav. 7, 239–250.

Li Y, Hao B.(2010) Structural basis of dimerization-dependent ubiquitination by the SCFFbx4 ubiquitin ligase. J. Biol. Chem. 285:13896–13906.

Li WF, Perry PJ, Prafulla NN, Schmidt W (2010) Ubiquitin-Specific protease 14 (UBP14) is involved in root responses to phosphate deficiency in Arabidopsis. Mol. Plant 3, 212–223.

Lin SI, Chiang SF, Lin WY, Chen JW, Tseng CY, Wu PC, Chiou TJ (2008) Regulatory network of microRNA399 and PHO2 by systemic signaling. Plant Physiol. 147, 732–746.

Lin WY, Huang TK, Chiou TJ (2013) NITROGEN LIMITATION ADAPTATION, a Target of MicroRNA827, Mediates Degradation of Plasma Membrane–Localized Phosphate Transporters to Maintain Phosphate Homeostasis in Arabidopsis. The Plant Cell Online 25, 4061-4074.

Lisec J., Schauer N., Kopka J., Willmitzer L. & Fernie A.R. (2006) Gas chromatography mass spectrometry-based metabolite profiling in plants. Nature Protocols 1, 387–396.

Liu, H, Yang, H, Wu, C, Feng, J, Liu, X, Qin, H, and Wang, D (2009) Overexpressing HRS1 Confers Hypersensitivity to Low Phosphate-Elicited Inhibition of Primary Root Growth in Arabidopsis thaliana. Journal of Integrative Plant Biology 51, 382-392.

Liu TY, Huang TK, Tseng CY, Lai YS, Lin SI, Lin WY, Chen JW, Chiou TJ (2012) PHO2-dependent degradation of PHO1 modulates phosphate homeostasis in Arabidopsis. Plant Cell 24, 2168– 2183.

Liu JQ, Allan D, Vance C (2010) Systemic Signaling and Local Sensing of Phosphate in Common Bean: Cross-Talk between Photosynthate and MicroRNA399. Mol Plant 3, 428 - 437.

Lopez-Bucio J, Cruiz-Ramirez A, Herrera-Estrella L (2003) The role of nutrient availability in regulating root architecture. Curr. Opin. Plant Biol. 6, 280–287.

Lopez-Bucio J, Hernández-Abreu E, Sánchez-Calderón L, Nieto- Jacobo MF, Simpson J, Herrera-Estrella L (2002) Phosphate availability alters architecture and causes changes in hormone sensitivity in the Arabidopsis root system. Plant Physiol. 129, 244– 256.

Luedemann A., Strassburg K., Erban A. & Kopka J. (2008) TagFinder for the quantitative analysis of gas chromatography-mass spectrometry (GC-MS)- based metabolite profiling experiments. Bioinformatics (Oxford, England) 24, 732–737.

Lynch JP, Brown KM (2001) Topsoil foraging: An architectural adaptation of plants to low phosphorus availability. Plant Soil 237, 225– 237.

Lynch, JP (2011) Root phenes for enhanced soil exploration and phosphorus acquisition: tools for future crops. Plant physiology 156, 1041-1049.

Lyzenga WJ, Booth JK, Stone SL (2012) The Arabidopsis RING-type E3 ligase XBAT32 mediates the proteasomal degradation of the ethylene biosynthetic enzyme, 1-aminocyclopropane-1-carboxylate synthase 7. Plant J. 71, 23–34.

Ma, Z, Baskin, TI, Brown, KM, and Lynch, JP (2003) Regulation of Root Elongation under Phosphorus Stress Involves Changes in Ethylene Responsiveness. Plant Physiology 131, 1381-1390.

Marrocco, K, Thomann, A, Parmentier, Y, Genschik, P, and Criqui, MC (2009) The APC/C E3 ligase remains active in most post-mitotic Arabidopsis cells and is required for proper vasculature development and organization. Development 136, 1475-1485.

Marschner, M (1995) Mineral Nutrition of Higher Plants. Academic Press Limited, London, UK.

Martín, AC, Del Pozo, JC, Iglesias, J, Rubio, V, Solano, R, De La Peña, A, Leyva, A, and Paz-Ares, J (2000) Influence of cytokinins on the expression of phosphate starvation responsive genes in Arabidopsis. The Plant Journal 24, 559-567.

Martin, C, and Paz-Ares, J (1997) MYB transcription factors in plants. Trends Genet. 13:67–73

Mavandad, M., Edwards, R., Liang, X., Lamb, C.J., and Dixon, R.A. (1990). Effects of trans-cinnamic acid on expression of the bean phenylalanine ammonia-lyase gene family. Plant Physiol. 94:671–680.

Mayzlish-Gati, E, De-Cuyper, C, Goormachtig, S, Beeckman, T, Vuylsteke, M, Brewer, PB, Beveridge, CA, Yermiyahu, U, Kaplan, Y, Enzer, Y, *et al* (2012) Strigolactones Are Involved in Root Response to Low Phosphate Conditions in Arabidopsis. Plant Physiology 160, 1329-1341.

Mele, G, Ori, N, Sato, Y, and Hake, S (2003) The knotted1-like homeobox gene BREVIPEDICELLUS regulates cell differentiation by modulating metabolic pathways. Genes Dev. 17:2088–2093.

Miao Y, Zentgraf U (2010) A HECT E3 ubiquitin ligase negatively regulates Arabidopsis leaf senescence through degradation of the transcription factor WRKY53. Plant J. 63, 179–188.

Miller MJ, Barrett-Wilt GA, Hua Z, Vierstra RD (2010) Proteomic analyses identify a diverse array of nuclear processes affected by small ubiquitin-like modifier conjugation in Arabidopsis. Proc. Natl. Acad. Sci. USA 107, 16512–16517.

Misson J, Raghothama KG, Jain A, Jouhet J, Block MA, Bligny R, Ortet P, Creff A, Somerville S, Rolland N, Doumas P, Nacry P, Herrerra-Estrella L, Nussaume L, Thibaud MC (2005) A genomewide transcriptional analysis using Arabidopsis thaliana Affymetrix gene chips determined plant responses to phosphate deprivation. Proc. Natl. Acad. Sci. USA 102, 11934–11939.

Miura K, Hasegawa PM (2010) Sumoylation and other ubiquitin-like post-translational modifications in plants. Trends Cell Biol. 4, 223– 232.

Miura K, Lee J, Gong Q, Ma S, Jin JB, Yoo CY, Miura T, Sato A, Bohnert HJ, Hasegawa PM (2011) SIZ1 regulation of phosphate starvation-induced root architecture remodeling involves the control of auxin accumulation. Plant Physiol. 2, 1000–1012.

Miura K, Rus A, Sharkhuu A, Yokoi S, Karthikeyan AS, Raghothama KG, Baek D, Koo YD, Jin JB, Bressan RA, Yun DJ, Hasegawa PM (2005) The Arabidopsis SUMO E3 ligase SIZ1 controls phosphate deficiency responses. Proc. Natl. Acad. Sci. USA 102, 7760–7765.

Molinier, J, Lechner, E, Dumbliauskas, E, and Genschik, P (2008) Regulation and role of Arabidopsis CUL4-DDB1A-DDB2 in maintaining genome integrity upon UV stress. PLoS Genet. 4, e1000093.

Moon J, Zhao Y, Dai X, Zhang W, Gray WM, Huq E, Estelle M (2007) A new CULLIN 1 mutant has altered responses to hormones and light in Arabidopsis. Plant Physiol. 143, 684–696.

Mora-García S, Vert G, Yin Y, Cano-Delgado A, Cheong H, Chory J (2004) Nuclear protein phosphatases with kelch-repeat domains modulate the response to brassinosteroids in Arabidopsis. Genes Dev 18: 448–460

Morcuende R, Bari R, Gibon Y, Zheng W, Pant BD, Blasing O, ¨ Usadel B, Czechowski T, Udvardi MK, Stitt M, Scheible WR (2007) Genome-wide reprogramming of metabolism and regulatory networks of Arabidopsis in response to phosphorus. Plant Cell Environ. 30, 85–112.

Muller R, Morant M, Jarmer H, Nilsson L, Nielsen TH (2007) Genome-wide analysis of the Arabidopsis leaf transcriptome reveals interaction of phosphate and sugar metabolism. Plant Physiol. 143, 156–171.

Nakamura, Y (2013) Phosphate starvation and membrane lipid remodeling in seed plants. Progress in Lipid Research 52, 43-50.

Nakasakoa M, Matsuokac D, Zikiharad K, Tokutomic S (2005) Quaternary structure of LOV-domain containing polypeptide of Arabidopsis FKF1 protein. FEBS Letters 579 (2005) 1067–1071.

Nielsen TH, Knapp A, Roper-Schwarz U, Stitt M (1998) The sugar-mediated regulation of genes encoding the small subunit of Rubisco and the regulatory subunit of ADP glucose pyrophosphorylase is modiWed by phosphate and nitrogen. Plant Cell Environ 21:443–454

Nilsson, L, MÜLler, R, and Nielsen, TH (2007) Increased expression of the MYB-related transcription factor, PHR1, leads to enhanced phosphate uptake in Arabidopsis thaliana. Plant, Cell & Environment 30, 1499-1512.

Ning Y, et al. (2011) The SINA E3 ligase OsDIS1 negatively regulates drought response in rice. Plant Physiol. Behav. 157, 242–255.

Ohi MD, Vander Kooi CW, Rosenberg JA, Chazin WJ, Gould KL (2003). Structural insights into the U-box, a domain associated with multi-ubiquitination. Nat. Struct. Biol. 10, 250–255.

Olsen, K.M., Lea, U.S., Slimestad, R., Verheul, M., and Lillo, C. (2008). Differential expression of four Arabidopsis PAL genes; PAL1 and PAL2 have functional specialization in abiotic environmental-triggered flavonoid synthesis. J. Plant Physiol. 165:1491–1499.

Pajerowska-Mukhtar, KM, Emerine, DK, and Mukhtar, MS (2013) Tell me more: roles of NPRs in plant immunity. Trends Plant Sci. 18, 402-411.

Pant BD, Buhtz A, Kehr J, Scheible WR (2008) MicroRNA399 is a long-distance signal for the regulation of plant phosphate homeostasis. Plant J. 53, 731–738.

Pant, B, Pant, P, Erban, A, Huhman, D, Kopka, J, and Scheible, W-R (2014) Identification of primary and secondary metabolites with phosphorus status-dependent abundance in Arabidopsis, and of the transcription factor PHR1 as a major regulator of metabolic changes during phosphorus limitation. Plant, Cell & Environment.

Pant, B, Musialak-Lange, M, Nuc, P, May, P, Buhtz, A, Kehr, J, Walther, D, and Scheible, W-R (2009) Identification of Nutrient-Responsive Arabidopsis and Rapeseed MicroRNAs by Comprehensive Real-Time Polymerase Chain Reaction Profiling and Small RNA Sequencing. Plant Physiol 150, 1541 - 1555.

Park, BS, Seo, JS, and Chua, N-H (2014) NITROGEN LIMITATION ADAPTATION Recruits PHOSPHATE2 to Target the Phosphate Transporter PT2 for Degradation during the Regulation of Arabidopsis Phosphate Homeostasis. The Plant Cell Online 26, 454-464.

Parry G, Calderon-Villalobos LI, Prigge M, Peret B, Dharmasiri S, Itoh H, Lechner E, Gray WM, Bennett M, Estelle M (2009) Complex regulation of the TIR1/AFB family of auxin receptors. Proc Natl Acad Sci USA 106: 22540–22545

Pedmale, UV, and Liscum, E (2007) Regulation of phototropic signaling in Arabidopsis via phosphorylation state changes in the phototropin 1-interacting protein NPH3. J. Biol. Chem. 282, 19992-20001

Perazza D, Herzog M, Hulskamp M, Brown S, Dorne AM, Bonneville JM (1999) Trichome cell growth in Arabidopsis thaliana can be derepressed by mutations in at least five genes. Genetics. 152, 461–476.

Peret B, Clément M, Nussaume L, Desnos T (2011) Root developmental adaptation to phosphate starvation: Better safe than sorry. Trends Plant Sci. 8, 442–450.

Perez-Torres CA, López-Bucio J, Cruz-Ramírez A, Ibarra-Laclette E, Dharmasiri S, Estelle M, Herrera-Estrella L (2008) Phosphate availability alters lateral root development in Arabidopsis by modulating auxin sensitivity via a mechanism involving the TIR1 auxin receptor. Plant Cell 20, 3258–3272.

Perez-Perez, JM, Serralbo, O, Vanstraelen, M, Gonzalez, C, Criqui, MC, Genschik, P, Kondorosi, E, and Scheres, B (2008) Specialization of CDC27 function in the Arabidopsis thaliana anaphase-promoting complex (APC/C). Plant J. 53, 78-89.

Pickart CM (2001) Mechanisms underlying ubiquitination. Annu. Rev. Biochem. 70:503–33.

Plaxton, WC, and Tran, HT (2011) Metabolic Adaptations of Phosphate-Starved Plants. Plant Physiology 156, 1006-1015.

Poirier Y, Thoma S, Somerville C, Schiefelbein J (1991) A mutant of Arabidopsis deficient in xylem loading of phosphate. Plant Physiol. 97, 1087–1093.

Poirier, Y, and Bucher, M (2002) Phosphate transport and homeostasis in Arabidopsis. The Arabidopsis book / American Society of Plant Biologists 1, e0024.

Prag S, Adams JC (2003) Molecular phylogeny of the kelch-repeat superfamily reveals an expansion of BTB/kelch proteins in animals. BMC Bioinformatics 4: 42

Pratelli R, Guerra DD, Yu S, Wogulis M, Kraft E, Frommer WB, Callis J, Pilot G (2012) The ubiquitin E3 ligase LOSS OF GDU2 is required for GLUTAMINE DUMPER1-induced amino acid secretion in Arabidopsis. Plant Physiol. 158, 1628–1642.

Qiao, H, Chang, KN, Yazaki, J, and Ecker, JR (2009) Interplay between ethylene, ETP1/ETP2 F-box proteins, and degradation of EIN2 triggers ethylene responses in Arabidopsis. Genes Dev. 23, 512-521.

Qiao H, Chang KN, Yazaki J, Ecker JR (2009) Interplay between ethylene, ETP1/ETP2 F-box proteins, and degradation of EIN2 triggers ethylene responses in Arabidopsis. Genes Dev 23: 512–521

Raab S, Drechsel G, Zarepou M, Hartung W, Koshiba T, Bittner F, Hoth S (2009) Identification of a novel E3 ubiquitin ligase that is required for suppression of premature senescence in Arabidopsis. Plant J. 59, 39–51.

Raasi S. & Wolf D. H. (2007) Ubiquitin receptors and ERAD: a network of pathways to the proteasome. Seminars in cell & developmental biology 18, 780-791, doi:10.1016/j.semcdb.2007.09.008.

Raghothama KG (1999) Phosphate acquisition. Annu. Rev. Plant Physiol. 50, 665–693.

Ren, H, Santner, A, del Pozo, JC, Murray, JA, and Estelle, M (2008) Degradation of the cyclin-dependent kinase inhibitor KRP1 is regulated by two different ubiquitin E3 ligases. Plant J. 53, 705-716.

Ribot, C, Wang, Y, and Poirier, Y (2008) Expression analyses of three members of the AtPHO1 family reveal differential interactions between signaling pathways involved in phosphate deficiency and the responses to auxin, cytokinin, and abscisic acid. Planta 227, 1025-1036.

Rishmawi, L, Pesch, M, Juengst, C, Schauss, AC, Schrader, A, and Hülskamp, M (2014) Non-Cell-Autonomous Regulation of Root Hair Patterning Genes by WRKY75 in Arabidopsis. Plant Physiology 165, 186-195.

Risseeuw, E.P., Daskalchuk, T.E., Banks, T.W., Liu, E., Cotelesage, J., Hellmann, H., Estelle, M., Somers, D.E., and Crosby, W.L. (2003). Protein interaction analysis of SCF ubiquitin E3 ligase subunits from Arabidopsis. Plant J. 34, 753-767.

Ritter, H, and Schulz, GE (2004) Structural basis for the entrance into the phenylpropanoid metabolism catalyzed by phenylalanine ammonia-lyase. Plant Cell 16:3426–3436.

Roberts, D, Pedmale, UV, Morrow, J, Sachdev, S, Lechner, E, Tang, X, Zheng, N, Hannink, M, Genschik, P, and Liscum, E (2011) Modulation of phototropic responsiveness in Arabidopsis through ubiquitination of phototropin 1 by the CUL3-Ring E3 ubiquitin ligase CRL3(NPH3). Plant Cell 23, 3627-3640.

Rohde, A., Morreel, K., Ralph, J., Goeminne, G., Hostyn, V., De Rycke, R., Kushnir, S., Van Doorsselaere, J., Joseleau, J.P., Vuylsteke, M., et al. (2004). Molecular phenotyping of the pal1 and pal2 mutants of Arabidopsis thaliana reveals far-reaching consequences on phenylpropanoid, amino acid, and carbohydrate metabolism. Plant Cell 16:2749–2771.

Rojas-Triana M, Bustos R, Espinosa-Ruiz A, Prat S, Paz-Ares J, Rubio V (2013) Roles of ubiquitination in the control of phosphate starvation responses in plants. J Integr Plant Biol. 55(1):40-53. doi: 10.1111/jipb.12017.

Roessner U., Wagner C., Kopka J., Trethewey R.N. & Willmitzer L. (2000) Technical advance: simultaneous analysis of metabolites in potato tuber by gas chromatography-mass spectrometry. The Plant Journal: For Cell and Molecular Biology 23, 131–142.

Rouached H, Arpat AB, Poirier Y (2010) Regulation of phosphate starvation responses in plants: Signaling players and cross-talks. Mol. Plant 2, 288–299.

Rubio, V, Bustos, R, Irigoyen, M, Cardona-López, X, Rojas-Triana, M, and Paz-Ares, J (2009) Plant hormones and nutrient signaling. Plant Molecular Biology 69, 361-373.

Rubio V, Linhares F, Solano R, Mart´ ın AC, Iglesias J, Leyva A, Paz-Ares J (2001) A conserved MYB transcription factor involved in phosphate starvation signalling both in vascular plants and unicellular algae. Genes Dev. 15, 2122–2133.

Rubio-Somoza I, Weigel D, Franco-Zorilla JM, Garc´ ıa JA, Paz-Ares J (2011) ceRNAs: miRNA target mimic mimics. Cell 7, 1431–1432.

Ruyter-Spira, C, Kohlen, W, Charnikhova, T, van Zeijl, A, van Bezouwen, L, de Ruijter, N, Cardoso, C, Lopez-Raez, JA, Matusova, R, Bours, R, et al (2011) Physiological Effects of the Synthetic

Sablowski, RW, Moyano, E, Culianez-Macia, FA, Schuch, W, Martin, C, and Bevan, M (1994) A flower-specific Myb protein activates transcription of phenylpropanoid biosynthetic genes. EMBO J. 13:128–137.

Sadanandom A, Bailey M, Ewan R, Lee J, Nelis S (2012) The ubiquitin-proteasome system: Central modifier of plant signalling. New Phytol. 196, 13–28.

Sadka A, DeWald DB, May GD, Park WD, Mullet JE (1994) Phosphate modulates transcription of soybean VspB and other sugar-inducible genes. Plant Cell 6:737–749

Sakai T, Mochizuki S, Haga K, Uehara Y, Suzuki A, Harada A, Wada T, Ishiguro S, Okada K (2012). The wavy growth 3 E3 ligase family controls the gravitropic response in Arabidopsis roots. Plant J. 70, 303–314.

Sakakibara, H (2006) CYTOKININS: Activity, Biosynthesis, and Translocation. Annual Review of Plant Biology. 57, 431-449.

Sambrook, J., Fritsch, E. F. & Maniatis, T. (1989) Molecular cloning: A Laboratory Manual. 2nd edition. . Cold Spring Harbor Laboratory Press, N.Y.

Samuel MA, Mudgil Y, Salt JN, Delmas F, Ramachandran S, Chilelli A, Goring DR (2008). Interactions between the S-domain receptor kinases and AtPUB–ARM E3 ubiquitin ligases suggest a conserved signaling pathway in Arabidopsis. Plant Physiol. 147, 2084–2095.

Saracco, S.A., Hansson, M., Scalf, M., Walker, J.M., Smith, L.M., and Vierstra, R.D. (2009). Tandem affinity purification and mass spectrometric analysis of ubiquitylated proteins in Arabidopsis. Plant J. 59:344–358.

Sawa, M, Nusinow, DA, Kay, SA, and Imaizumi, T (2007) FKF1 and GIGANTEA complex formation is required for day-length measurement in Arabidopsis. Science 318, 261-265.

Schauer N., Steinhauser D., Strelkov S., Schomburg D., Allison G., Moritz T., . . . Kopka J. (2005) GC-MS libraries for the rapid identification of metabolites in complex biological samples. FEBS Letters 579, 1332–1337.

Scheible WR, Morcuende R, Czechowski T, Fritz C, Osuna D, Palacios-Rojas N, Schindelasch D, Thimm O, Udvardi MK, Stitt M. (2004)Genome-wide reprogramming of primary and secondary metabolism, protein synthesis, cellular growth processes, and the regulatory infrastructure of Arabidopsis in response to nitrogen. Plant Physiol. 136(1):2483-99. Review.

Scheible W-R, Rojas-Triana M. (2015) Sensing, signaLling, and CONTROL of phosphate starvation in plants: molecular players and applications. Annual Plant Reviews Volume 48: Phosphorus Metabolism in Plants.DOI: 10.1002/9781118958841.ch2

Scheffner M, Nuber U, Huibregtse JM (1995). Protein ubiquitination involving an E1–E2–E3 enzyme ubiquitin thioester cascade. Nature. 373, 81–83.

Schiefelbein, J (2003) Cell-fate specification in the epidermis: A common patterning mechanism in the root and shoot. Curr. Opin. Plant Biol. 6, 74–78.

Schroeder, DF, Gahrtz, M, Maxwell, BB, Cook, RK, Kan, JM, Alonso, JM, Ecker, JR, and Chory, J (2002) De-etiolated 1 and damaged DNA binding protein 1 interact to regulate Arabidopsis photomorphogenesis. Curr. Biol. 12, 1462-1472.

Schluepmann, H., Pellny, T., van Dijken, A., Smeekens, S., and Paul, M. (2003). Trehalose 6-phosphate is indispensable for carbohydrate utilization and growth in Arabidopsis thaliana. Proc. Natl. Acad. Sci. USA 100, 6849–6854.

Schulman, BA, Carrano, AC, Jeffrey, PD, Bowen, Z, Kinnucan, ER, Finnin, MS, Elledge, SJ, Harper, JW, Pagano, M, and Pavletich, NP (2000) Insights into SCF ubiquitin ligases from the structure of the Skp1-Skp2 complex. Nature 408, 381-386.

Schumann N, Navarro-Quezada A, Ullrich K, Kuhl C, Quint M. (2011) Molecular Evolution and Selection Patterns of Plant F-Box Proteins with C-Terminal Kelch Repeats. Plant Physiol. 155(2): 835–850. doi: 10.1104/pp.110.166579.

Schwarz SE, Rosa JL, Scheffner M (1998) Characterization of human hect domain family members and their interaction with UbcH5 and UbcH7. J. Biol. Chem. 273, 12148–12154.

Searle, MS, Layfield, R, Hagen, T (2011) Inhibition of cullin RING ligases by cycle inhibiting factor: evidence for interference with Nedd8-induced conformational control J. Mol. Biol. 413, 430–437.

Secco, D, Jabnoune, M, Walker, H, Shou, H, Wu, P, Poirier, Y, and Whelan, J (2013) Spatio-temporal transcript profiling of rice roots and shoots in response to phosphate starvation and recovery. The Plant cell 25, 4285-4304.

Seo, KI, Lee, JH, Nezames, CD, Zhong, S, Song, E, Byun, MO, and Deng, XW (2014) ABD1 is an Arabidopsis DCAF substrate receptor for CUL4-DDB1-based E3 ligases that acts as a negative regulator of abscisic acid signaling. Plant Cell 26, 695-711.

Seo DH, Ryu MY, Jammes F, Hwang JH, Turek M, Kang BG, Kwak JM, Kim WT (2012a) Roles of four Arabidopsis U-box E3 ubiquitin ligases in negative regulation of ABA-mediated drought stress responses. Plant Physiol 160, 556–568.

Seo YS, Choi JY, Kim SJ, Kim EY, Shin JS, and Kim WT (2012b) Constitutive expression of CaRma1H1, a hot pepper ER-localized RING E3 ubiquitin ligase, increases tolerance to drought and salt stresses in transgenic tomato plants. Plant Cell Rep 31, 1659–1665.

Shabek N, Herman-Bachinsky Y, Buchsbaum S, Lewinson O, Haj-Yahya M, Hejjaoui M, Lashuel HA, Sommer T, Brik A, Ciechanover A (2012) The size of the proteasomal substrate determines whether its degradation will be mediated by mono- or polyubiquitylation. Mol. Cell 48, 87–97.

Shen G, Adam Z, Zhang H (2007a) The E3 ligase AtCHIP ubiquitylates FtsH1, a component of the chloroplast FtsH protease, and affects protein degradation in chloroplasts. Plant J. 52, 309–321.

Shen G, Yan J, Pasapula V, Luo J, He C, Clarke AK, Zhang H (2007b) The chloroplast protease subunit ClpP4 is a substrate of the E3 ligase AtCHIP and plays an important role in chloroplast function. Plant J. 49, 228–237.

Shen, C, Wang, S, Zhang, S, Xu, Y, Qian, Q, Qi, Y, and Jiang, DA (2013) OsARF16, a transcription factor, is required for auxin and phosphate starvation response in rice (Oryza sativa L.). Plant, Cell & Environment 36, 607-620.

Shi, Z, Maximova, S, Liu, Y, Verica, J, and Guiltinan, MJ (2012) The Salicylic Acid Receptor NRP3 Is a Negative Regulator of the Transcriptional Defense Response during Early Flower Development in Arabidopsis. Mol. Plant 6, 802-816.

Shibahara T, Kawasaki H, Hirano H (2002) Identification of the 19S regulatory particle subunits from the rice 26S proteasome. Eur. J. Biochem. 269:1474–83.

Sigismund S, Polo S, Di Fiore PP (2004) Signaling through monoubiquitination. Curr. Top Microbiol. Immunol. 286, 149–185.

Smalle J, Vierstra RD (2004) The ubiquitin 26S proteasome proteolytic pathway. Annu. Rev. Plant Biol. 55, 555–590.

Smith AP, Jain A, Deal RB, Nagarajan VK, Poling MD, Raghothama KG, Meagher RB (2010) Histone H2A.Z regulates the expression of several classes of phosphate starvation response genes but not as a transcriptional activator. Plant Physiol. 152, 217–225.

Smith, SE, Jakobsen, I, Groenlund, M, and Smith, FA (2011) Roles of arbuscular mycorrhizas in plant phosphorus (P) nutrition: interactions between pathways of P uptake in arbuscular mycorrhizal (AM) roots have important implications for understanding and manipulating plant P acquisition. Plant Physiology 156, 1050-1057.

Smith, M, Willmann, M, Wu, G, Berardini, T, Moller, B, Weijers, D, and Poethig, R (2009) Cyclophilin 40 is required for microRNA activity in Arabidopsis. Proceedings of the National Academy of Sciences 106, 5424 - 5429.

Solfanelli C, Poggi A, Loreti E, Alpi A, Perata P (2006) Sucrose-Specific Induction of the Anthocyanin Biosynthetic Pathway in Arabidopsis. Plant Physiology. 140, 637–646.

Sparkes, I. A., Runions, J., Kearns, A. & Hawes, C. (2006) Rapid, transient expression of fluorescent fusion proteins in tobacco plants and generation of stably transformed plants. Nature protocols 1, 2019-2025, doi:10.1038/nprot.2006.286.

Spoel, SH, Mou, Z, Tada, Y, Spivey, NW, Genschik, P, and Dong, X (2009) Proteasome-mediated turnover of the transcription coactivator NPR1 plays dual roles in regulating plant immunity. Cell 137, 860-872.

Stefanovic A, Ribot C, Rouached H, Wang Y, Chong J, Belbahri L, Delessert S, Poirier Y (2007) Members of the PHO1 gene family show limited functional redundancy in phosphate transfer to the shoot, and are regulated by phosphate deficiency via distinct pathways. Plant J. 50, 982–994.

Stirnberg, P, Furner, IJ, and Ottoline Leyser, HM (2007) MAX2 participates in an SCF complex which acts locally at the node to suppress shoot branching. Plant J. 50, 80-94.

Stone SL, Hauksdottir H, Troy A, Herschleb J, Kraft E, Callis J (2005). Functional analysis of the RING-type ubiquitin ligase family of Arabidopsis. Plant Physiol. 137, 13–30.

Strader, LC, Ritchie, S, Soule, JD, McGinnis, KM, and Steber, CM (2004) Recessive-interfering mutations in the gibberellin signaling gene SLEEPY1 are rescued by overexpression of its homologue, SNEEZY. Proc. Natl. Acad. Sci. 101, 12771-12776.

Strehmel N., Hummel J., Erban A., Strassburg K. & Kopka J. (2008) Retention index thresholds for compound matching in GC-MS metabolite profiling. Journal of Chromatography. B, Analytical Technologies in the Biomedical and Life Sciences 871, 182–190.

Stuttmann, J, Parker, JE, Noel, LD (2009) COP9 signalosome- and 26S proteasome-dependent regulation of SCFTIR1 accumulation in Arabidopsis. J. Biol. Chem. 284, 7920–7930.

Sulpice, R, Ishihara, H, Schlereth, A, Cawthray, GR, Encke, B, Giavalisco, P, Ivakov, A, Arrivault, S, Jost, R, Krohn, N, et al (2014) Low levels of ribosomal RNA partly account for the very high photosynthetic phosphorus-use efficiency of Proteaceae species. Plant, Cell & Environment 37, 1276-1298.

Sun L, Shi L, Li W, Yu W, Liang J, Zhang H, Yang X, Wang Y, Li R, Yao X, et al (2009) JFK, a kelch domain-containing F-box protein, links the SCF complex to p53 regulation. Proc Natl Acad Sci USA 106: 10195–10200

Sunkar, R, and Zhu, J-K (2004) Novel and Stress-Regulated MicroRNAs and Other Small RNAs from Arabidopsis. The Plant Cell Online 16, 2001-2019.

Suzuki H, et al. (2000) Homodimer of two F-box proteins βTrCP1 or βTrCP2 binds to IκBα for signaldependent ubiquitination. J. Biol. Chem. 275:2877–2884.

Takahashi A, Takeda K, Ohnishi T (1991) Light-induced anthocyanin reduces the extent of damage to DNA in UV-irradiated Centaurea cyanus cells in culture. Plant Cell Physiol. 32, 541–547.

Taylor, CB, Bariola, PA, delCardayre, SB, Raines, RT, and Green, PJ (1993) RNS2: a senescence-associated RNase of Arabidopsis that diverged from the S-RNases before speciation. Proceedings of the National Academy of Sciences of the United States of America 90, 5118-5122.

Thibaud MC, Arrighi JF, Bayle V, Chiarenza S, Creff A, Bustos R, Paz-Ares J, Poirier Y, Nussaume L (2010) Dissection of local and systemic transcriptional responses to phosphate starvation in Arabidopsis. Plant J. 64, 775–789.

Thines, B, Katsir, L, Melotto, M, Niu, Y, Mandaokar, A, Liu, G, Nomura, K, He, SY, Howe, GA, and Browse, J (2007) JAZ repressor proteins are targets of the SCF(COI1) complex during jasmonate signalling. Nature 448, 661-665.

Thomann A, Lechner E, Hansen M, Dumbliauskas E, Parmentier Y, Kieber J, Scheres B, Genschik P (2009) Arabidopsis CULLIN3 genes regulate primary root growth and patterning by ethylene-dependent and-independent mechanisms. PLoS Genet. 5, e1000328.

Thomas JH (2006) Adaptive evolution in two large families of ubiquitinligase adapters in nematodes and plants. Genome Res 16: 1017–1030

Tian J, Wang C, Zhang Q, He X, Whelan J, Shou H (2012) Overexpression of OsPAP10a, a root-associated acid phosphatase, increased extracellular organic phosphorus utilization in rice. J. Integr. Plant Biol. 54, 631–639.

Ticconi CA, Abel S (2004) Short on phosphate: Plant surveillance and countermeasures. Trends Plant Sci. 9, 548–555.

Tiwari SB, Wang XJ, Hagen G, Guilfoyle TJ (2001) Aux/IAA proteins are active repressors and their stability and activity are modulated by auxin. Plant Cell 13, 2809–2822.

Tomsig JL, Snyder SL, Creutz CE (2003) Identification of targets for calcium signaling through the copine family of proteins. Characterization of a coiled-coil copine-binding motif. J. Biol. Chem. 278, 10048–10054.

Tran HT, Plaxton WC (2008) Proteomic analysis of alterations in the secretome of Arabidopsis thaliana suspension cells subjected to nutritional phosphate deficiency. Proteomics 8, 4317–4326.

Trull MC, Guiltinan MJ, Lynch JP, Deikman J (1997) The responses of wild-type and ABA mutant Arabidopsis thaliana plants to phosphorus starvation. Plant Cell Environ. 20, 85–92

Tsiantis, M (2001) Control of shoot cell fate: beyond homeoboxes. Plant Cell 13:733–738.

Tsukaya H, Ohshima T, Naito S, Chino M, Komeda Y (1991) Sugardependent expression of the CHS-A gene for chalcone synthase from petunia in transgenic Arabidopsis. Plant Physiol 97: 1414–1421

Tuteja JH, Clough SJ, Chan WC, Vodkin LO. (2004) Tissue-specific gene silencing mediated by a naturally occurring chalcone synthase gene cluster in Glycine max. Plant Cell. 16(4):819-35.

Uhde-Stone, C, Zinn, KE, Ramirez-Yáñez, M, Li, A, Vance, CP, and Allan, DL (2003) Nylon Filter Arrays Reveal Differential Gene Expression in Proteoid Roots of White Lupin in Response to Phosphorus Deficiency. Plant Physiology 131, 1064-1079.

Ulrich HD (2005) Mutual interactions between the SUMO and ubiquitin systems: A plea of no contest. Trends Cell Biol. 15, 525–532.

Umehara, M, Hanada, A, Magome, H, Takeda-Kamiya, N, and Yamaguchi, S (2010) Contribution of Strigolactones to the Inhibition of Tiller Bud Outgrowth under Phosphate Deficiency in Rice. Plant and Cell Physiology 51, 1118-1126.

Usadel B, Nagel A, Steinhauser D, Gibon Y, Bläsing OE, Redestig H, Sreenivasulu N, Krall L, Hannah MA, Poree F, Fernie AR, Stitt M (2006) PageMan: An interactive ontology tool to generate, display, and annotate overview graphs for profiling experiments. BMC Bioinformatics, 7:535.

Vaccari, DA (2009) Phosphorus: a looming crisis. Scientific American 300, 54-59.

Valdes-López O, Arenas-Huertero C, Ramírez M, Girard L, Sanchez F, Vance CP, Luis Reyes J, Hernandez G (2008) Essential role of MYB transcription factor: PvPHR1 and microRNA: PvmiR399 in phosphorus-deficiency signalling in common bean roots. Plant Cell Environ. 12, 1834–1843

Van Kauwenbergh, SJ, Stewart, M, and Mikkelsen, R (2013) World Reserves of Phosphate Rock... a Dynamic and Unfolding Story. Better Crops 97, 18-20.

Van Leene, J, Hollunder, J, Eeckhout, D, Persiau, G, Van De Slijke, E, Stals, H, Van Isterdael, G, Verkest, A, Neirynck, S, Buffel, Y, De Bodt, S, Maere, S, Laukens, K, Pharazyn, A, Ferreira, PC, Eloy, N, Renne, C, Meyer, C, Faure, JD, Steinbrenner, J, Beynon, J, Larkin, JC, Van de Peer, Y, Hilson, P, Kuiper, M, De Veylder, L, Van Onckelen, H, Inze, D, Witters, E, and De Jaeger, G (2010) Targeted interactomics reveals a complex core cell cycle machinery in Arabidopsis thaliana. Mol. Syst. Biol. 6, 397.

Vance CP (2010) Quantitative trait loci, epigenetics, sugars, and microRNAs: Quaternaries in phosphate acquisition and use. Plant Physiol. 154, 582–588.

Vance CP, Uhde-Stone C, Allan DL (2003) Phosphorus acquisition and use: Critical adaptations by plants for securing a nonrenewable resource. New Phytol. 157, 423–447.

Vanholme, R, Demedts, B, Morreel, K, Ralph, J, and Boerjan, W (2010) Lignin biosynthesis and structure. Plant Physiol. 153:895– 905.

Vanstraelen, M, Baloban, M, Da Ines, O, Cultrone, A, Lammens, T, Boudolf, V, Brown, SC, De Veylder, L, Mergaert, P, and Kondorosi, E (2009) APC/C-CCS52A complexes control meristem maintenance in the Arabidopsis root. Proc. Natl. Acad. Sci. 106, 11806-11811.

Vierstra RD (1996) Proteolysis in plants: mechanisms and functions. Plant Mol. Biol. 32:275–302.

Vierstra RD (2003) The ubiquitin/26S proteasome pathway, the complex last chapter in the life of many plant proteins. Trends Plant Sci. 8:135–42.

Vierstra, RD (2009) The ubiquitin-26S proteasome system at the nexus of plant biology. Nature reviews. Molecular cell biology 10, 385-397, doi:10.1038/nrm2688.

Vodermaier, HC, Gieffers, C, Maurer-Stroh, S, Eisenhaber, F, and Peters, JM (2003) TPR subunits of the anaphase-promoting complex mediate binding to the activator protein CDH1. Curr. Biol. 13, 1459- 1468.

Voges D, Zwickl P, Baumeister W (1999) The 26S proteasome: a molecular machine designed for controlled proteolysis. Annu. Rev. Biochem. 68:1015–68.

Vogt, T (2010) Phenylpropanoid biosynthesis. Mol. Plant 3:2–20.

Voinnet, O., Rivas, S., Mestre, P. & Baulcombe, D. (2003) An enhanced transient expression system in plants based on suppression of gene silencing by the p19 protein of tomato bushy stunt virus. The Plant journal : for cell and molecular biology 33, 949-956.

Wagner C., Sefkow M. & Kopka J. (2003) Construction and application of a mass spectral and retention time index database generated from plant GC/EI-TOF-MS metabolite profiles. Phytochemistry 62, 887–900.

Wang, L, Dong, J, Gao, Z, and Liu, D (2012) The Arabidopsis gene HYPERSENSITIVE TO PHOSPHATE STARVATION 3 encodes ETHYLENE OVERPRODUCTION 1. Plant and Cell Physiology 53, 1093-1105.

Wang, X, Yi, K, Tao, Y, Wang, F, Wu, Z, Jiang, D, Chen, XIN, Zhu, L, and Wu, P (2006) Cytokinin represses phosphate-starvation response through increasing of intracellular phosphate level. Plant, Cell & Environment 29, 1924-1935.

Wang Y, Ribot C, Rezzonico E, Poirier Y (2004) Structure and expression profile of the Arabidopsis PHO1 gene family indicates a broad role in inorganic phosphate homeostasis. Plant Physiol. 135, 400–411.

Wang, J, Sun, J, Miao, J, Guo, J, Shi, Z, He, M, Chen, Y, Zhao, X, Li, B, Han, F, et al (2013a) A phosphate starvation response regulator Ta-PHR1 is involved in phosphate signalling and increases grain yield in wheat. Annals of Botany 111, 1139-1153.

Wang, S, Zhang, S, Sun, C, Xu, Y, Chen, Y, Yu, C, Qian, Q, Jiang, D-A, and Qi, Y (2014) Auxin response factor (OsARF12), a novel regulator for phosphate homeostasis in rice (Oryza sativa). New Phytologist 201, 91-103.

Wang, KL, Yoshida, H, Lurin, C, and Ecker, JR (2004a) Regulation of ethylene gas biosynthesis by the Arabidopsis ETO1 protein. Nature 428, 945-950.

Wasaki J, Yonetani R, Kuroda S (2003) Transcriptomic analysis of metabolic changes by phosphorus stress in rice plant roots. Plant Cell Environ. 26, 1515–1523.

Watt M, Evans JR (1999) Proteoid roots. Physiology and development. Plant Physiol. 121, 317–324.

Weber H, Bernhardt A, Dieterle M, Hano P, Mutlu A, Estelle M, Genschik P, Hellmann H (2005) Arabidopsis AtCUL3a and AtCUL3b form complexes with members of the BTB/POZ–MATH protein family. Plant Physiol. 137, 83–93.

Weigel, D. & Glazebrook, J. (20002) Arabidopsis: A Laboratory Manual. . CSHL Press.

Welcker, M. & Clurman, B. E. (2007) Fbw7/hCDC4 dimerization regulates its substrate interactions. Cell Div. 2, 7.

Whetten, R, and Sederoff, R (1995) Lignin biosynthesis. Plant Cell 7:1001–1013.

Wilkinson, C. R. *et al*. (2001) Proteins containing the UBA domain are able to bind to multi-ubiquitin chains. Nature cell biology 3, 939-943, doi:10.1038/ncb1001-939).

Williamson LC, Ribrioux SP, Fitter AH, Ottoline Leyser HM (2001) Phosphate availability regulates root system architecture in Arabidopsis. Plant Physiol. 126, 875–882.

Wissuwa, M, Gamat, G, and Ismail, AM (2005) Is root growth under phosphorus deficiency affected by source or sink limitations? Journal of Experimental Botany 56, 1943-1950.

Woodcock, D. M. et al. (1989) Quantitative evaluation of Escherichia coli host strains for tolerance to cytosine methylation in plasmid and phage recombinants. Nucleic acids research 17, 3469-3478.

Wu P, Ma L, Hou X, Wang M, Wu Y, Liu F, Deng XW (2003) Phosphate starvation triggers distinct alterations of genome expression in Arabidopsis roots and leaves. Plant Physiol. 132, 1260–1271.

Wykoff DD, Grossman, AR, Weeks DP, Usuda H, Shimogawara K (1999) Psr1, a nuclear localized protein that regulates phosphorus metabolism in Chlamydomonas. Proc. Natl. Acad. Sci. USA 96, 15336–15341.

Xie, DX, Feys, BF, James, S, Nieto-Rostro, M, and Turner, JG 36 of 36 (1998) COI1: an Arabidopsis gene required for jasmonate-regulated defense and fertility. Science 280, 1091-1094.

Xu, F, Liu, Q, Chen, L, Kuang, J, Walk, T, Wang, J, and Liao, H (2013) Genome-wide identification of soybean microRNAs and their targets reveals their organ-specificity and responses to phosphate starvation. BMC Genomics 14, 1-30.

Xu G, Ma H, Nei M, Kong H (2009) Evolution of F-box genes in plants: different modes of sequence divergence and their relationships with functional diversification. Proc Natl Acad Sci USA 106: 835–840

Xu, C, Wang, Y, Yu, Y, Duan, J, Liao, Z, Xiong, G, Meng, X, Liu, G, Qian, Q, and Li, J (2012) Degradation of MONOCULM 1 by APC/ C(TAD1) regulates rice tillering. Nat. Commun. 3, 750.

Xu, Y, Cao, H, and Chong, K (2010b) APC-targeted RAA1 degradation mediates the cell cycle and root development in plants. Plant Signal Behav. 5, 218-223.

Yan J, Wang J, Li Q, Hwang JR, Patterson C, Zhang H (2003) AtCHIP, a U-box-containing E3 ubiquitin ligase, plays a critical role in temperature stress tolerance in Arabidopsis. Plant Physiol. 132, 861–869.

Yang XJ, Finnegan PM (2010) Regulation of phosphate starvation responses in higher plants. Ann. Bot. 4, 513–526.

Yang, S, Sweetman, JP, Amirsadeghi, S, Barghchi, M, Huttly, AK, Chung, WI, and Twell, D (2001) Novel anther-specific myb genes 26 Molecular Plant 8, 17–27, January 2015 ª The Author 2015. Molecular Plant Regulation of Phenylalanine Ammonia-Lyase in Plants from tobacco as putative regulators of phenylalanine ammonia-lyase expression. Plant Physiol. 126:1738–1753.

Yang P, Fu H, Walker J, Papa CM, Smalle J, *et al*. (2004) Purification of the Arabidopsis 26S proteasome: biochemical and molecular analyses revealed the presence of multiple isoforms. J. Biol. Chem. 279:6401–13.

Yang X, Kalluri UC, Jawdy S, Gunter LE, Yin T, Tschaplinski TJ, Weston DJ, Ranjan P, Tuskan GA (2008) The F-box gene family is expanded in herbaceous annual plants relative to woody perennial plants. Plant Physiol 148: 1189–1200

Yanofsky MF, Nester EW (1986) Molecular characterization of a host-range-determining locus from Agrobacterium tumefaciens. K Bacteriol. 168, 244-250.

Yen JL, et al. (2012) Signal-induced disassembly of the SCF ubiquitin ligase complex by Cdc48/p97. Mol. Cell. 48:288–297.

Yi K, Wu Z, Zhou J, Du L, Guo L, Wu Y, Wu P (2005) OsPTF1, a novel transcription factor involved in tolerance to phosphate starvation in rice. Plant Physiol. 138, 2087–2096.

Yin, R, Messner, B, Faus-Kessler, T, Hoffmann, T, Schwab, W, Hajirezaei, MR, von Saint Paul, V, Heller, W, and Schaffner, AR (2012) Feedback inhibition of the general phenylpropanoid and flavonol biosynthetic pathways upon a compromised flavonol-3-Oglycosylation. J. Exp. Bot. 63:2465–2478.

Yoneyama, K, Yoneyama, K, Takeuchi, Y, and Sekimoto, H (2007) Phosphorus deficiency in red clover promotes exudation of orobanchol, the signal for mycorrhizal symbionts and germination stimulant for root parasites. Planta 225, 1031-1038.

Yoshida, H, Nagata, M, Saito, K, Wang, KL, and Ecker, JR (2005) Arabidopsis ETO1 specifically interacts with and negatively regulates type 2 1-aminocyclopropane-1-carboxylate synthases. BMC Plant Biol. 5, 14.

Yu, H, Luo, N, Sun, L, and Liu, D (2012) HPS4/SABRE regulates plant responses to phosphate starvation through antagonistic interaction with ethylene signalling. Journal of Experimental Botany 63, 4527-4538.

Yuan S, *et al*. (2012) A ubiquitin ligase of symbiosis receptor kinase involved in nodule organogenesis. Plant Physiol. 160, 106–117.

Zhang X, Gou M, Liu C-L (2013) Arabidopsis Kelch Repeat F-Box Proteins Regulate Phenylpropanoid Biosynthesis via Controlling the Turnover of Phenylalanine Ammonia-Lyase. The Plant Cell. 25(12):4994-5010. doi: 10.1105/tpc.113.119644.

Zhang, Q, Wang, C, Tian, J, Li, K, and Shou, H (2011) Identification of rice purple acid phosphatases related to posphate starvation signalling. Plant Biology 13, 7-15.

Zhang F, Gonzalez A, Zhao M, Payne CT, Lloyd A (2003) A network of redundant bHLH proteins functions in all TTG1-dependent pathways of Arabidopsis. Development 130, 4859–4869.

Zhang L, Skolnick J (1998) What should the Z-score of native protein structures be? Protein Sci. 1998 May; 7(5): 1201–1207.

Zhang, W, Ito, H, Quint, M, Huang, H, noel, Ld, and Gray, WM (2008a) Genetic analysis of CAND1–CUL1 interactions in Arabidopsis supports a role for CAND1-mediated cycling of the SCFTIR1 complex. Proc. Natl Acad. Sci. U S A. 105, 8470–8475.

Zhang, Y, Xu, W, Li, Z, Deng, XW, Wu, W, and Xue, Y (2008b) Fbox protein DOR functions as a novel inhibitory factor for abscisic acidinduced stomatal closure under drought stress in Arabidopsis. Plant Physiol. 148, 2121-2133.

Zhang, YJ, Lynch, JP, and Brown, KM (2003) Ethylene and phosphorus availability have interacting yet distinct effects on root hair development. Journal of Experimental Botany 54, 2351-2361.

Zhang, Y, Cheng, YT, Qu, N, Zhao, Q, Bi, D, and Li, X (2006) Negative regulation of defense responses in Arabidopsis by two NPR1 paralogs. Plant J. 48, 647-656.

Zhang, L, Du, L, Shen, C, Yang, Y, and Poovaiah, BW (2014) Regulation of plant immunity through ubiquitin-mediated modulation of Ca(2+)-calmodulin-AtSR1/CAMTA3 signaling. Plant J. 78, 269-281.

Zhang, Z, Yang, J, Kong, EH, Chao, WC, Morris, EP, da Fonseca, PC, and Barford, D (2013) Recombinant expression, reconstitution and structure of human anaphase-promoting complex (APC/C). Biochem J. 449, 365-371.

Zheng, N, et al (2002b) Structure of the Cul1–Rbx1–Skp1–F boxSkp2 SCF ubiquitin ligase complex: N6east COP9/signalosome suppresses cullin activity through recruitment of the deubiquitylating enzyme Ubp12p. Mol. Cell. 11, 927–938. Nature. 416, 703–709.

Zheng, N., Schulman, B.A., Song, L., Miller, J.J., Jeffrey, P.D., Wang, P., Chu, C., Koepp, D.M., Elledge, S.J., Pagano, M., Conaway, R.C., Conaway, J.W., Harper, J.W., and Pavletich, N.P. (2002b). Structure of the Cul1-Rbx1-Skp1-F boxSkp2 SCF ubiquitin ligase complex. Nature 416, 703-709. Deshaies, R. (1999). SCF and Cullin/RING H2-based Ubiquitin ligases. Annu. Rev. Cell Dev. Biol. 15, 435-467.

Zhou J, Jiao F, Wu Z, Li Y, Wang X, He X, Zhong W, Wu P (2008) OsPHR2 is involved in phosphate-starvation signaling and excessive phosphate accumulation in shoots of plants. Plant Physiol. 146, 1673–1686.

Zhou, J, Lee, C, Zhong, R, and Ye, ZH (2009) MYB58 and MYB63 are transcriptional activators of the lignin biosynthetic pathway during secondary cell wall formation in Arabidopsis. Plant Cell 21: 248–266.

Zhu, D, Maier, A, Lee, JH, Laubinger, S, Saijo, Y, Wang, H, Qu, LJ, Hoecker, U, and Deng, XW (2008) Biochemical characterization of Arabidopsis complexes containing CONSTITUTIVELY PHOTOMORPHOGENIC1 and SUPPRESSOR OF PHYA proteins in light control of plant development. Plant Cell 20, 2307-2323.

Zhu, J, Kaeppler, SM, and Lynch, JP (2005) Topsoil foraging and phosphorus acquisition efficiency in maize (Zea mays). Functional Plant Biology 32, 749-762

Zhuang, M, Calabrese, MF, Liu, J, Waddell, MB, Nourse, A, Hammel, M, Miller, DJ, Walden, H, Duda, DM, Seyedin, SN, Hoggard, T, Harper, JW, White, KP, and Schulman, BA (2009). Structures of SPOP-substrate complexes: insights into molecular architectures of BTB-Cul3 ubiquitin ligases. Mol. Cell 36, 39-50.

Zimmermann, S, and Hahlbrock, K (1975) Light-induced changes of enzyme activities in parsley cell suspension cultures. Purification and some properties of phenylalanine ammonia-lyase (E.C.4.3.1.5). Arch. Biochem. Biophys. 166:54–62.